Hawaii National Marine Renewable Energy Center (HINMREC)

U.S. Department of Energy Award Number: DE-FG36-08GO18180

Task 3: Wave Resource Model, Wave Field Measurements and Data Analysis

Wave Energy Resource Characterization at the U.S. Navy Wave Energy Test Site and Other Locations in Hawaiʻi

Prepared by:
UH Department of Ocean and Resource Engineering

Prepared for:
Hawaii Natural Energy Institute, University of Hawaii

November 2014

HNEI
Hawaiʻi Natural Energy Institute
University of Hawaiʻi at Mānoa

Wave Energy Resource Characterization at the US Navy Wave Energy Test Site and other Locations in Hawai‘i

Prepared by:

Ning Li and Kwok Fai Cheung

Department of Ocean and Resources Engineering
University of Hawai‘i

Prepared for:

luisvega@hawaii.edu
Hawai‘i National Marine Renewable Energy Center
Hawai‘i Natural Energy Institute
University of Hawai‘i

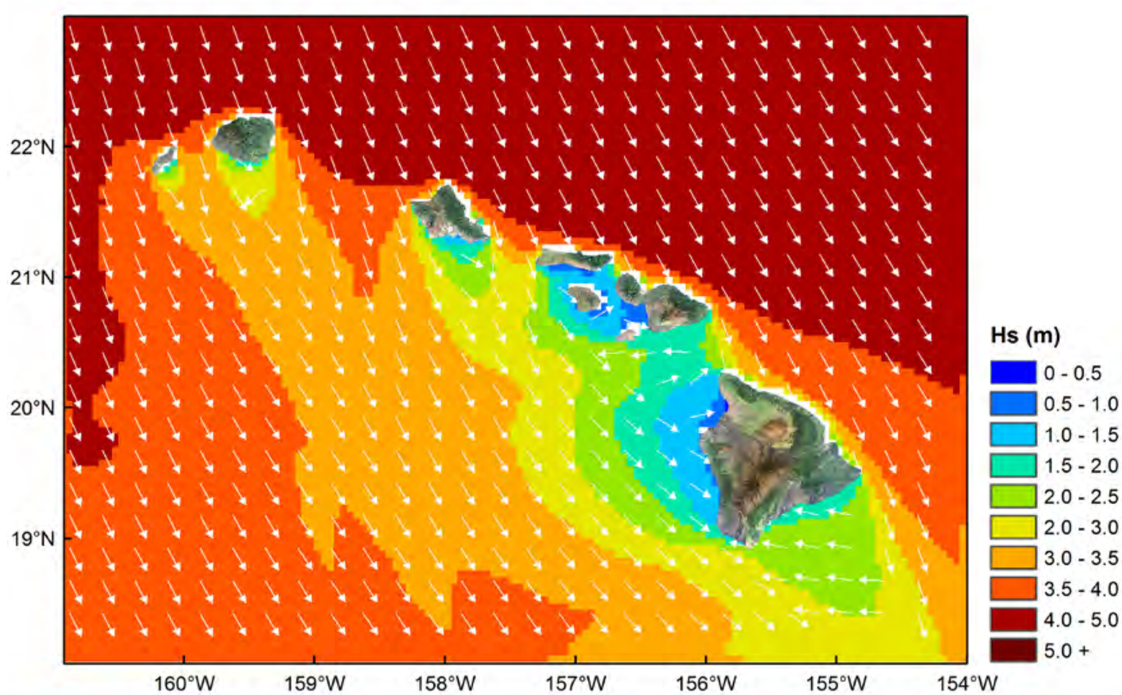

This material is based upon work supported by the US Department of Energy under Award Number DE-FG36-08GO18180

November 1, 2014

Summary

Numerical wave hindcasting from surface winds provides an important source of information for wave energy resource assessment and climate research. We utilized the third-generation ocean and coastal wave models, WAVEWATCH III and SWAN (Simulating WAves Nearshore), in a system of nested grids to provide high-resolution wave parameters around the islands of Oahu, Maui, Kauai, and Hawaiʻi from 1979 to 2013. The wind forcing includes the Climate Forecast System Reanalysis (CFSR) for the globe and downscaled winds by the Weather Research and Forecasting (WRF) model around the Hawaiian Islands. Measurements from 14 buoys provide validation of the hindcast across the Hawaiʻi region. The hindcast reproduces the wave climate, statistical distributions, and episodic events recorded at both offshore and nearshore buoys. After validation, the sea state and wave power parameters are compiled at six sites around the islands. Two of the sites are located within the US Navy Wave Energy Test Site (WETS) offshore of the Marine Corps Base in Kaneohe, Oahu. One is collocated with a Waverider™ buoy at 81 m water depth, where tests will be conducted and the other at a shallower depth of 58 m is a potential site. The other 4 are potential sites at Kilauea, Pauwela, Upolu, and South Point at the north shore of Kauai, the north shore of Maui, and the north and south shores of Hawaiʻi Island, respectively. The results show year-round wave activities with significant increases of wave power from the summer to the winter months accompanied by a transition from the wind waves to swells. At WETS, the analysis shows 60% of the energy resources come from conditions with significant wave height above 2 m that occur less than 25% of the time during 1979 to 2013. The diversified and persistent wave activities make WETS and the other five potential sites suitable for testing and development of wave energy convertors.

Table of Contents

List of Figures

List of Tables

1. Introduction

The wave climate in Hawai‘i is unique because of the mid-Pacific location and massive archipelago. Figure 1 provides a location map and an illustration of the wind wave and swell patterns around the major Hawaiian Islands. Extratropical storms near the Kuril and Aleutian Islands generate swells from the northwest to north during the winter months. The south facing shores experience gentle swells from the year-round Southern Hemisphere Westerlies that are augmented by mid-latitude cyclones off Antarctica during the summer. The trade winds generate waves from the northeast to east throughout the year. In addition, passing cold fronts and subtropical storms might generate wind waves and short-period swells toward the islands from different directions during the winter months. The wave conditions are recorded by a number of nearshore and offshore buoys across the state. The diversified and persistent wave activities indicate the potential for development of wave energy resources in Hawai‘i.

The Wave Energy Test Site (WETS) on windward Oahu, developed and operated with funding from the Department of Energy and the Department of Navy, provides the infrastructure for testing and development of wave energy convertors. Figure 2 shows the location of WETS and buoys around Oahu. A Waverider™ buoy is deployed at WETS in 81 m of water. Kaneohe II at about 1 km to the southeast is a potential site. Both sites are exposed to the north swells and east wind waves, but are sheltered from the south swells. Three other buoys are currently in operation to provide the wave conditions around the Oahu. Preliminary assessment of wave records (Li and Cheung, 2014) and local logistics identify a number of neighbor island locations for wave energy resources development. Figure 3 shows the locations of a potential site off Kilauea, Kauai and an adjacent buoy that was in operation from 1982 to 1996. The site on the

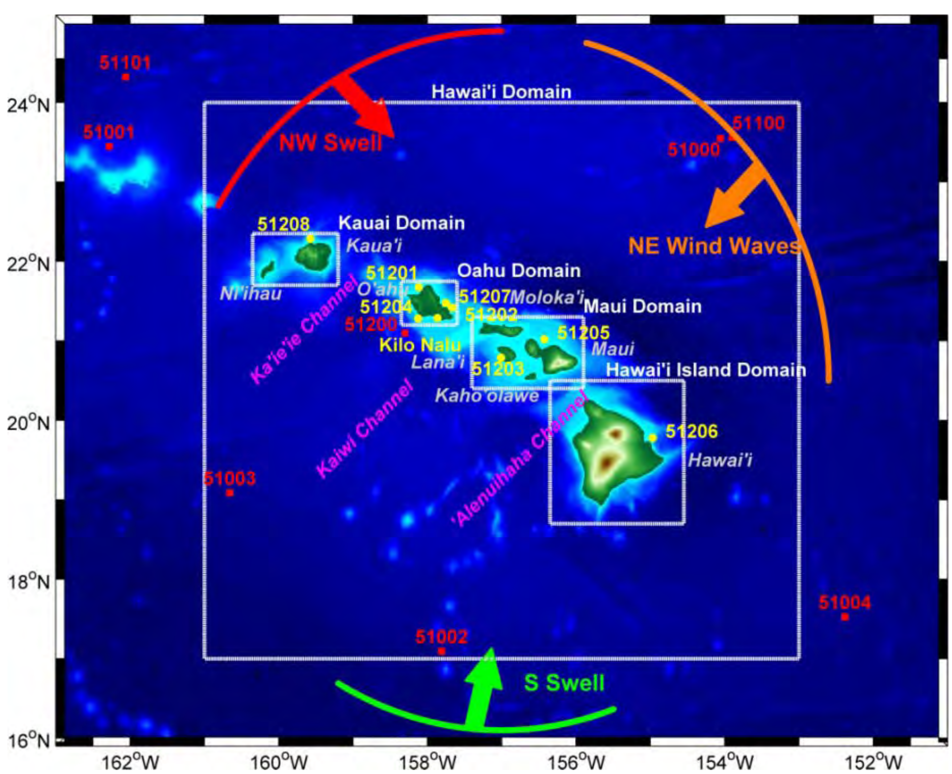

Figure 1- Hawai‘i wave climate, buoys, and hindcast coverage.

North-facing shore is exposed to the north swells and the year round wind waves. A site off Pauwela, Maui is exposed to similar wave conditions. Figure 4 shows its location along with those of two buoys currently in operation. Hawai‘i Island has two potential sites off Upolu and South Point and a buoy near Hilo as shown in Figure 5. These two sites are exposed to heightened wind waves due to acceleration of the east trade winds around the island (Stopa *et al.*, 2011).

Figure 2- Locations of buoys (pin), WETS, and a potential site (balloon) around Oahu.

Figure 3- Locations of a buoy (pin) and a potential site (balloon) around Kauai.

Figure 4- Locations of buoys (pin) and a potential site (balloon) around Maui.

Figure 5- Locations of a buoy (pin) and potential sites (balloon) around Hawai‘i Island.

Table 1 list the water depths and coordinates of the sites and buoys along with their data coverage. The long records at offshore buoys #51001, #51003, #51002, #51004, #51100 and #51101 provide general wave conditions for the state. The nearshore buoys, Waimea #51201, Barbers Point #51204, Barking Sands #39, Kaumalapau #51203, and Hilo #51206 do not record the wave conditions directly relevant to the sites located on different sides of the islands. Other buoys such as #51205 and #51207 are close to Pauwela and WETS, but do not have sufficient wave data for wave energy analysis. The buoy Mokapu # 51202 is close to WETS and Kaneohe II. Its location southeast of the Kaneohe headland is in the shadow of the northwest swells despite its long record. The wave energy resources assessment at WETS and other sites are best accomplished by numerical models, while the extensive records provide a good opportunity to validate the model results.

Third generation spectral wave models, such as WAVEWATCH III of Tolman (2008) and SWAN (Simulating WAves Nearshore) of Booij *et al.* (1999) and SWAN Team (2011), can provide a reliable tool for modeling of the multi-modal sea states in Hawaiʻi. Despite being developed for open oceans and shelf seas, WAVEWATCH III is able to describe shadowing of the wave field by the Hawaiian Islands and heightened seas with small fetches in interisland channels and around headlands (Stopa *et al.*, 2011, 2013b; Foster *et al.*, 2014). The SWAN model is better suited for near-shore environments due to the ability to account for triad wave interactions and depth-limited wave breaking in shallow water. Filipot and Cheung (2012) provided additional parameterizations in SWAN to model coastal processes in tropical island environments. The nesting of WAVEWATCH III and SWAN has become a standard to model wave generation and propagation from the open ocean to the shore.

Table 1 - Locations of 14 Buoys for Model Validation and Sites for Wave Energy Assessment

Buoy/Site	Location	Latitude (°N)	Longitude (°W)	Depth (m)	Temporal Coverage
51001	Northwestern Hawaiʻi	23.445	162.279	3430	1981.2-2009.12
51002	Southwest Hawaiʻi	17.094	157.808	5002	1984.9-2013.1
51003	Western Hawaiʻi	19.018	160.582	4919	1984.11-2013.6
51004	Southeastern Hawaiʻi	17.602	152.395	5230	1984.11-2013.6
51100	Northern Hawaiʻi	23.558	153.900	4754.9	2009.4-2013.6
51101	Northwestern Hawaiʻi	24.321	162.058	4791.5	2008.2-2013.6
WETS[1] (51207)	Oahu	21.4775	157.7526	81	2012.10-2013.6
Kaneohe II	Oahu	21.472	157.747	58	-
51204	Oahu	21.281	158.124	302	2010.10-2013.6
51201	Oahu	21.669	158.120	200	2001.12-2013.6
51202	Oahu	21.414	157.679	82	2000.8-2013.6
39	Kauai	22.00667	159.8333	109.8	1982.10-1996.11
Kilauea	Kauai	22.236	159.422	53	-
51205	Maui	21.0195	156.4272	193	2011.12-2013.6
51203	Lanai	20.78778	157.0098	201	2007.5-2013.6
Pauwela	Maui	20.958	156.322	73	-
51206	Hawaiʻi	19.78143	154.968	347	2012.3-2013.6
Upolu	Hawaiʻi	20.275	155.863	47	-
South Point	Hawaiʻi	18.91	155.681	40	-

[1] Kaneohe Bay Waverider Buoy (CDIP #198/NDBC 51207) deployed at the Wave Energy Test Site (WETS).

High-quality global and regional wind forcing is critical in modeling of the ocean wave conditions in Hawaiʻi. The newly released Climate Forecast System Reanalysis (CFSR) of Saha *et al.* (2010) contains clear signals of climate cycles and provides better descriptions of the upper percentile winds among available global reanalysis datasets (Stopa *et al.*, 2013a; Stopa and Cheung, 2014). The state-of-the-art dataset was generated from a suite of coupled ocean, land and atmospheric models with assimilation of observations from many data sources like buoy, ship, aircraft, and satellite observations. It provides hourly surface winds at 0.5° resolution on a spherical global grid from 1979 to 2010 and 0.25° resolution from 2011 onward. The Hawaiʻi archipelago modifies the trade wind flow and creates localized weather patterns that are not amenable to the global models in CFSR. The Weather Research and Forecasting (WRF) model of Skamarock and Klemp (2008) with proper initial and boundary conditions from CFSR can describe mesoscale phenomena such as diurnal thermal forcing of sea and land breezes, flow acceleration and deceleration around topographic features, and wakes on the leeside of islands.

In this report, we describe a long-term hindcast study using the spectral models WAVEWATCH III and SWAN in a system of global, regional, and nearshore computational grids to characterize the wave conditions and energy resources at WETS and the other potential sites. The wind forcing includes CFSR for the entire globe and downscaled WRF winds for the Hawaiʻi region to account for the multi-modal sea state. Section 2 describes the setup of the spectral wave and atmospheric models and defines the characteristic wave energy parameters. Section 3 provides validation of the hindcast with measurements from available offshore and nearshore buoys across the state. The standard wave parameters and 2D spectra at WETS and the other potential sites are used in a detailed wave resource assessment in Section 4. This is followed by a summary of the findings in Section 5.

2. Methodology

2.1 Model Setup

The present study utilizes a system of nested global, regional, and island-scale spectral wave models based on WAVEWATCH III and SWAN with wind forcing from the global CFSR and Hawai‘i regional WRF datasets. Figure 1 illustrates the setup of the regional and island-scale nested grids within global WAVEWATCH III. The series of nested grids capture physical processes at increasing temporal and spatial resolution toward each island. Global WAVEWATCH III, which resolves the oceans from 77.5°S to 77.5°N latitude at 0.5 arc-degree (~55 km near Hawai‘i) resolution, is coupled with the Hawai‘i regional grid from 199 to 206°E and 18 to 23°N at 3 arc-min (~5.5 km) resolution. The coupled model outputs 2D wave spectra along the boundary of the SWAN domain for Oahu, Kauai, Maui and Hawai‘i Island.

The Oahu SWAN domain extends from 201.65 to 202.40°E and 21.2 to 21.75°N at 18 arc-sec (~550 m) resolution. With the same grid resolution, the Kauai SWAN domain extend from 199.65 to 200.8°E and 21.7 to 22.35°N, the Maui SWAN domain from 202.6 to 204.1°E and 20.4 to 21.3°N, and the Hawai‘i Island domain from 203.8 to 205.3°E and 18.85 to 20.35°N. The bathymetry comes from a blended datasets comprising ETOPO1, multibeam, and LiDAR data at 1 arcmin (~1,800 m), 50 m, and 3 m resolution respectively (Cheung *et al.*, 2013). Hydrographic surveys and digitized nautical charts supplement the near-shore bathymetry, where the water lacks clarity for LiDAR surveys. The Generic Mapping Tools (GMT) of Wessel and Smith (1991) blends the datasets for development of the computational grids. The SWAN spectrum is discretized by 24 equal directional bins from 0 to 360° and 25 exponentially increasing frequency bins from 0.0418 to 1 Hz.

The Hawai‘i regional wind forcing was developed by Prof. Yi-Leng Chen and his team in the UH Department of Meteorology. A two-way nested grid system with horizontal resolution of 18 and 6 km and 196 × 185 and 292 × 196 cells covers the central Pacific and the Hawaiian Islands in the WRF model, which is forced and initialized by the global CFSR dataset. The WRF model produced daily 36-h simulations, which were combined to produce a continuous dataset from 1979 to 2013. The 6 km WRF winds for the Hawai‘i region together with the 0.5° CFSR winds for the entire globe define the forcing for the wave model system, which in turn outputs hourly wave parameters over the computational grid system and wave spectra at the buoy and the site locations showed in Table 1 for model validation and computation of energy parameters.

2.2 Wave Energy Parameters

For consistency with the methodology proposed by Lenee-Bluhm *et al* (2011) to characterize sea state and wave energy resources off Oregon, we use the following six parameters: omnidirectional wave power (also referred as wave power flux), significant wave height, energy period, spectral width, direction of the maximum directionally resolved wave power, and directionality coefficient.

The omnidirectional wave power is defined by

$$J = \sum_{ij} \rho g C_{gi} S_{ij} \Delta f_i \Delta\theta_j \quad \text{(Watts/m)} \tag{1}$$

where S = wave spectrum, θ = wave direction, f = wave frequency, C_g = group speed, g = gravitational acceleration, ρ = water density, and i and j are indices for frequency and direction bins. The significant wave height H_s, energy period T_e, and spectral width ϵ_0 are given by:

$$H_s = 4\sqrt{m_0} \tag{2}$$

$$T_e = \frac{m_{-1}}{m_0} \tag{3}$$

$$\epsilon_0 = \sqrt{\frac{m_0 m_{-2}}{m_{-1}^2} - 1} \tag{4}$$

in which the nth spectral moment is defined as

$$m_n = \sum_i f_i^n S_i \Delta f_i \tag{5}$$

The spectral width measures the spread of energy over frequency and its value would increase disproportionately for multi-modal spectra. The directionally resolved wave power can be calculated by

$$J_\theta = \sum_{ij} \rho g C_{gi} S_{ij} \Delta f_i \Delta\theta_j \cos(\theta - \theta_j)\, \delta \quad \begin{cases} \delta = 1 \text{ if } \cos(\theta - \theta_j) \geq 0 \\ \delta = 0 \text{ if } \cos(\theta - \theta_j) < 0 \end{cases} \tag{6}$$

The directionality coefficient is the ratio of the maximum directionally resolved wave power $\max(J_\theta)$ to the omnidirectional wave power J

$$d_\theta = \frac{\max(J_\theta)}{J} \tag{7}$$

which has a maximum value of one for unidirectional seas.

These wave energy parameters are supplemented by the wavelength λ computed from T_e and water depth using the linear dispersion relation. The steepness defined by H_s/λ provides a general indication of the nonlinearity in the wave field. In addition to the significant wave height, we utilize the peak period T_p and peak direction defined at the highest spectral density for wave data analysis and sea state characterization.

2.3 Error Metrics

We use a number of error metrics to measure the difference between the recorded and hindcast significant wave heights. These include the mean error, root-mean-square error, and normalized root-mean-square error defined as

$$ME = \frac{1}{n} \sum_{i=1}^{n} (y_i - x_i) \tag{7}$$

$$RMSE = \sqrt{\frac{1}{n} \sum_{i=1}^{n} (y_i - x_i)^2} \tag{8}$$

$$NRMSE = \frac{\sqrt{\frac{1}{n}\sum_{i=1}^{n}(y_i - x_i)^2}}{\max(x_i) - \min(x_i)} \quad (9)$$

where (x_i, y_i) denote the recorded and hindcast data pairs and n is the number of data pairs. It should be noted that the records are not continuous and might not exactly match the model output times. We utilized the hindcast wave height at the nearest time stamp of the record to compile the data pair sequence.

In addition, the overall agreement between the recorded data and wave hindcast can be illustrated by the correlation coefficient and scattered index as

$$COR = \frac{\sum_{i=1}^{n}(y_i - \bar{y})(x_i - \bar{x})}{\sqrt{\sum_{i=1}^{n}(y_i - \bar{y})^2}\sqrt{\sum_{i=1}^{n}(x_i - \bar{x})^2}} \quad (10)$$

$$SI = \frac{1}{\bar{x}}\sqrt{\frac{1}{n}\sum_{i=1}^{n}[(y_i - \bar{y}) - (x_i - \bar{x})]^2} \quad (11)$$

where the over bar indicates time average. The correlation coefficient has a value of one while the scattered index becomes zero for perfect match. The bias between the data pairs can be illustrated through a regression line in the scatter plot. The quantile-quantile plot compares the percentile distributions of the recorded and hindcast datasets independent of the time stamps.

The error metrics provide an overall assessment of the hindcast against the recorded data for validation and quality control. It should be noted that the observations also contain errors and are simply used as a reference for comparison.

3. Hindcast Waves and Validation

3.1 Regional Wave Climate

The WAVEWATCH III and SWAN hindcast produces 34 years of significant wave height, peak period, and direction at one hour intervals in the Hawaiʻi region as well as wave spectra at locations of the near-shore buoys and potential sites. The long-duration hindcast provides a comprehensive dataset on the Hawaiʻi wave climate, which comprises north and south swells as well as occasional subtropical storm waves superposed on the year-round northeast wind seas.

Trade wind waves are the most common in Hawaiʻi. Figure 6 shows the hindcast wind and wave fields of a typical event at 3:00 AM June 28, 2012 UTC. The 8~12 m/s steady wind flow from the northeast generates 2.0~2.8 m significant wave height with 7.1~8.1 s peak period around the Hawaiian Islands. The Hawaiian Islands play a dominant role in the local wind pattern characterized by deceleration of the approaching flow, speed-up in the channels, and leeward wake formation. Heightened wave activities are evident in channels between the islands due to local acceleration of the winds. Shadows of the dominant wind waves develop leeward of the islands and expose a small-amplitude south swell in the background. Figure 7 provides a better illustration of the south swell when the wind waves are weaker at midnight August 30, 2007 UTC. This is a relatively strong south swell with a significant wave height close to 2 m and a peak period of 16 s. The swell energy propagates through the island chain into the incoming wind waves.

The episodic northwest swell is much more energetic. Figure 8 shows a major swell with 4.6 m significant wave height and 16.8 s peak period at 9 AM March 16, 2010 UTC. The swell dominates the seas generated by 6~12 m/s winds from the east. Background wind waves are evident in the shadows of the swell especially along the ʻAlenuihāhā Channel between Maui and Hawaiʻi Island .

The subtropical region around Hawaiʻi experiences on average two local (Kona) storms per winter (Caruso and Businger, 2006). The centers of these events are typically located north of the Hawaiian Islands. These slow-moving systems can bring strong winds and large waves from different directions to Hawaiʻi over a period of several days. Figure 9 shows the wind and wave fields from a selected Kona storm. The cyclonic system covers most of the Central North Pacific with a strong southwesterly flow of 12~15 m/s toward the Hawaiian Island chain at 9:00 AM January 11, 1980 UTC. The winds accelerate in the ʻAlenuihāhā Channel. A swell of 5~7 m significant wave height with 11~12.5 s peak period approaches the west. Locally generated wind waves from the southwest are evident in the channel and leeward of Hawaiʻi Island.

The selected events have demonstrated the multi-modal sea states and the need to model the basin-wide processes to reproduce the wave conditions in Hawaiʻi. The modification of the wind flow by the Hawaiian Islands has profound effects on the local wave conditions especially in the channels. In addition, island sheltering is an important factor defining the wave field along the island chain.

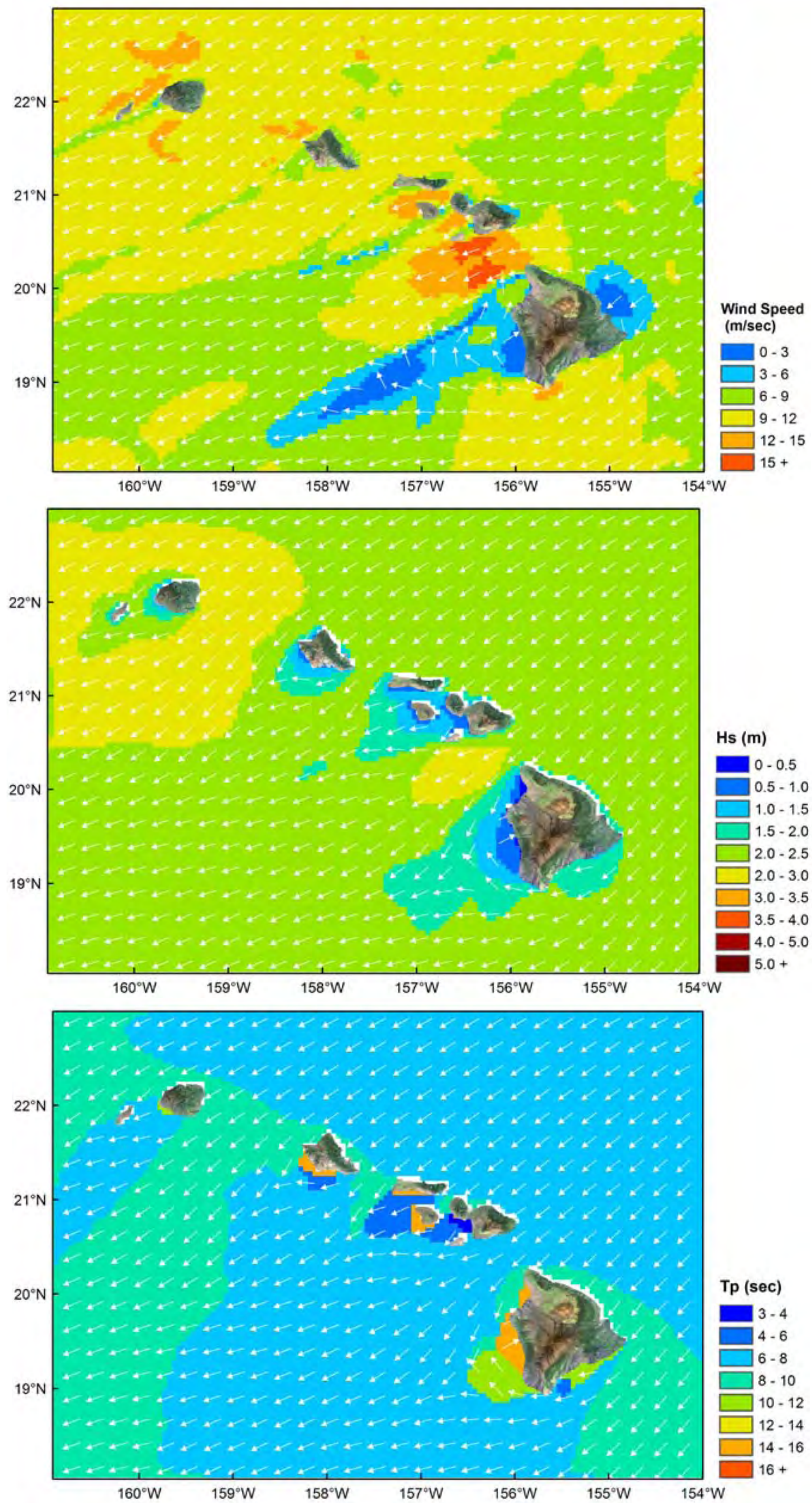

Figure 6- Wind velocity, significant wave height, and peak period during a trade wind event at 3:00 AM June 28, 2012UTC.

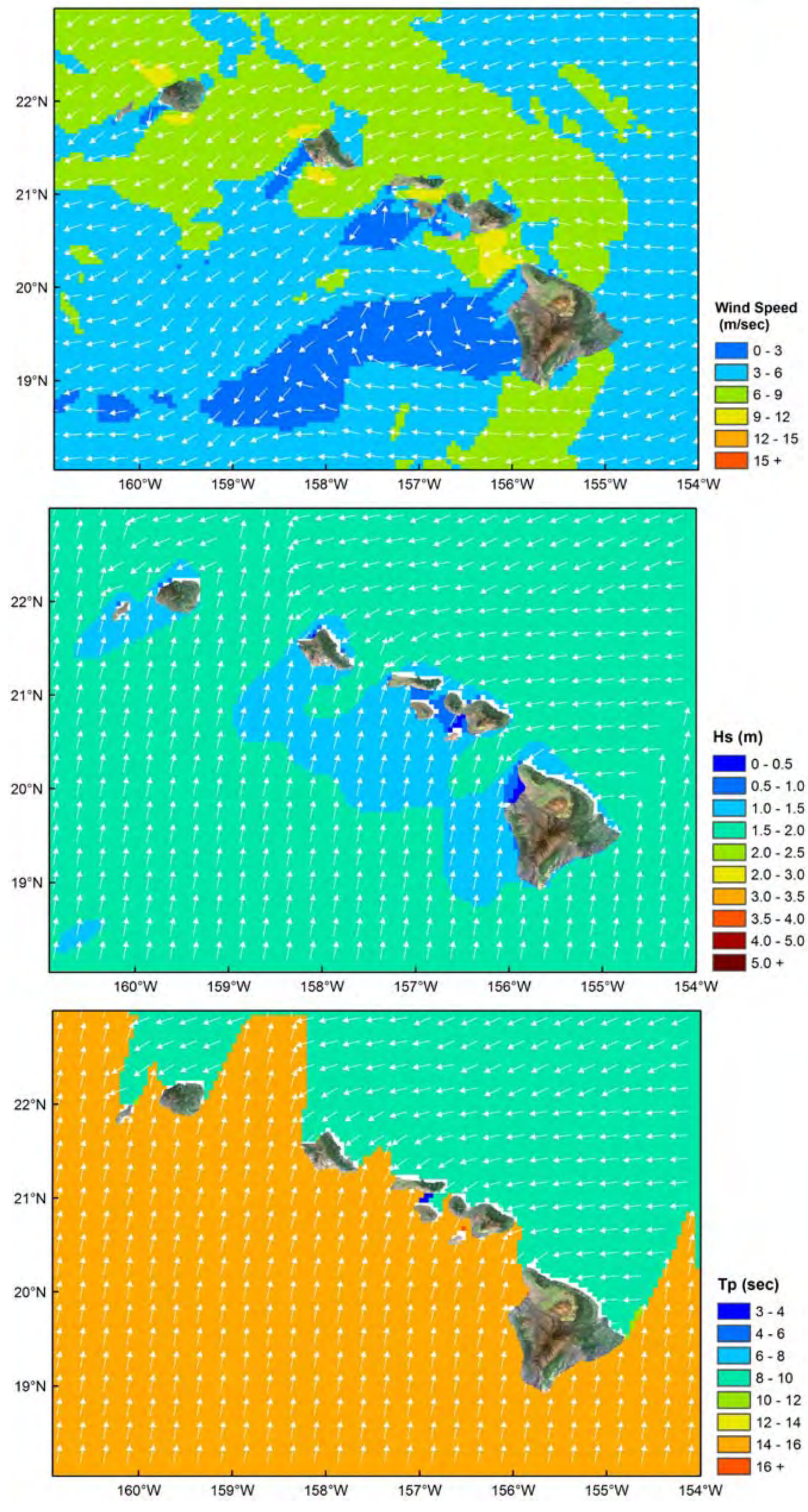

Figure 7- Wind velocity, significant wave height and peak period during a south swell event at 0:00 AM August 30, 2007 UTC.

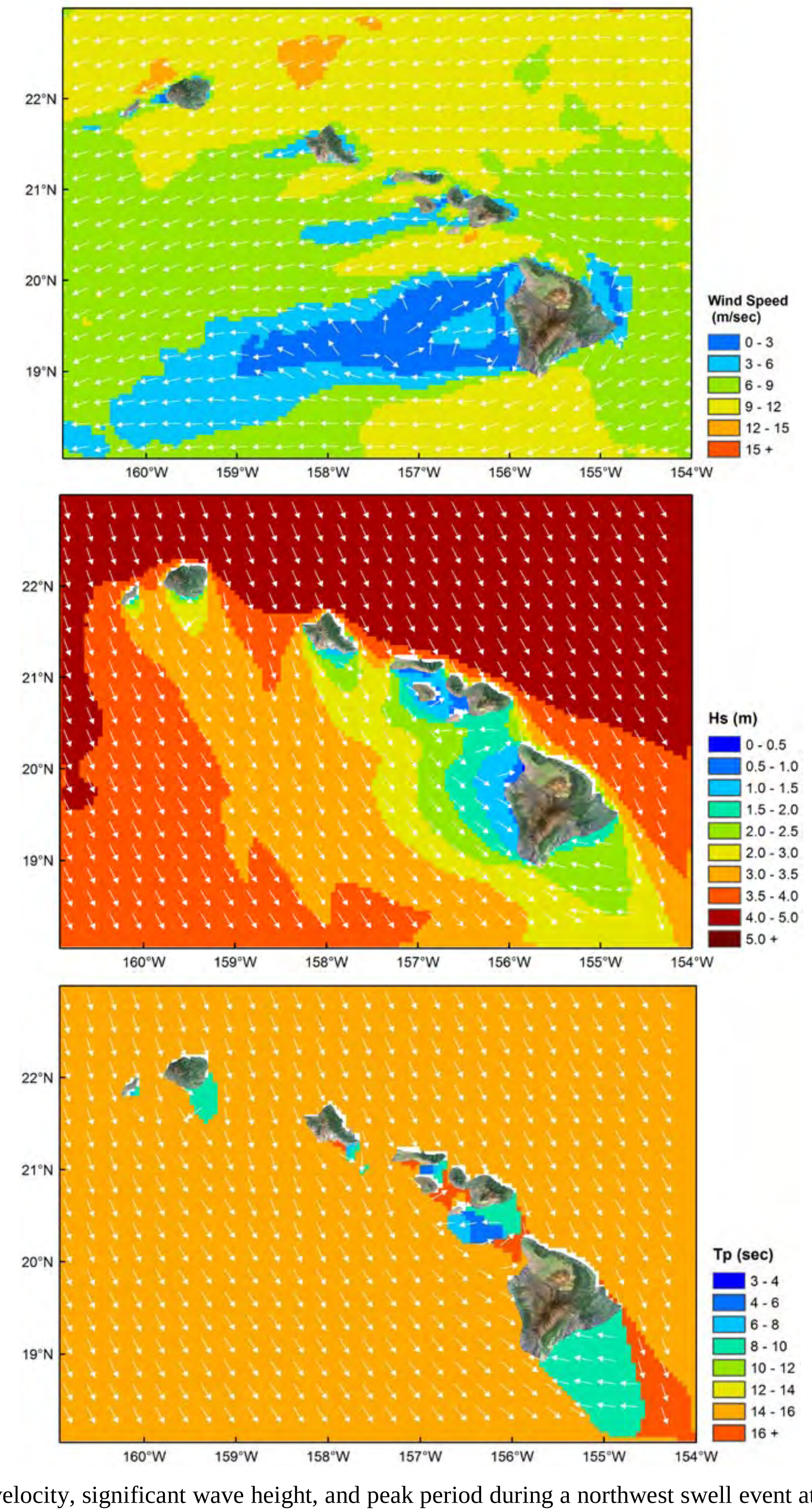

Figure 8- Wind velocity, significant wave height, and peak period during a northwest swell event at 9:00 AM March 16, 2010 UTC.

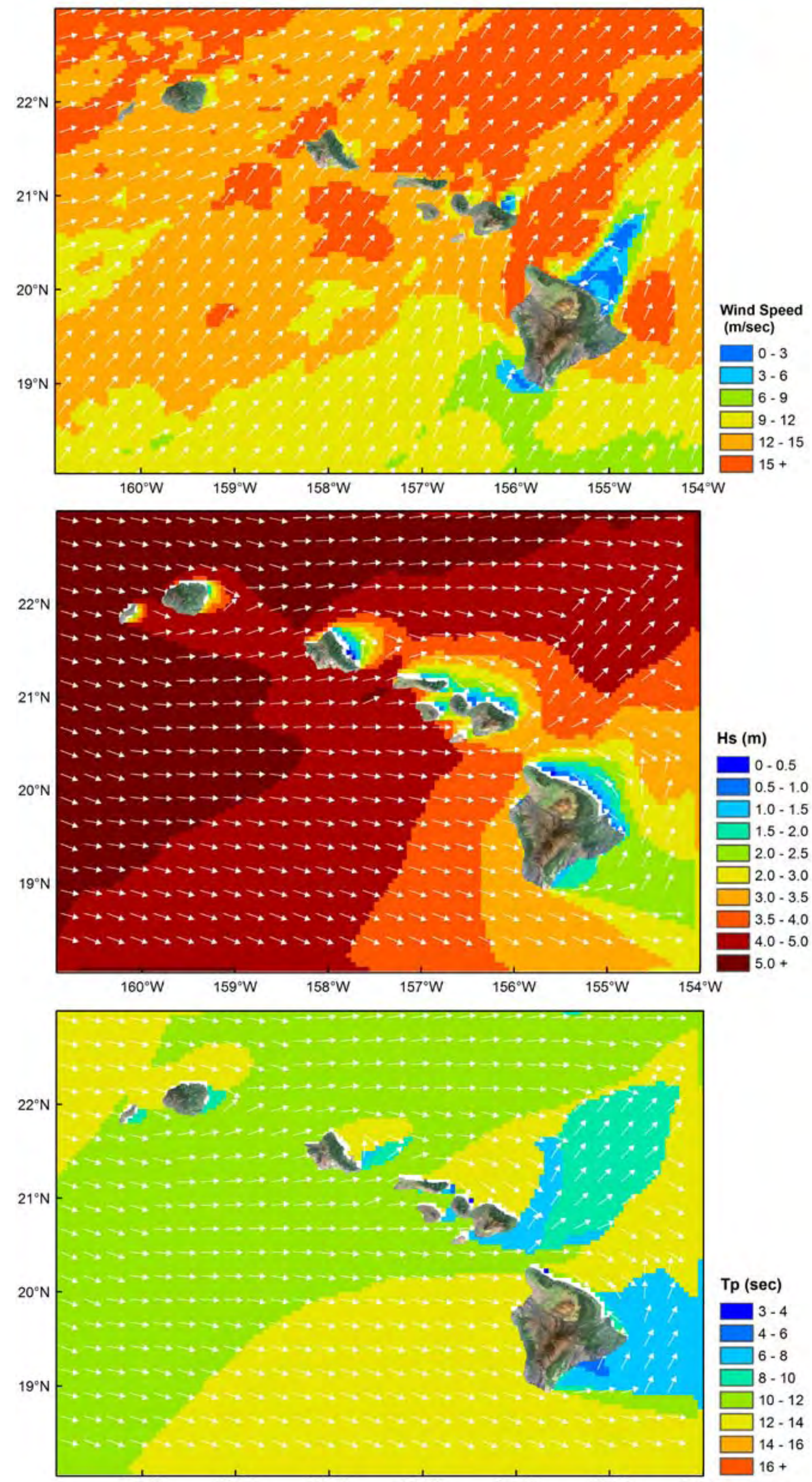

Figure 9- Wind velocity, significant wave height, and peak period during a Kona storm at 9:00 AM January 11, 1980UTC.

3.2 Validation with Regional Buoys

The 29 years of records from buoys #51001, #51003, #51002, #51004 located northwest, southwest, south, and southeast of the island chain as well as the recent 5 years of records from buoys #51100 and #51101 to the northeast and northwest provide a comprehensive dataset to validate the WAVEWATCH III hindcast (see Figure 1 for buoy locations). Figures 10 to 23 compare the time series of significant wave height, peak period, and available peak direction from the hindcast and the recorded data. The hindcast accurately reproduces the seasonal patterns as well as the individual events over the entire period albeit with several gaps in the records when the buoys were not in operation. The data shows a general decrease of the wave height from north to south due to sheltering of the north swells by the island chain. The highly seasonal wave conditions show large northwest swells in the winter and moderate wind waves and south swell throughout the year. The peak direction at #51001 after 2005 and #51004, #51100 and #51101 after 2009 provides a better illustration of the dominating components. Although south swells occur year round, their low energy levels are masked by the more energetic north swells or wind waves and usually have little influence on the peak period or direction.

Figures 24-29 provides the scatter plots of the recorded and hindcast significant wave heights at buoys #51001, #51003, #51002, #51004, #51100 and #51101. Since the hindcast predicts the wave height reasonably well, the apparent large scatter might be due to offset of the swell arrival times. The timing offsets should be similar across the Hawaiian Islands and consequently lead to the small range of scattered indices from 0.16 to 0.17 at five of the six buoys. Nevertheless, 90% of the hindcast wave heights are within ±0.58 m of the measurements, the RMSEs are less than 0.21 m, and the NRMSE is less than 3.1% among the six buoys. The small mean errors of 0.06 to 0.28 m and the high correlation coefficients of 0.85 to 0.91 indicate minimal biases and good overall agreement between the two datasets.

The quantile-quantile (Q-Q) plots in Figures 30-35 eliminate the timing errors and compare directly the percentile distributions of the hindcast and recorded wave heights. Hindcast wave heights up to 3 m are generally within ±5% of the recorded values and account for 80 to 89% of the occurrence at the buoys. The model produces increasing overestimation of the wave heights above 3 m likely associated with the north swell events. An exception occurs at buoy #51004 to the southeast of Hawai‘i Island in the shadow of the northwest swells probably due to the lack of diffraction in WAVEWATCH III. The underestimation of the extreme record of 12 m at buoy #51001 is due to the resolution of the parameterized atmospheric processes and the global computational grid (Stopa and Cheung, 2014). Both the hindcast and recorded wave heights show a decreasing trend of the large events from west to east and from north to south due to sheltering by the islands.

A convenient way to illustrate the multi-modal sea states off Hawai‘i is through comparison of “rose” plots at the four buoys with directional measurements. Figures 36-37, 38-39, 40-41 and 42-43 compare the rose plots of the recorded and hindcast significant wave heights and peak periods at buoy # 51001 from 2005 to 2009, buoy #51004 from 2012 to 2013, and buoys #51100 and #51101 from 2009 to 2013. The peak period and direction associated with the spectral density correspond to the dominant component and might not fully characterize a multi-modal sea state. The spectral peak might also be influenced by the model parameterization and resolution. Nevertheless, parameters estimated with WAVEWATCH III are representative of the actual measurements under open ocean conditions. The results illustrate the dominant north swells and east wind waves as well as their variation from west to east along the island chain. The year-round south swells are masked by the dominant components most of the time. The occasional wind waves and short-period swells from north, northwest, and west are likely associated with passing cold fronts or Kona storms around the islands. Kona storms can also generate similar wave activities from north to east that cannot be easily differentiated from the trade wind waves.

3.3 Validation with Nearshore Buoys

There are eight near-shore buoys listed in Table 1 and their records allow validation of the hindcast wave conditions from SWAN for each island or island group. Figures 44 to 47 compare the hindcast and recorded significant wave heights, peak periods, and directions and Figures 48 to 51 show the scattered plots of the significant wave heights at the Waimea, Barbers Point, Mokapu, and WETS buoys around Oahu. The model captures the individual swell and wind wave events as well as the seasonal patterns in the time series comparison. At the Waimea buoy, the recorded significant wave height and peak period of the north swell reach 7 m and 22 s in winter. Northeast wind waves of typical 1 to 2 m height and 5 to 12 s period dominate during the summer. The corresponding scattered plot shows small mean and root-mean-square errors of 0.18 and 0.13 m of the computed significant wave height. The two datasets have a high correlation coefficient of 0.92, but the largest scatter index of 0.19 among the buoys. The nearly parallel linear regression and best match lines illustrate the relationship between hindcast model estimates and buoy measurements for both the wind wave and swell events. Despite the large spread, 90% of the hindcast estimates are within ±0.45 m of the regressed line.

There is a decreasing trend of the wave height from north to south. Compared to the exposed Waimea buoy, the Barbers Point buoy recorded lower significant wave heights of 3 to 4 m from northwest swells due to sheltering by Kauai and Oahu. The hindcast model resolves the peak period and direction of the swells reasonably well, but could not fully capture the short-period wind waves wrapped around Diamond Head from southeast and some of the south swells. However, the scatter plot shows good agreement of the hindcast and recorded significant wave heights for the smaller events, but underestimate the more energetic northwest swells likely due to the low spatial resolution, which cannot fully resolve the steep seafloor near the buoy. This results in a small slope of 0.65 for the regression line and a low correlation coefficient of 0.78 despite the small mean error of -0.06 m.

The proximity of the Mokapu and WETS buoys results in similar records of the wave conditions. The former also recorded occasional southeast wind waves due to its more open location. The hindcast model reproduces the persistent east wind waves reasonably well, but slightly underestimates the significant wave height of the intermittent north swells, which reach of up to 4 to 6 m in the record. The corresponding scatter plots show slopes of 0.89 and 0.92 for the regression lines and 90% of the hindcast wave heights are within ±0.34 and 0.31 m of the records at Mokapu and WETS. The correlation coefficient of 0.94 at WETS is the highest among the four buoys around Oahu.

The Q-Q plots in Figures 52-55 sort the computed and recorded significant wave heights for comparison of their percentile distributions at the buoys around Oahu. The difference between hindcast and recorded values are within ±0.5 m for wave height up to 6 m at Waimea Buoy, 3.5 m at Barbers Point, 6.2 m at Mokapu, and 4.0 m at WETS. The hindcast model yields slight overestimates of wave height at Waimea, but shows underestimates at Barbers Point, Mokapu, and WETS for wave heights above 1.3, 4.5, and 3.5 m corresponding to the 60.0, 99.9, and 99.2 percentiles respectively. The underestimation at Barbers Point is likely due to the low resolution of the steep seafloor, where the buoy is located. The lower predictions of the large events at Mokapu and WETS might be explained by the lack of diffraction in SWAN for the energetic northwest swells.

The records from the buoys off Barking Sands, north Kauai; Pauwela and Kaumalapau, north and west Maui; and Hilo, east Hawaiʻi Island provide additional validation of the nearshore wave conditions from SWAN. Figures 56-59 compare the time series of hindcast and recorded wave parameters for these buoys. The buoy at Barking Sand recorded large winter swell events with significant wave heights up to 7 m due to its exposed location to the northwest. The records at Pauwela and Hilo, which are sheltered from the more energetic northwest swells, show less distinct seasonal variations. Kaumalapau only recorded south swells and small amplitude northwest swells that wrapped around Kauai from the west. The large recorded wave height of 4.3 m on Dec 05, 2007 coincides with a Kona storm (http://earthobservatory.nasa.gov/ NaturalHazards/view.php?id=19423).

With reference to the scatter plots in figures 60-63, the mean errors of the hindcast significant wave height are 0.37, 0.2, -0.12, and -0.006 m with 90% of data within ±0.67, ±0.48, ±0.89, ±0.37 m of the measured data at Barking Sands, Pauwela, Kaumalapau, and Hilo respectively. The slopes of the regression lines are close to one at more open locations such as Barking Sands and Pauwela, while the smaller slopes at Kaumalapau and Hilo indicates underestimations of the large northwest swell events due to the lack of diffraction in SWAN. The large scatter and low correlation at Kaumalapau is likely due to its sheltered location from the north swells and trade wind waves. Figures 64-67 shows the Q-Q plots to compare the distributions of the hindcast and recorded datasets. The hindcast at Barking Sands, which is open to the north swells and northeast wind waves, overestimates the significant wave height as in the case of the offshore buoys open to those events. Pauwela has similar exposure and shows the same patterns as Waimea that slightly overestimates the wave height before tapering off at the extreme events. Kaumalapu located to the southwest of Lanai show overall underestimation of the hindcast wave height as at Barbers Point in a similar environment. Hilo is similar to Mokapu, which is shielded to some extent from the northwest swells. This results in underestimation of large events with wave height above 3.0 m.

Figures 68 to 81 compare the rose plots of the significant wave height and peak period at the near-shore buoys. The comparisons show overall agreement of the directional distribution and occurrences of the dominating wave components on the respective sides of the island. Located at 200 m water depth north of Oahu, the Waimea buoy is exposed to northeast wind waves and north swells. The Barbers Point and Kaumalapau buoys, located off the southwest shore of the respective islands, are open to swells from the northwest and south, and former also experiences some refracted wind waves from the east. Mokapu and WETS off east Oahu and Pauwela off north Maui, which are sheltered from the south swells and to a certain extent the northwest swells, mainly comprise wind waves from the northeast and swells from the north. The Hilo buoy off the northeast-facing shore of Hawaiʻi Island experiences the northwest swells and east wind waves. The hindcast model, in general, captures the trend and reproduces the majority of the measurements. The results have better agreement with the large events recorded at locations exposed to the northwest swells, but shows underestimation at locations sheltered by headlands and islands.

A convenient approach to illustrate the sea state is through the wave spectrum. Figures 82 and 83 provide the recorded and hindcast 2D and 1D spectra from WETS at 4:00 PM May 5, 2013 to illustrate typical trade wind waves in the summer months. The recorded 2D spectrum is from an image downloaded from http://cdip.ucsd.edu/?ximg=search&xsearch=198&xsearch_type=Station_ID. Because of different spectral resolution, the hindcast spectrum has a different color scale to highlight the detailed features for a qualitative comparison. Despite the different values of the peak energy density, the recorded and hindcast estimates provide good agreement of the peak direction and period and essentially the same significant wave heights of 1.19 and 1.17 m respectively. North swells occur along with trade wind waves during the winter months. Figures 84 and 85 compare the recorded and computed 2D and 1D spectra at 1:00 AM January 4, 2013 for illustration. The spectra have a distinct peak from the north-northwest as well as broad-banded signals of the wind waves from the east-northeast. The agreement between the recorded and computed spectra is also maintained for a multi-modal sea state.

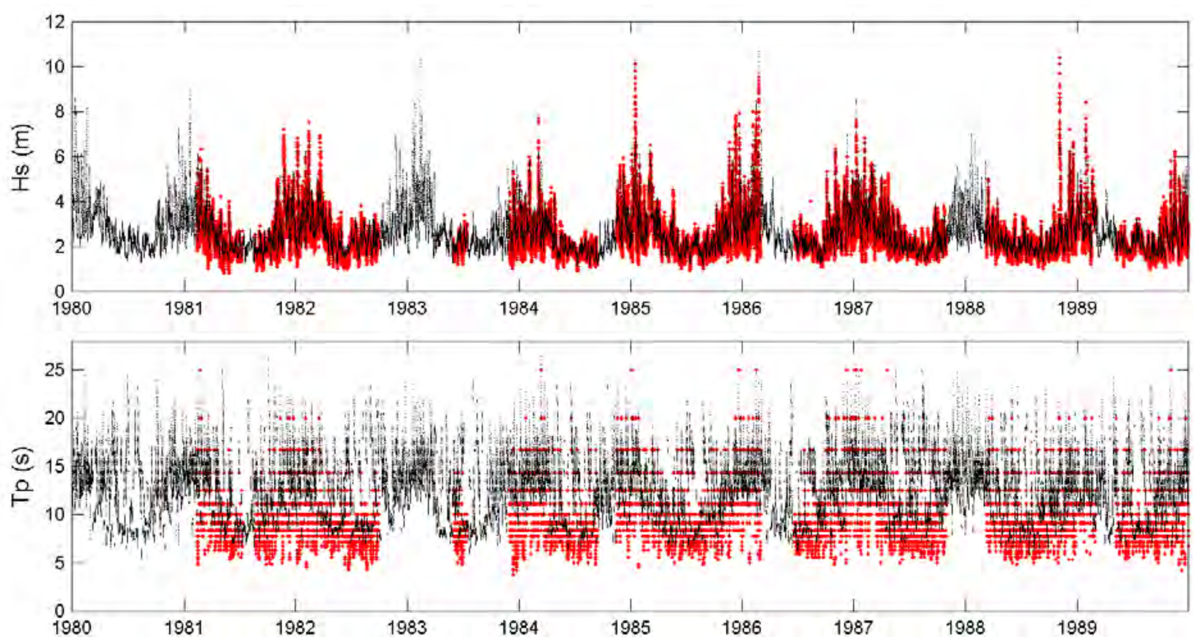

Figure 10- Comparison of recorded (red) and hindcast (black) wave parameters at buoy #51001 from 1980 to 1989.

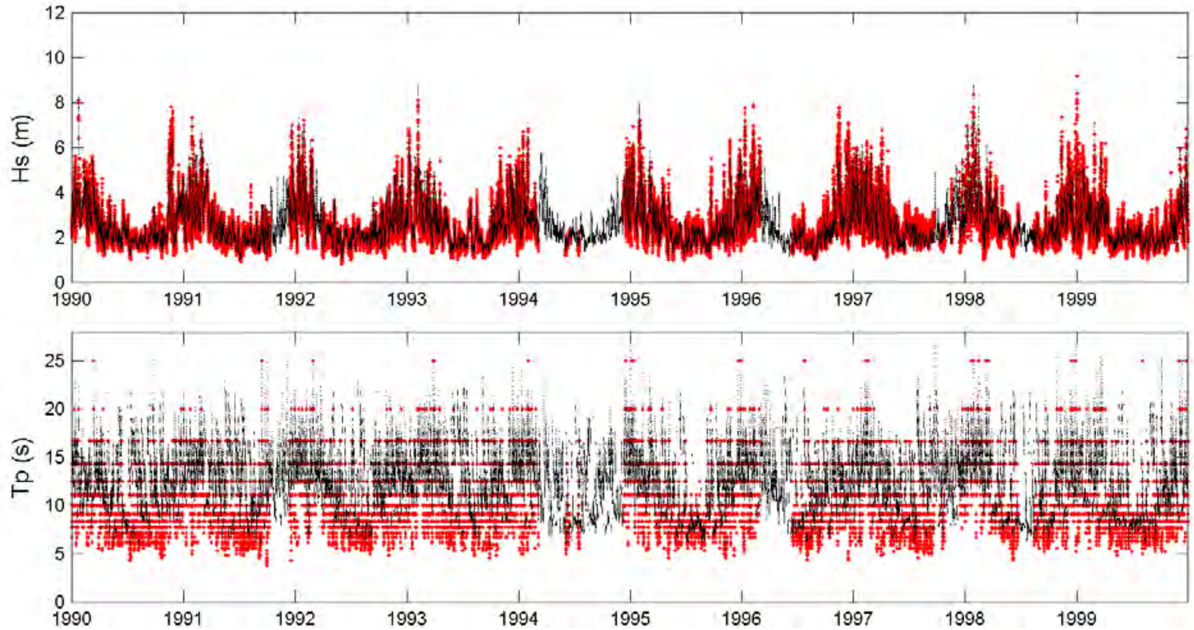

Figure 11- Comparison of recorded (red) and hindcast (black) wave parameters at buoy #51001 from 1990 to 1999.

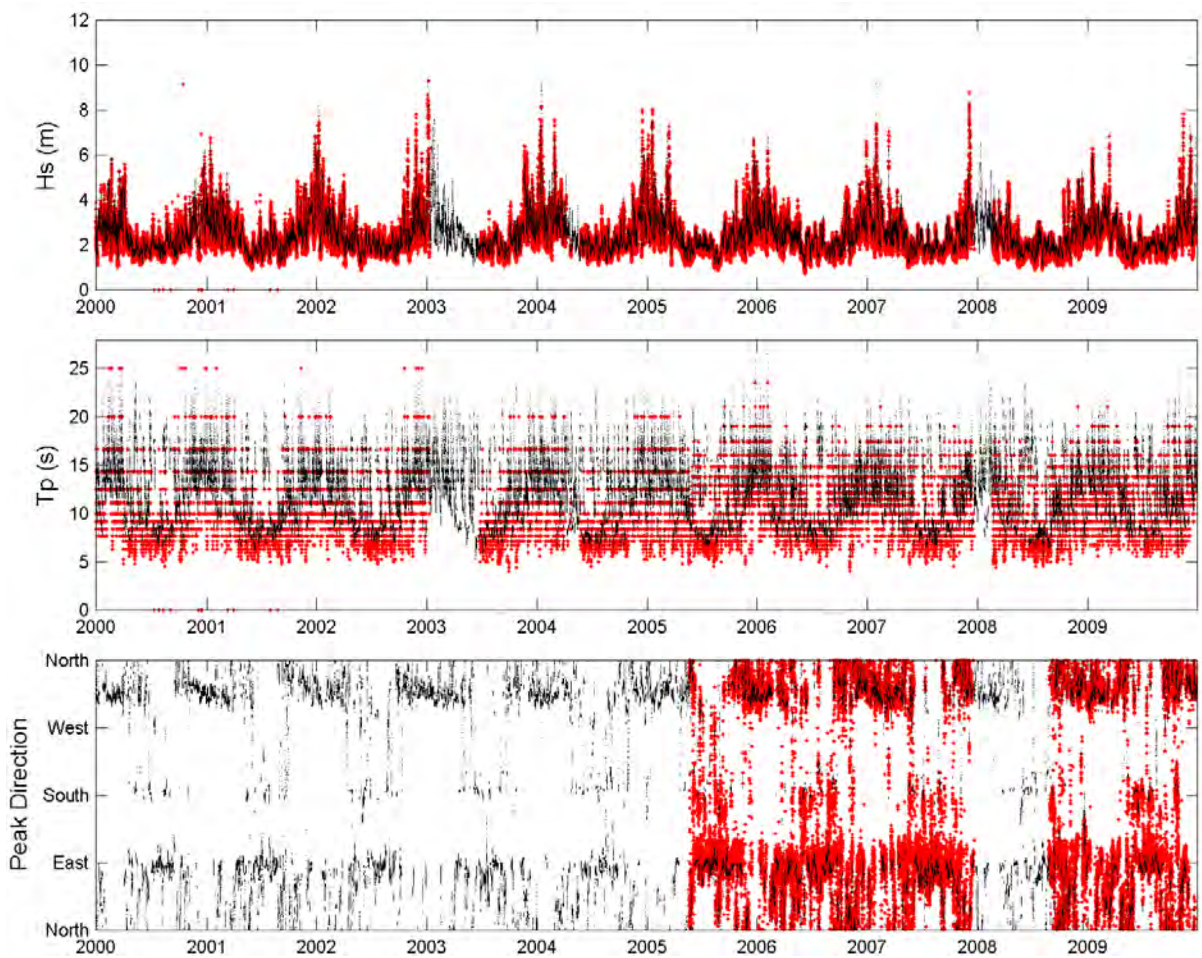

Figure 12- Comparison of recorded (red) and hindcast (black) wave parameters at buoy #51001 from 2000 to 2009.

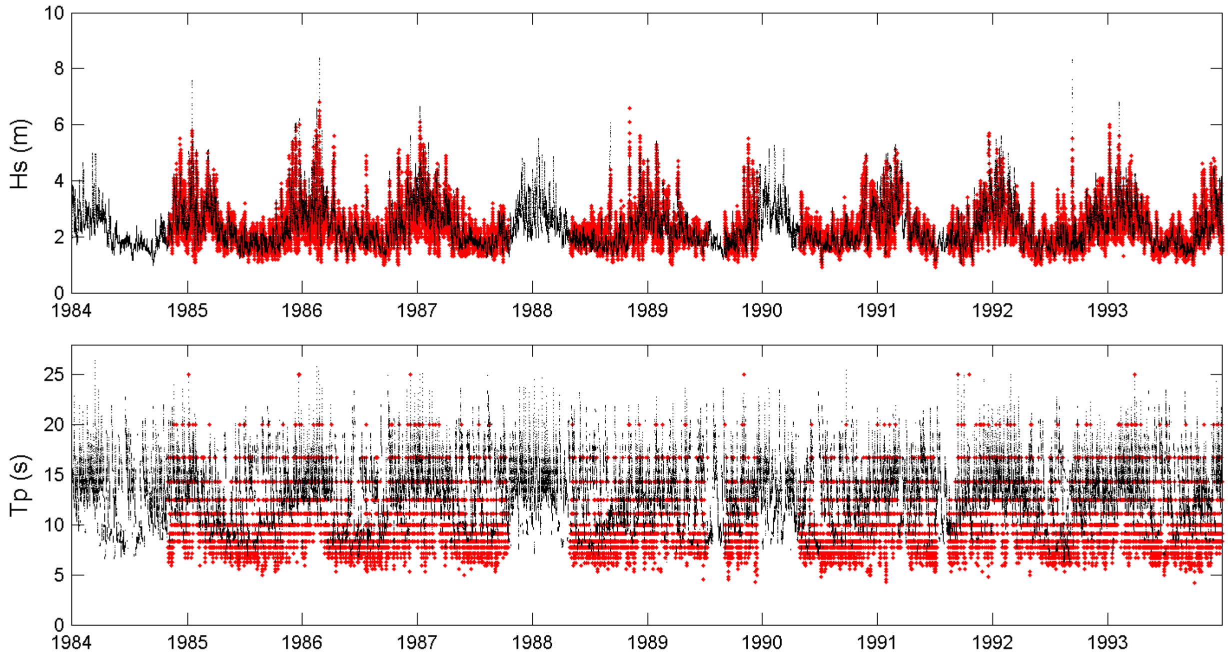

Figure 13- Comparison of recorded (red) and hindcast (black) wave parameters at buoy #51003 from 1984 to 1993.

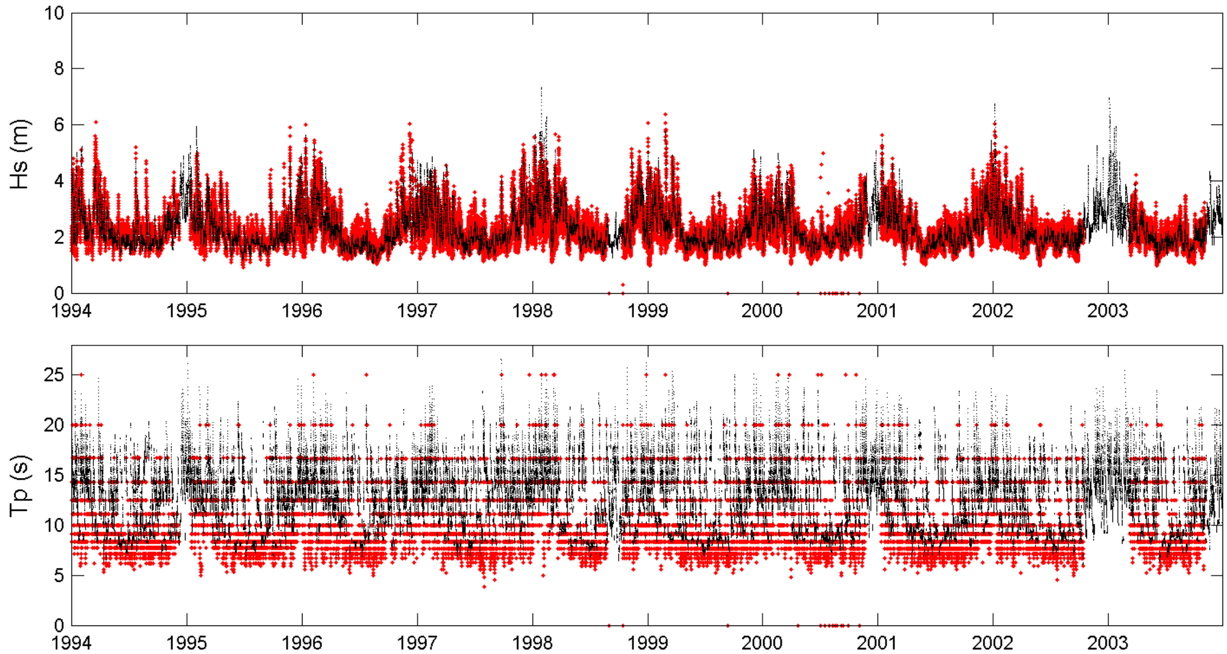

Figure 14- Comparison of recorded (red) and hindcast (black) wave parameters at buoy #51003 from 1994 to 2003.

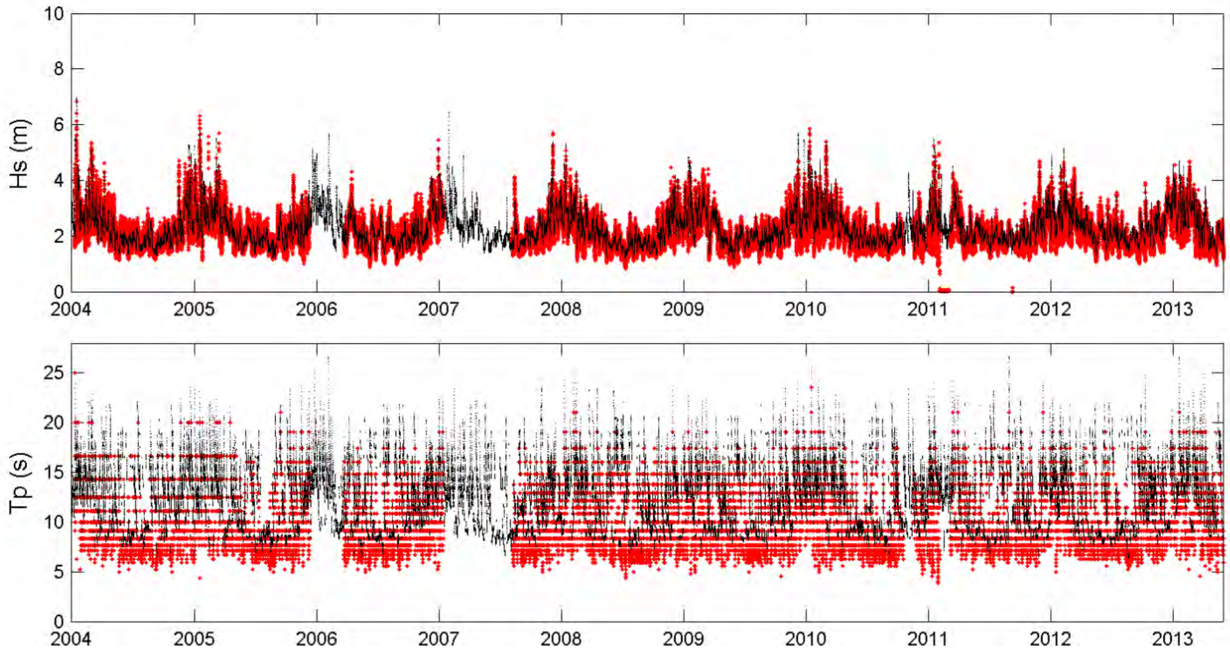

Figure 15- Comparison of recorded (red) and hindcast (black) wave parameters at buoy #51003 from 2004 to 2013.

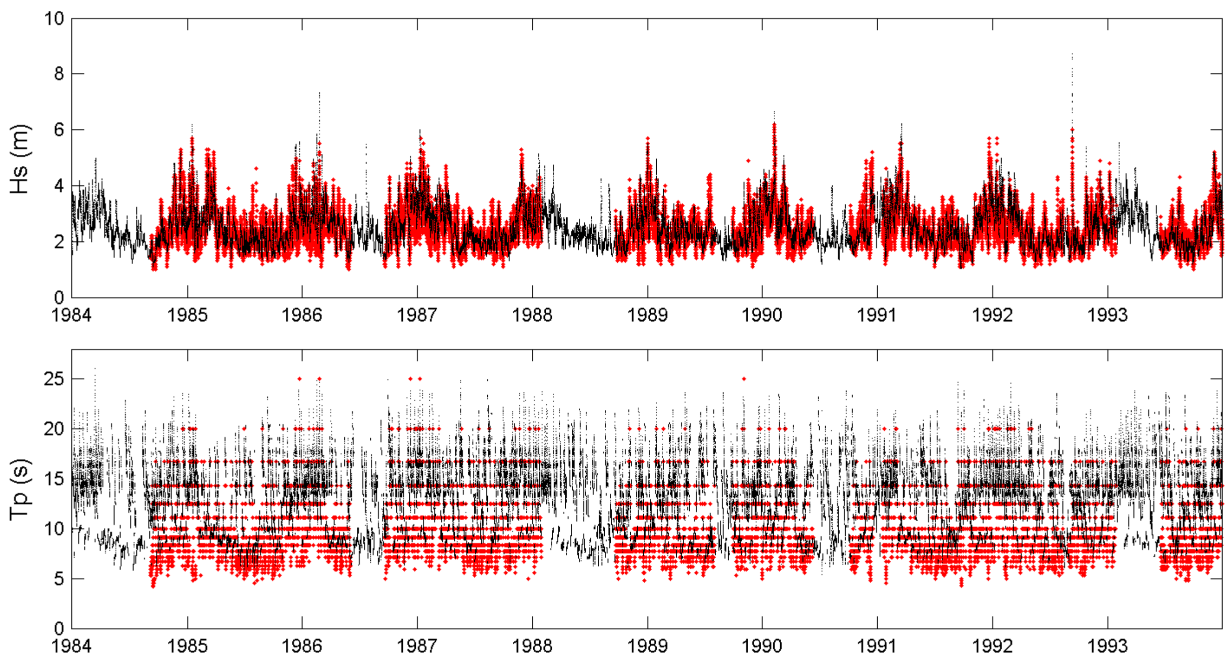

Figure 16- Comparison of recorded (red) and hindcast (black) wave parameters at buoy #51002 from 1984 to 1993.

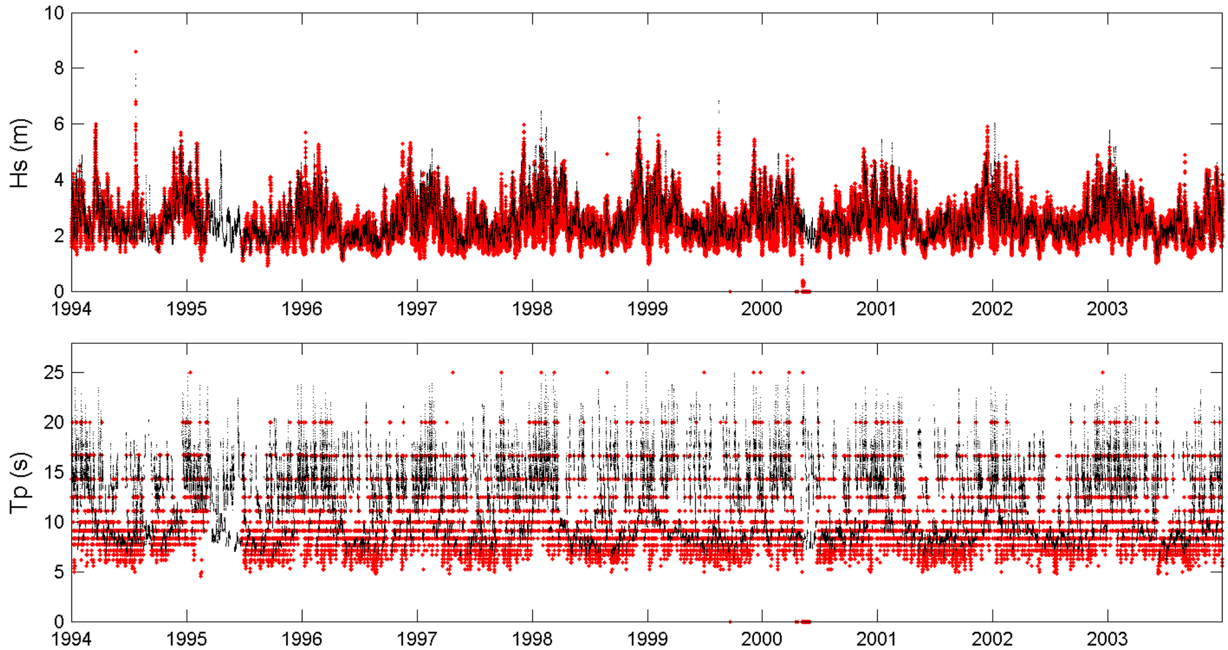

Figure 17- Comparison of recorded (red) and hindcast (black) wave parameters at buoy #51002 from 1994 to 2003.

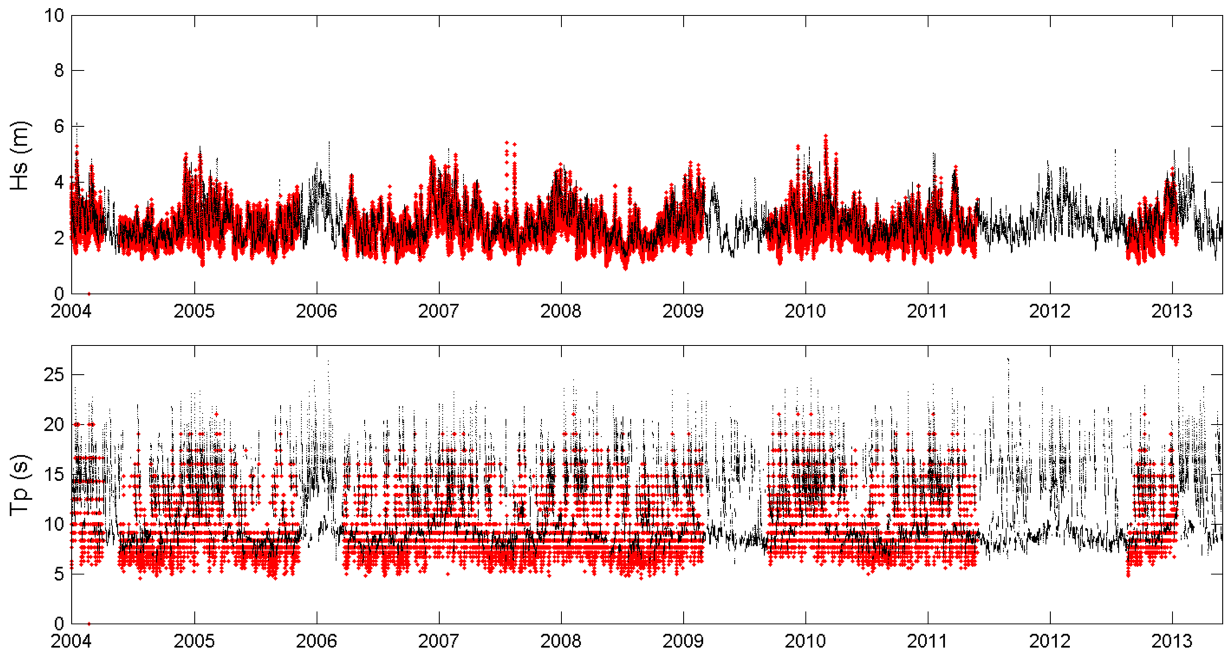

Figure 18- Comparison of recorded (red) and hindcast (black) wave parameters at buoy #51002 from 2004 to 2013.

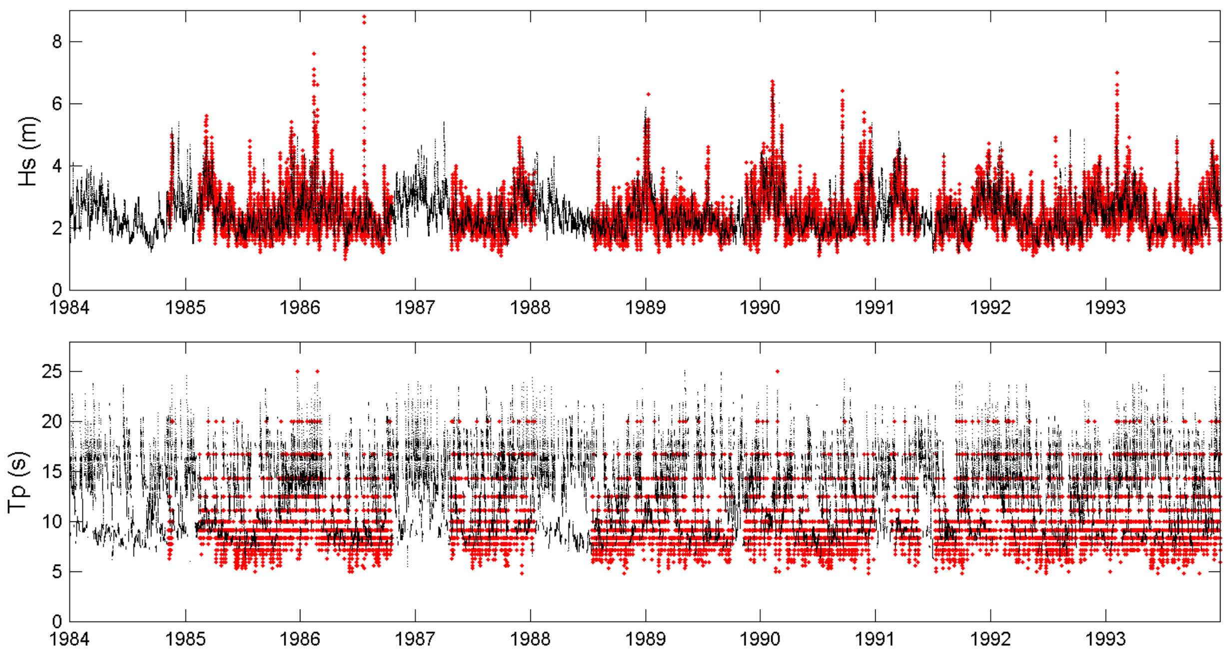

Figure 19- Comparison of recorded (red) and hindcast (black) wave parameters at buoy #51004 from 1984 to 1993.

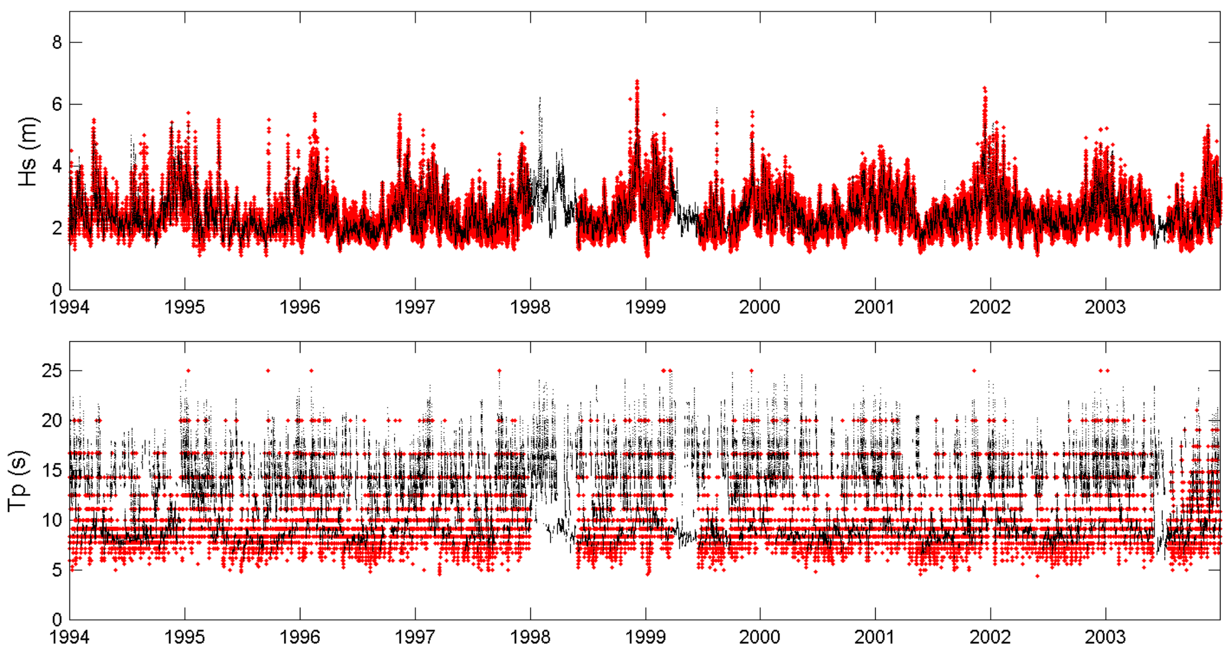

Figure 20- Comparison of recorded (red) and hindcast (black) wave parameters at buoy #51004 from 1994 to 2003.

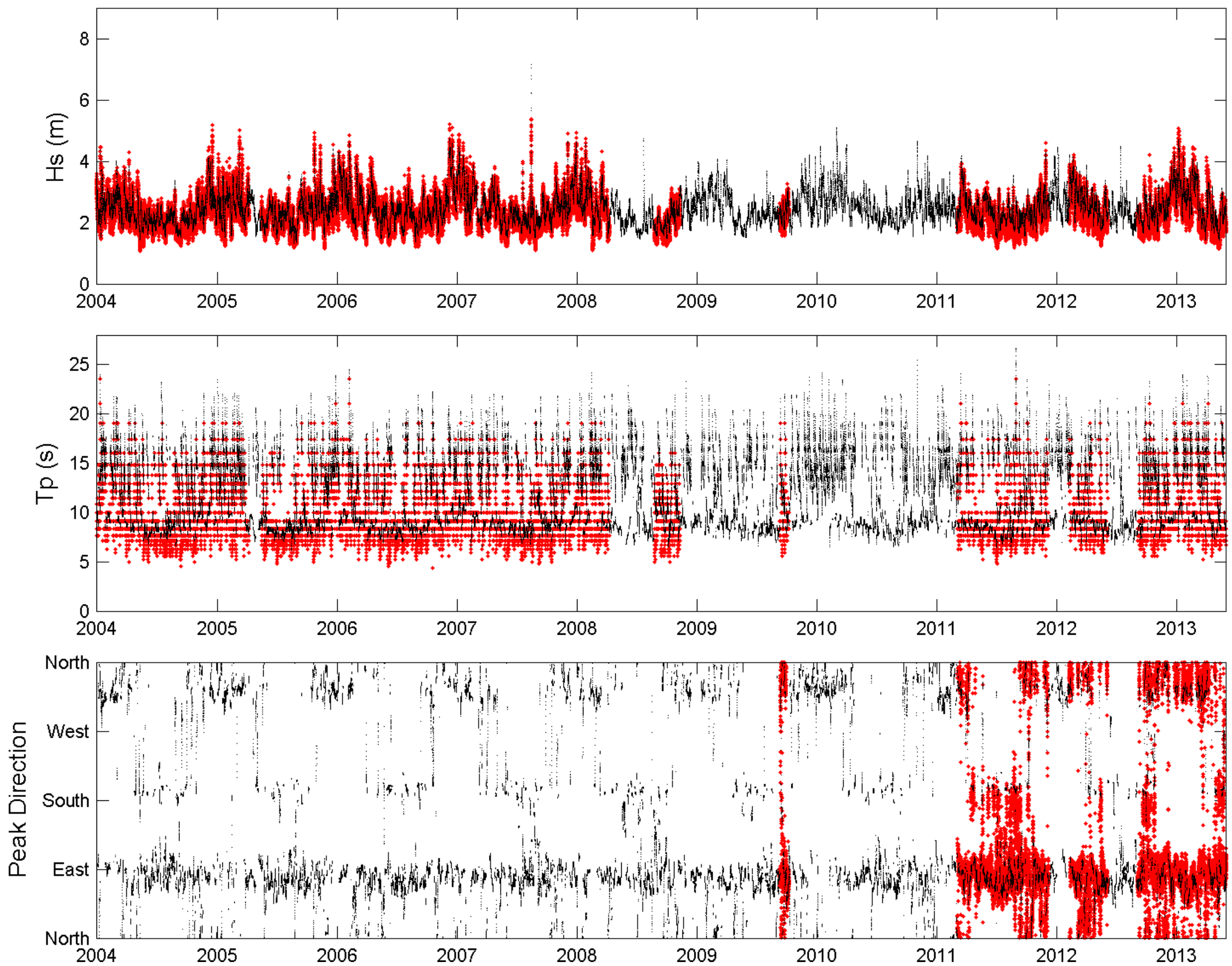

Figure 21- Comparison of recorded (red) and hindcast (black) wave parameters at buoy #51004 from 2004 to 2013.

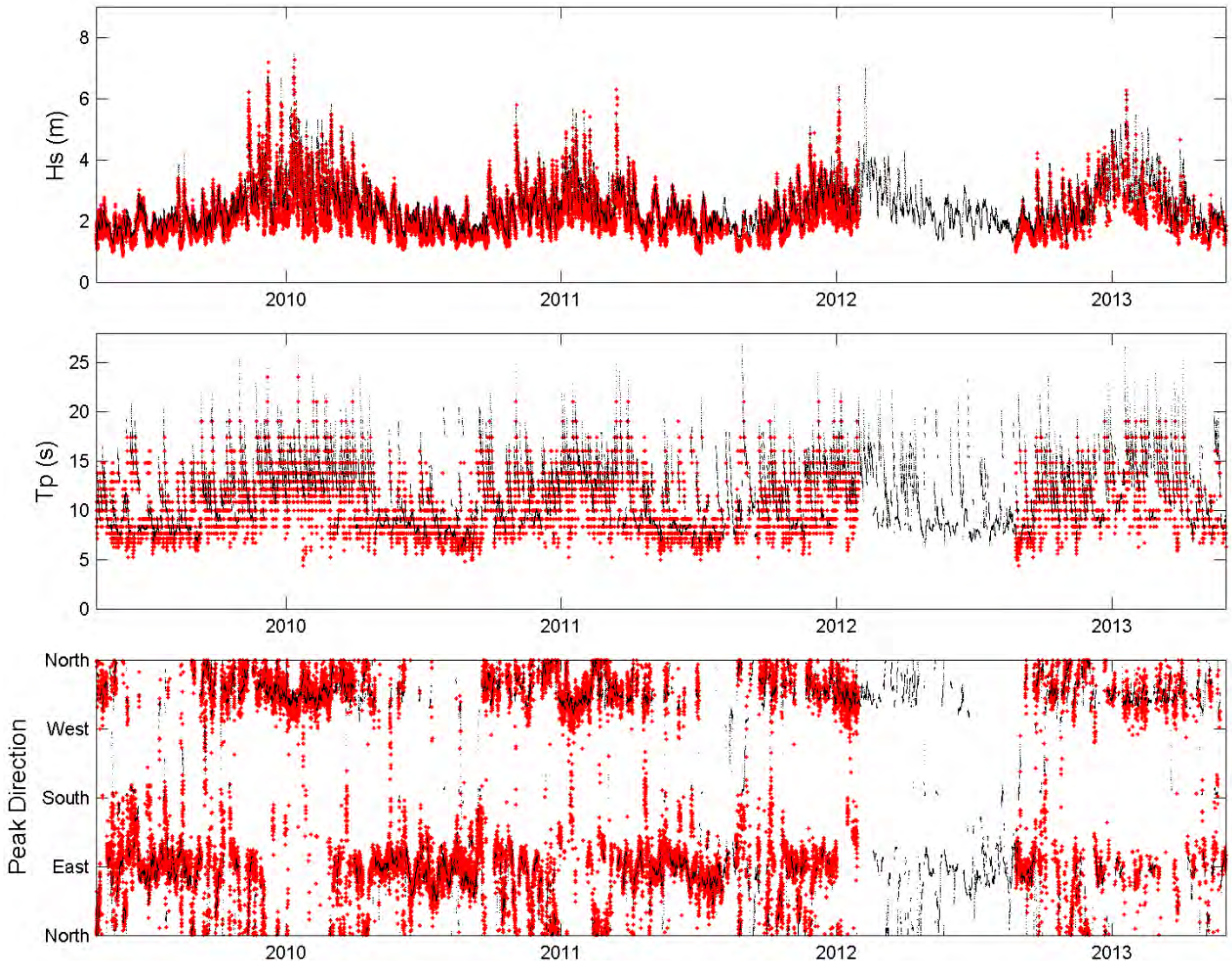

Figure 22- Comparison of recorded (red) and hindcast (black) wave parameters at buoy #51100 from 2009 to 2013.

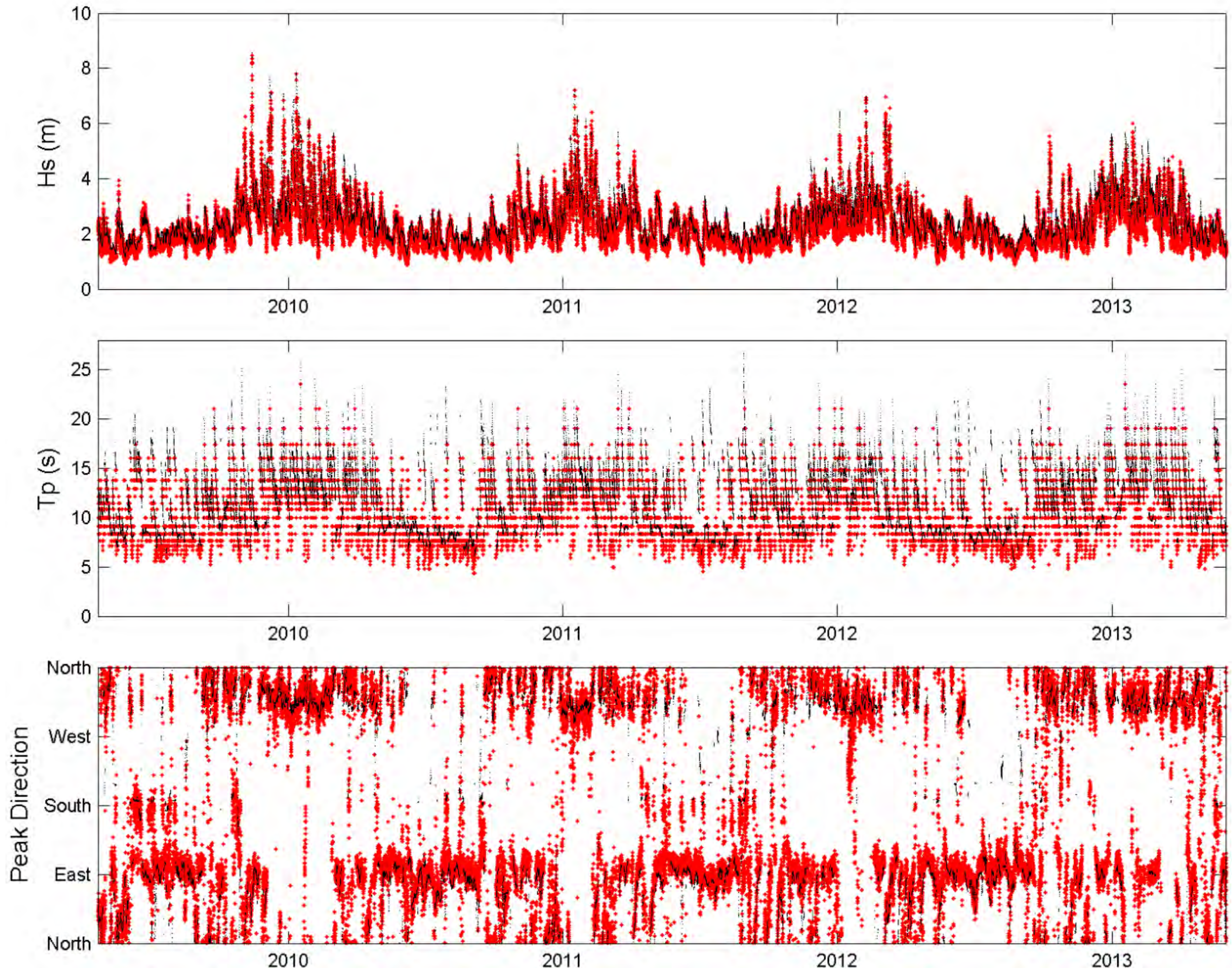

Figure 23- Comparison of recorded (red) and hindcast (black) wave parameters at buoy #51101 from 2009 to 2013.

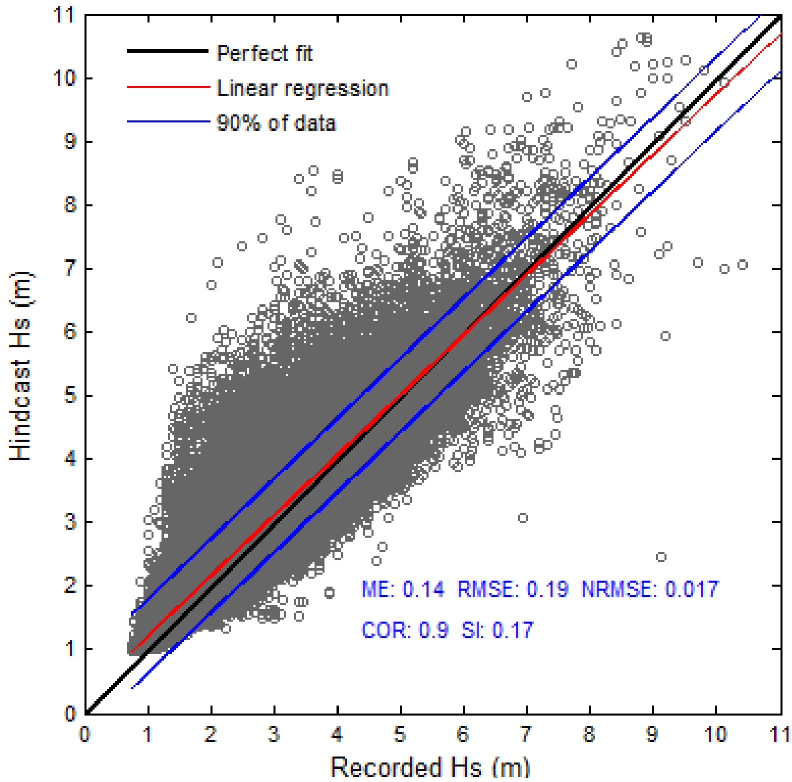

Figure 24- Scatter plot of recorded and hindcast significant wave heights at buoy #51001.

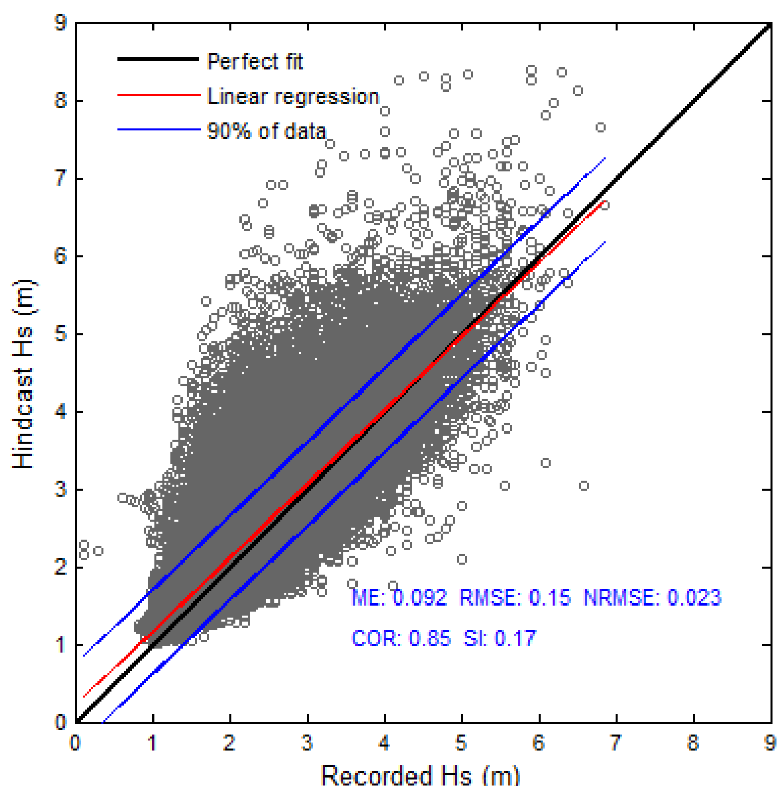

Figure 25- Scatter plot of recorded and hindcast significant wave heights at buoy #51003.

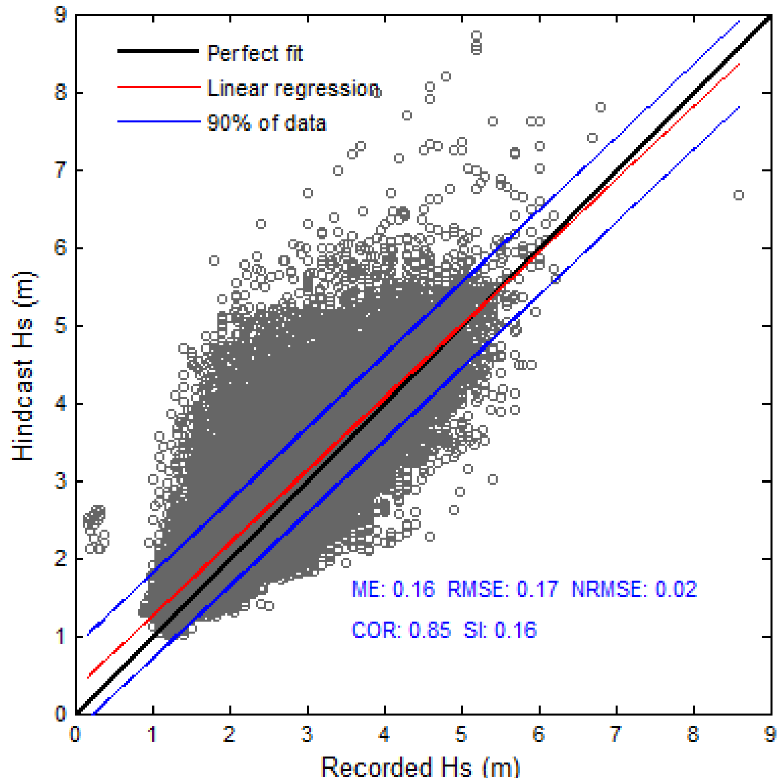

Figure 26- Scatter plot of recorded and hindcast significant wave heights at buoy #51002.

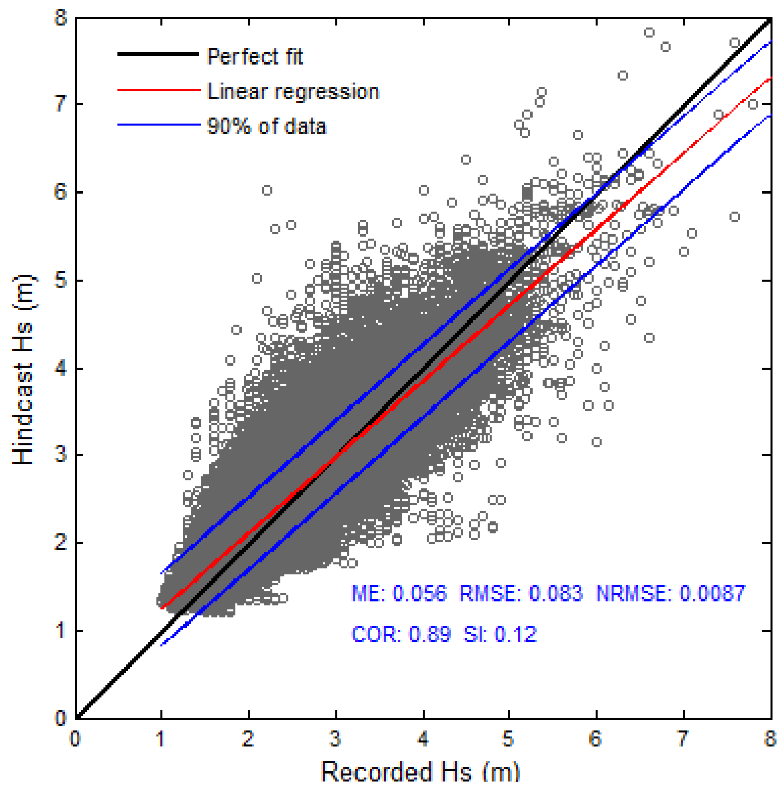

Figure 27- Scatter plot of recorded and hindcast significant wave heights at buoy #51004.

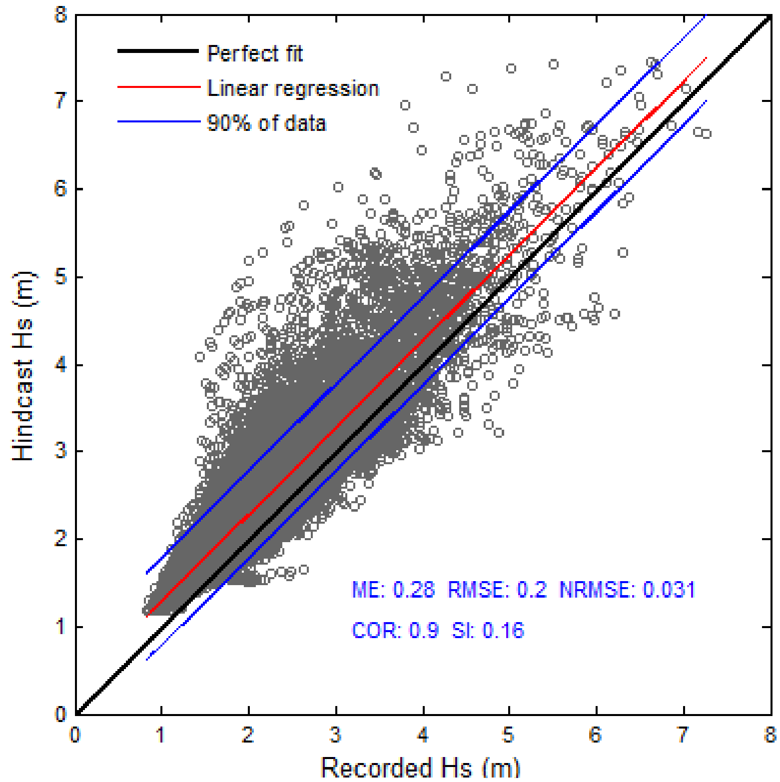

Figure 28- Scatter plot of recorded and hindcast significant wave heights at buoy #51100.

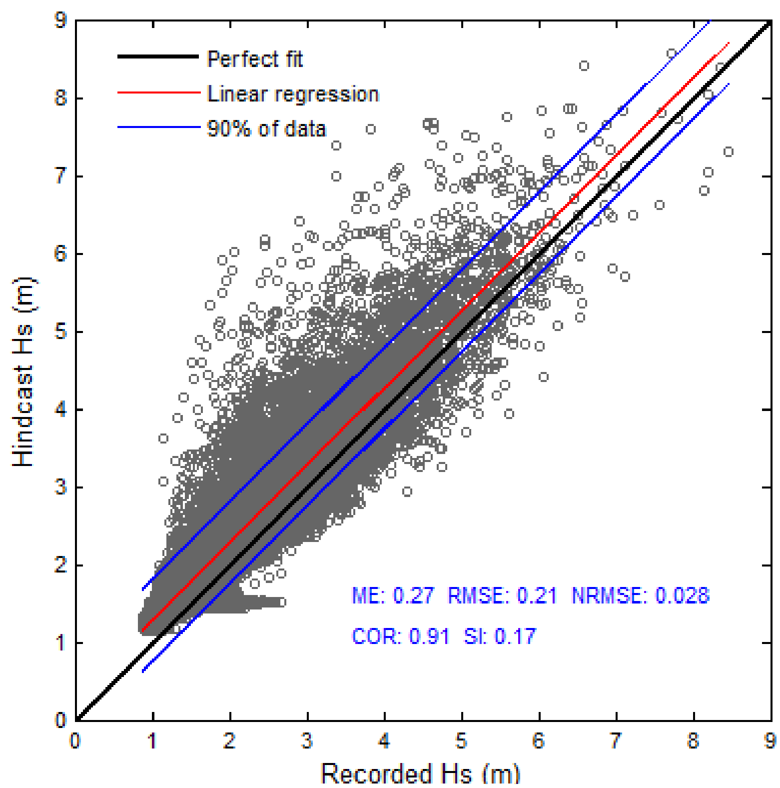

Figure 29- Scatter plot of recorded and hindcast significant wave heights at buoy #51101.

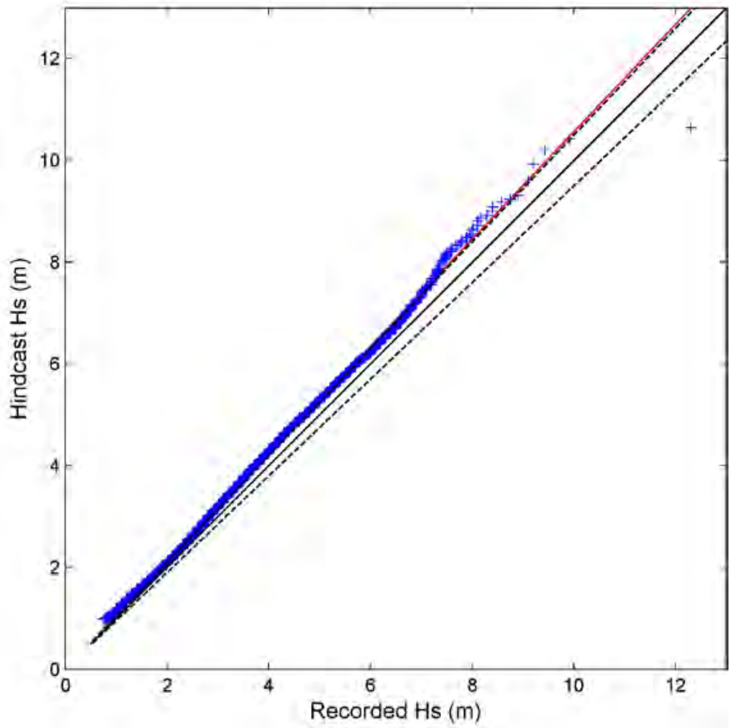

Figure 30- Quantile-quantile plot of recorded and hindcast significant wave heights at buoy #51001. Blue crosses represent data pair at 0.002 percentile increment, black line denotes perfect match, black dash lines delineate the ±5% error bounds, and red line is the linear regression.

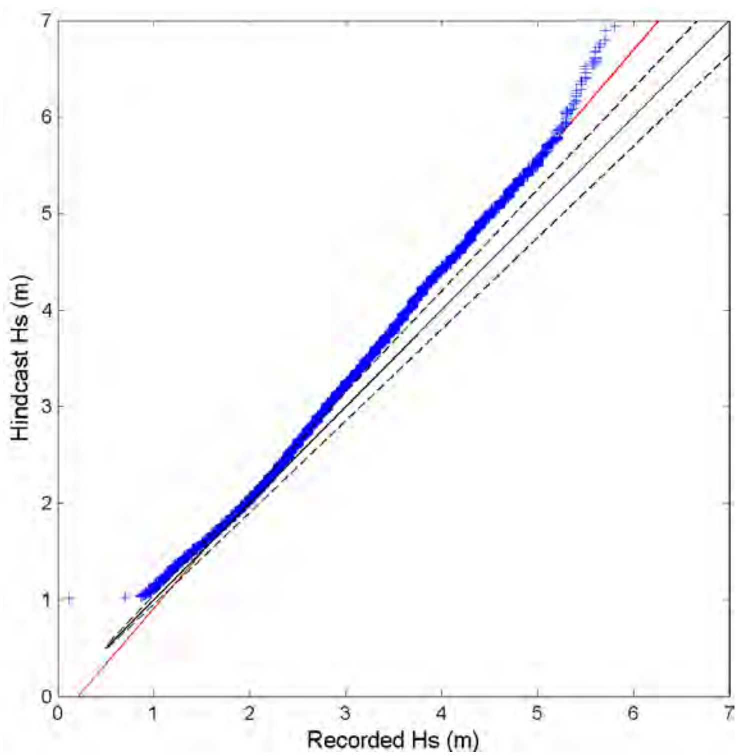

Figure 31- Quantile-quantile plot of recorded and hindcast significant wave heights at buoy #51003. Blue crosses represent data pair at 0.002 percentile increment, black line denotes perfect match, black dash lines delineate the ±5% error bounds, and red line is the linear regression.

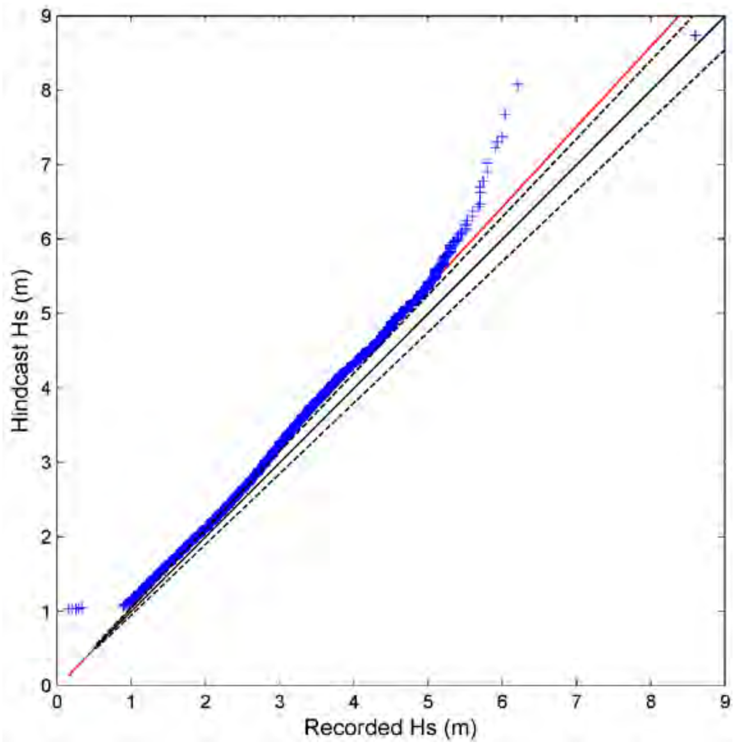

Figure 32- Quantile-quantile plot of recorded and hindcast significant wave heights at buoy #51002. Blue crosses represent data pair at 0.002 percentile increment, black line denotes perfect match, black dash lines delineate the ±5% error bounds, and red line is the linear regression.

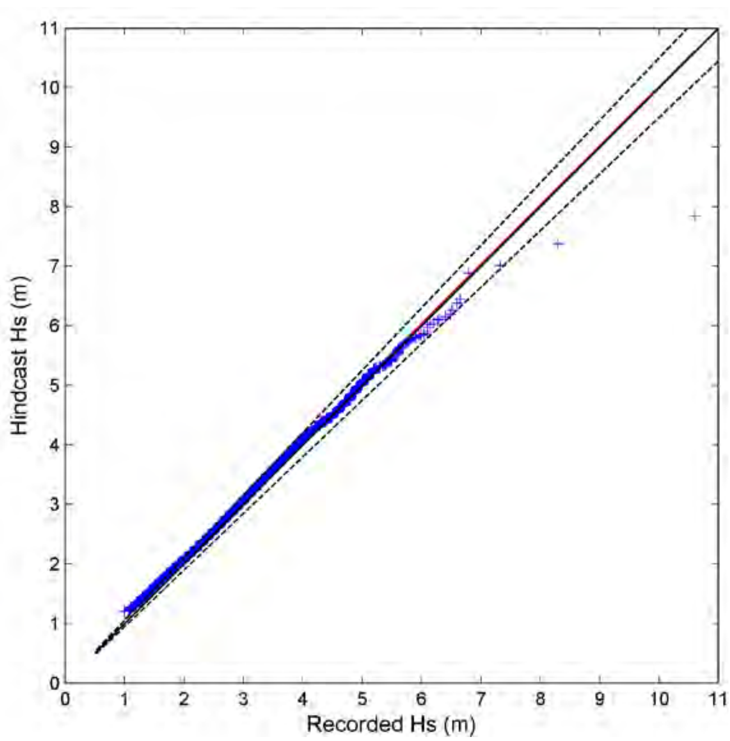

Figure 33- Quantile-quantile plot of recorded and hindcast significant wave heights at buoy #51004. Blue crosses represent data pair at 0.002 percentile increment, black line denotes perfect match, black dash lines delineate the ±5% error bounds, and red line is the linear regression.

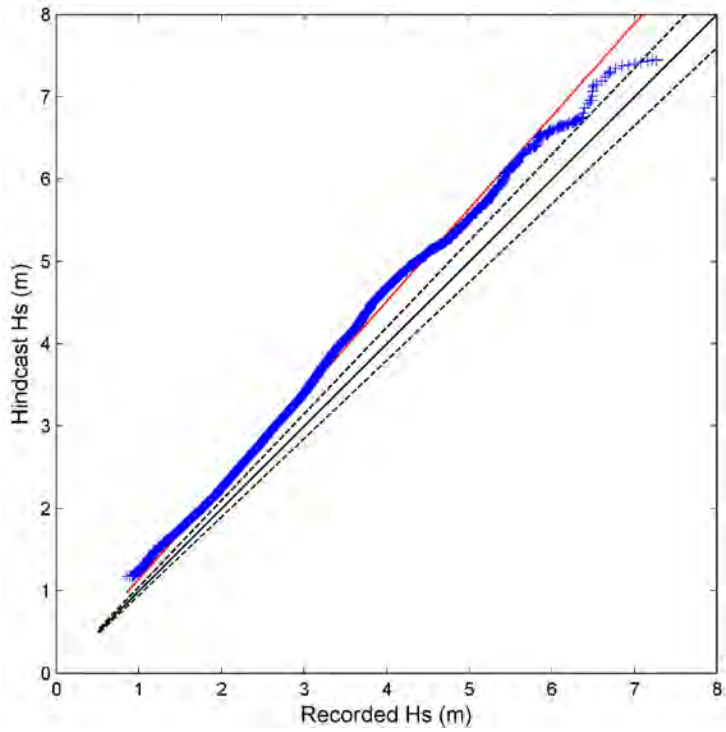

Figure 34- Quantile-quantile plot of recorded and hindcast significant wave heights at buoy #51100. Blue crosses represent data pair at 0.002 percentile increment, black line denotes perfect match, black dash lines delineate the ±5% error bounds, and red line is the linear regression.

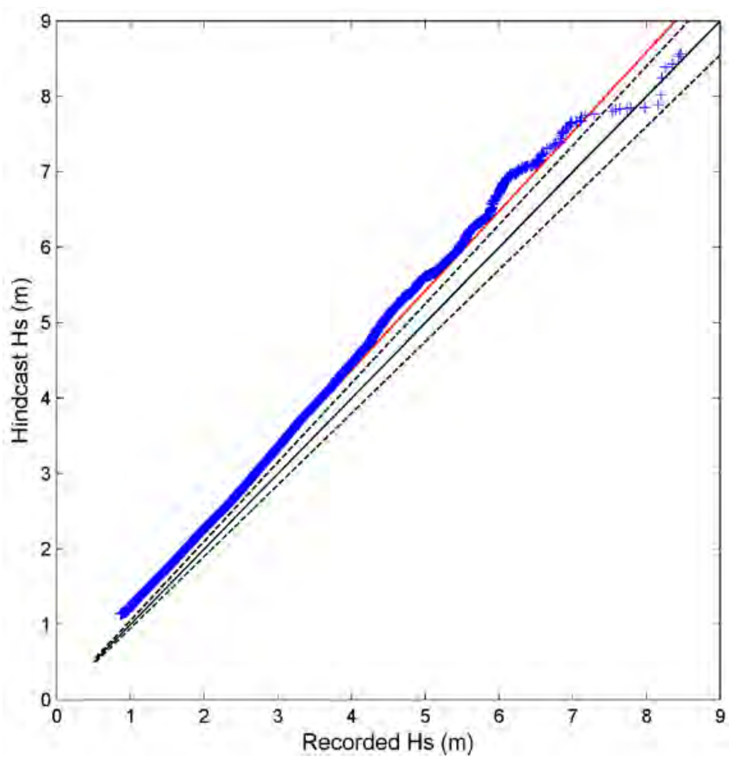

Figure 35- Quantile-quantile plot of recorded and hindcast significant wave heights at buoy #51101. Blue crosses represent data pair at 0.002 percentile increment, black line denotes perfect match, black dash lines delineate the ±5% error bounds, and red line is the linear regression.

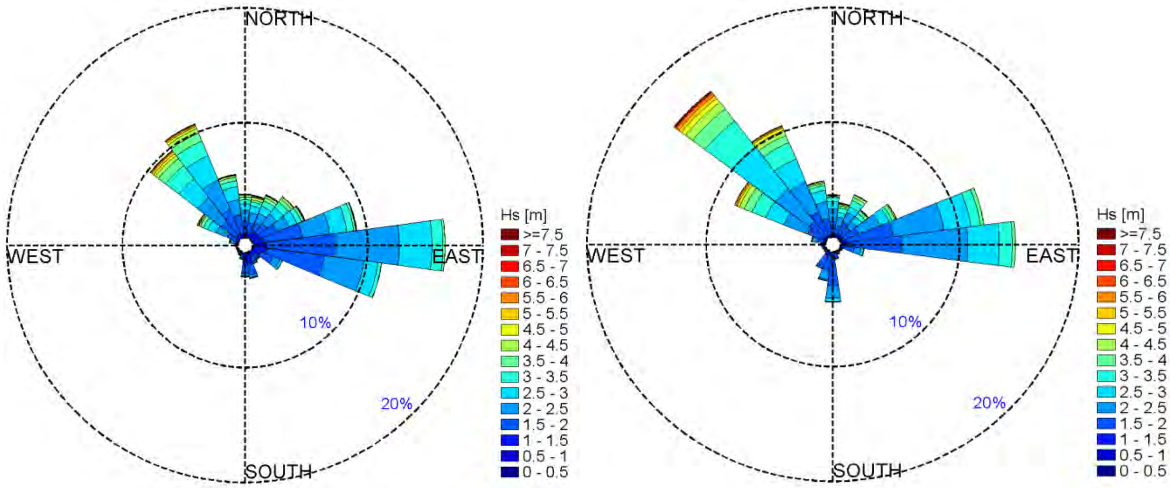

Figure 36- Rose plots of recorded (left) and hindcast (right) significant wave heights at buoy #51001.

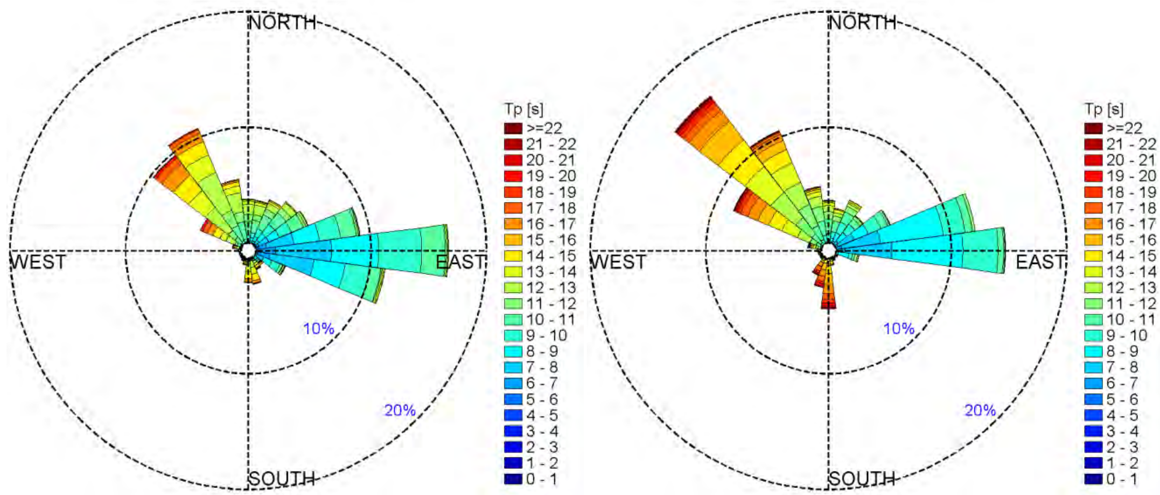

Figure 37- Rose plots of recorded (left) and hindcast (right) peak periods at buoy #51001.

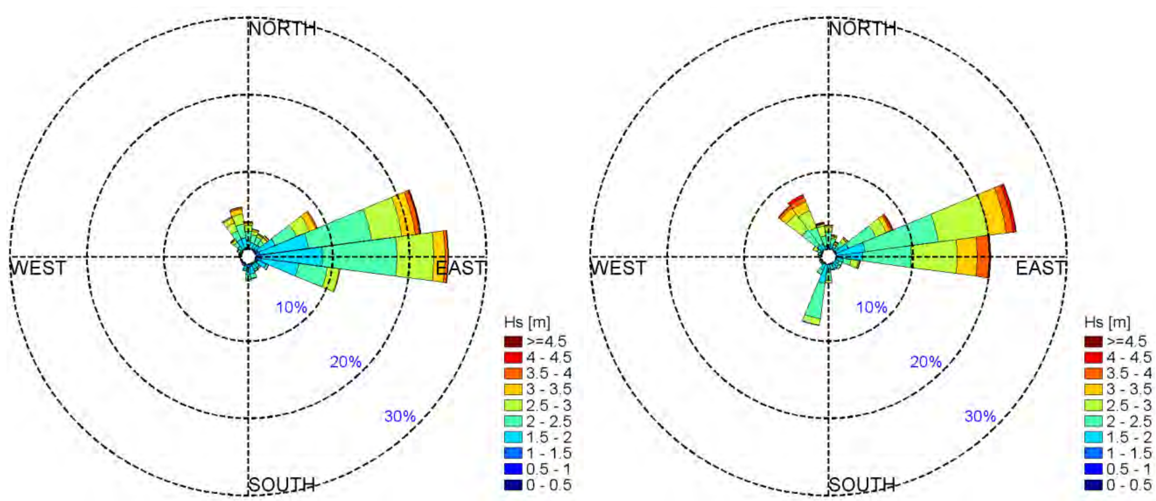

Figure 38- Rose plots of recorded (left) and hindcast (right) significant wave heights at buoy #51004.

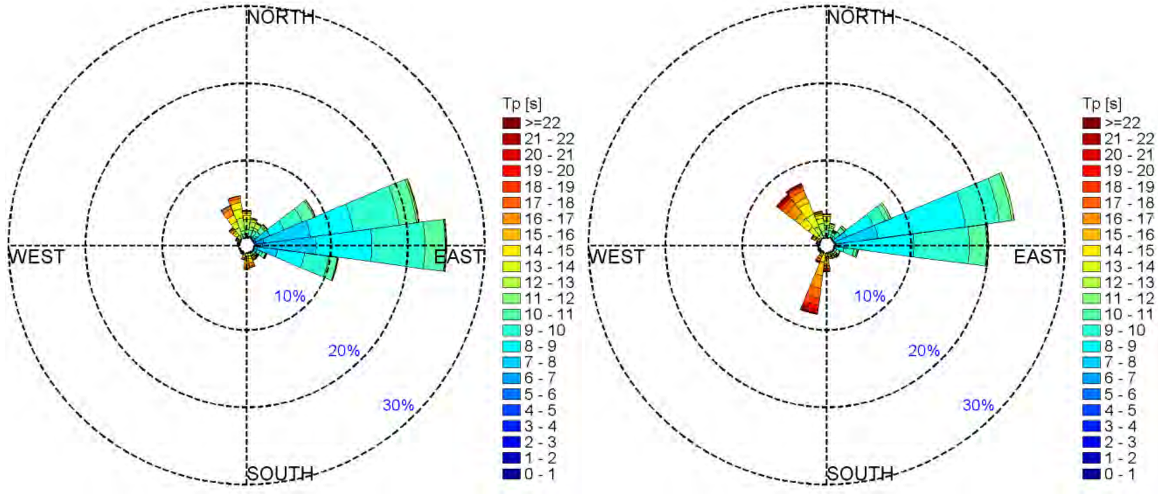

Figure 39- Rose plots of recorded (left) and hindcast (right) peak periods at buoy #51004.

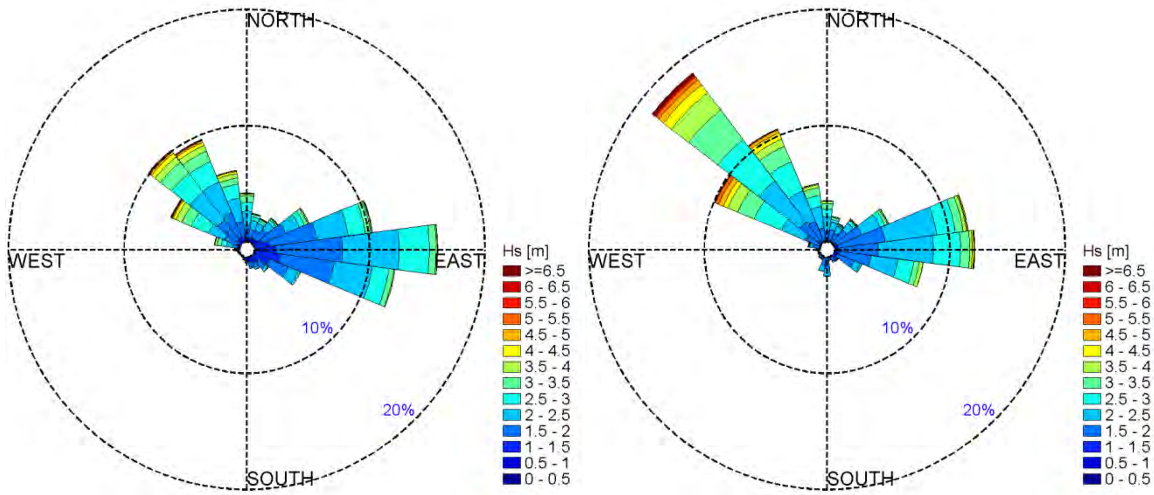

Figure 40- Rose plots of recorded (left) and hindcast (right) significant wave heights at buoy #51100.

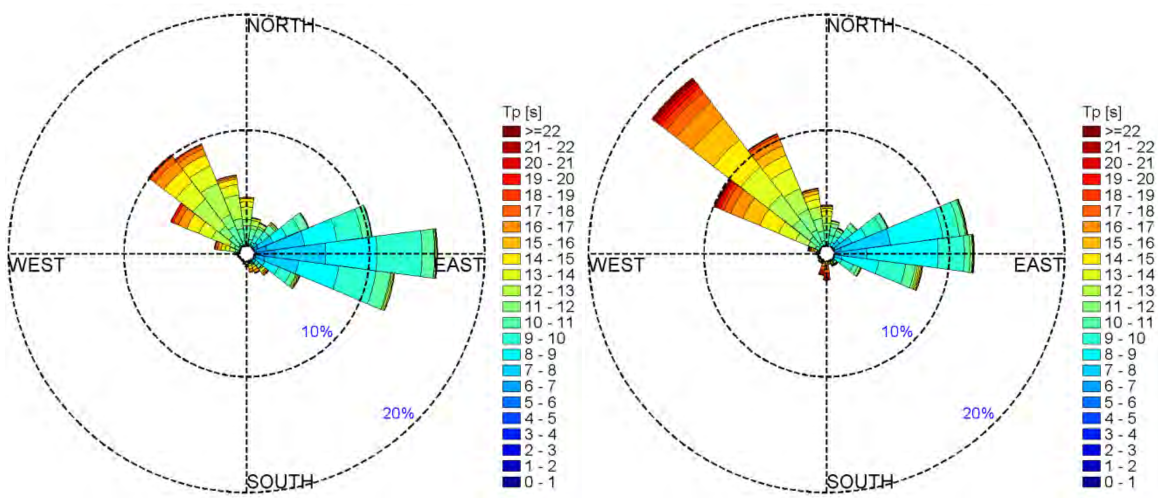

Figure 41- Rose plots of recorded (left) and hindcast (right) peak periods at buoy #51100.

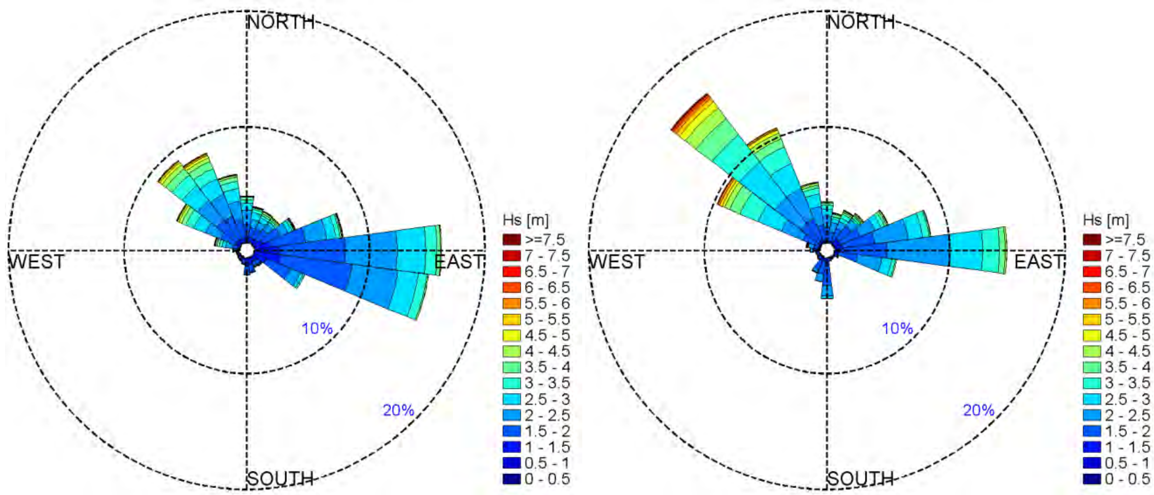

Figure 42- Rose plots of recorded (left) and hindcast (right) significant wave heights at buoy #51101.

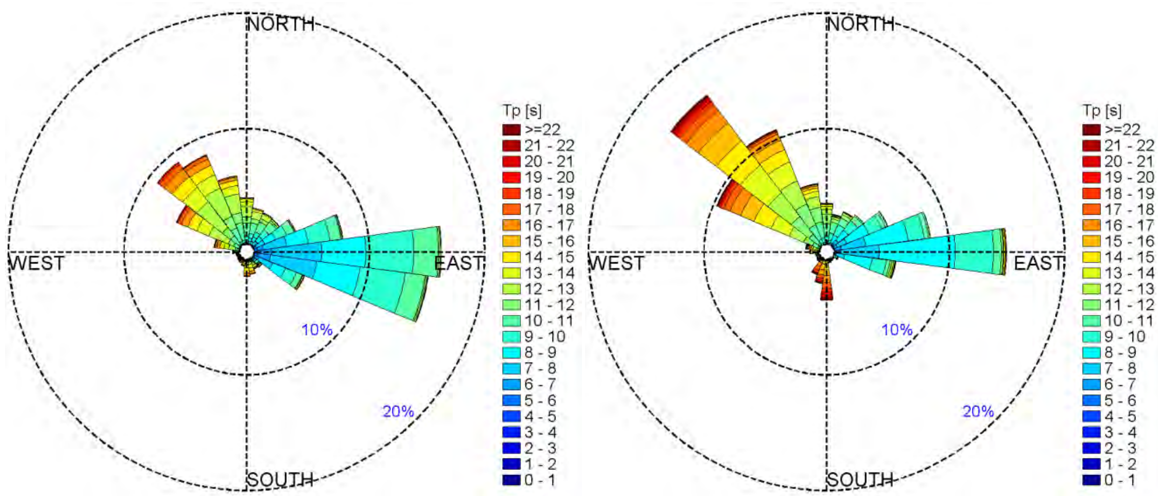

Figure 43- Rose plots of recorded (left) and hindcast (right) peak periods at buoy # 51101.

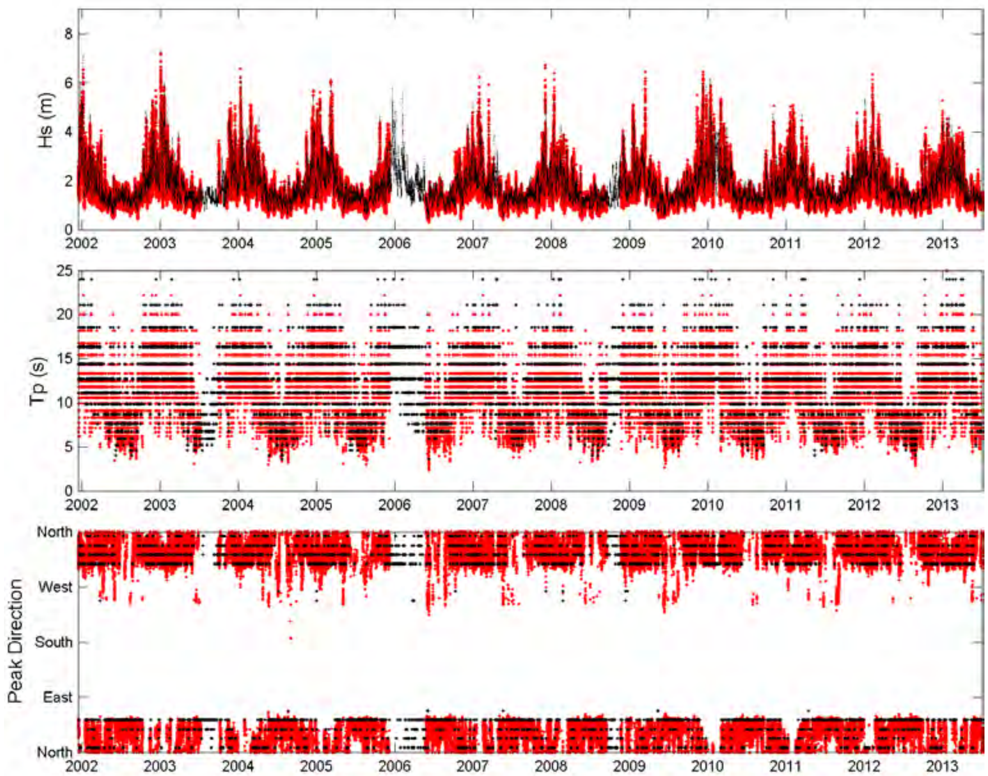

Figure 44- Comparison of recorded (red) and hindcast (black) wave parameters at the Waimea buoy.

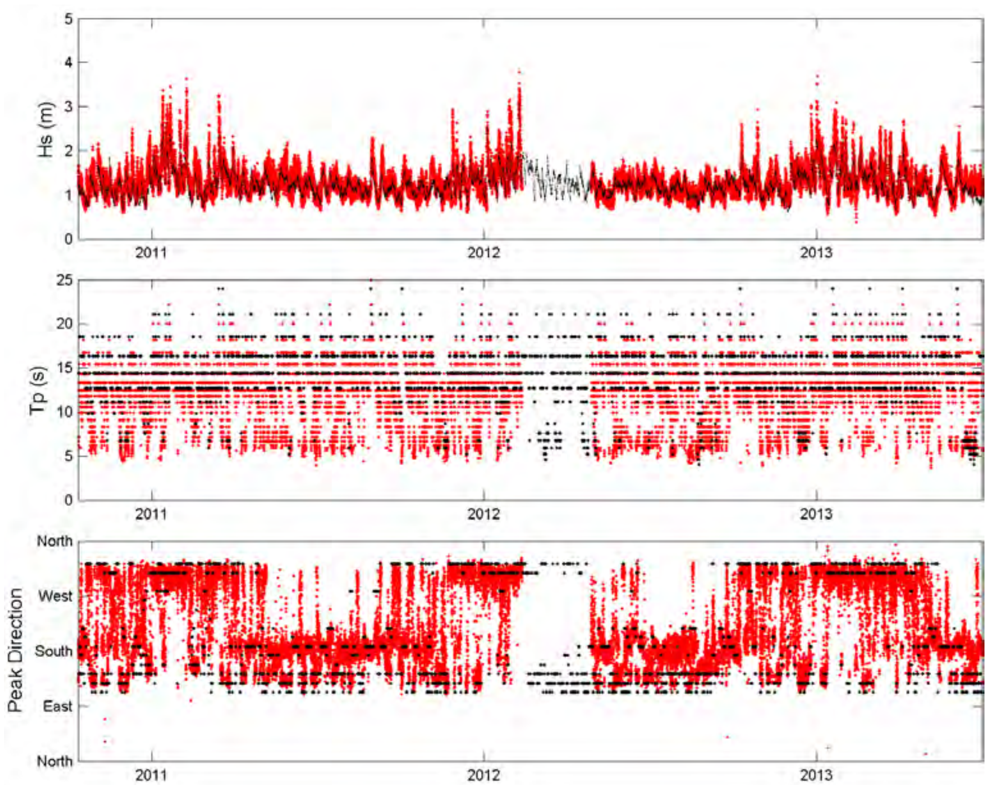

Figure 45 - Comparison of recorded (red) and hindcast (black) wave parameters at the Barbers Point buoy.

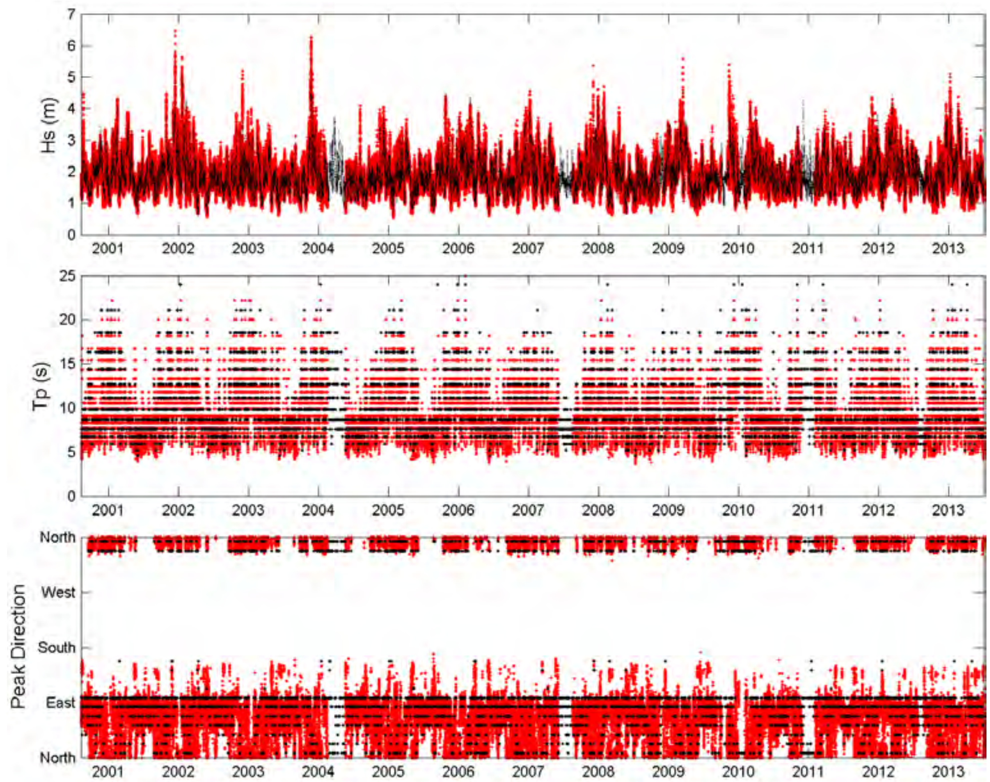

Figure 46- Comparison of recorded (red) and hindcast (black) wave parameters at the Mokapu buoy.

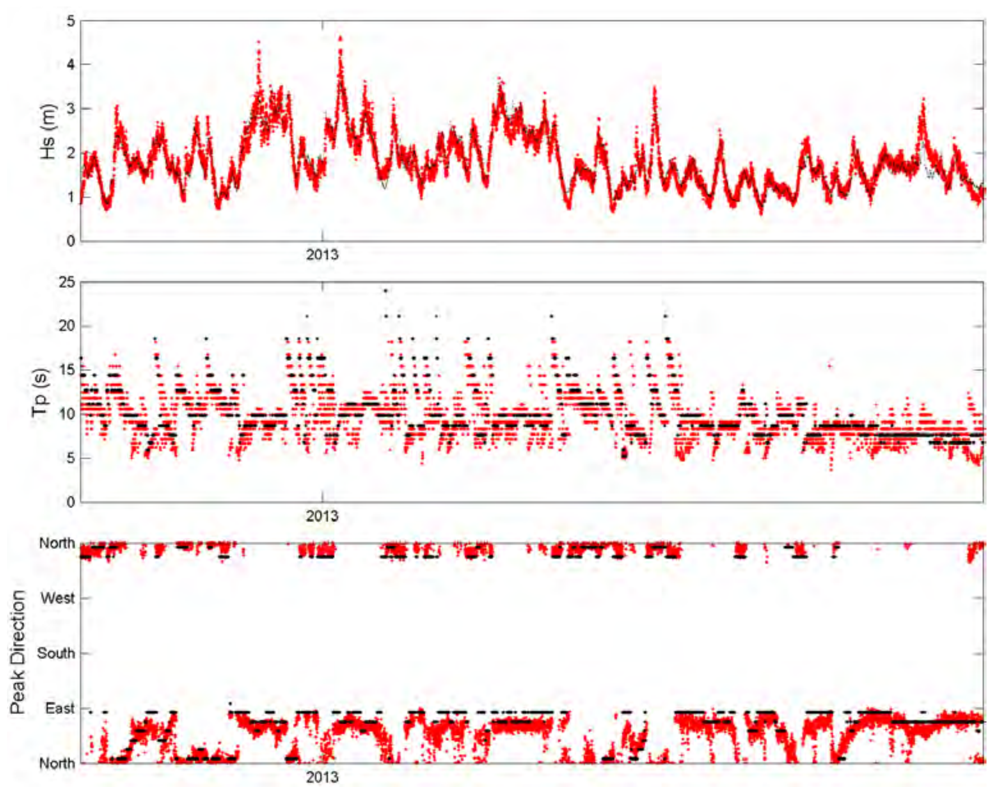

Figure 47- Comparison of recorded (red) and hindcast (black) wave parameters at the WETS buoy.

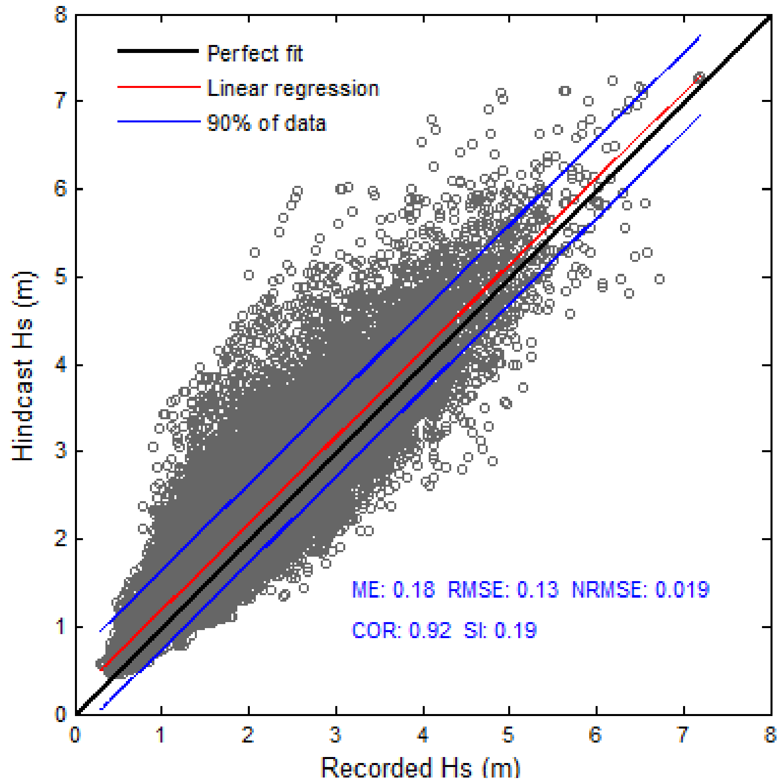

Figure 48- Scatter plot of recorded and hindcast significant wave heights at the Waimea buoy.

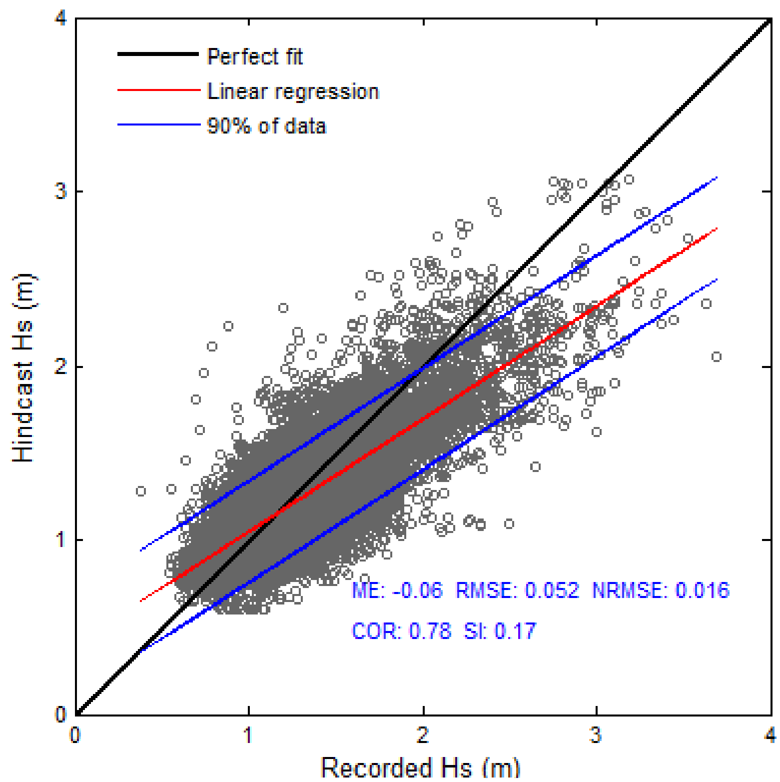

Figure 49- Scatter plot of recorded and hindcast significant wave heights at the Barbers Point buoy.

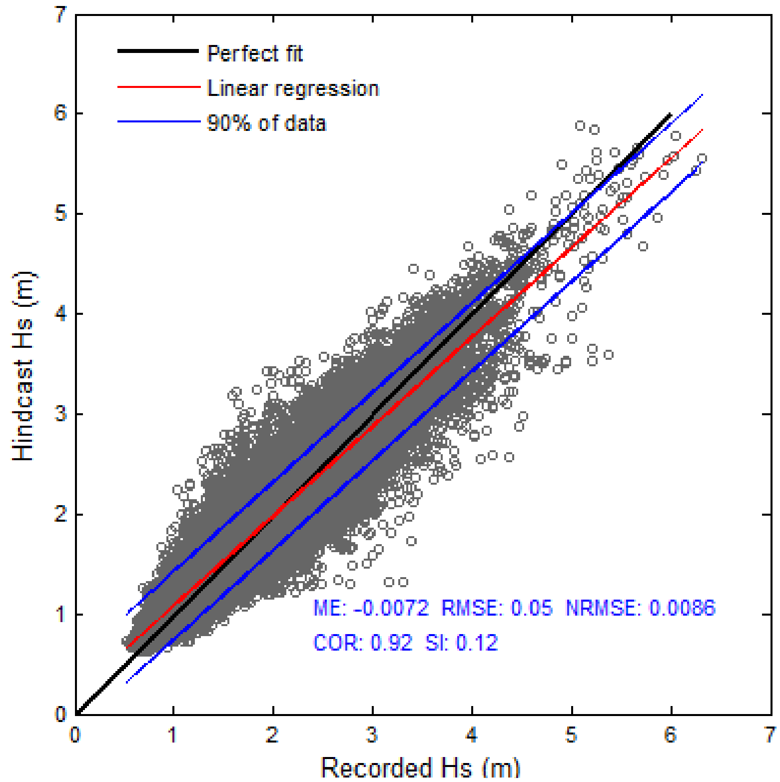

Figure 50- Scatter plot of recorded and hindcast significant wave heights at the Mokapu buoy.

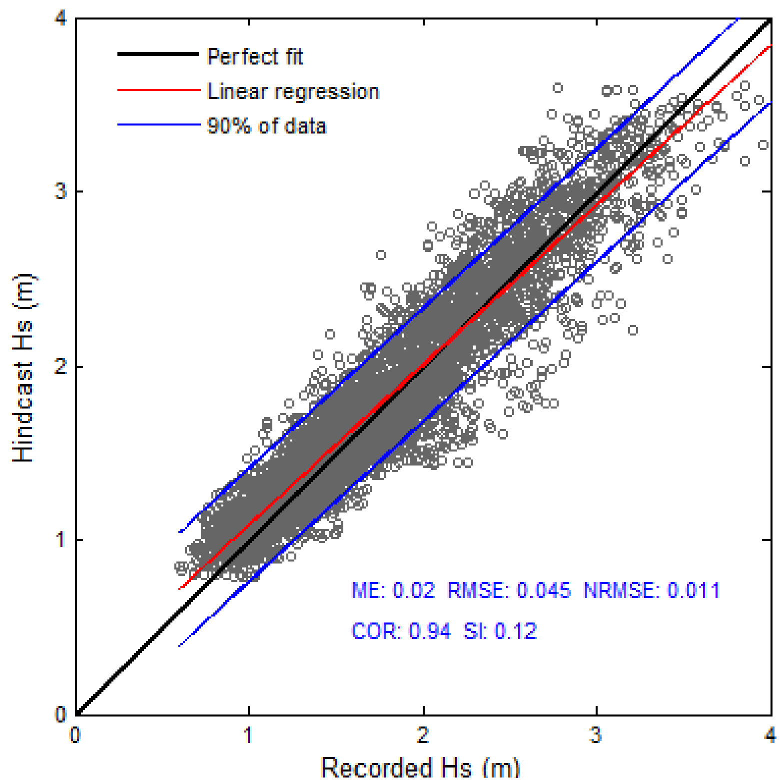

Figure 51- Scatter plot of recorded and hindcast significant wave heights at the WETS buoy.

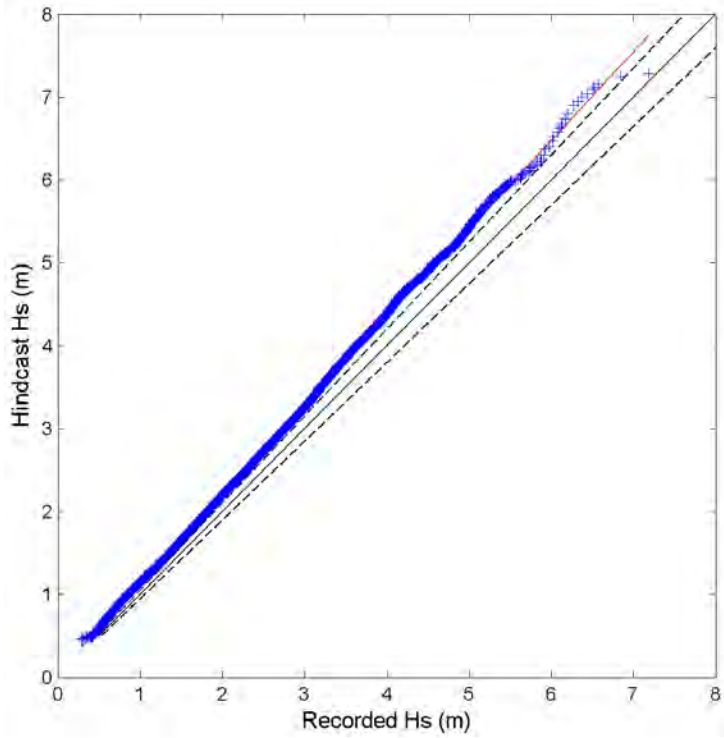

Figure 52- Quantile-quantile plot of recorded and hindcast significant wave heights at the Waimea buoy. Blue crosses represent data pair at 0.002 percentile increment, black line denotes perfect match, black dash lines delineate the ±5% error bounds, and red line is the linear regression.

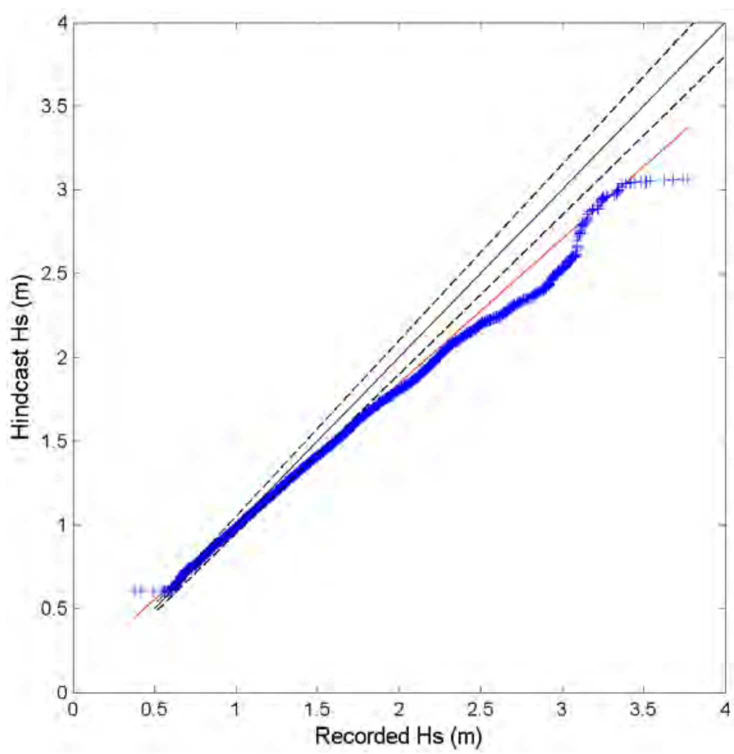

Figure 53- Quantile-quantile plot of recorded and hindcast significant wave heights at the Barbers Point buoy. Blue crosses represent data pair at 0.002 percentile increment, black line denotes perfect match, black dash lines delineate the ±5% error bounds, and red line is the linear regression.

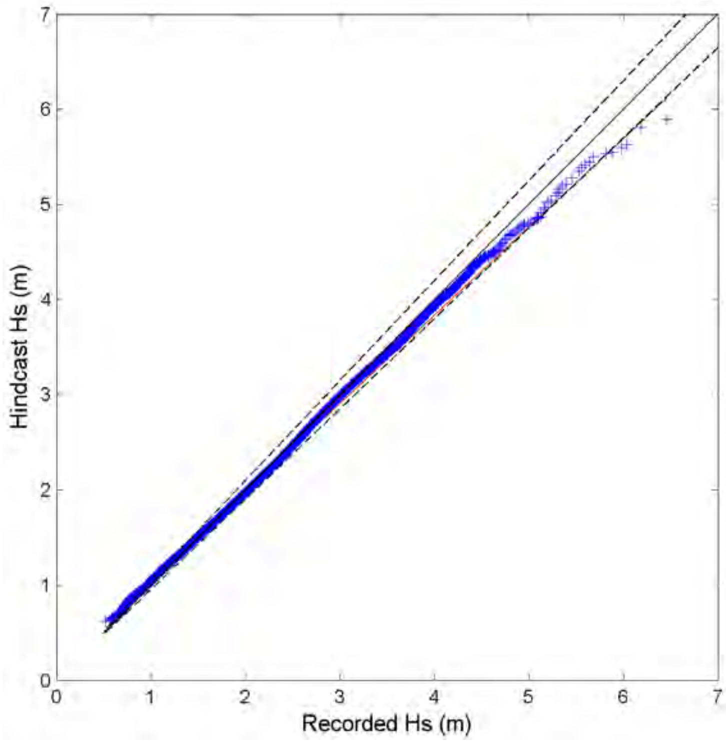

Figure 54- Quantile-quantile plot of recorded and hindcast significant wave heights at Mokapu buoy. Blue crosses represent data pair at 0.002 percentile increment, black line denotes perfect match, black dash lines delineate the ±5% error bounds, and red line is the linear regression.

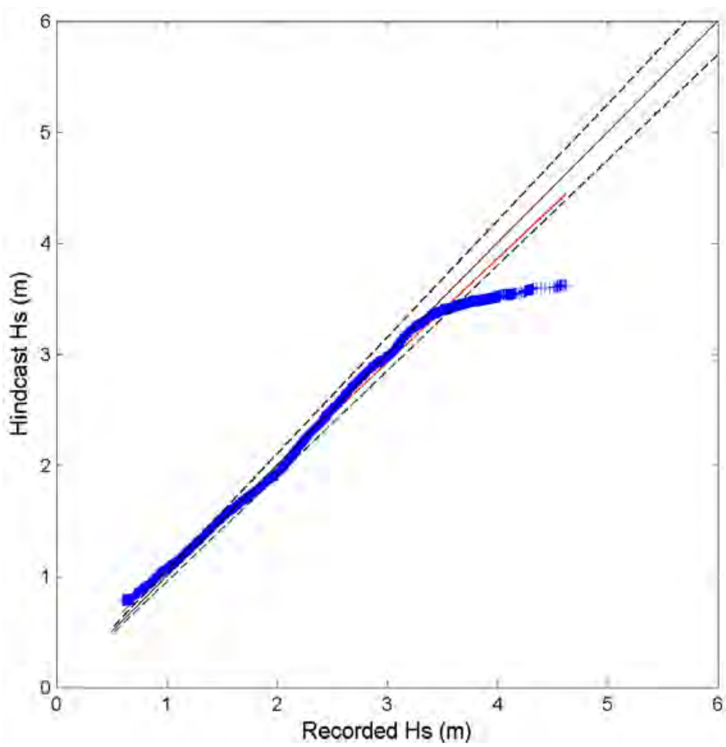

Figure 55- Quantile-quantile plot of recorded and hindcast significant wave heights at the WETS buoy. Blue crosses represent data pair at 0.002 percentile increment, black line denotes perfect match, black dash lines delineate the ±5% error bounds, and red line is the linear regression.

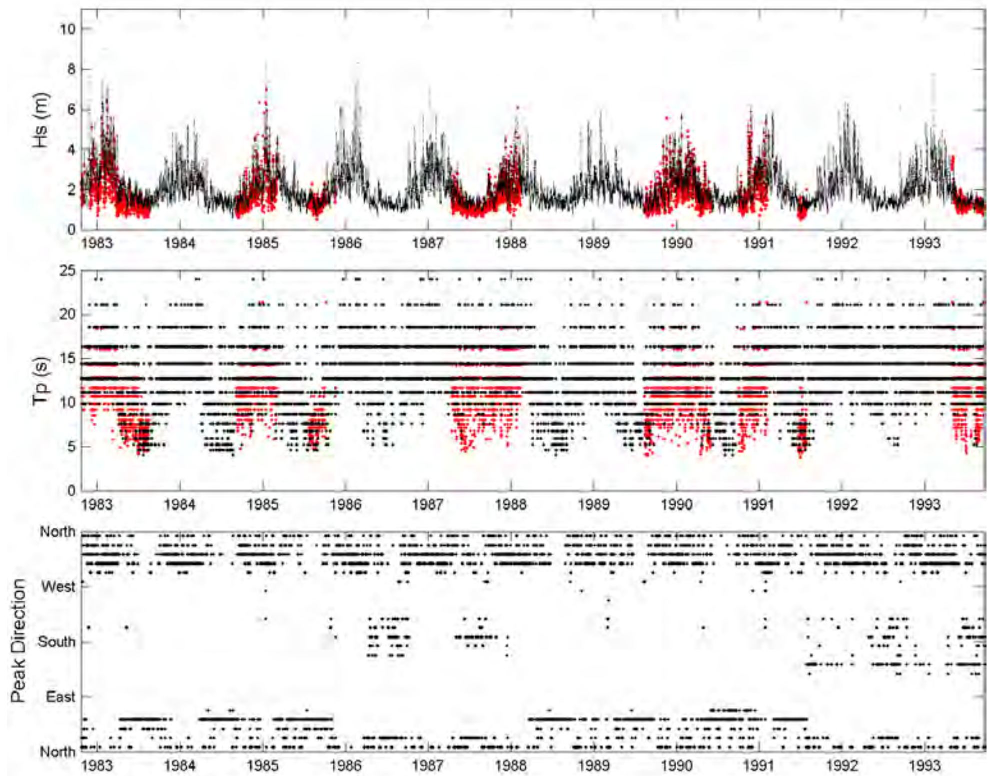

Figure 56- Comparison of recorded (red) and hindcast (black) wave parameters at the Barking Sands buoy.

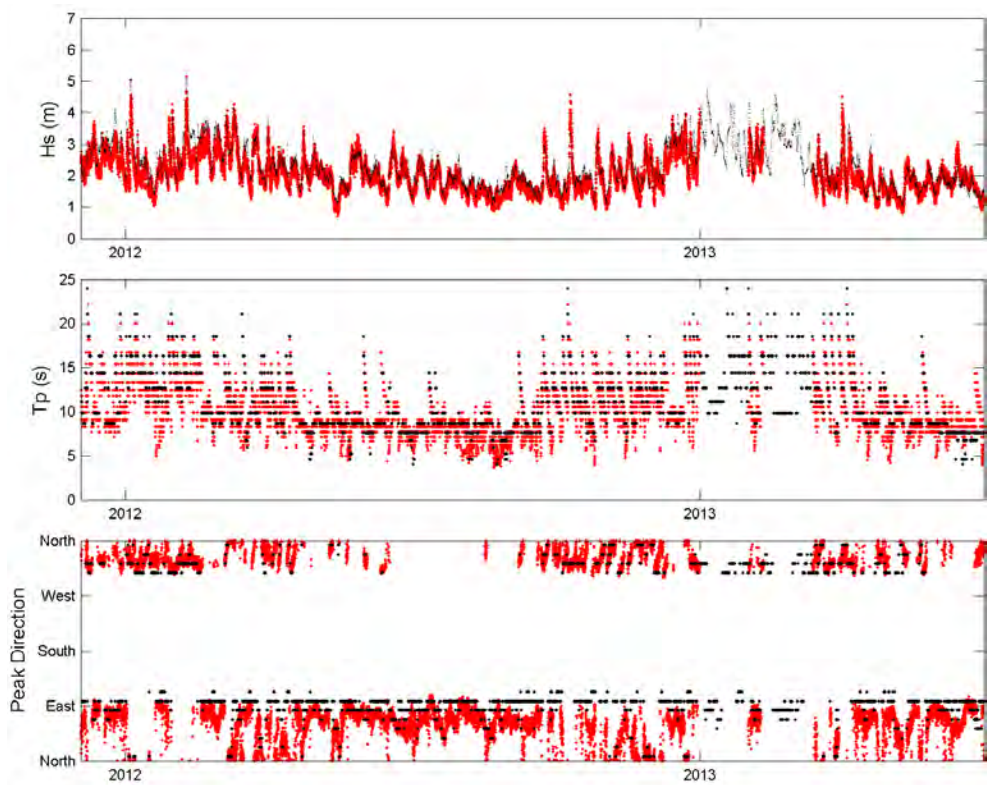

Figure 57- Comparison of recorded (red) and hindcast (black) wave parameters at the Pauwela buoy.

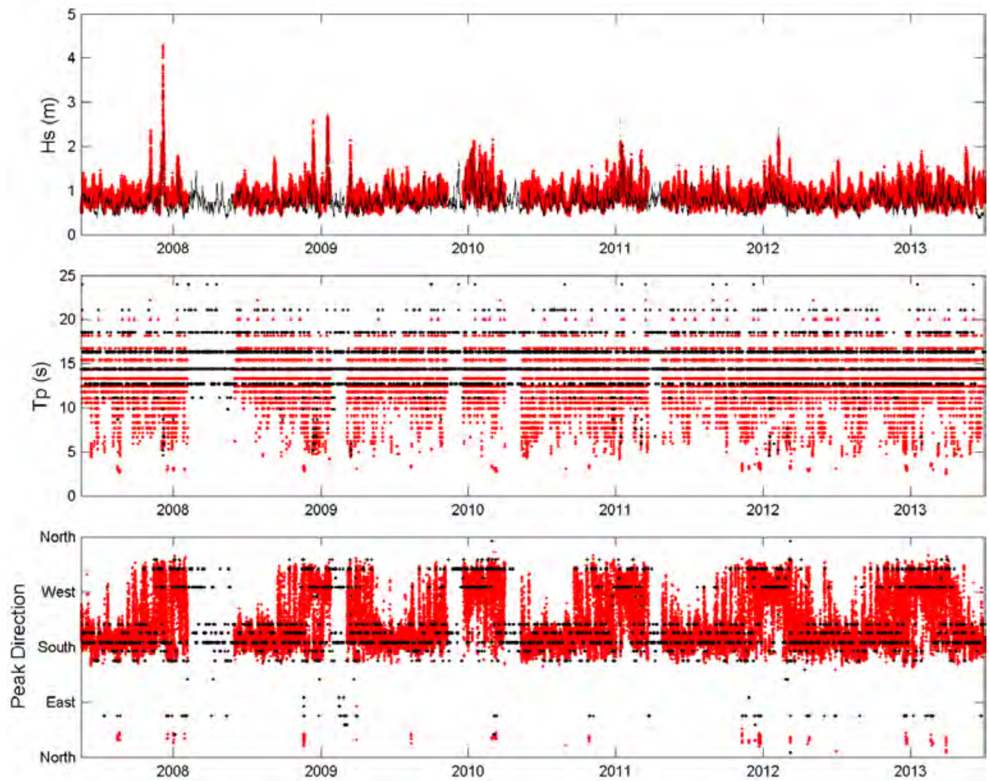

Figure 58- Comparison of recorded (red) and hindcast (black) wave parameters at the Kaumalapau buoy.

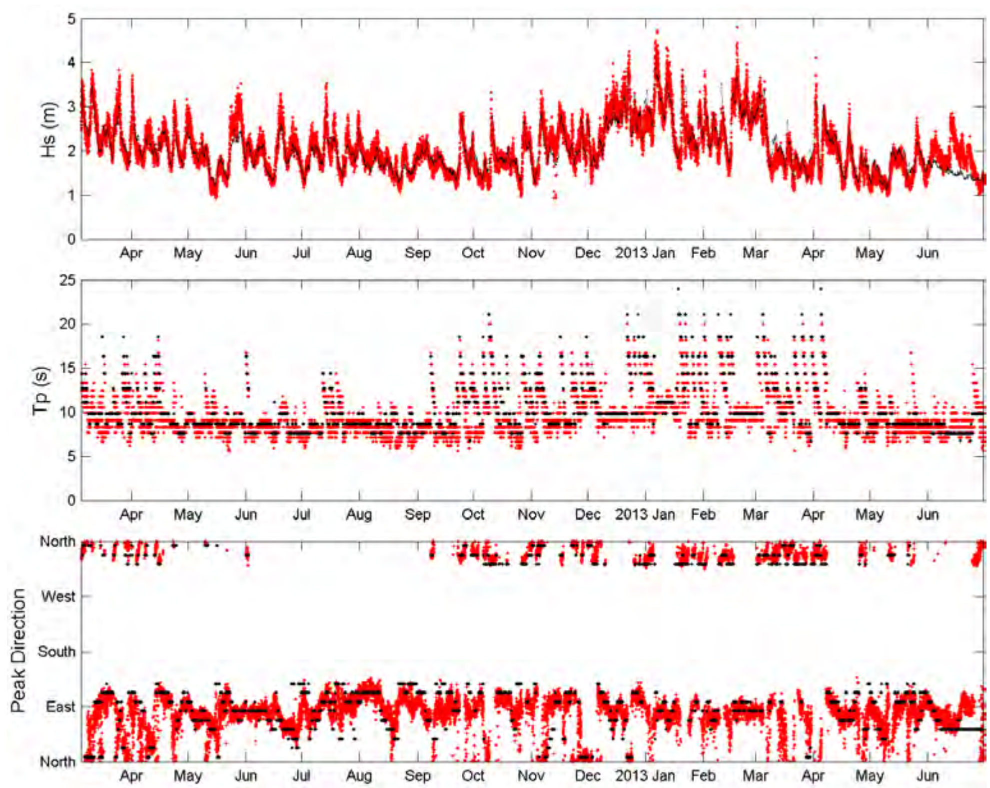

Figure 59- Comparison of recorded (red) and hindcast (black) wave parameters at the Hilo buoy.

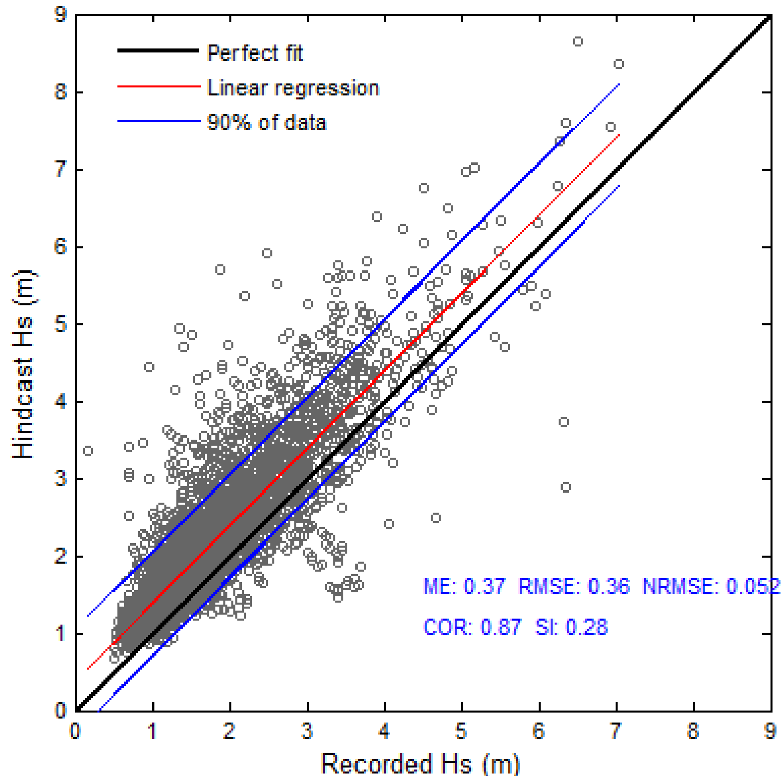

Figure 60- Scatter plot of recorded and hindcast significant wave heights at the Barking Sands buoy.

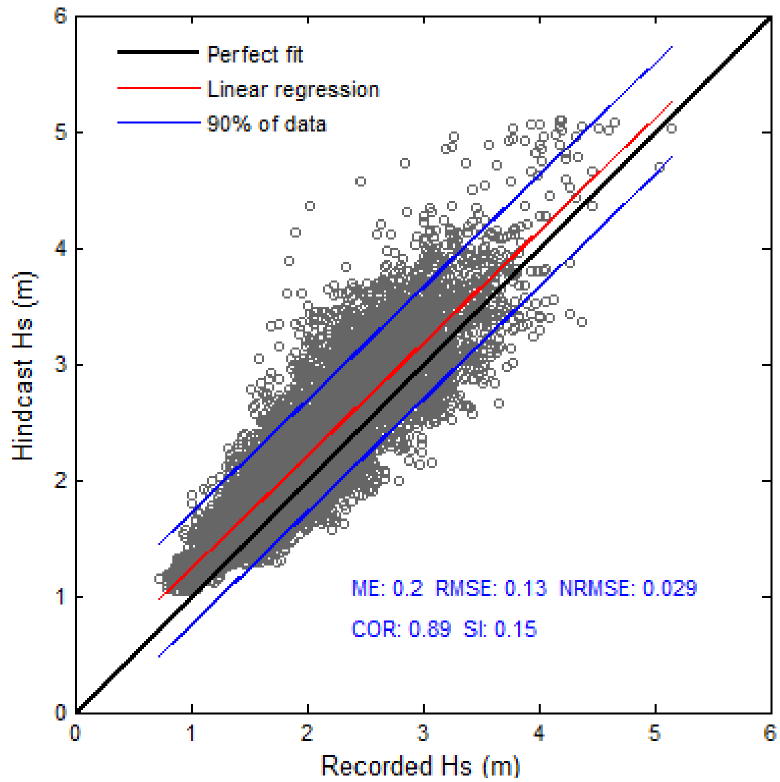

Figure 61- Scatter plot of recorded and hindcast significant wave heights at the Pauwela buoy.

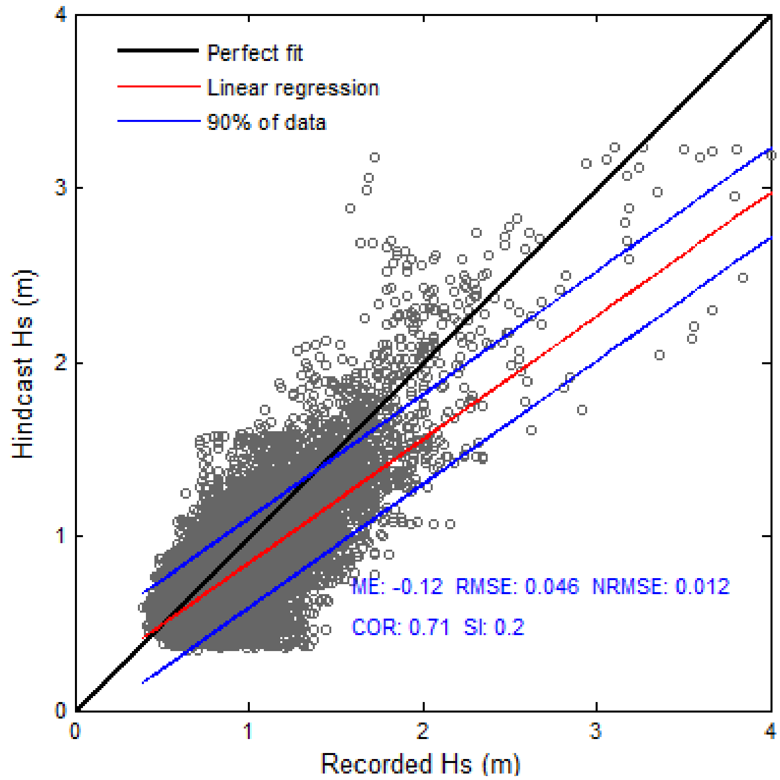

Figure 62- Scatter plot of recorded and hindcast significant wave heights at the Kaumalapau buoy.

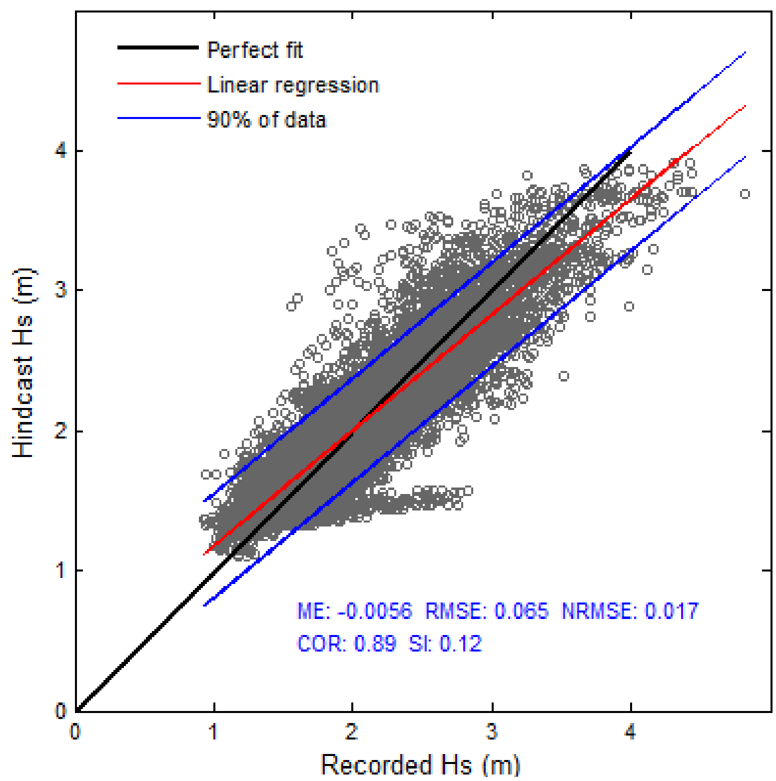

Figure 63- Scatter plot of recorded and hindcast significant wave heights at the Hilo buoy.

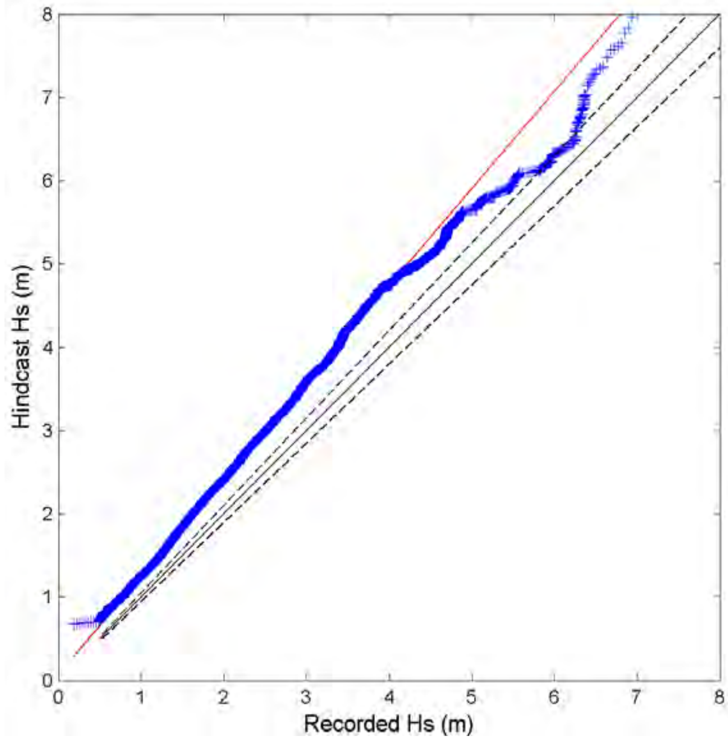

Figure 64- Quantile-quantile plot of recorded and hindcast significant wave heights at the Barking Sands buoy. Blue crosses represent data pair at 0.002 percentile increment, black line denotes perfect match, black dash lines delineate the ±5% error bounds, and red line is the linear regression.

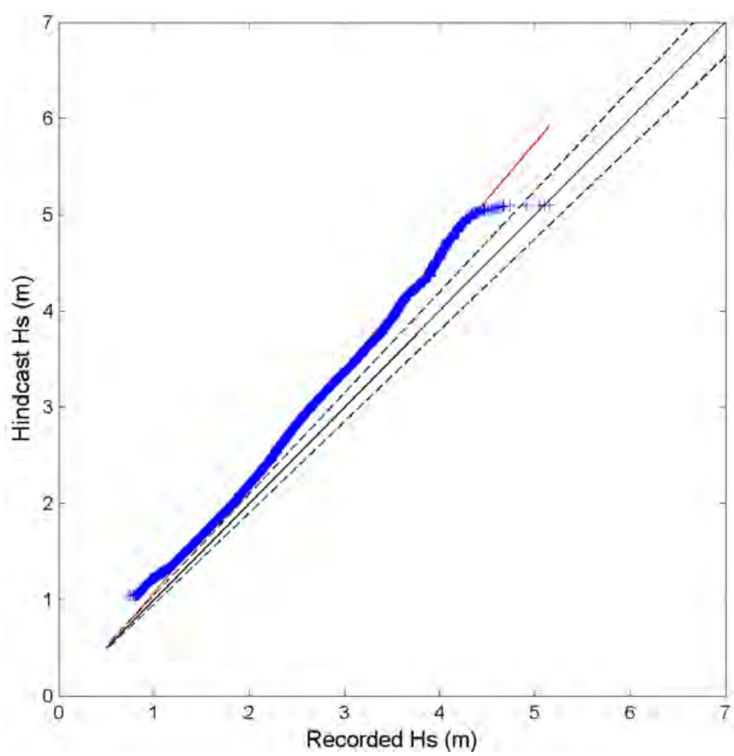

Figure 65- Quantile-quantile plot of recorded and hindcast significant wave heights at the Pauwela buoy. Blue crosses represent data pair at 0.002 percentile increment, black line denotes perfect match, black dash lines delineate the ±5% error bounds, and red line is the linear regression.

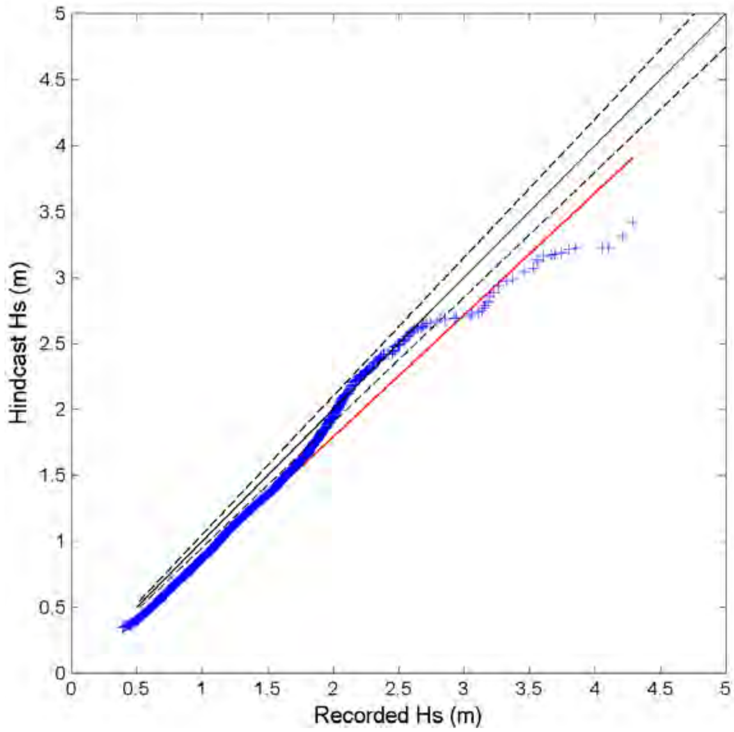

Figure 66- Quantile-quantile plot of recorded and hindcast significant wave heights at the Kaumalapau buoy. Blue crosses represent data pair at 0.002 percentile increment, black line denotes perfect match, black dash lines delineate the ±5% error bounds, and red line is the linear regression.

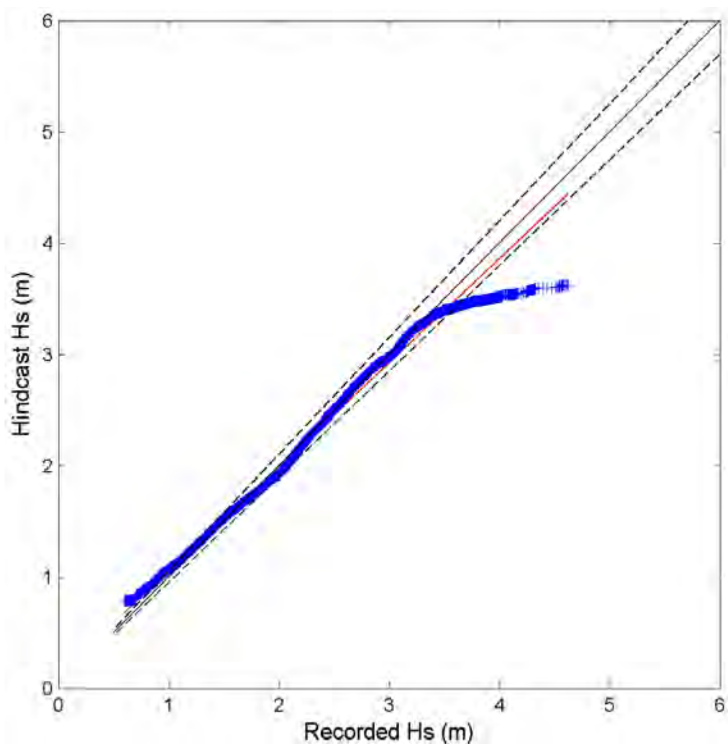

Figure 67- Quantile-quantile plot of recorded and hindcast significant wave heights at the Hilo buoy. Blue crosses represent data pair at 0.002 percentile increment, black line denotes perfect match, black dash lines delineate the ±5% error bounds, and red line is the linear regression.

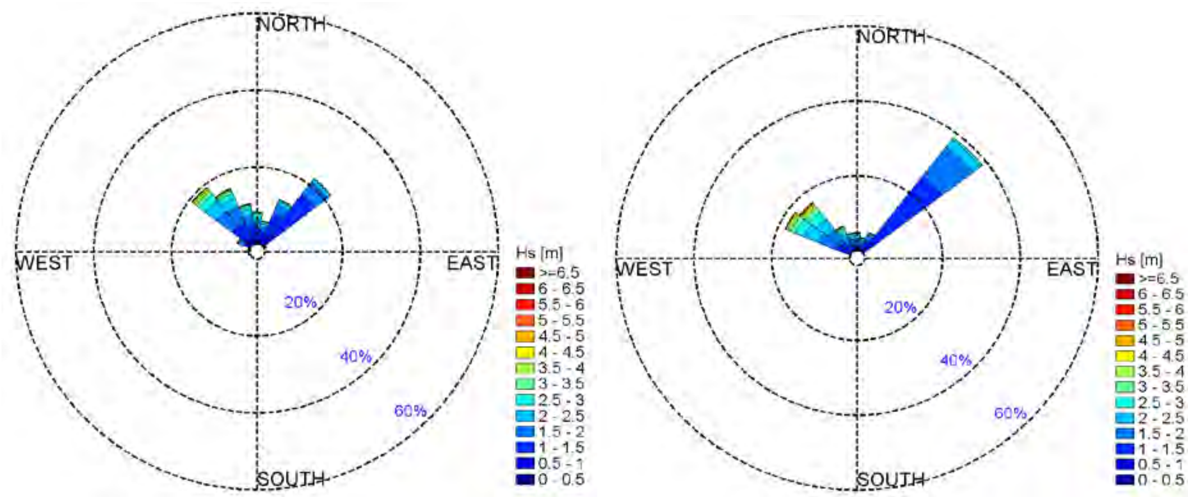

Figure 68- Rose plots of recorded (left) and hindcast (right) significant wave heights at the Waimea buoy.

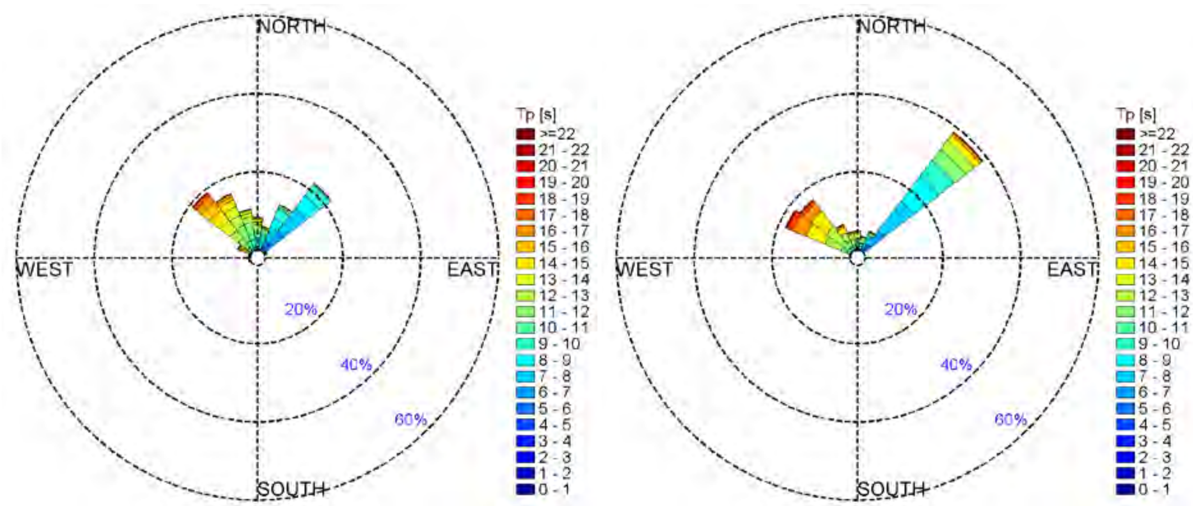

Figure 69- Rose plots of recorded (left) and hindcast (right) peak periods at the Waimea buoy.

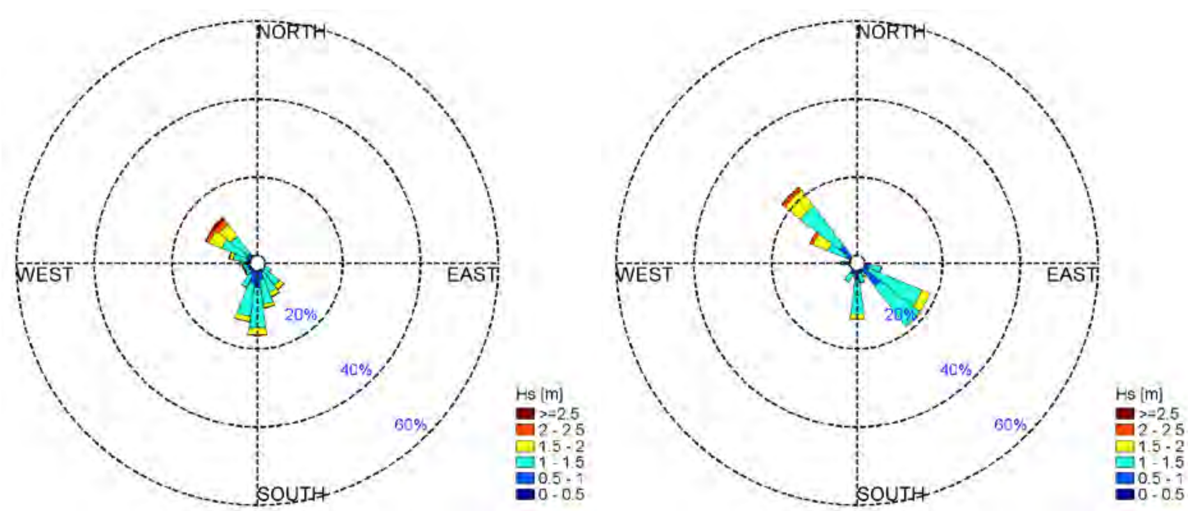

Figure 70- Rose plots of recorded (left) and hindcast (right) significant wave heights at the Barbers Point buoy.

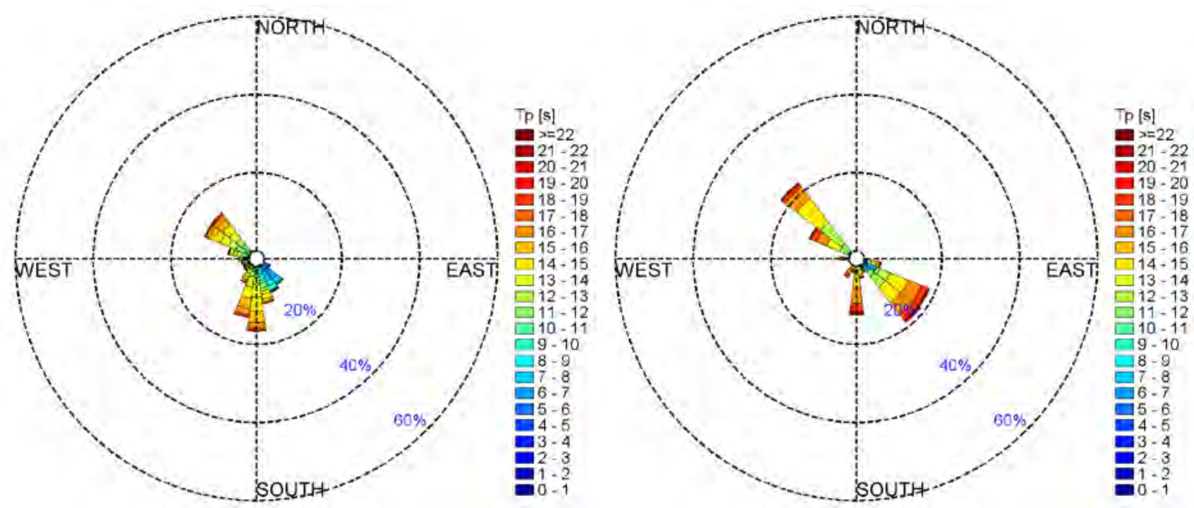

Figure 71- Rose plots of recorded (left) and hindcast (right) peak periods at the Barbers Point buoy.

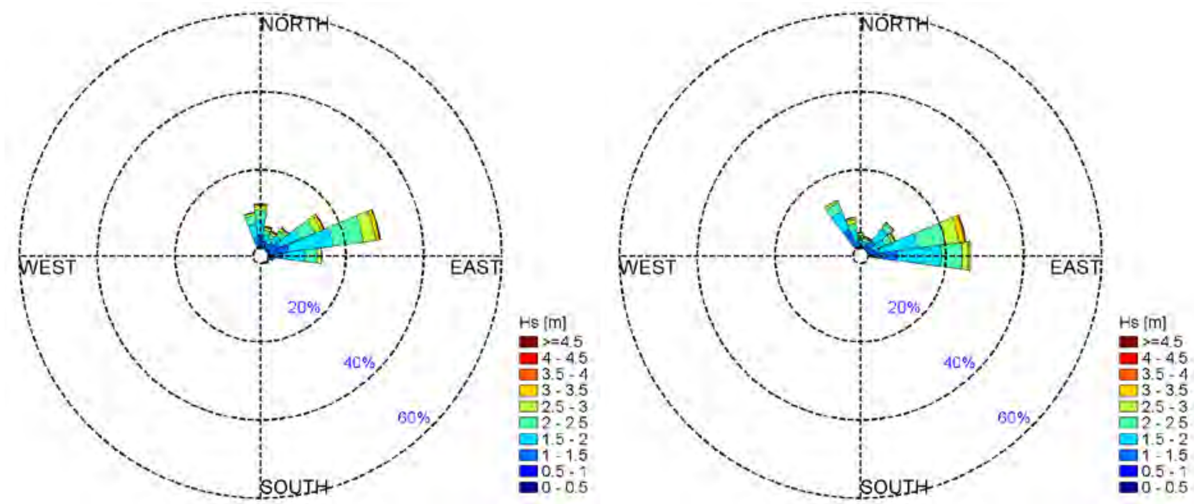

Figure 72-Rose plots of recorded (left) and hindcast (right) significant wave heights at the Mokapu buoy.

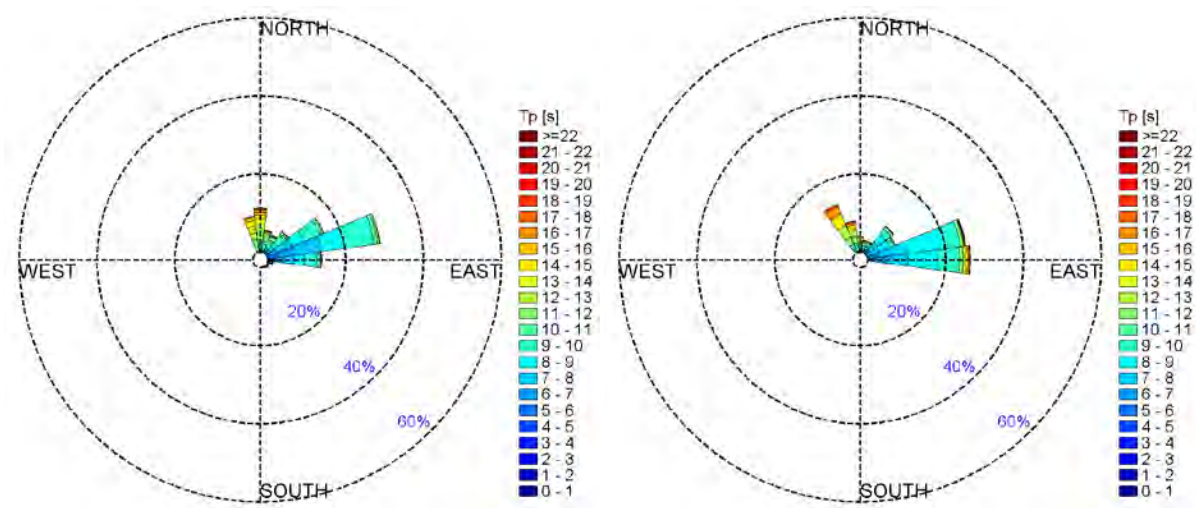

Figure 73- Rose plots of recorded (left) and hindcast (right) peak periods at the Mokapu buoy.

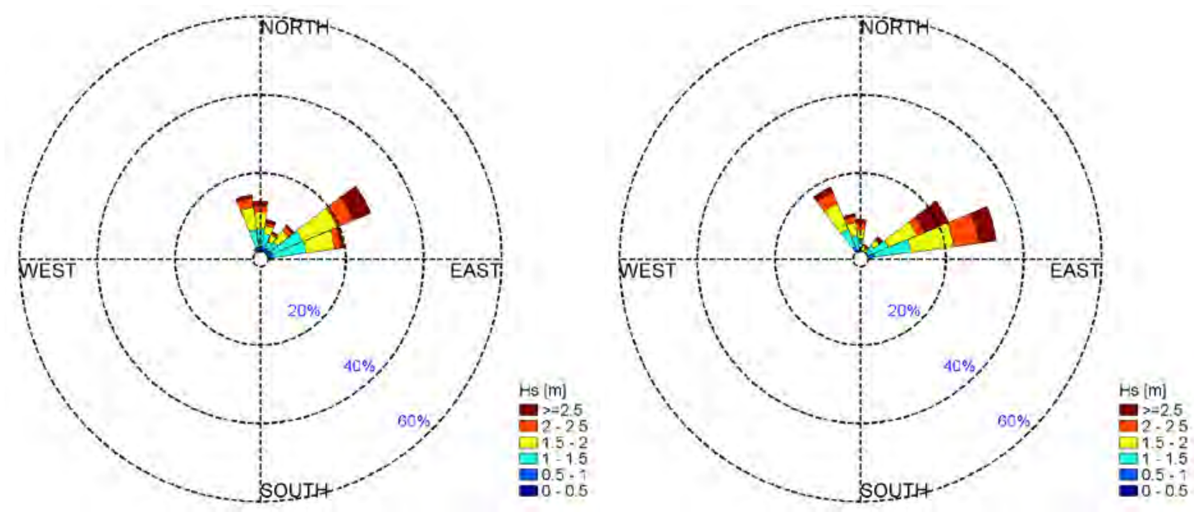

Figure 74- Rose plots of recorded (left) and hindcast (right) significant wave heights at the WETS buoy.

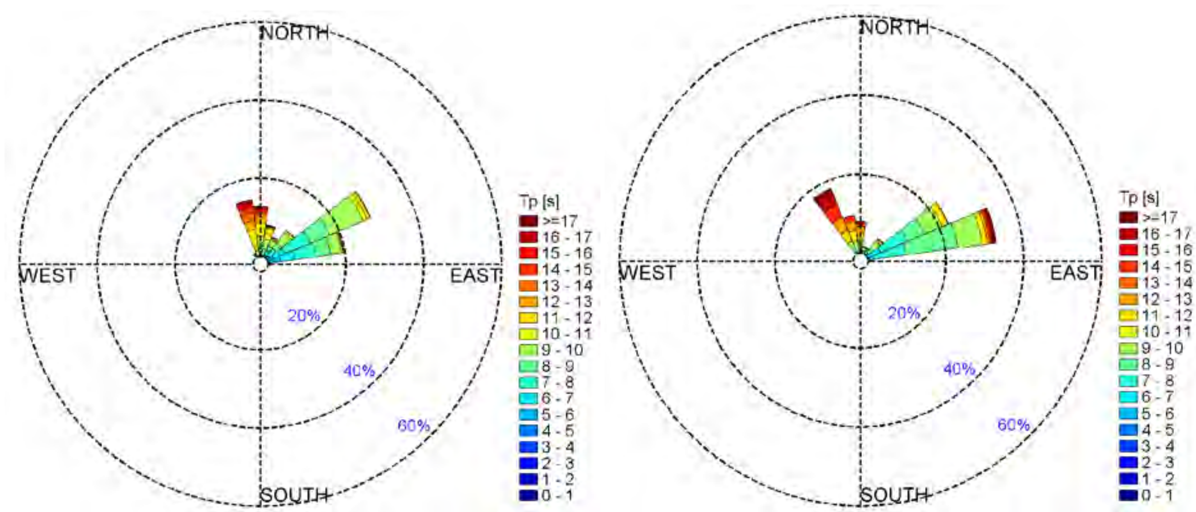

Figure 75- Rose plots of recorded (left) and hindcast (right) peak periods at the WETS buoy.

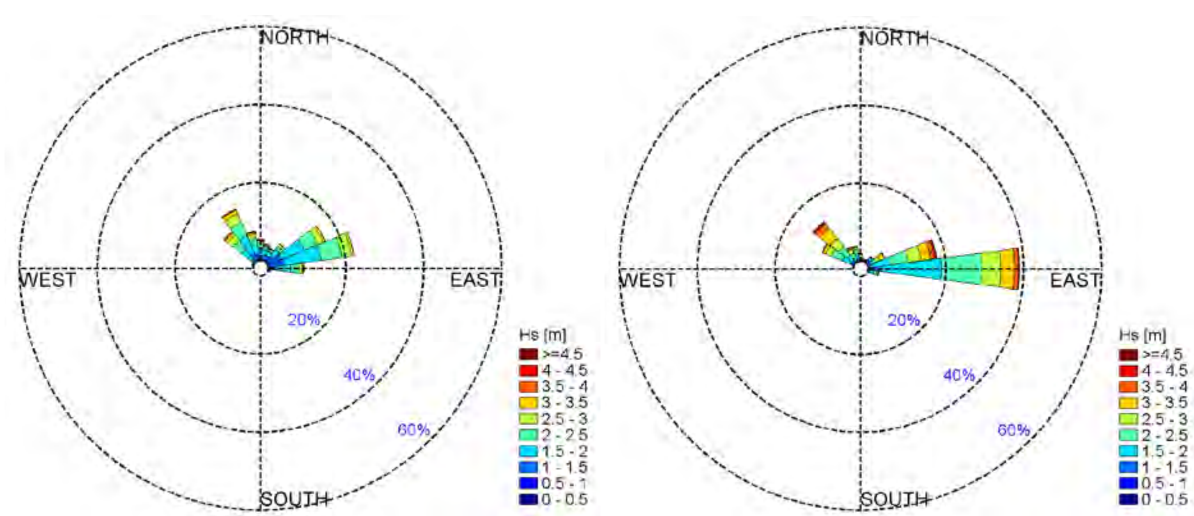

Figure 76- Rose plots of recorded (left) and hindcast (right) significant wave heights at the Pauwela buoy.

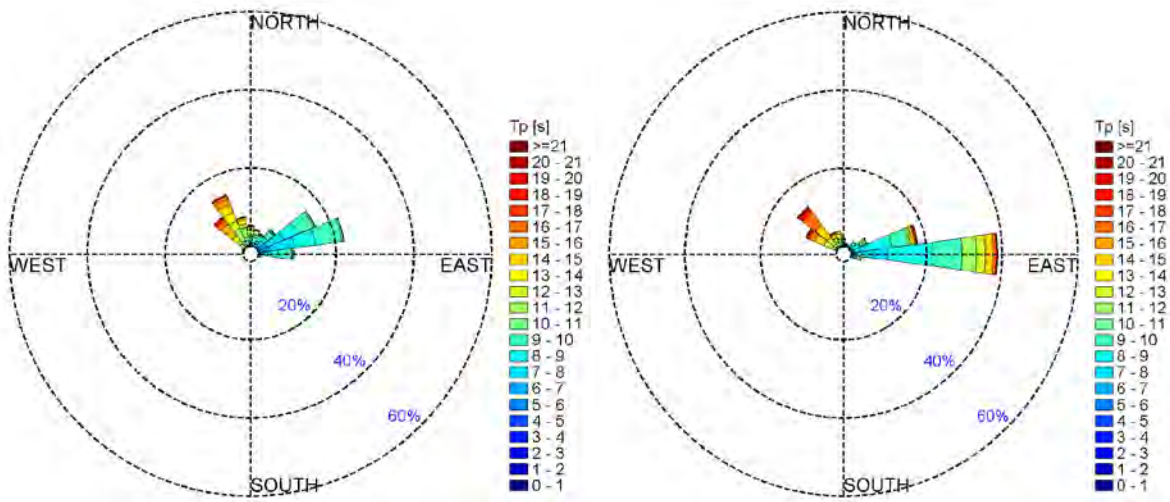

Figure 77- Rose plots of recorded (left) and hindcast (right) peak periods at the Pauwela buoy.

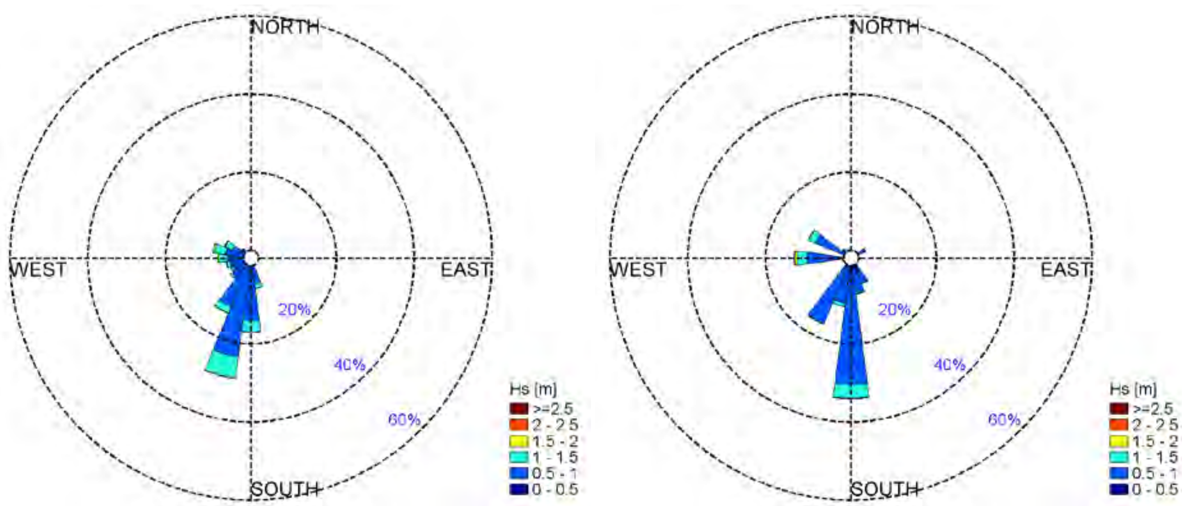

Figure 78- Rose plots of recorded (left) and hindcast (right) significant wave heights at the Kaumalapau buoy.

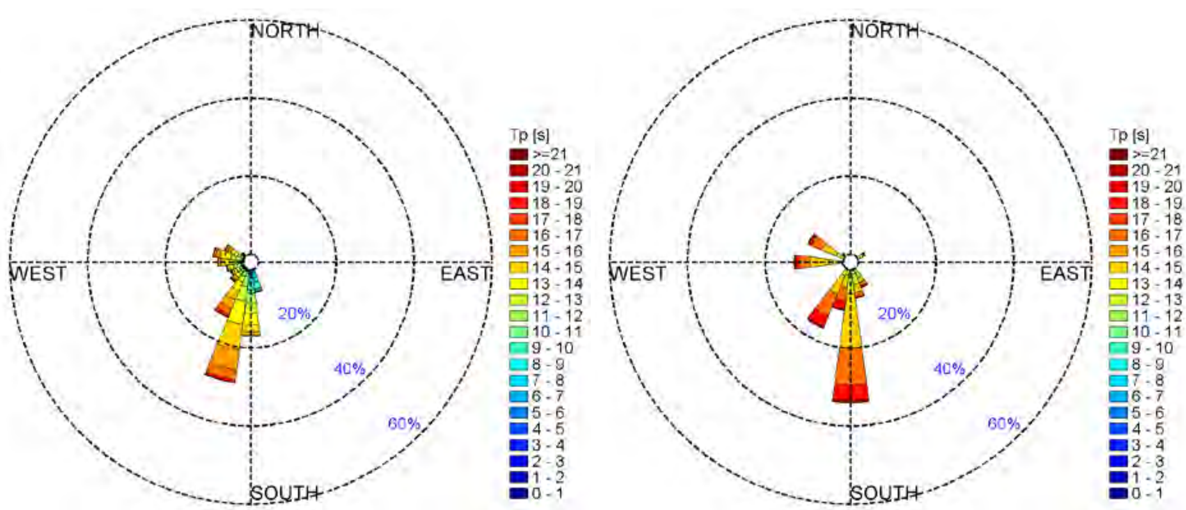

Figure 79- Rose plots of recorded (left) and hindcast (right) peak periods at the Kaumalapau buoy.

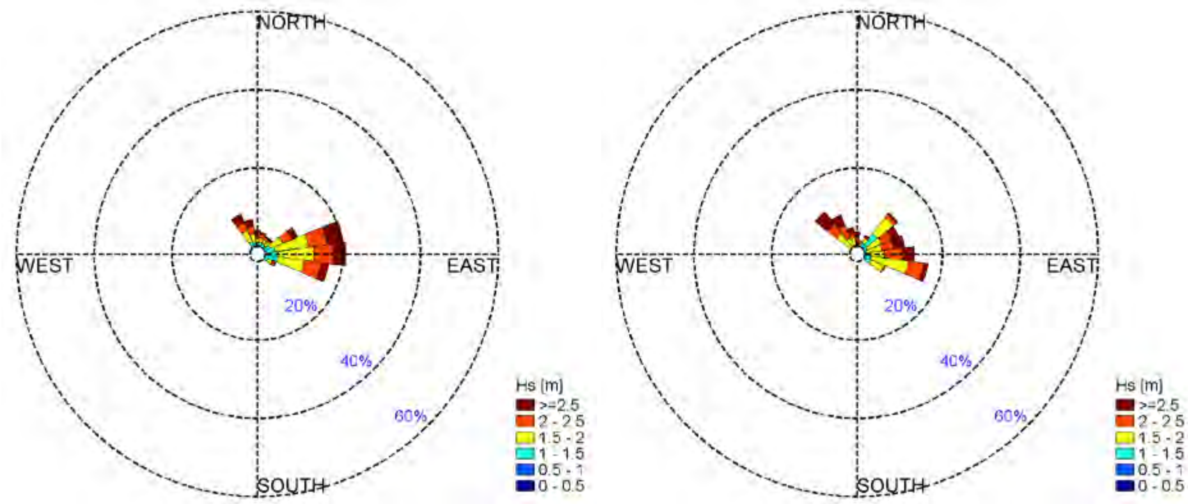

Figure 80- Rose plots of recorded (left) and hindcast (right) significant wave heights at the Hilo buoy.

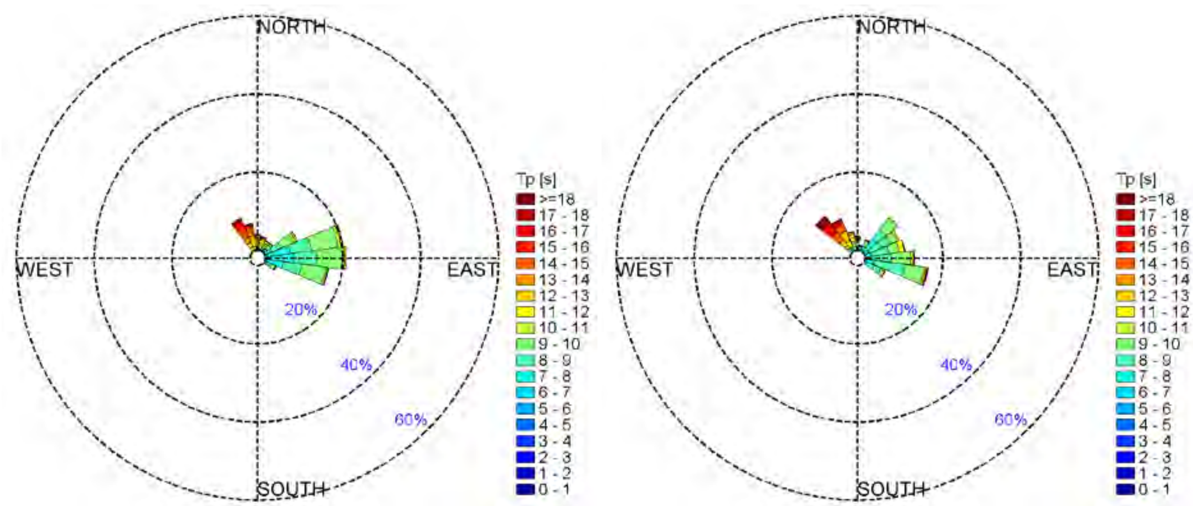

Figure 81- Rose plots of recorded (left) and hindcast (right) peak periods at the Hilo buoy.

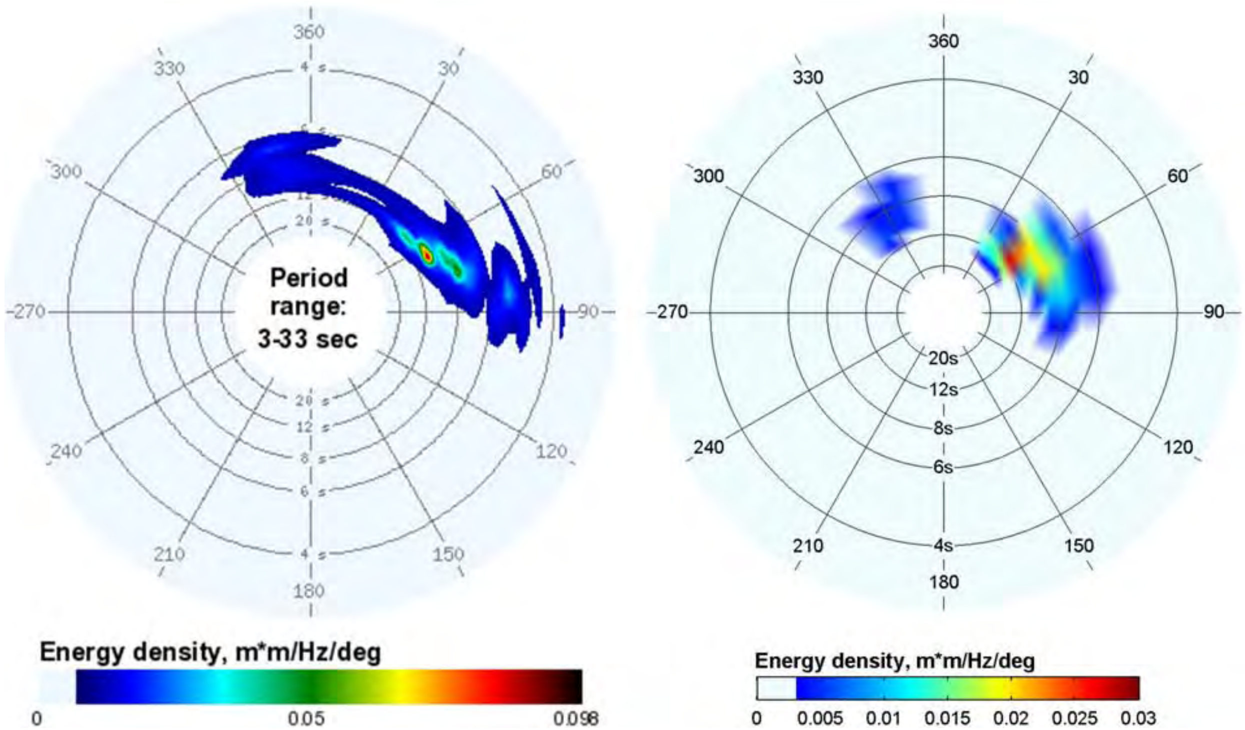

Figure 82- Two-dimensional spectra estimated from WETS Waverider records (left) and hindcast model (right) at 4:00 PM May 5, 2013.

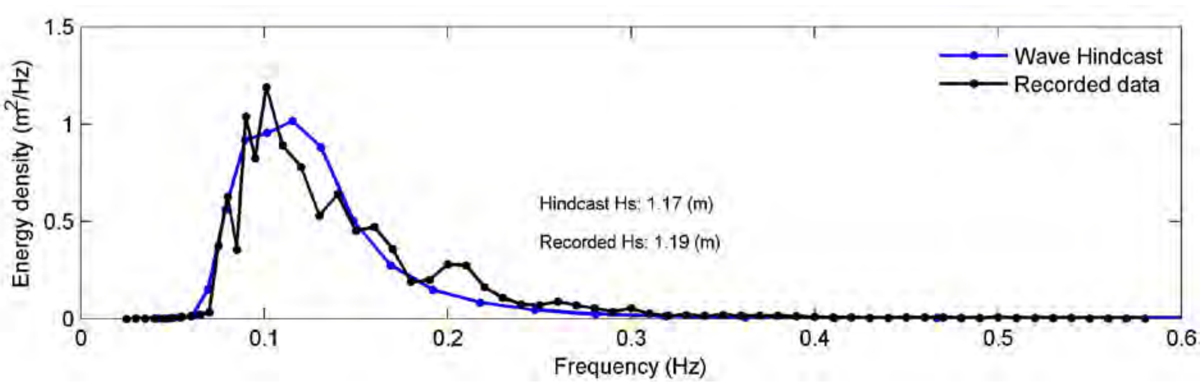

Figure 83- One-dimensional spectra estimated from WETS Waverider records and hindcast model at 4:00 PM May 5, 2013.

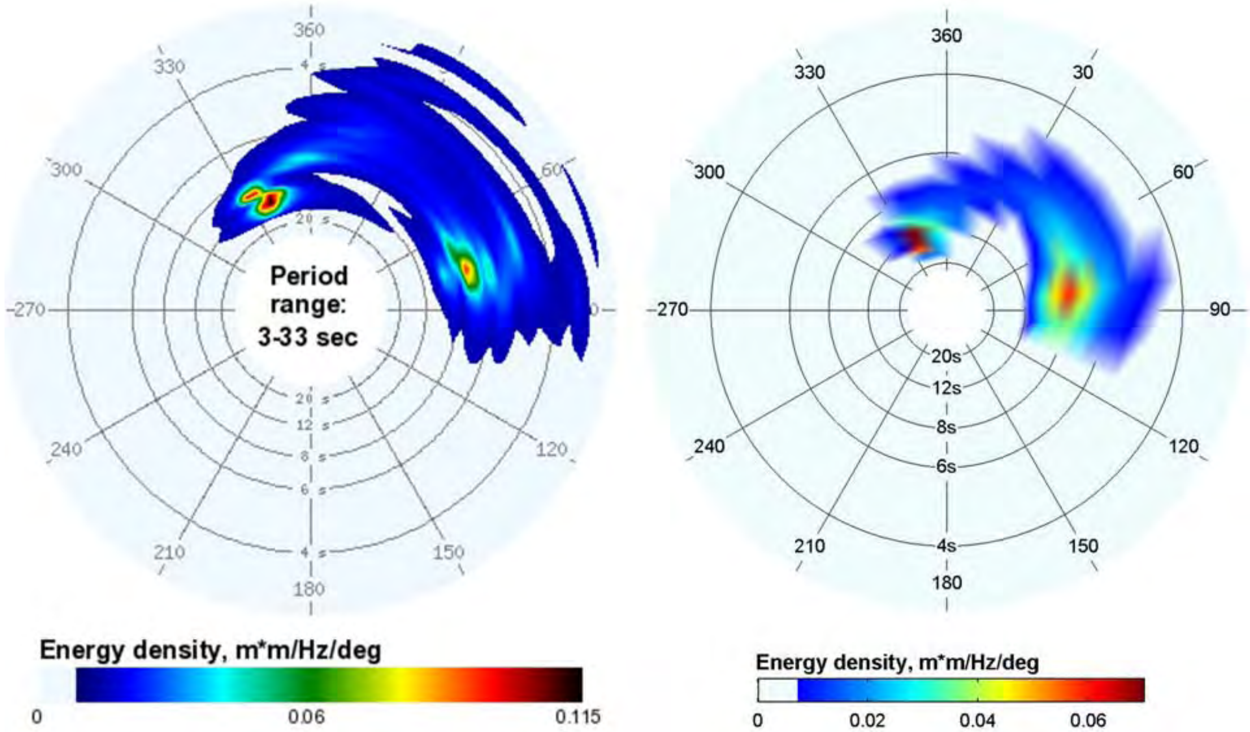

Figure 84- Two-dimensional spectra estimated from WETS Waverider records (left) and hindcast model (right) at 1:00 AM January 4, 2013.

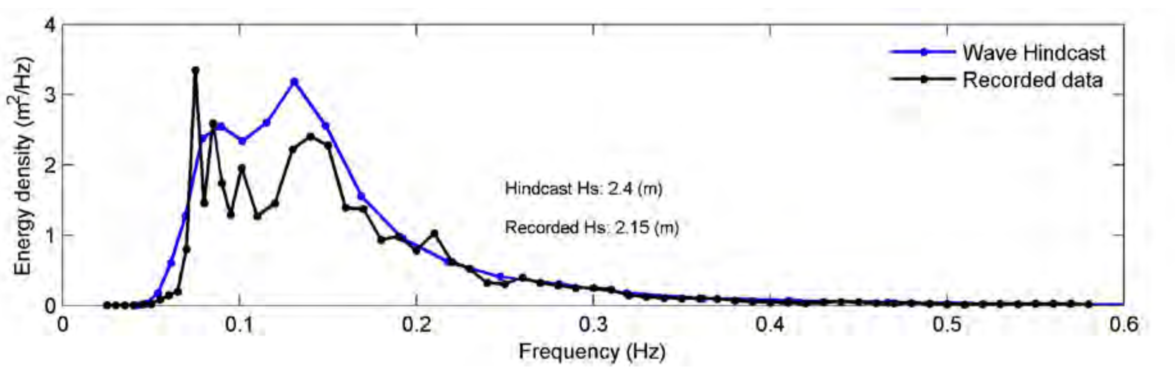

Figure 85- One-dimensional spectra estimated from WETS Waverider records and hindcast model at 1:00 AM January 4, 2013.

4. Wave Energy Resource Assessment

After validating the model with offshore and nearshore buoy measurements, we compiled statistics of the sea state and wave power parameters from the SWAN hindcast at WETS and the other five potential sites around the islands. Although the climate is not stationary, the 34-year hindcast covers several interannual cycles to reduce biases in the statistics (Stopa *et al*., 2013a). WETS and the potential site Kaneohe II, which are located offshore of the Marine Corps Base in Kaneohe, Oahu, share similar wave conditions. The other 4 potential sites at Kilauea, Pauwela, Upolu, and South Point of the neighbor islands are exposed to different wave components to contrast the statistics of the Oahu sites.

4.1 WETS and Kaneohe II, Oahu

WETS and the adjacent site Kaneohe II on the windward shore of Oahu are dominated by year-round wind waves from the east and swells from North Pacific storms in the winter. We compiled monthly statistics of the hindcast wave parameters from 1979 through 2013 to characterize the sea state and energy resource.

Figures 86 to 91 illustrate the seasonal distributions of the significant wave height, wave power, energy period, spectral width, direction of the maximum directionally resolved wave power, and the directionality coefficient at WETS (see Section 2.2 for definition). The plots show the monthly mean values as well as the 5^{th} and 95^{th} percentiles to indicate the range. The north swells augment the wave energy during the winter months. The monthly average significant wave height increases from 1.47 m in August to 2.0 m in December. The mean wave power flux follows the same pattern with 7.7 kW/m in August and 21.7 kW/m in December. The monthly average parameters highlight seasonal wave characteristics useful for planning and operations of wave energy converters. Since the wind wave and swell events have time scale of several days, their variations can be better illustrated with the daily mean significant wave height and power in Figures A1 and A2 for WETS and Kaneohe II (see Appendix A).

The wind waves become dominant in the summer resulting in shorter energy periods. The monthly mean energy period decreases from 9.7 s in January to 6.6 s in July. The swells have a lesser influence on the spectral width due to their narrow frequency bands, but dominate the mean direction of the maximum resolved wave power. The mean direction varies from ENE in the summer to NNE in the winter associated with the arrival of the north swells amidst the background wind waves. The 5th and 95th percentage range corresponds to the window of incident wave directions at the semi-sheltered site. The wind waves show a slightly higher directionality coefficient in the summer in the absence of the north swells. Kaneohe II in shallower water follows the same seasonal patterns with slightly lower wave power, but the same energy period and spectral width and similar directional characteristics as shown in Figures 92 to 97. Tables B1 and B2 in Appendix B provide the monthly mean wave energy parameters estimated for WETS and Kaneohe II.

The six wave energy parameters are supplemented by the wavelength and wave steepness to illustrate the wave characteristics. Figures 98 and 99 show the monthly average as well as the 5 and 95 percentile at WETS. The wavelength decreases, while the steepness increases, from the winter to the summer due to transition of the swell to wind-wave dominated ocean conditions. The larger wave steepness indicates more nonlinear wave characteristics that might pose an issue for scaling of wave power from predefined linear transfer functions. Figures 100 and 101 show similar patterns for Kaneohe II. Overall, the monthly statistics show a larger range during the winter months due to the episodic north swell events.

Tables 2 and 3 sort the 1979-2013 wave hindcast by binned significant wave heights and energy periods, while Tables 4 and 5 provide the total wave energy flux (kWh/m) for WETS and Kaneohe II. The results for the two sites are very similar due to their proximity. The wind waves, in the range of 1-2 m significant wave height and 6-8 s energy period, have high occurrence of 40% and contribute to 23 % of the total energy at WETS. Tables 6 and 7 summarize the average wave power flux (kW/m) for the two sites. Despite the lower occurrence, the northwest swells have higher average wave power due to their longer energy periods and larger wave heights (Power $\approx H_s^2 T_e$). Since typical wave energy converters are tuned to specific periods, the energy flux and power estimated from a multi-modal sea state require additional interpretations. A rational approach would be to develop those parameters for the respective wave components through partition of the wave spectrum (e.g., Arinaga and Cheung, 2012).

Figure 102 plots the cumulative distributions of the hindcast significant wave height and the associated wave energy in terms of the percentage total at each site. WETS consists of slightly larger waves due to its more exposed location and deeper water. The waves at WETS and Kaneohe II are greater than 2.0 m for 25% and 19% of the time, but account for 69% and 61% of the total energy respectively. The wave period is not sensitive to the water depth. Figure 103 shows very similar cumulative distributions of the wave energy period and the associated wave energy contribution to the total at the two sites. The occurrences with wave energy period greater than 8 s is 42%, but contribute to approximately 65% of total energy at both locations. Figure 104 shows that the wave power flux at WETS and Kaneohe II is over 15 kW/m for 31% and 26% of time and that those events account for 63% and 59% of total energy respectively.

In summary, the results at WETS show strong seasonal variations of the wave conditions and resources for testing and evaluation of a wide variety of wave energy convertors.

4.2 Potential Sites on Neighbor Islands

The wave climate varies along the Hawaiian Island chain and the shores of the same island. The four potential sites on the neighbor islands present a range of wave conditions to supplement WETS. Figures 105 to 108 show the monthly statistics of the significant wave height at Kilauea, Pauwela, Upolu and South Point. The mean significant wave height increases from 1.2 to 2.56 m at Kilauea and 1.55 to 2.67 m at Pauwela from August to January and maintains in a small range of 1.37-1.79 m throughout the year at Upolu. South Point has the largest monthly average wave height of 1.83 m among the four sites in the summer and a gradual increase to 2.2 m in the winter.

The wave power in Figures 109 to 112 follows the same trend as the significant wave height at each site. Kilauea and Pauwela off the north shores of Kauai and Maui have similar seasonal patterns as WETS dominated by energetic winter swells. The mean wave power increases from less than 10 to over 50 kW/m from summer to winter. Upolu, which is located at the northern tip of Hawaiʻi Island, is shielded from the energetic northwest swells in the winter months and the south swells throughout the year. The monthly statistics show a lower level of power with more subtle seasonable variations compared to other sites. South Point is exposed to the heightened trade wind flow around Hawai‘i Island with significant local wave generation (Stopa *et al.*, 2011). Its wave power is augmented by year-round south swells and local storms to the west of the main Hawaiian Islands to exceed the monthly mean of 14 kW/m in the summer and up to 25 kW/m in the winter. Figures A3 to A6 in Appendix A show the daily mean significant wave height and power for Kilauea, Pauwela, Upolu, and South Point.

Figures 113 to 116 show the distributions of the energy period at the four sites. The dominating north swell dramatically increases the mean energy period from 6.6 to 11.8 s at Kilauea and 6.4 to 11.3 s at Pauwela in wintertime. Dominated by the year-around trade wind waves with intermittent north swells in winter, Upolu has 6.4 s mean wave energy period in June with only a slight increase to 8.8 s in January. With a mix of south swells and trade wind waves, South Point has a small range of the averaged wave energy period of 8.3-9.1 s throughout the year. The locally generated seas together with the persistent south swells also contribute to a largest spectral width among the four sites as illustrated in Figures 117 to 120.

The wave direction and its spreading also play a role in the efficiency of some wave energy converters. Figures 121 to 124 show the direction of the maximum directionally resolved wave power at the four sites. At Kilauea, Pauwela, and Upolu, the direction typically follows the dominant wave component that transitions from northeast to north from the summer to the winter. The direction at South Point changes from south during the summer to southwest in the winter due to mixing of the south swells with waves generated by local storms from the west and northwest swells that wrap around the Kauai and Oahu. Figures 125 to 128 plot the directionality coefficient at the four sites, among which, Kilauea gives the largest value in the winter due to its open location to the energetic northwest swells. The year-round south swells and wind waves at South Point result in the lowest directionality coefficient. Figures 129 to 136 show discernible increase of the wave length and decrease of the wave steepness at Kilauea, Pauwela, and Upolu site from the summer to winter, while almost the same wave length and wave steepness throughout the year at South Point. Tables B3 and B6 in Appendix B list the monthly mean wave energy parameters estimated for Kilauea, Pauwela, Upolu and South Point.

Tables 8-10 shows the occurrence, the wave energy flux (kWh/m), and the average wave power flux (kW/m) by binned significant wave heights and energy periods for Kilauea. Waves with significant wave height in 1.0-1.25 m and wave energy period in 6.25-6.50s have the highest occurrence, but contribute disproportionately less to the total wave energy flux because of the low level of average wave power. Tables 11-13, 14-16, and 17-19 show the same set of information and similar patterns for Pauwela, Upolu, and South Point respectively.

Figure 137 shows the cumulative distributions of the significant wave height and the associated wave energy in terms of the percentage total at each site. Events with significant wave height above 2 m occur 31%, 45%, 17% and 37% of the time, but account for 81%, 88%, 57%, and 76% of the total energy at Kilauea, Pauwela, Upolu and South Point, respectively. Figure 138 shows the results in terms of the energy period. Waves with energy period longer than 8 s have 58%, 51%, 28% and 69% occurrence and contribute disproportionately to 89%, 80%, 46% and 79% of the energy at Kilauea, Pauwela, Upolu and South Point, respectively. Figure 139 shows the cumulative distribution of the wave power flux and the corresponding contribution to the total wave energy. The events with wave power over 15 kW/m occurs 42%, 50%, 20%, and 54% of the time at Kilauea, Pauwela, Upolu and South Point, but produce 83%, 84%, 48%, and 76%

of the total wave energy respectively. Upolu at the northern tip of Hawai‘i Island has the lowest values among the four sites despite its direct exposure to the year-round trade wind waves. Similar to WETS and Kaneohe II, the occasional large waves contribute to the majority of the total energy at the potential sites.

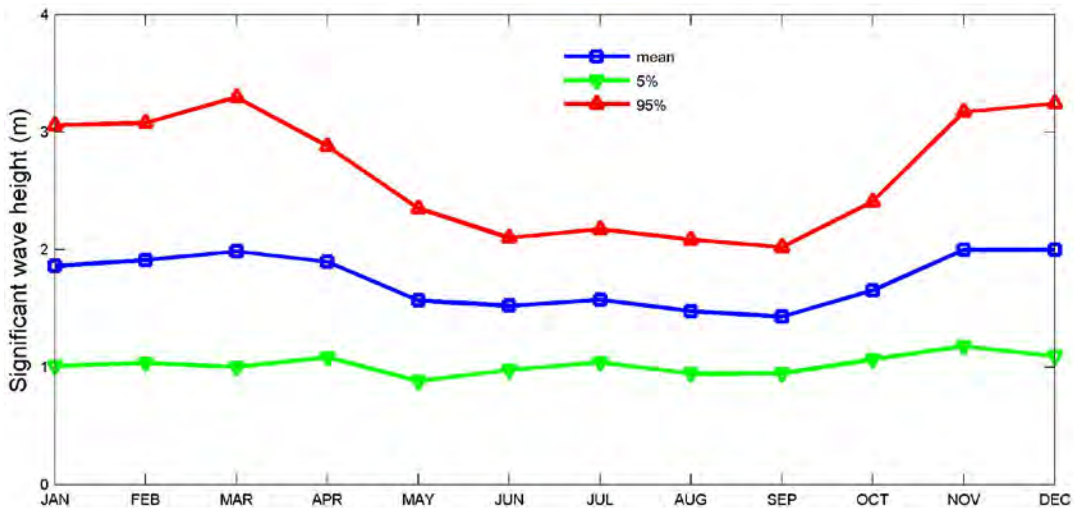

Figure 86– Monthly statistics of significant wave height at WETS.

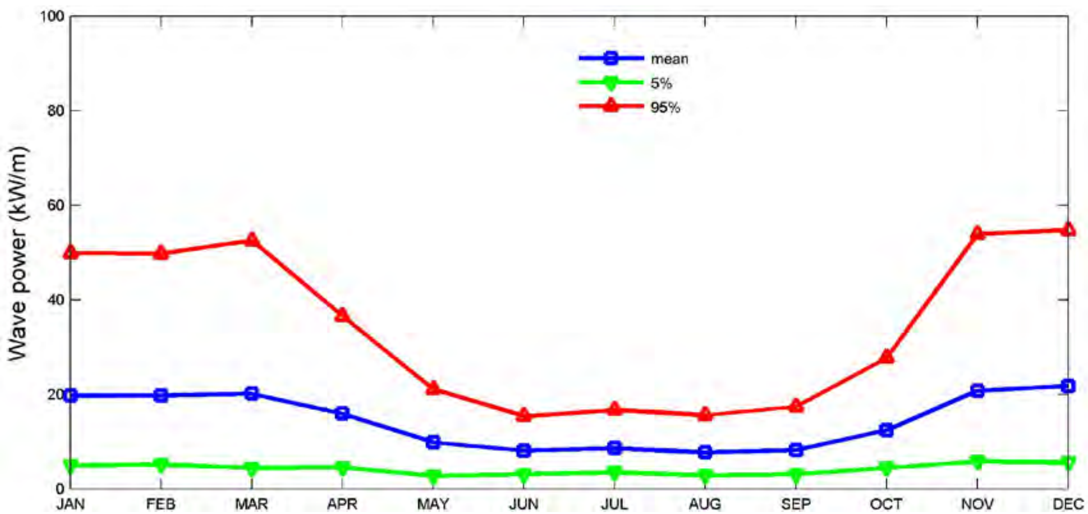

Figure 87– Monthly statistics of wave power at WETS.

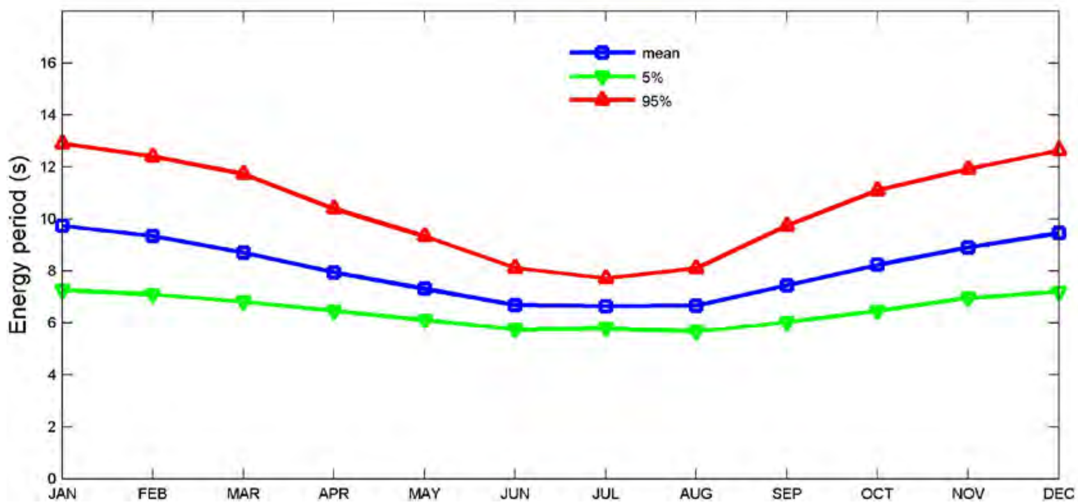

Figure 88– Monthly statistics of energy period at WETS.

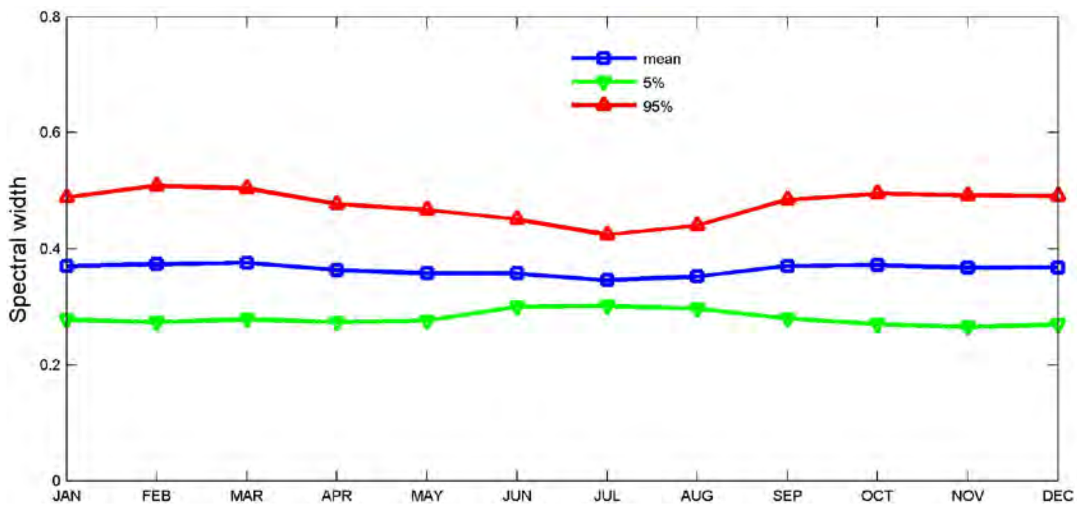

Figure 89– Monthly statistics of spectral width at WETS.

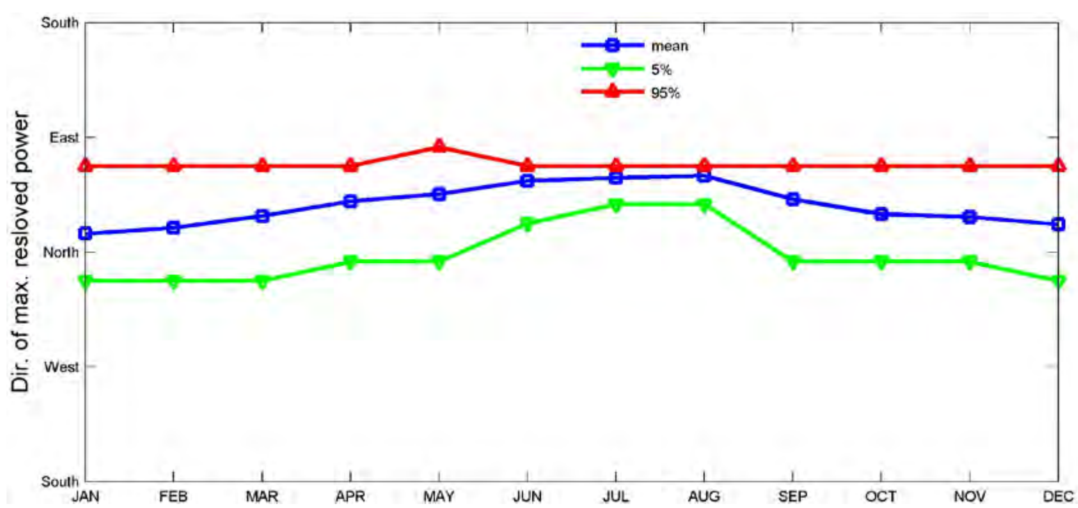

Figure 90– Monthly statistics of direction of maximum directionally resolved wave power at WETS.

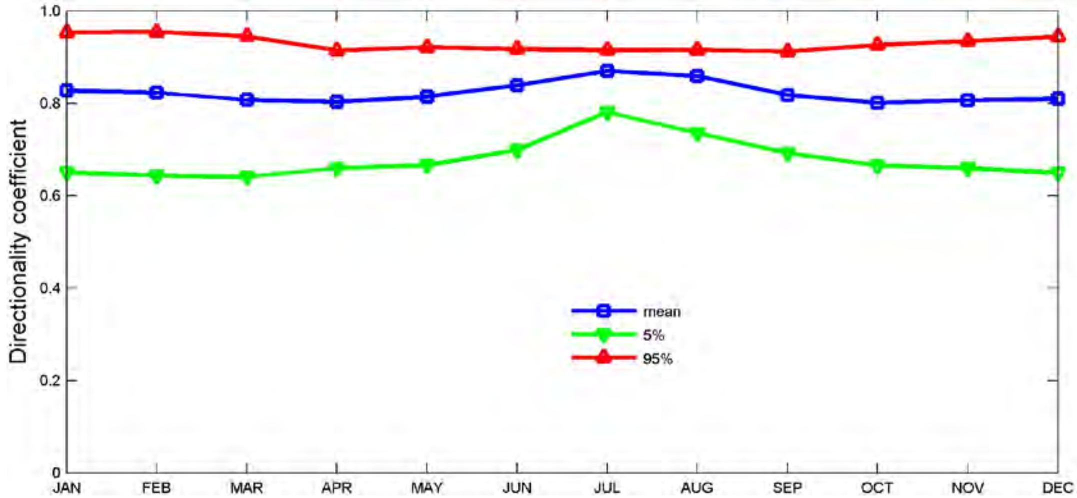

Figure 91– Monthly statistics of directionality coefficient at WETS.

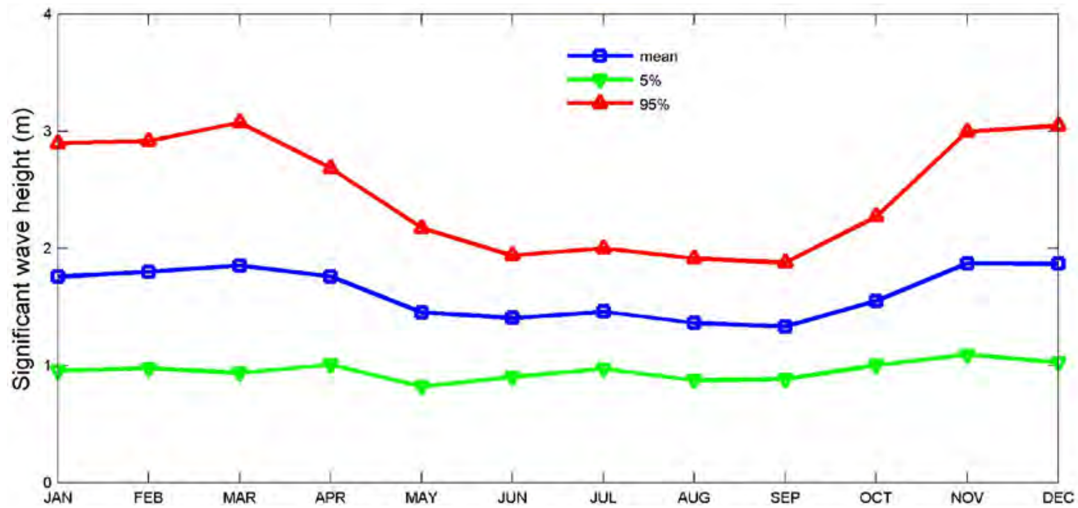

Figure 92– Monthly statistics of significant wave height at site Kaneohe II.

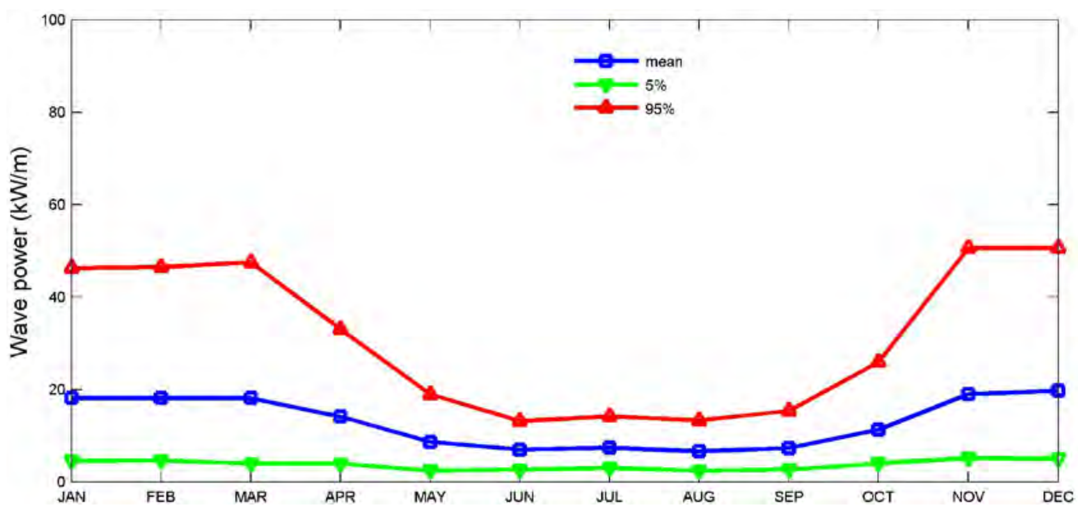

Figure 93– Monthly statistics of wave power at site Kaneohe II.

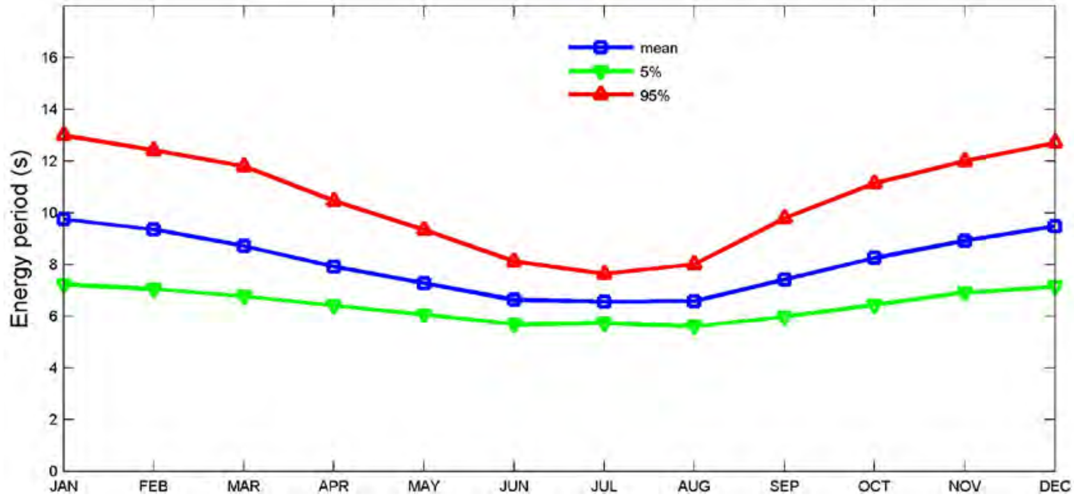

Figure 94– Monthly statistics of energy period at site Kaneohe II.

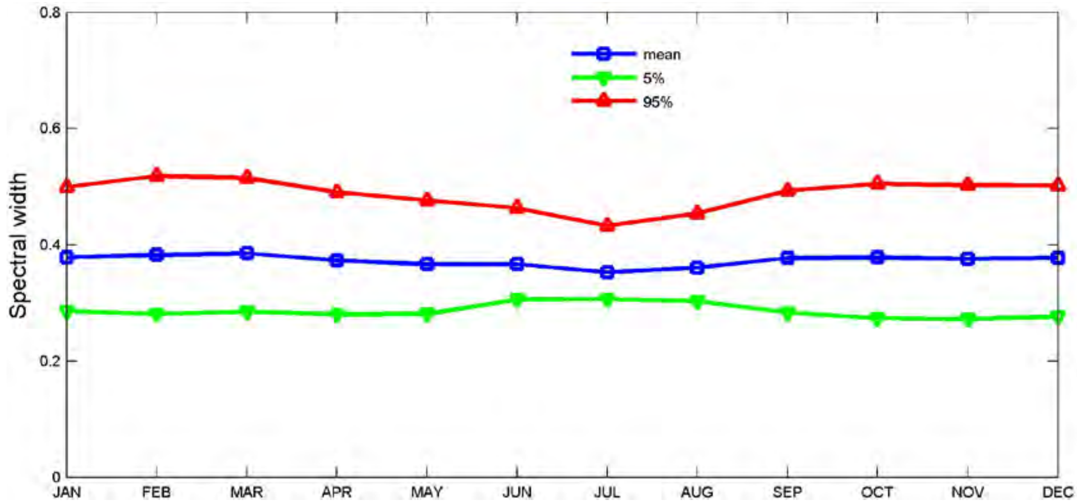

Figure 95– Monthly statistics of spectral width at site Kaneohe II.

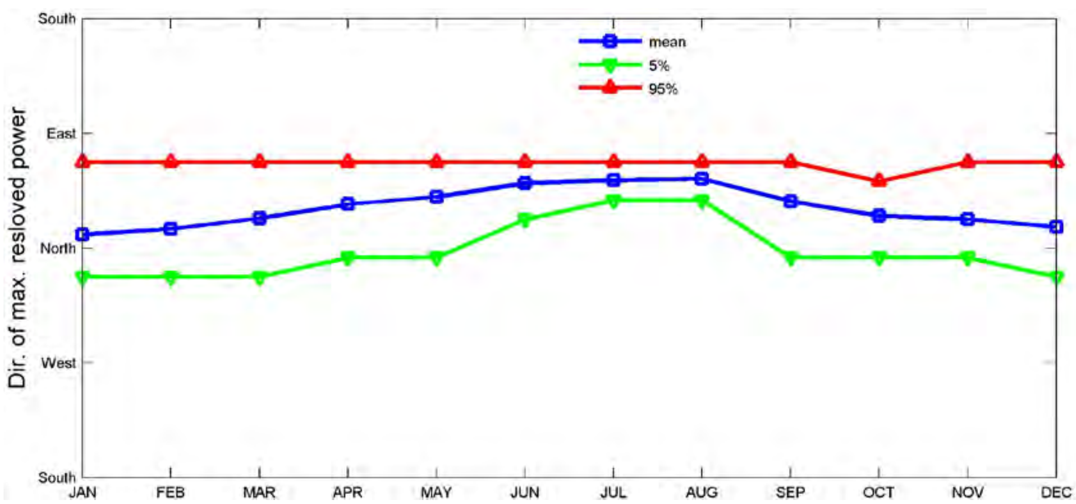

Figure 96– Monthly statistics of direction of maximum directionally resolved wave power at site Kaneohe II.

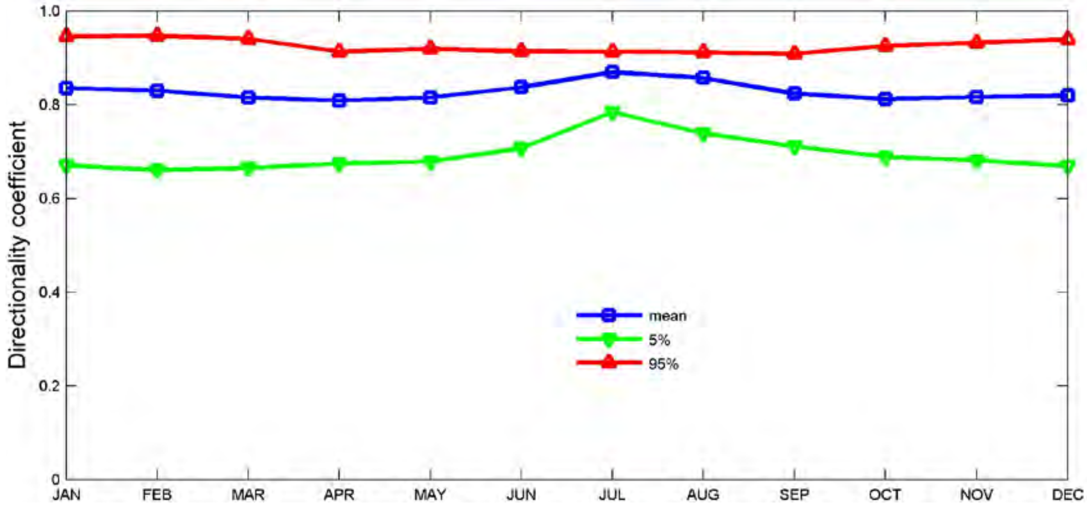

Figure 97– Monthly statistics of directionality coefficient at site Kaneohe II.

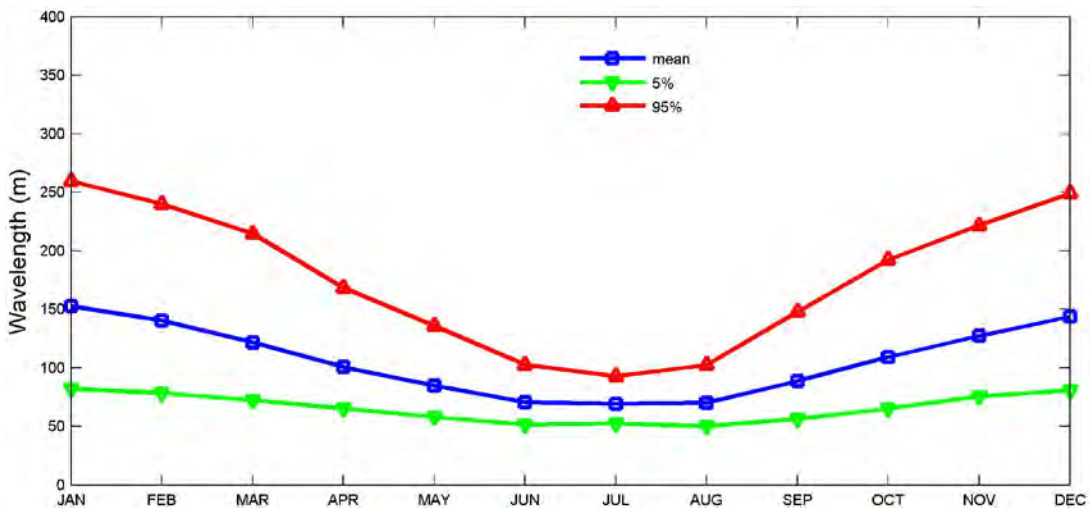

Figure 98– Monthly statistics of wavelength at WETS.

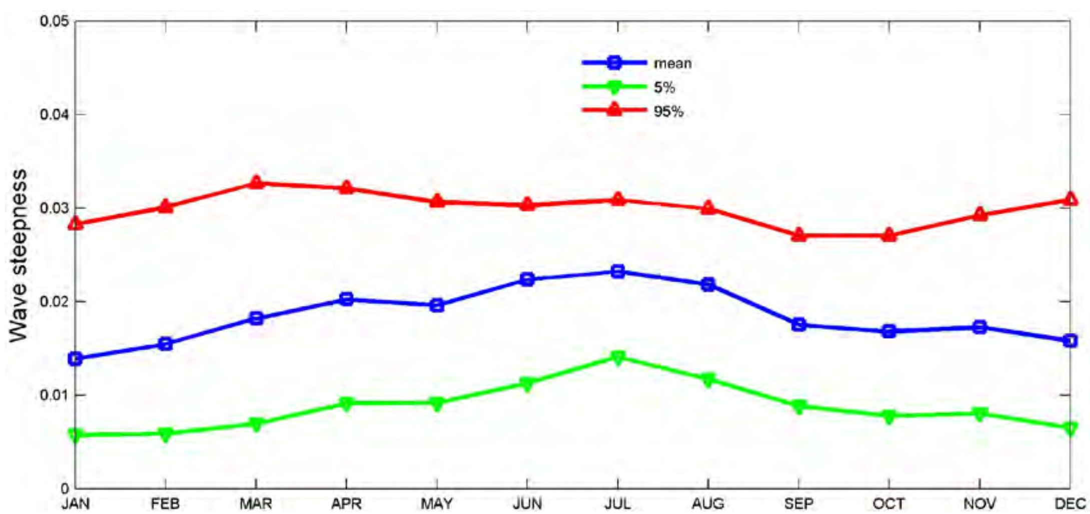

Figure 99– Monthly statistics of wave steepness at WETS.

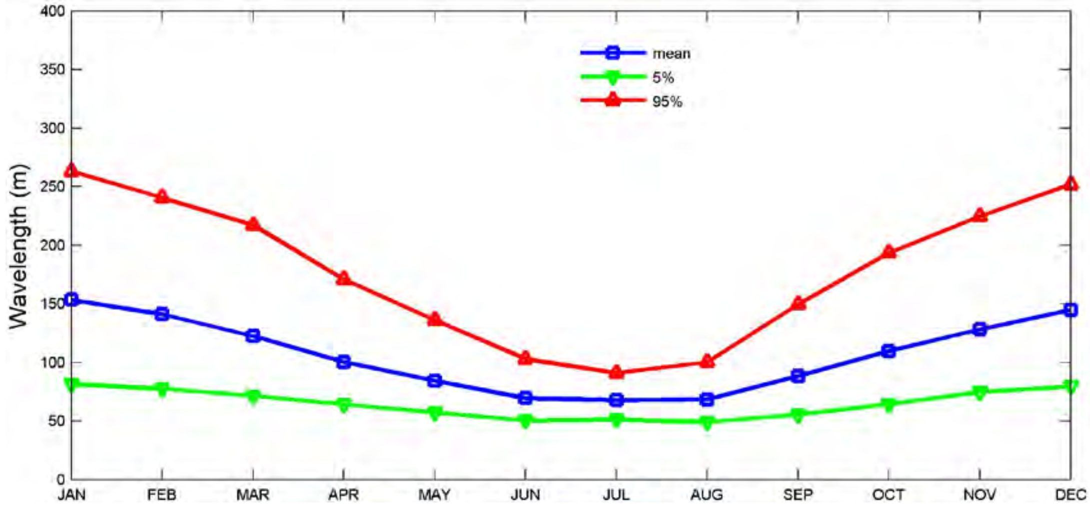

Figure 100– Monthly statistics of wavelength at site Kaneohe II.

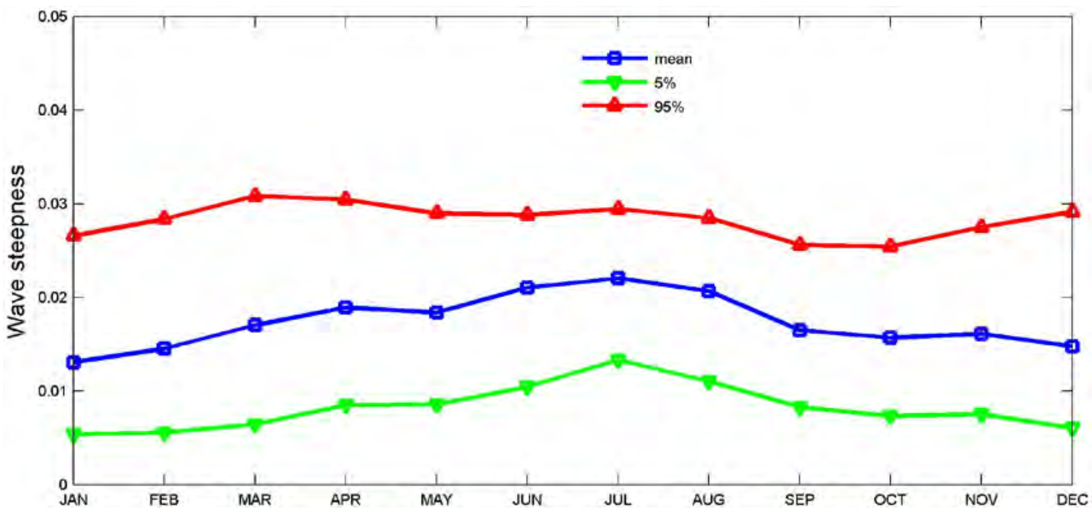

Figure 101– Monthly statistics of wave steepness at site Kaneohe II.

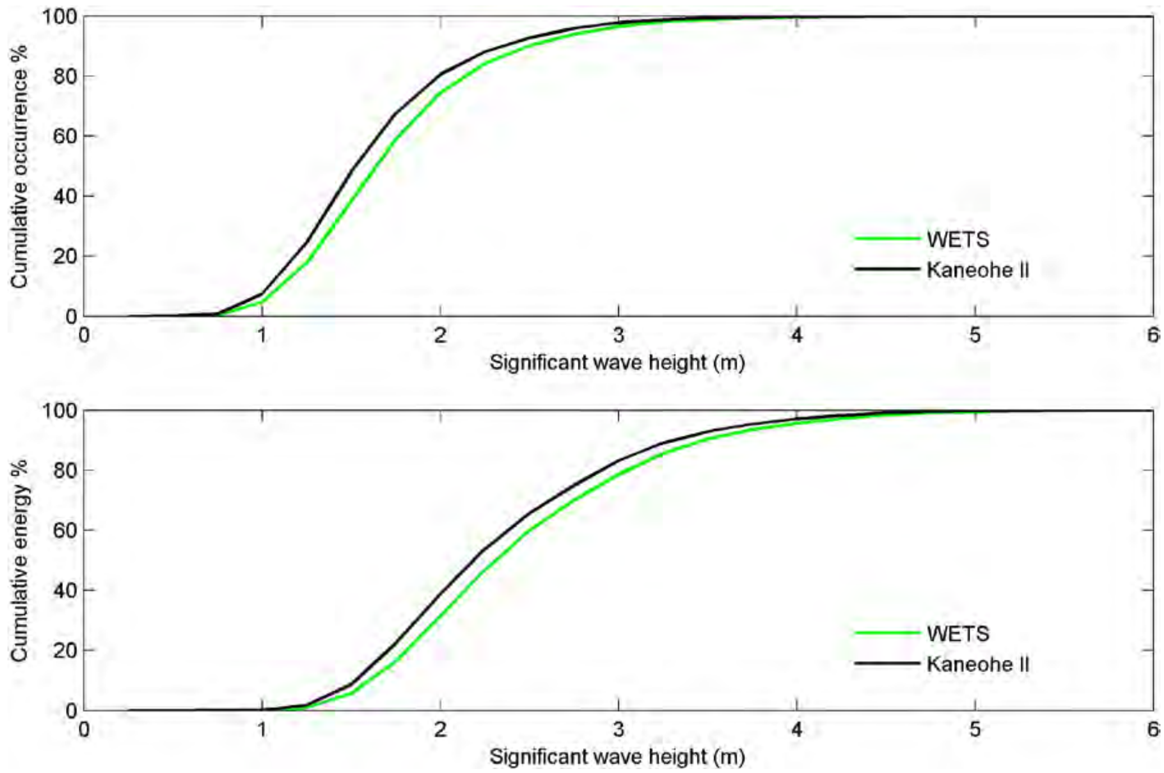

Figure 102– Cumulative distributions of significant wave height (upper) and the associated wave energy (lower) in terms of the percentage total at WETS and site Kaneohe II.

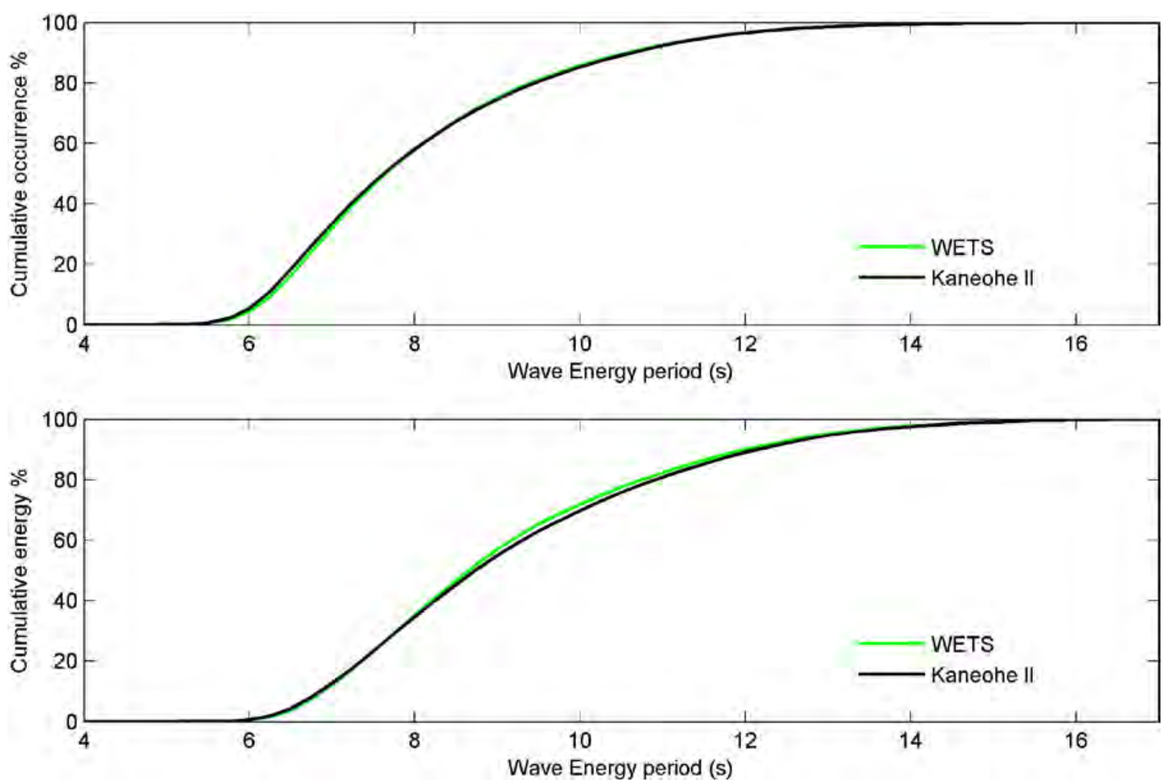

Figure 103– Cumulative distributions of wave energy period (upper) and the associated wave energy (lower) in terms of the percentage total at WETS and site Kaneohe II.

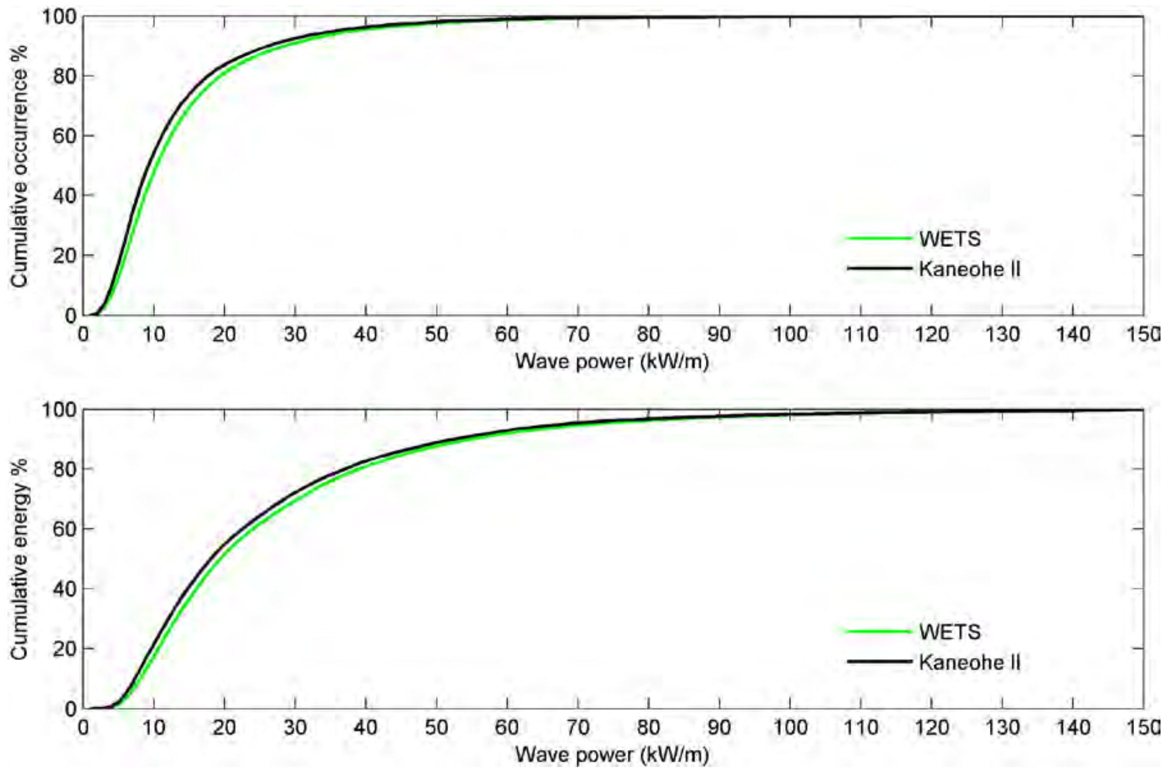

Figure 104 – Cumulative distributions of wave power (upper) and the associated wave energy (lower) in terms of the percentage total at WETS and site Kaneohe II.

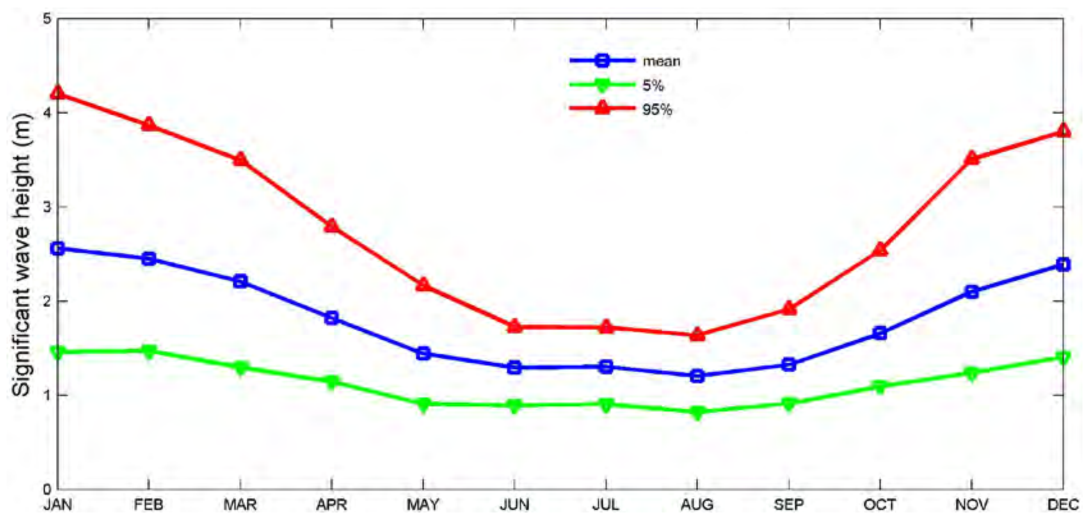

Figure 105– Monthly statistics of significant wave height at site Kilauea.

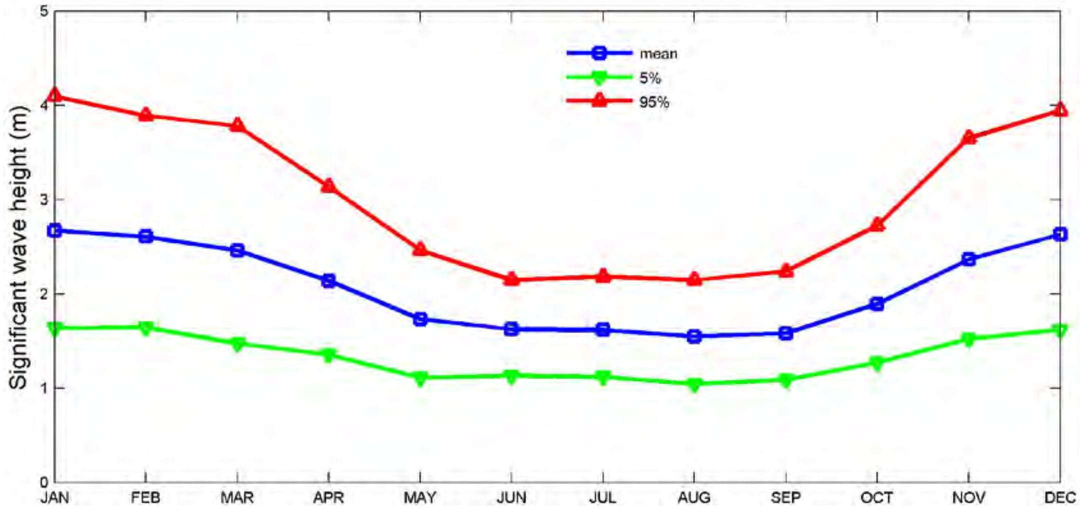

Figure 106– Monthly statistics of significant wave height at the site Pauwela.

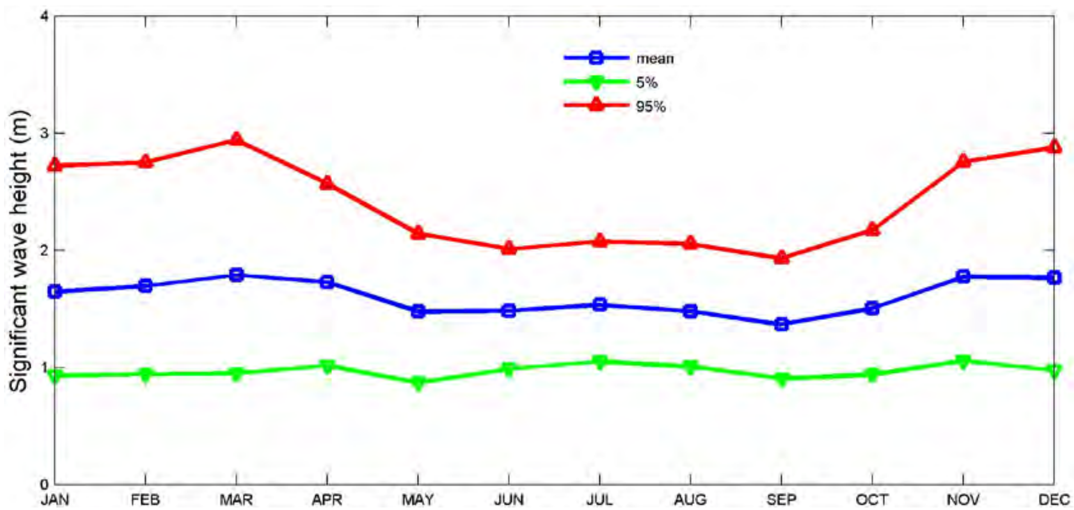

Figure 107– Monthly statistics of significant wave height at site Upolu.

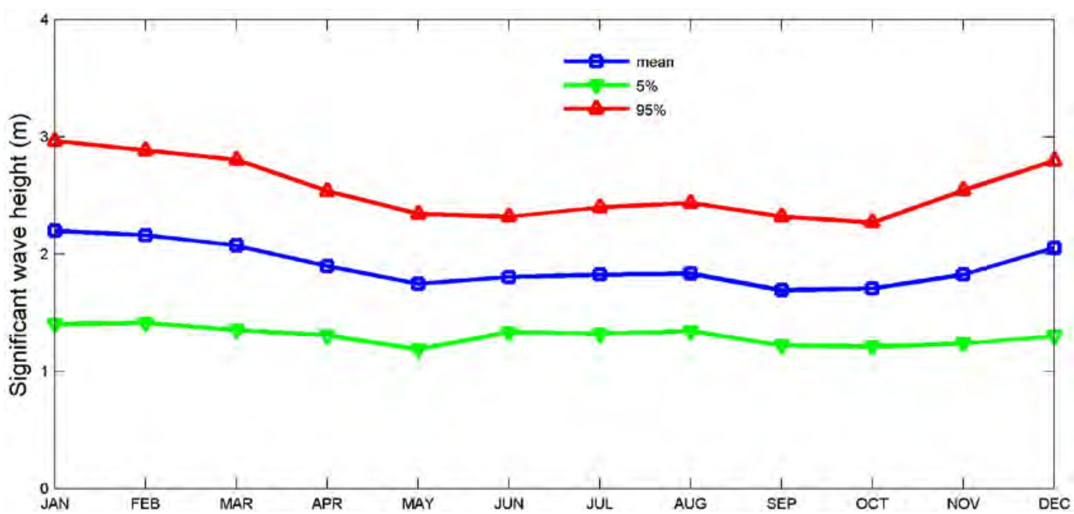

Figure 108– Monthly statistics of significant wave height at site South Point.

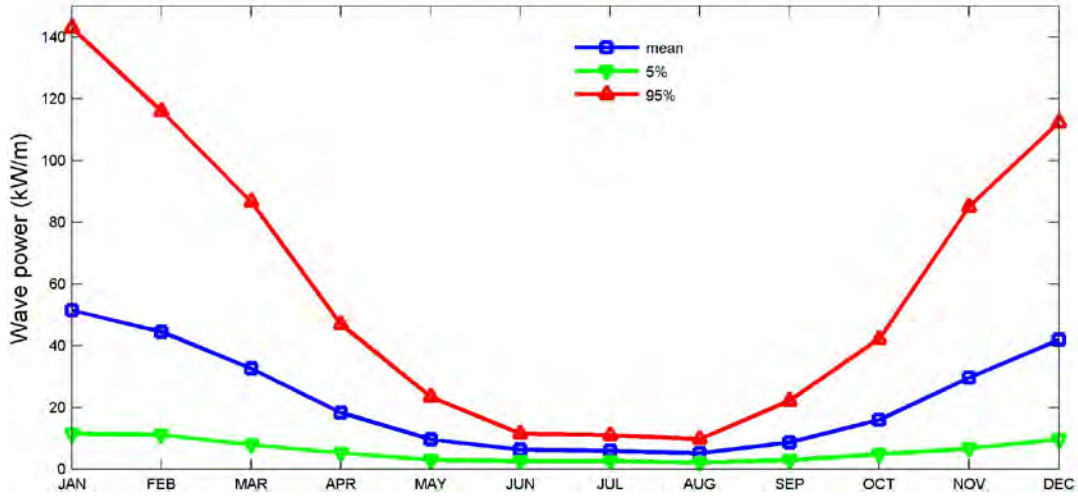

Figure 109– Monthly statistics of wave power at site Kilauea.

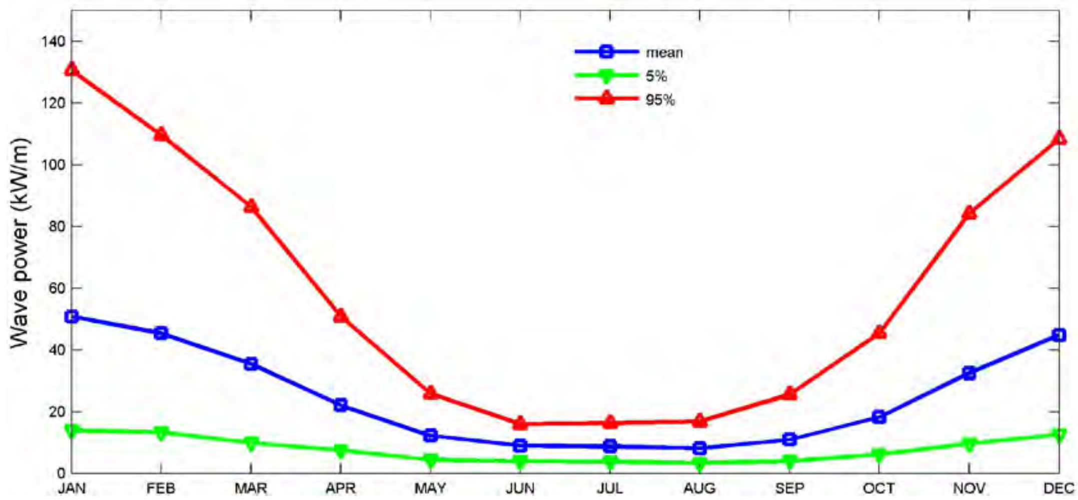

Figure 110– Monthly statistics of wave power at site Pauwela.

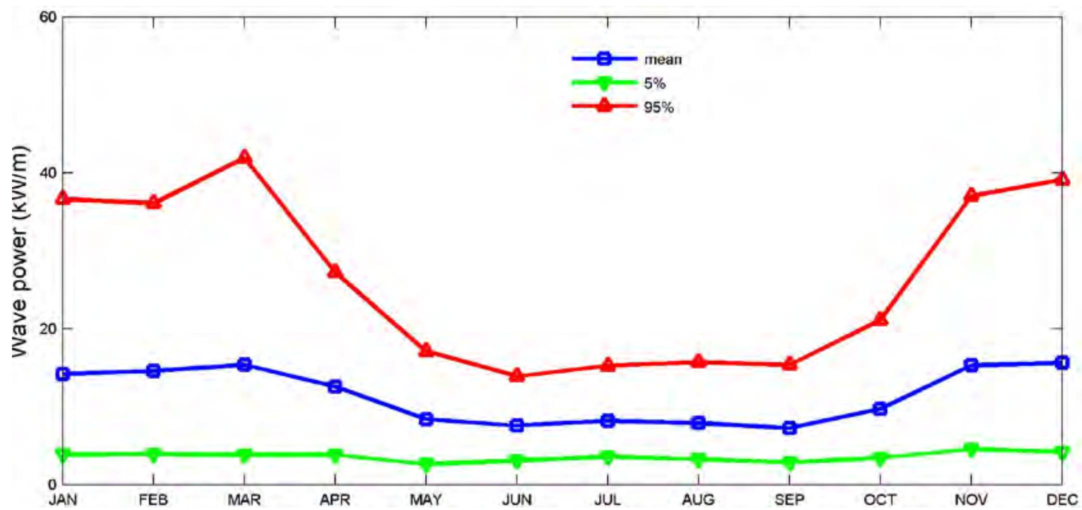

Figure 111– Monthly statistics of wave power at site Upolu.

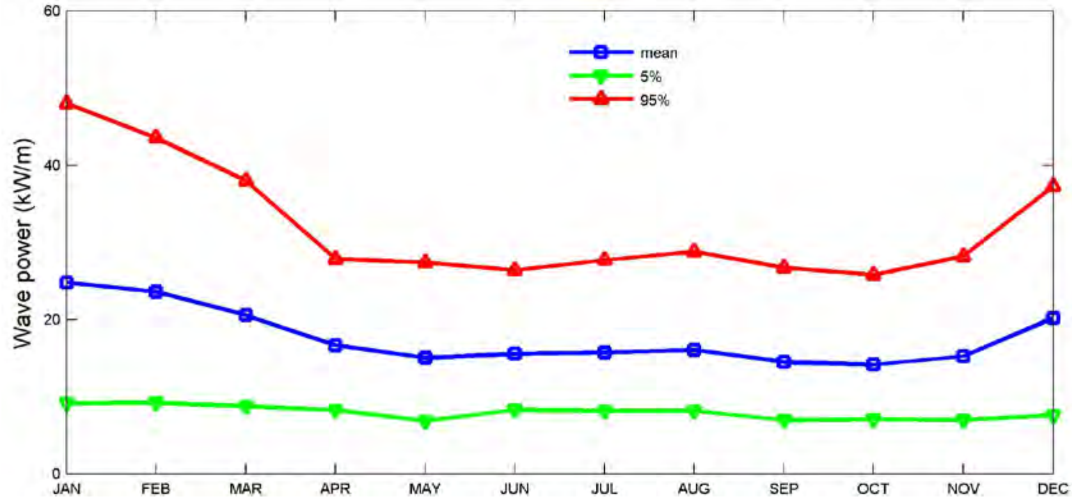

Figure 112– Monthly statistics of wave power at site South Point.

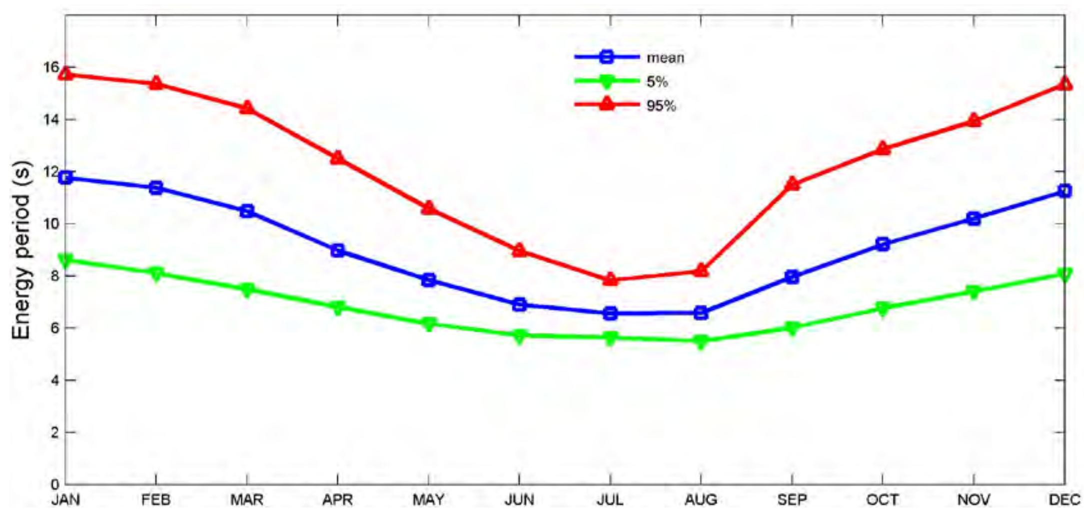

Figure 113– Monthly statistics of energy period at site Kilauea.

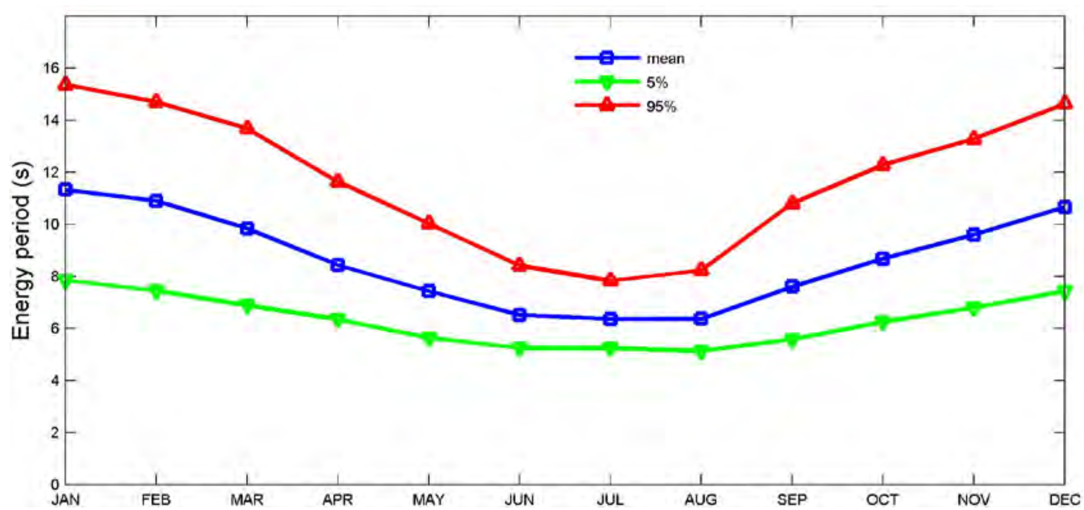

Figure 114– Monthly statistics of energy period at site Pauwela.

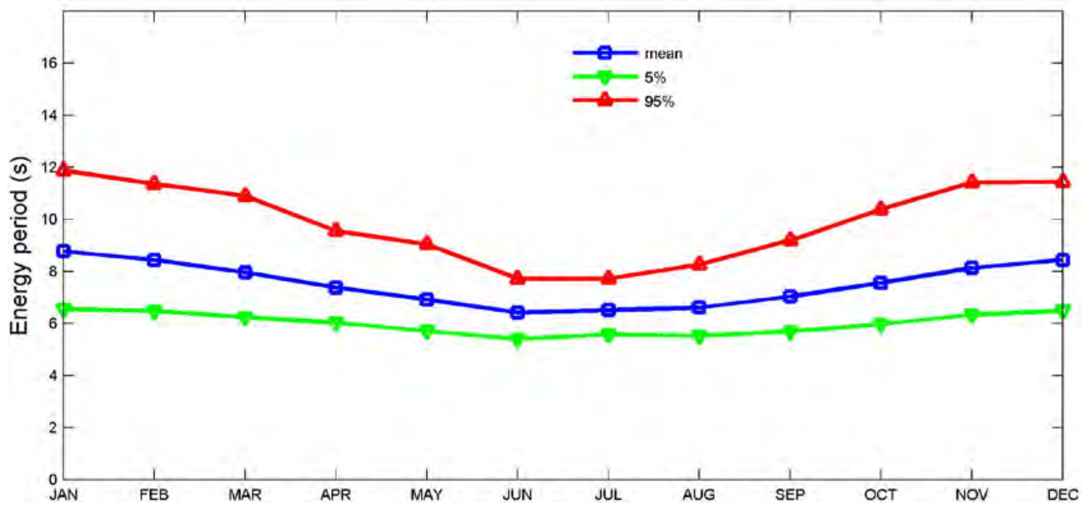

Figure 115– Monthly statistics of energy period at site Upolu.

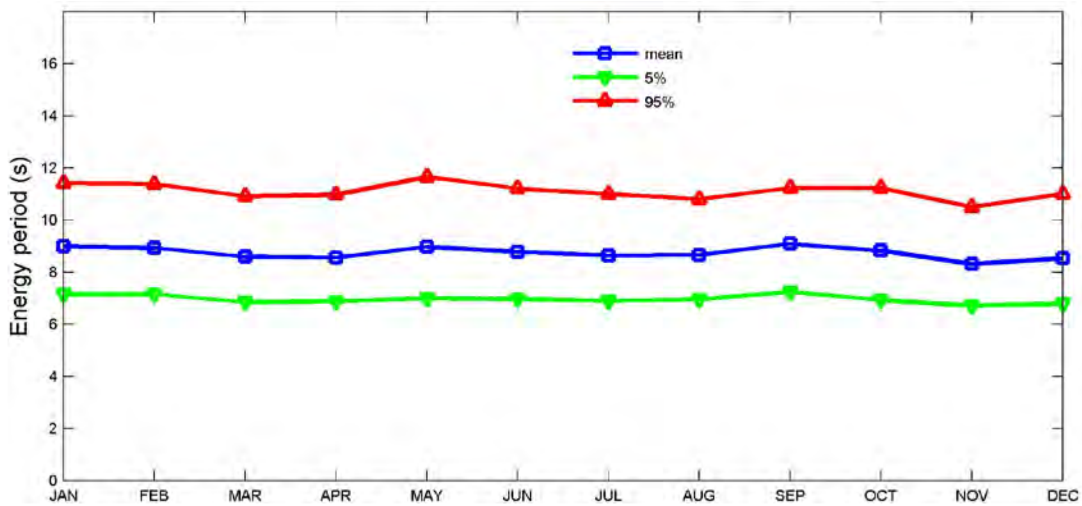

Figure 116– Monthly statistics of energy period at site South Point.

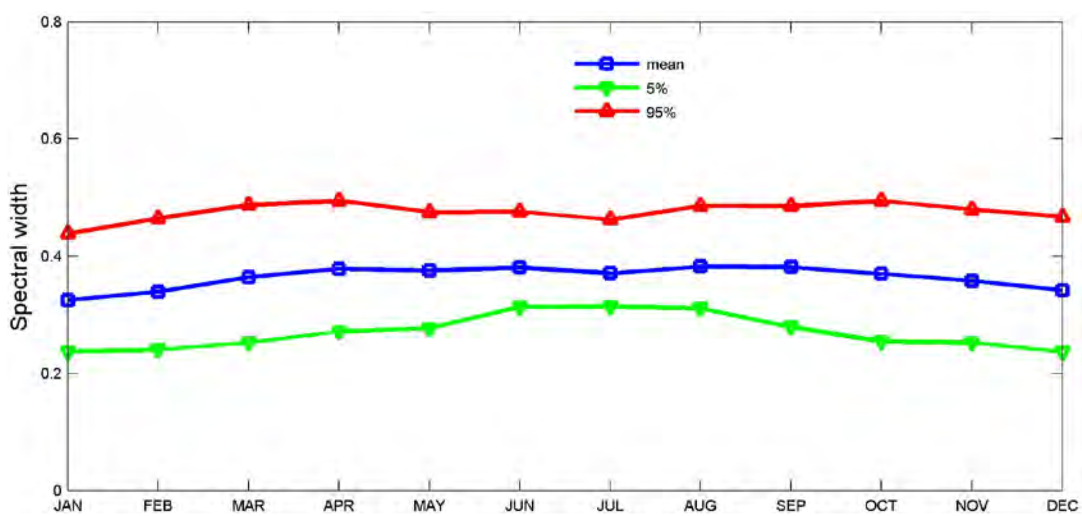

Figure 117– Monthly statistics of spectral width at site Kilauea.

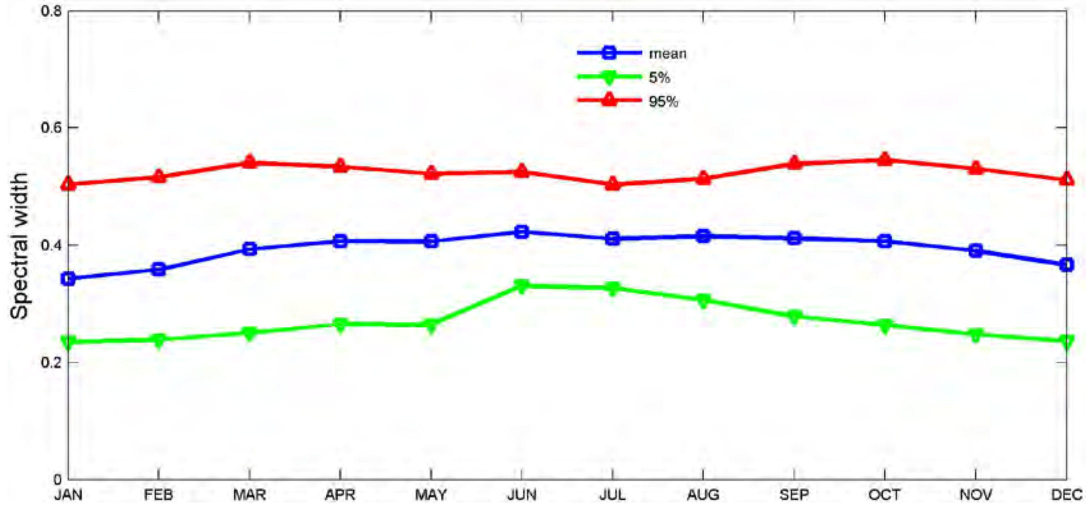

Figure 118– Monthly statistics of spectral width at site Pauwela.

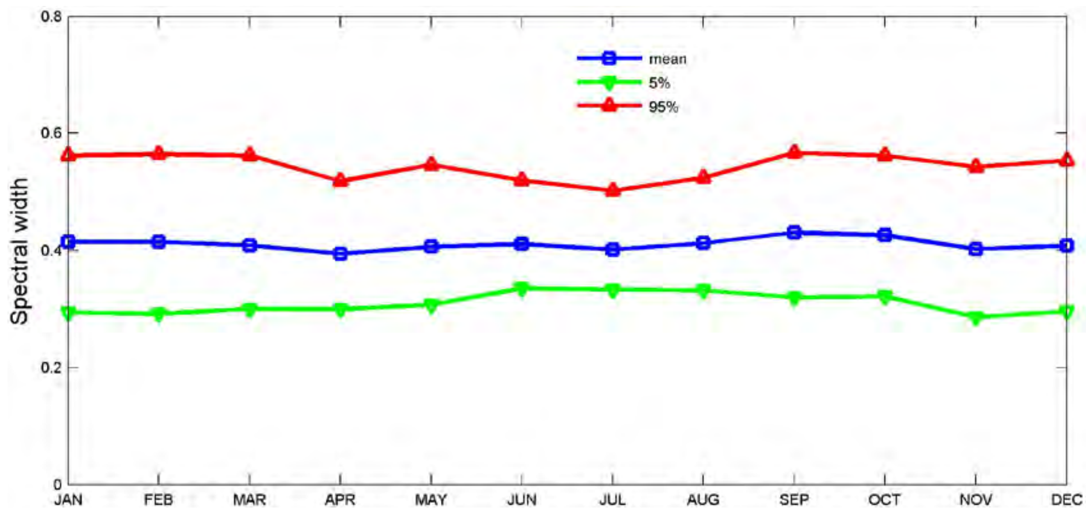

Figure 119– Monthly statistics of spectral width at site Upolu.

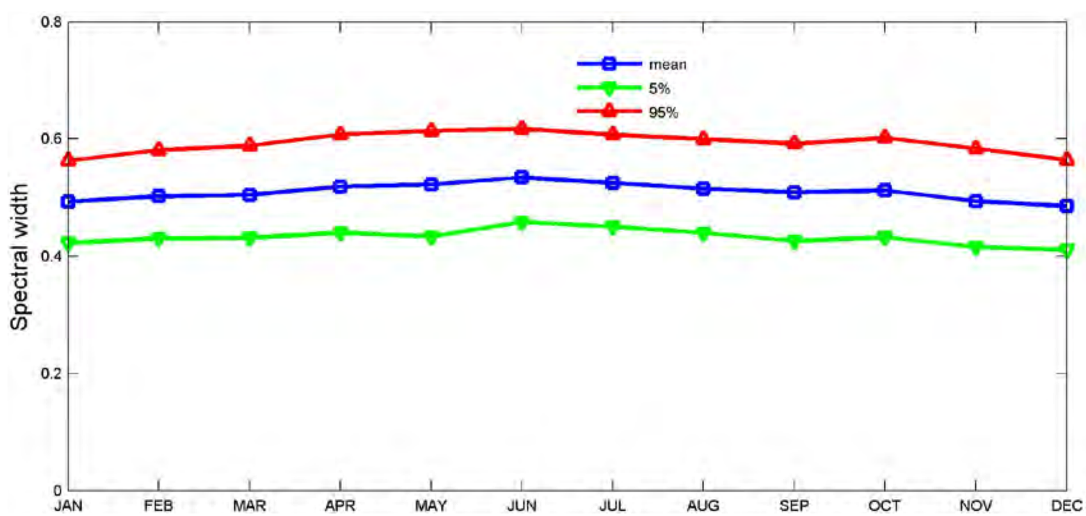

Figure 120– Monthly statistics of spectral width at site South Point.

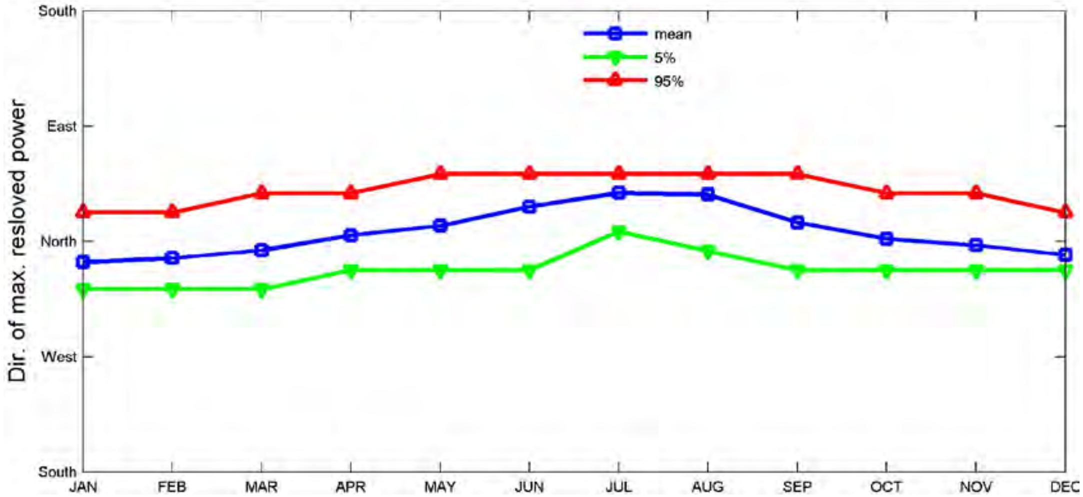

Figure 121– Monthly statistics of direction of maximum directionally resolved wave power at site Kilauea.

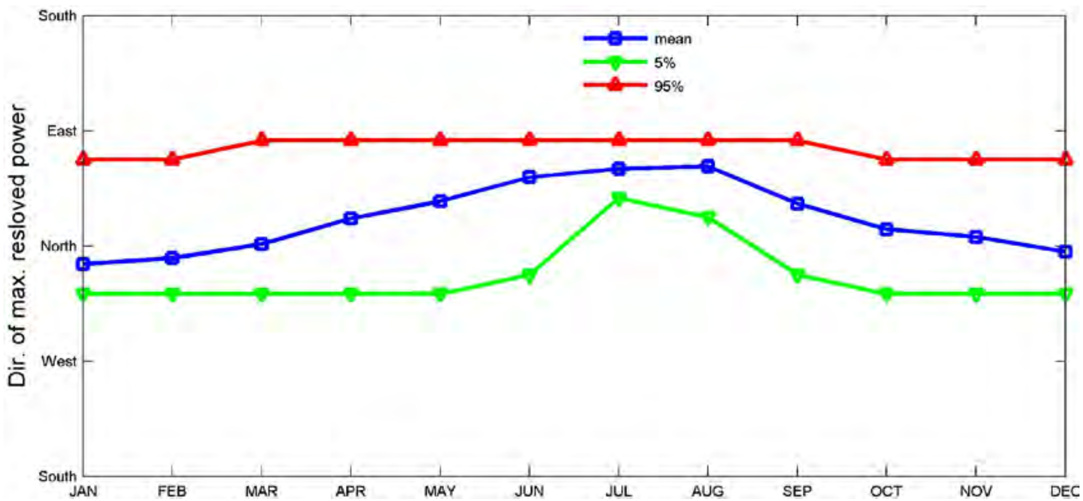

Figure 122– Monthly statistics of direction of maximum directionally resolved wave power at site Pauwela.

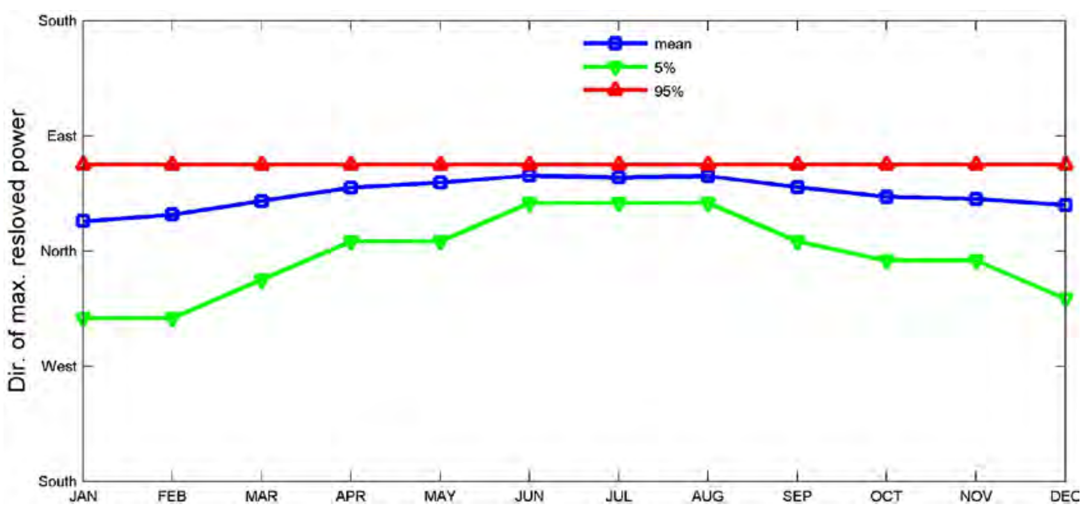

Figure 123– Monthly statistics of direction of maximum directionally resolved wave power at site Upolu.

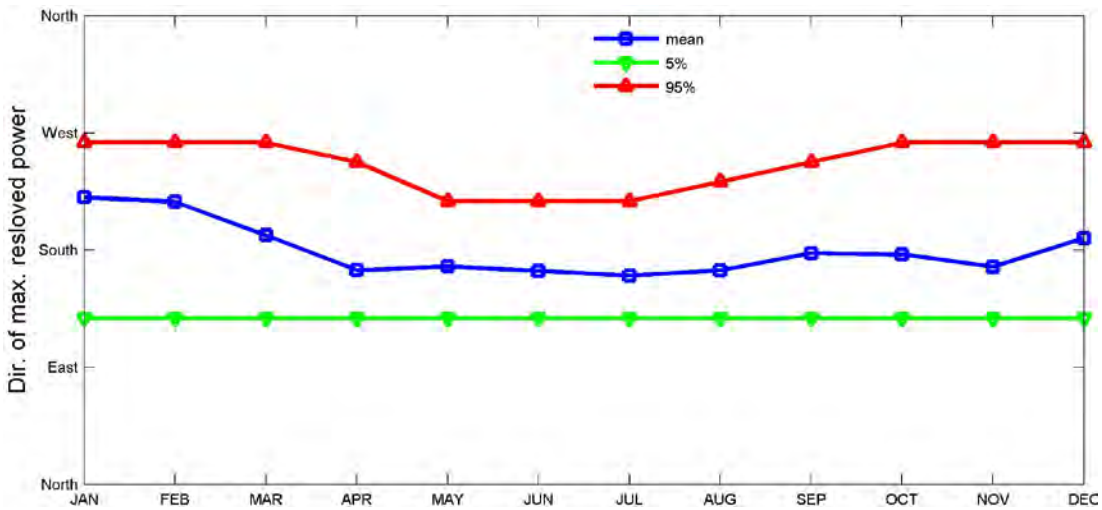

Figure 124– Monthly statistics of direction of maximum directionally resolved wave power at site South Point.

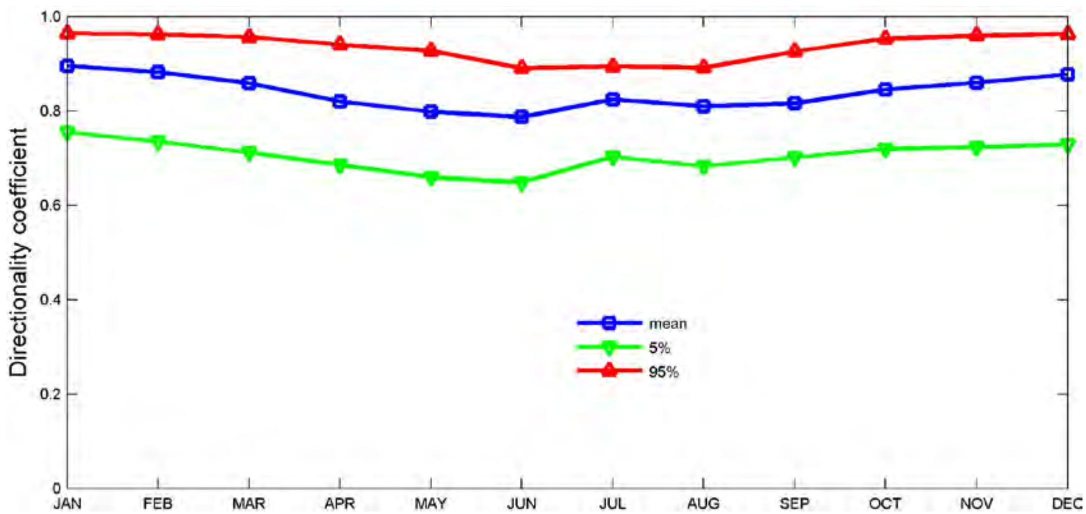

Figure 125– Monthly statistics of directionality coefficient at site Kilauea.

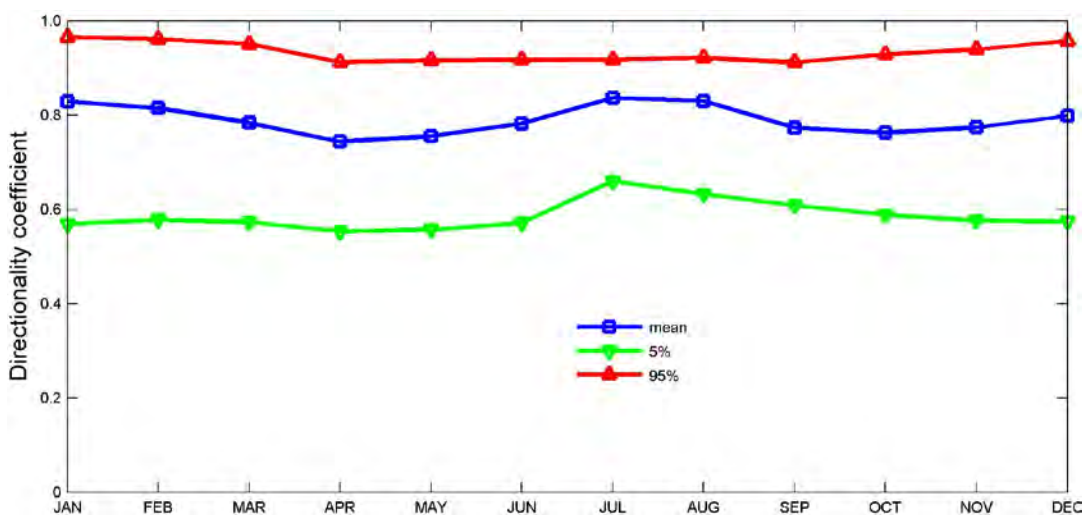

Figure 126– Monthly statistics of directionality coefficient at site Pauwela.

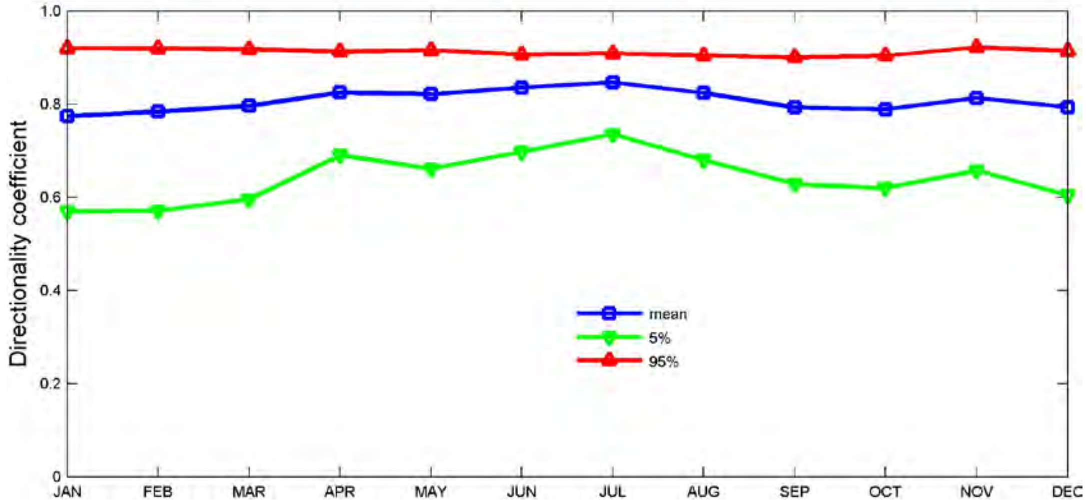

Figure 127– Monthly statistics of directionality coefficient at site Upolu.

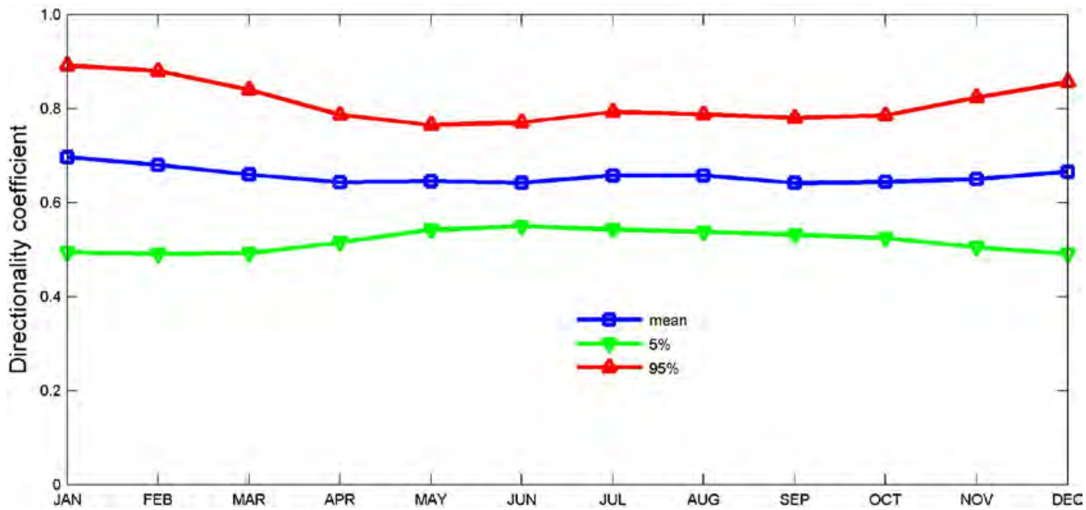

Figure 128– Monthly statistics of directionality coefficient at site South Point.

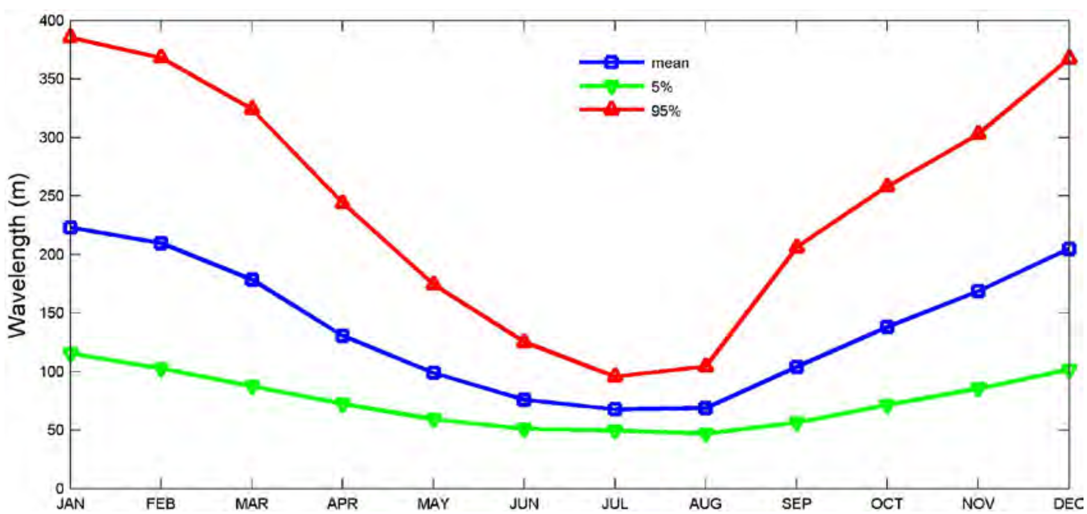

Figure 129– Monthly statistics of wavelength at site Kilauea.

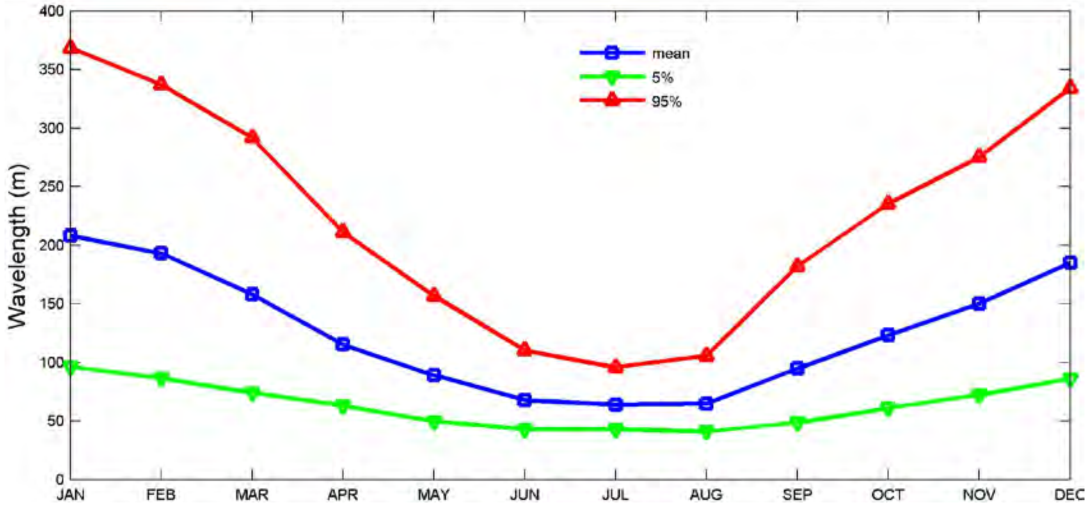

Figure 130– Monthly statistics of wavelength at site Pauwela.

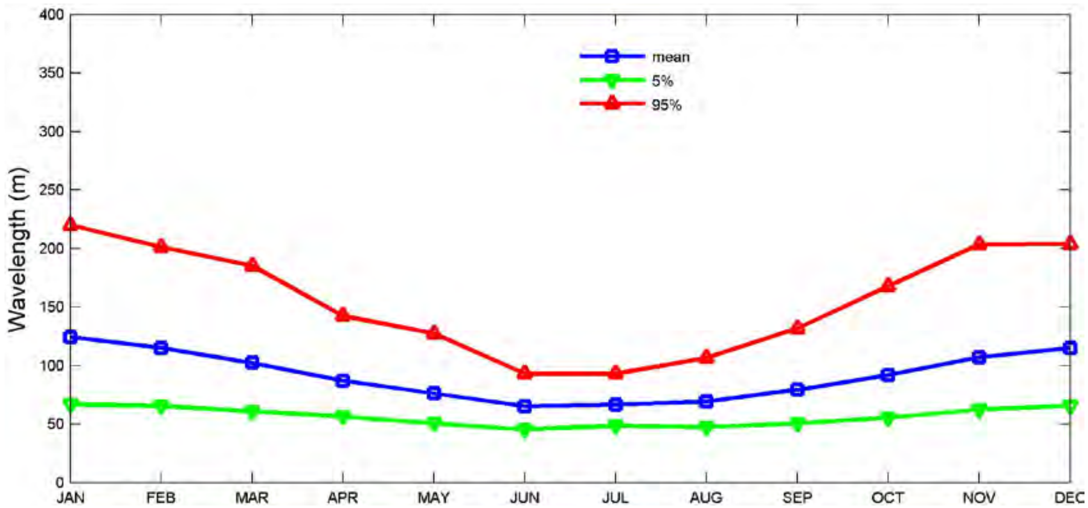

Figure 131– Monthly statistics of wavelength at site Upolu.

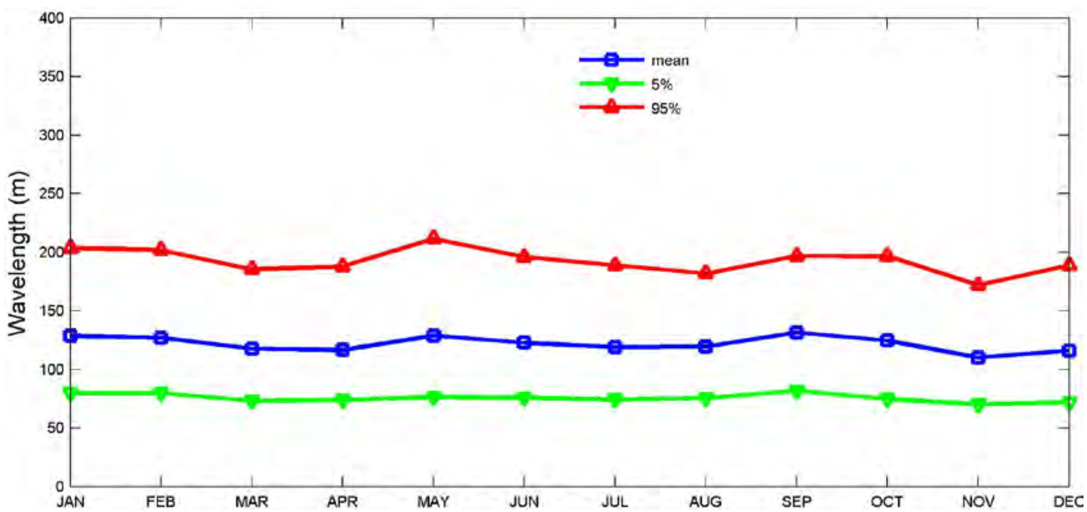

Figure 132– Monthly statistics of wavelength at site South Point.

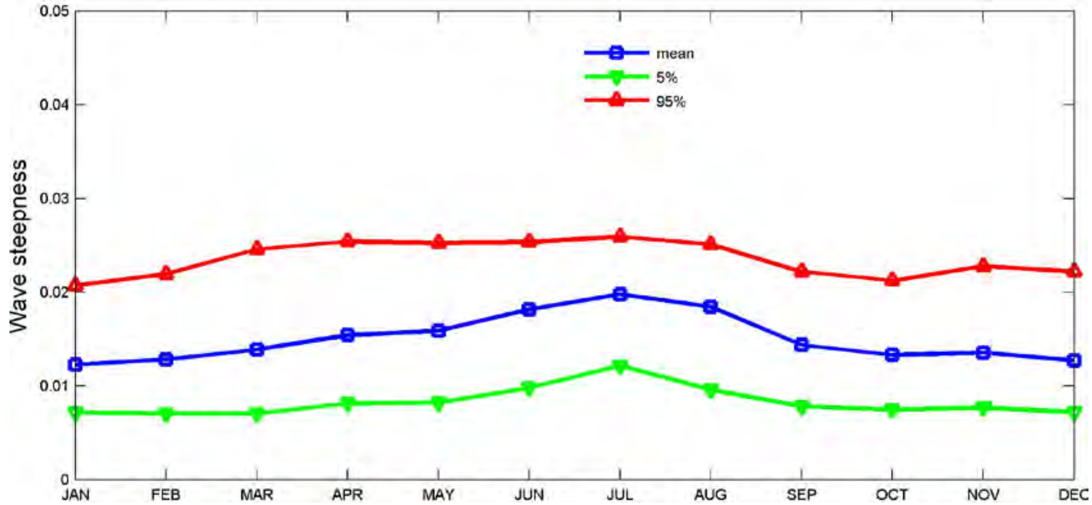

Figure 133– Monthly statistics of wave steepness at site Kilauea.

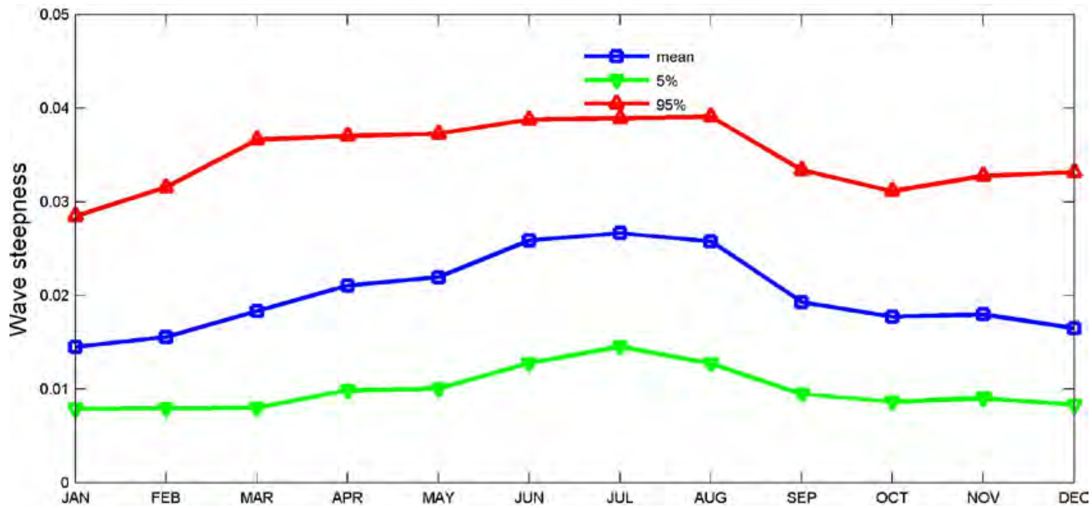

Figure 134– Monthly statistics of wave steepness at site Pauwela.

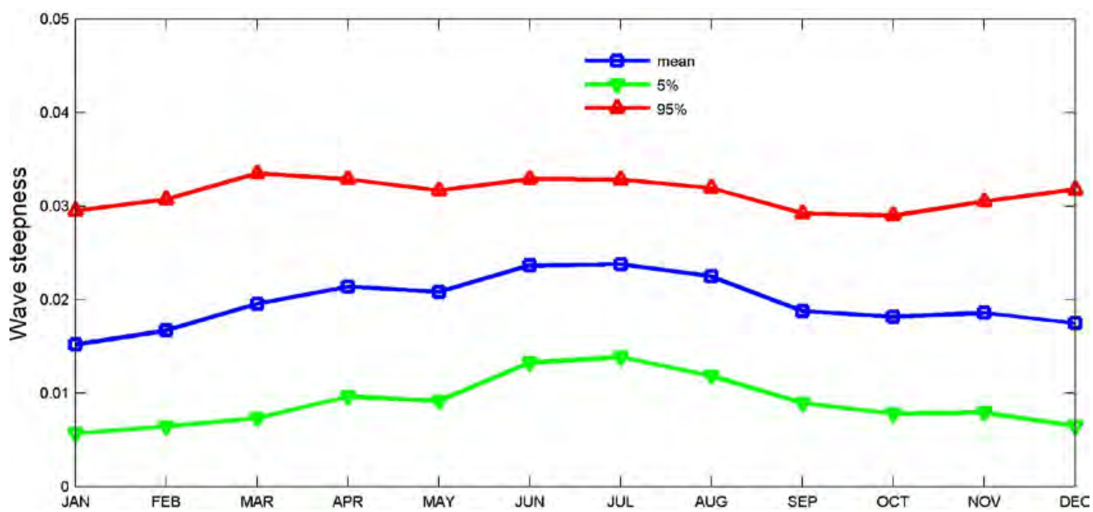

Figure 135– Monthly statistics of wave steepness at site Upolu.

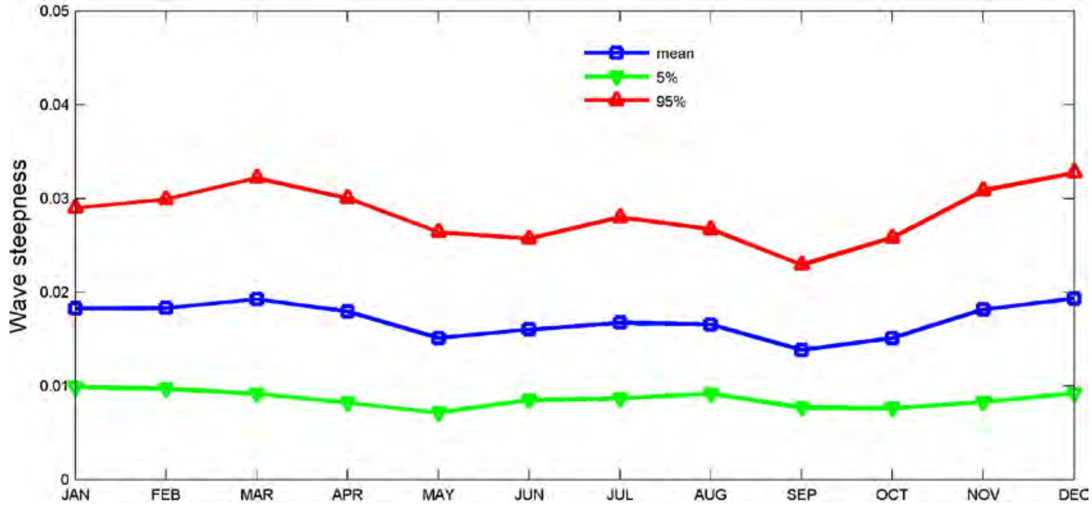

Figure 136– Monthly statistics of wave steepness at site South Point.

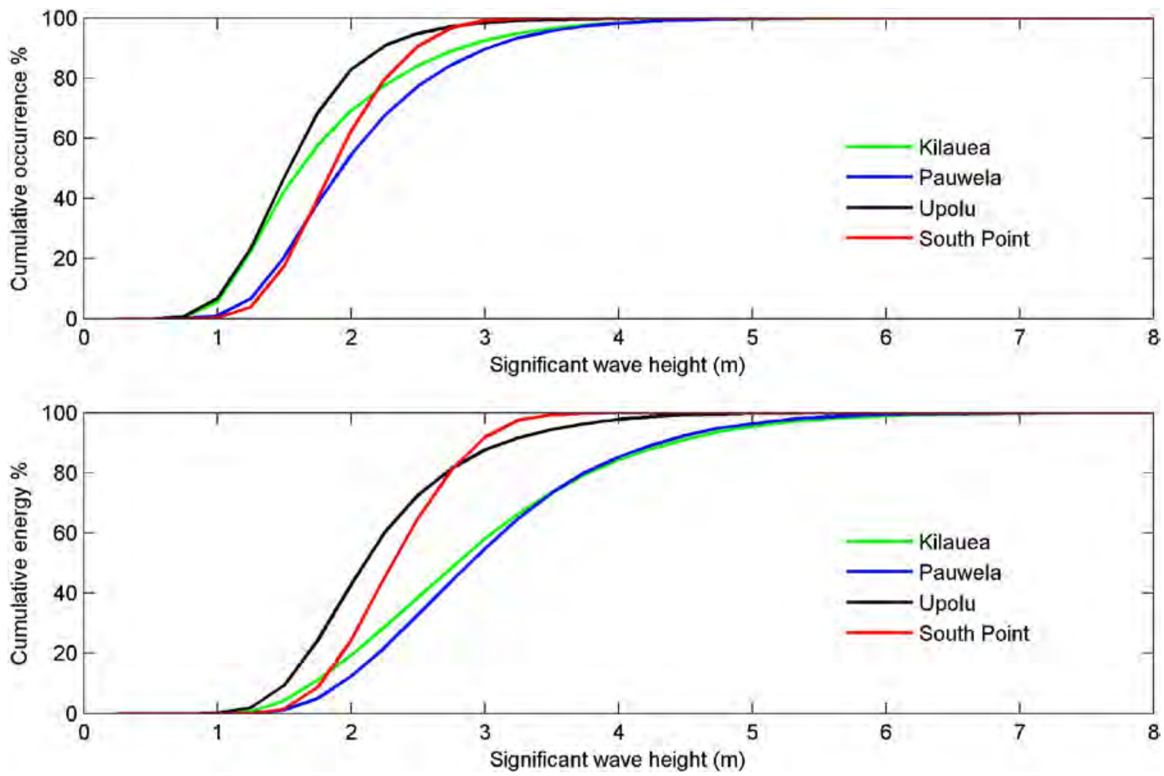

Figure 137– Cumulative distributions of significant wave height (upper) and the associated wave energy (lower) in terms of the percentage total at site Kilauea, Pauwela, Upolu, and South Point.

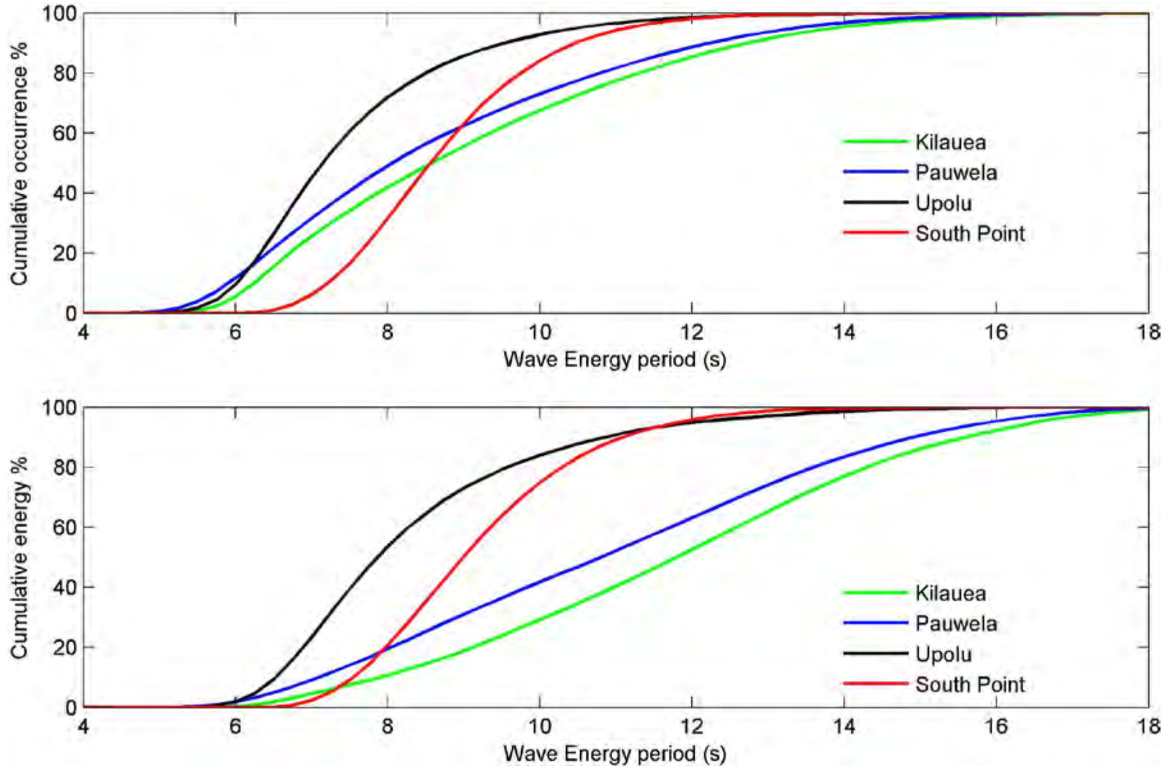

Figure 138– Cumulative distributions of wave energy period (upper) and the associated wave energy (lower) in terms of the percentage total at site Kilauea, Pauwela, Upolu, and South Point.

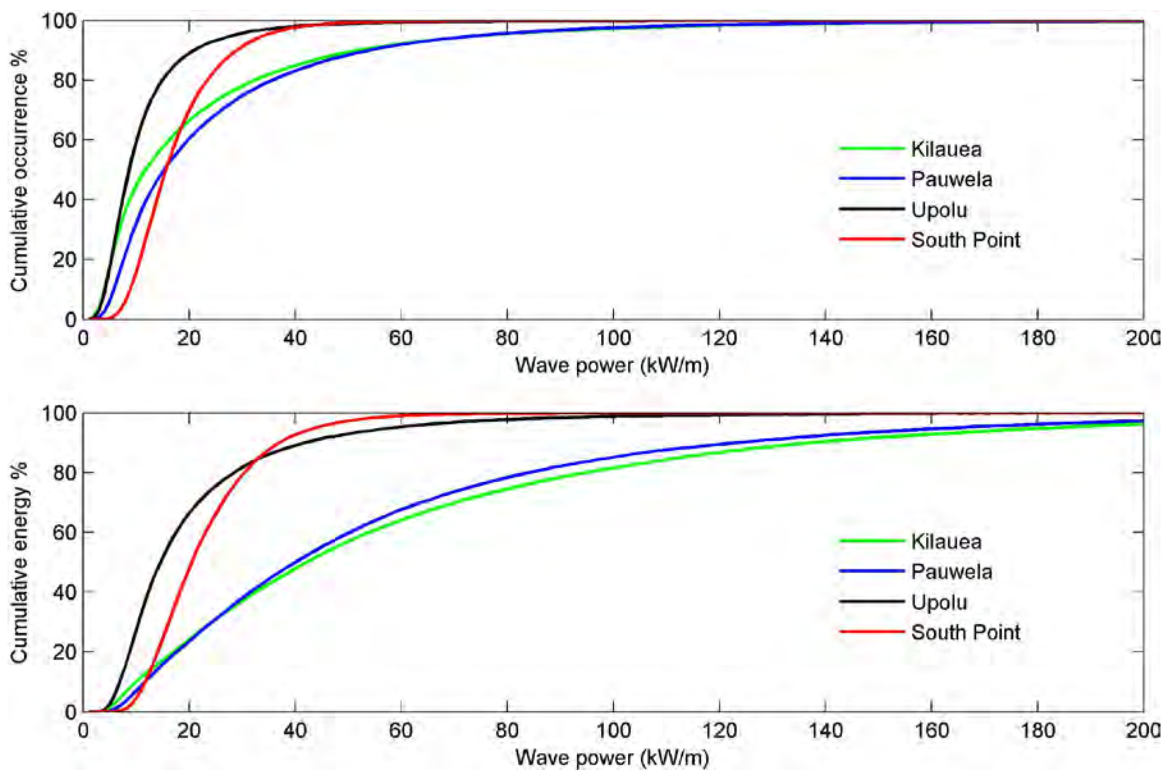

Figure 139– Cumulative distributions of wave power (upper) and the associated wave energy (lower) in terms of the percentage total at site Kilauea, Pauwela, Upolu, and South Point.

Table 2 Occurrence (hours) of Hindcast T_e Versus H_s at WETS during 1979-2013

	Te (s)																									
H_S (m)	4.75-5.00	5.00-5.25	5.25-5.50	5.50-5.75	5.75-6.00	6.00-6.25	6.25-6.50	6.50-6.75	6.75-7.00	7.00-7.25	7.25-7.50	7.50-7.75	7.75-8.00	8.00-8.25	8.25-8.50	8.50-8.75	8.75-9.00	9.00-9.25	9.25-9.50	9.50-9.75	9.75-100	10.0-10.25	10.25-10.50	10.50-10.75	10.75-11.00	11.00-11.25
0.25-0.50														1	2	4										
0.50-0.75			16	33	45	80	82	71	61	136	134	107	103	76	84	53	22	27	18	11	6	2	9	10	9	5
0.75-1.00	2	61	254	357	566	552	724	834	1042	849	843	869	827	816	792	676	540	480	334	269	261	216	178	168	154	125
1.00-1.25	5	123	656	1298	1954	2668	2768	2673	2743	2392	2306	1946	1955	1969	1773	1518	1500	1320	1206	1053	954	882	764	533	491	409
1.25-1.50		22	323	1448	3749	5748	6117	5554	4671	3979	3125	2813	2741	2556	2260	1996	1780	1709	1696	1490	1266	968	1076	959	822	726
1.50-1.75			14	266	1771	4608	6672	6889	5616	4365	3425	2981	2837	2304	2396	2061	1912	1825	1572	1287	1216	1141	1079	959	1002	870
1.75-2.00				5	169	1181	3742	4923	4771	4247	3774	3046	2186	1873	1875	1684	1644	1489	1162	1046	871	902	771	683	584	668
2.00-2.25					4	65	836	2030	3248	3327	2974	2260	1743	1589	1321	1069	981	910	859	722	593	656	605	503	409	394
2.25-2.50						6	50	444	1244	2116	2079	1589	1405	1004	809	709	595	598	490	493	469	424	383	334	321	278
2.50-2.75							1	23	189	698	1302	1182	1274	856	807	770	464	370	397	350	334	306	272	261	270	189
2.75-3.00									15	149	642	929	1042	801	568	456	345	294	170	262	242	235	186	138	154	141
3.00-3.25										7	105	387	576	578	494	390	222	177	97	132	163	130	111	103	86	74
3.25-3.50											5	59	191	380	357	274	149	116	94	71	85	61	72	79	55	26
3.50-3.75												6	59	152	212	216	170	132	70	60	49	34	18	13	32	38
3.75-4.00													13	46	85	120	93	126	62	25	48	20	8	10	16	19
4.00-4.25														4	60	82	111	65	49	15	14	18	11	14	6	15
4.25-4.50															6	25	63	33	33	16	10	18	7	11	11	5
4.50-4.75																4	29	19	30	6	11	12	8	3	1	2
4.75-5.00																	3	23	23	17	4	3	1	3		
5.00-5.25																		4	1	17		3	3			
5.25-2.50																					6	9	1			
5.50-5.75																					8	1				

	Te (s)																								
H_S (m)	11.25-11.50	11.50-11.75	11.75-12.00	12.00-12.25	12.25-12.50	12.50-12.75	12.75-13.00	13.00-13.25	13.25-13.50	13.50-13.75	13.75-14.00	14.00-14.25	14.25-14.50	14.50-14.75	14.75-15.00	15.00-15.25	15.25-15.50	15.50-15.75	15.75-16.00	16.00-16.25	16.25-16.50	16.50-16.75	16.75-17.00	>17.00	
0.25-0.50																									7
0.50-0.75	1	2	2	2																					1207
0.75-1.00	102	78	28	50	22	8	7	4	6	5	3		1												13103
1.00-1.25	322	207	138	105	87	73	78	46	45	32	25	10	15	4	2										39048
1.25-1.50	547	428	287	248	239	174	137	118	72	54	38	30	31	10	10	3	2	1							62023
1.50-1.75	633	556	415	248	227	217	156	77	82	65	63	47	35	28	23	15	5	4	9		1				61974
1.75-2.00	563	450	398	338	256	218	174	125	129	67	61	59	32	32	32	42	13	8	8	2		1	1		46305
2.00-2.25	382	360	275	280	220	173	166	118	103	74	65	62	46	44	31	20	15	10	13	9	3	2		2	29571
2.25-2.50	234	221	228	201	185	141	116	98	74	51	52	43	41	39	36	18	11	9	3	4	5	3	2		17655
2.50-2.75	181	170	190	138	122	92	73	66	86	76	57	55	31	15	6	14	7	12	7	8	2	1	1		11725
2.75-3.00	167	127	129	125	133	95	52	42	32	23	24	36	35	14	12	11	10	1	1	5				2	7845
3.00-3.25	79	84	75	73	90	69	42	22	11	13	14	19	22	18	12	11	12	5	4	3			2		4512
3.25-3.50	53	46	26	27	40	20	20	25	17	28	15	6	2	4		4	2	4	3	1	2	1			2420
3.50-3.75	22	22	19	25	10	15	10	22	8	4	8	7	5	3	3	1			1						1446
3.75-4.00	23	20	18	23	10	8	5	7	12	5	5	10	12	4	8	3			1	1					866
4.00-4.25	11	4	10	22	8	6	7	4	4	3	7	15	9	17	6	9	1	1	3						611
4.25-4.50	7	1	2	10	8	11	6	15	9																307
4.50-4.75		2	9	5	6	8	8																		163
4.75-5.00							3	3																	83
5.00-5.25								2	4	1															35
5.25-5.50									1	3															20
5.50-5.75																									9
																									300935

Table 3 Occurrence (hours) of Hindcast T_e Versus H_s at the Kaneohe II site during 1979-2013

	Te (s)																									
H_S (m)	4.75-5.00	5.00-5.25	5.25-5.50	5.50-5.75	5.75-6.00	6.00-6.25	6.25-6.50	6.50-6.75	6.75-7.00	7.00-7.25	7.25-7.50	7.50-7.75	7.75-8.00	8.00-8.25	8.25-8.50	8.50-8.75	8.75-9.00	9.00-9.25	9.25-9.50	9.50-9.75	9.75-100	10.0-10.25	10.25-10.50	10.50-10.75	10.75-11.00	11.00-11.25
0.25-0.50								6	5		8		1	1	1	9	1									
0.50-0.75		16	31	66	101	162	118	169	253	221	209	234	196	120	155	119	98	79	58	28	21	23	10	23	15	15
0.75-1.00	15	128	475	597	824	1106	1224	1268	1398	1211	1236	1199	1084	1179	1123	1004	872	738	544	414	425	364	267	266	206	195
1.00-1.25	4	151	841	2060	3247	4160	4112	3801	3500	3069	2806	2299	2317	2412	2002	1722	1757	1607	1550	1271	1285	964	925	749	633	547
1.25-1.50		17	323	1437	4324	7069	7468	6600	5319	4410	3570	3223	3103	2549	2440	2241	2014	1947	1732	1552	1324	1205	1100	1107	1000	837
1.50-1.75				153	1350	3682	6296	6285	5278	4273	3599	3147	2449	2125	2321	1905	1851	1697	1483	1235	1165	1109	1041	955	999	776
1.75-2.00					56	682	2490	3705	3847	3819	3246	2481	1970	1780	1569	1428	1404	1266	1119	1018	867	813	691	657	542	602
2.00-2.25					3	38	318	1372	2075	2602	2218	1743	1521	1196	926	827	750	617	714	670	540	553	530	421	364	368
2.25-2.50						1	9	119	587	1141	1458	1332	1217	886	725	656	563	524	445	482	407	362	307	362	280	256
2.50-2.75							1	9	69	478	941	1036	941	800	678	675	367	313	290	285	346	300	242	221	194	181
2.75-3.00									3	54	295	509	681	541	497	398	257	196	130	200	211	154	196	116	119	98
3.00-3.25										2	29	101	251	349	392	287	137	128	112	87	102	109	110	105	76	65
3.25-3.50											1	9	113	163	207	156	168	155	82	60	63	47	36	26	44	42
3.50-3.75													26	65	113	115	81	113	50	43	42	39	9	12	25	33
3.75-4.00													2	22	31	97	79	64	28	14	12	26	7	13	8	5
4.00-4.25															6	23	24	36	21	15	8	21	11	7	10	9
4.25-4.50															1	5	25	27	21	12	6	12	5	4	2	2
4.50-4.75																		8	18	11	2	5	1	2		
4.75-5.00																				3	4	10	2	2		
5.00-5.25																					11					

	Te (s)																							
H_S (m)	11.25-11.50	11.50-11.75	11.75-12.00	12.00-12.25	12.25-12.50	12.50-12.75	12.75-13.00	13.00-13.25	13.25-13.50	13.50-13.75	13.75-14.00	14.00-14.25	14.25-14.50	14.50-14.75	14.75-15.00	15.00-15.25	15.25-15.50	15.50-15.75	15.75-16.00	16.00-16.25	16.25-16.50	16.50-16.75	16.75-17.00	>17.00	
0.25-0.50																									32
0.50-0.75	8	7	3	4	7																				2569
0.75-1.00	136	128	63	51	45	23	19	11	14	10	7	6	3												19878
1.00-1.25	439	265	199	146	130	103	99	65	61	38	29	25	18	11	4										51423
1.25-1.50	641	530	335	267	246	200	178	130	74	71	56	28	44	19	10	11	1	2	2						70756
1.50-1.75	720	571	543	330	260	229	173	105	111	79	66	53	30	40	26	14	20	6	7	1	1	1			58560
1.75-2.00	553	435	373	324	264	187	194	116	126	99	64	70	51	36	38	31	26	11	11	7	1	1		2	39072
2.00-2.25	344	362	267	284	239	164	153	125	98	80	75	63	53	24	45	29	18	17	11	7	2	3	2	2	22833
2.25-2.50	180	201	201	144	155	127	104	94	99	46	52	38	33	27	30	34	11	10	3	5	5	4	2	2	13726
2.50-2.75	180	161	150	168	113	93	71	72	71	55	44	58	40	15	9	8	5	9	8	6	2	1		2	9708
2.75-3.00	153	127	114	99	111	97	35	35	28	24	23	26	27	20	10	12	12			4				1	5613
3.00-3.25	57	57	45	43	77	60	33	22	14	11	18	18	16	16	15	10	12	6	5	3			1	2	2983
3.25-3.50	36	34	23	10	26	32	24	23	15	15	17	5	3	4	1	1		2	2	1	2	1			1649
3.50-3.75	27	18	21	29	12	16	10	14	12	6	6	8	7	3	4	2				1					962
3.75-4.00	17	11	13	10	12	4	0	1	7	6	7	7	9	9	3	6	1			2					533
4.00-4.25	21	3	4	9	17	9	11	11	4		2	13	6	12	11	5	3	2	1	2					337
4.25-4.50		2	2	7	13	12	8	10	8							2	2								188
4.50-4.75					8	1	8	1																	65
4.75-5.00								3	3																27
5.00-5.25									2	6															19
5.25-5.50										2															2
																									300935

Table 4 Total Hindcast Wave Energy Flux (kWh/m) by T_e and H_s at WETS during 1979-2013

		Te (s)																									
		4.75-5.00	5.00-5.25	5.25-5.50	5.50-5.75	5.75-6.00	6.00-6.25	6.25-6.50	6.50-6.75	6.75-7.00	7.00-7.25	7.25-7.50	7.50-7.75	7.75-8.00	8.00-8.25	8.25-8.50	8.50-8.75	8.75-9.00	9.00-9.25	9.25-9.50	9.50-9.75	9.75-10.0	10.0-10.25	10.25-10.50	10.50-10.75	10.75-11.00	11.00-11.25
	0.25-0.50														1	2	4										
	0.50-0.75			19	40	62	114	120	104	100	207	222	196	206	152	167	109	49	63	43	28	16	5	26	29	26	14
	0.75-1.00	5	121	578	834	1371	1394	1942	2299	2862	2430	2490	2638	2629	2709	2751	2412	2029	1823	1316	1113	1116	958	821	790	738	626
	1.00-1.25	13	394	2210	4696	7568	10687	11512	11585	12225	11077	11019	9528	9978	10337	9585	8513	8678	7938	7531	6758	6299	5956	5384	3816	3682	3153
	1.25-1.50		99	1563	7477	20641	33089	36949	35014	30527	26804	21987	20516	20718	19851	18108	16561	15288	15023	15291	14017	12316	9660	11032	10136	9035	8192
	1.50-1.75			86	1814	13134	36014	54983	59416	50341	40775	33179	30054	29370	24758	26836	23734	22642	22364	19887	16823	16348	15957	15453	14165	15132	13509
	1.75-2.00				46	1601	12054	40309	55663	56628	52595	48682	40770	30195	26877	27630	25952	26041	24380	19719	18168	15545	16674	14682	13362	11704	13639
	2.00-2.25					51	853	11472	29388	49215	52528	48850	38638	30966	29231	24962	20974	19828	19037	18580	16086	13682	15492	14719	12566	10565	10475
	2.25-2.50						98	836	7862	23210	41918	42771	33894	31214	22943	19246	17434	15202	15632	13299	13677	13600	12517	11693	10529	10290	9169
	2.50-2.75							21	502	4287	16670	32724	30831	34324	24179	23547	23316	14392	11805	13142	11963	11774	11222	10175	9997	10612	7678
H_S (m)	2.75-3.00									406	4185	19075	28871	33702	26781	19807	16340	12748	11221	6778	10624	10096	10130	8302	6304	7272	6805
	3.00-3.25										236	3644	14017	21812	22871	20341	16535	9728	7994	4559	6348	8113	6664	5895	5615	4843	4287
	3.25-3.50											206	2487	8381	17395	16958	13544	7567	6155	5136	3937	5000	3618	4415	4975	3556	1713
	3.50-3.75												285	3017	7975	11620	12056	9996	8001	4420	3865	3295	2381	1288	934	2378	2926
	3.75-4.00													742	2759	5284	7807	6243	8747	4438	1877	3723	1560	632	840	1351	1689
	4.00-4.25														271	4241	5983	8491	5131	3991	1264	1217	1575	1003	1312	588	1542
	4.25-4.50															470	2006	5294	2899	2981	1477	964	1841	732	1195	1216	565
	4.50-4.75																359	2758	1881	3063	631	1222	1339	887	355	123	243
	4.75-5.00																	306	2460	2569	1990	471	373	124	392		
	5.00-5.25																		476	121	2136		427	412			
	5.25-2.50																					896	1344	148			
	5.50-5.75																					1280	165				

		Te (s)																							
		11.25-11.50	11.50-11.75	11.75-12.00	12.00-12.25	12.25-12.50	12.50-12.75	12.75-13.00	13.00-13.25	13.25-13.50	13.50-13.75	13.75-14.00	14.00-14.25	14.25-14.50	14.50-14.75	14.75-15.00	15.00-15.25	15.25-15.50	15.50-15.75	15.75-16.00	16.00-16.25	16.25-16.50	16.50-16.75	16.75-17.00	>17.00
	0.25-0.50																								
	0.50-0.75	3	6	7	7																				
	0.75-1.00	524	392	152	258	129	47	47	28	40	34	20		8											
	1.00-1.25	2578	1729	1163	907	769	650	732	430	433	294	240	109	175	45	20									
	1.25-1.50	6379	5148	3535	3103	3054	2269	1877	1635	1027	813	571	453	477	161	158	52	38	20						
	1.50-1.75	10211	9208	7154	4325	4067	4019	2893	1489	1621	1316	1294	1001	769	629	525	360	120	99	212		29			
	1.75-2.00	11884	9763	8897	7716	6082	5312	4379	3186	3314	1815	1711	1709	931	976	986	1278	411	254	281	71		35	40	
	2.00-2.25	10365	9969	7912	8318	6691	5414	5300	3852	3441	2578	2286	2238	1725	1639	1219	770	603	420	531	389	134	97		97
	2.25-2.50	7925	7643	8179	7384	6898	5377	4569	3986	3092	2156	2267	1934	1837	1830	1779	894	537	445	155	237	272	174	114	
	2.50-2.75	7579	7300	8387	6281	5652	4372	3531	3259	4344	3905	3028	3016	1742	875	365	786	421	742	448	516	127	62	70	
H_S (m)	2.75-3.00	8373	6465	6808	6757	7368	5430	3002	2481	1943	1440	1542	2332	2293	931	848	791	750	68	72	407				171
	3.00-3.25	4676	5059	4656	4662	5879	4618	2897	1541	785	952	1026	1455	1734	1453	995	950	1034	453	372	289			202	
	3.25-3.50	3657	3275	1876	2001	3082	1557	1596	2075	1441	2439	1329	534	194	382		377	191	411	314	110	220	108		
	3.50-3.75	1747	1769	1598	2198	871	1326	916	2073	778	395	806	744	529	334	338	115			126					
	3.75-4.00	2066	1872	1738	2221	983	811	511	739	1317	578	573	1191	1484	526	1009	383			140	151				
	4.00-4.25	1167	418	1072	2480	918	718	855	508	495	375	915	2050	1249	2374	882	1328	152	157	479					
	4.25-4.50	789	115	252	1243	1023	1448	791	2093	1296															
	4.50-4.75		261	1246	701	857	1176	1210																	
	4.75-5.00							494	528																
	5.00-5.25								373	783	205														
	5.25-5.50									206	628														
	5.50-5.75																								

Table 5 Total Hindcast Wave Energy Flux (kWh/m) by T_e and H_s at the Kaneohe II site during 1979-2013

	Te (s)																									
H_S (m)	4.75-5.00	5.00-5.25	5.25-5.50	5.50-5.75	5.75-6.00	6.00-6.25	6.25-6.50	6.50-6.75	6.75-7.00	7.00-7.25	7.25-7.50	7.50-7.75	7.75-8.00	8.00-8.25	8.25-8.50	8.50-8.75	8.75-9.00	9.00-9.25	9.25-9.50	9.50-9.75	9.75-10.0	10.0-10.25	10.25-10.50	10.50-10.75	10.75-11.00	11.00-11.25
0.25-0.50								5	4		7		1	1	1	9	1									
0.50-0.75		21	35	84	139	233	164	267	435	350	352	429	385	244	322	259	223	192	145	72	57	62	30	67	45	47
0.75-1.00	30	264	1055	1386	1992	2836	3261	3487	3974	3607	3737	3814	3573	4076	4006	3705	3434	3003	2286	1792	1900	1681	1277	1327	1017	1006
1.00-1.25	12	468	2825	7471	12539	16854	17332	16599	15849	14609	13762	11626	12251	13126	11304	10139	10509	10124	10150	8524	8897	6840	6736	5643	4915	4373
1.25-1.50		74	1522	7295	23678	40822	45321	42063	35420	30596	25678	24065	24116	20553	20480	19433	18170	17979	16408	15347	13407	12740	11904	12293	11526	9917
1.50-1.75				1054	9834	28731	52430	54933	48462	41161	36229	32927	26348	23871	26974	22910	23138	21875	19781	16914	16416	16226	15637	14767	15809	12676
1.75-2.00					531	6963	27038	42673	46543	48567	42857	34043	28300	26686	24156	22815	23173	21528	19689	18520	16297	15746	13756	13505	11452	12874
2.00-2.25					38	502	4346	20012	32039	42300	37572	30726	28104	22813	18316	16940	15947	13512	16134	15779	13062	13782	13560	11091	9840	10168
2.25-2.50						17	151	2151	11182	22974	30809	29359	27952	21270	18040	16862	14903	14378	12646	14100	12325	11236	9851	11912	9483	8967
2.50-2.75							20	201	1581	11624	24057	27828	26301	23391	20380	20583	11905	10601	10103	10249	12835	11342	9476	8880	7971	7738
2.75-3.00									80	1582	8957	16249	22831	18876	18046	14973	9960	7785	5385	8609	9296	7009	9195	5580	5852	4946
3.00-3.25										68	1051	3821	9813	14272	16759	12802	6283	6138	5478	4443	5284	5870	6131	6030	4411	3878
3.25-3.50											41	390	5202	7748	10299	8036	9065	8634	4682	3577	3831	2980	2283	1696	3011	3005
3.50-3.75													1338	3639	6414	6884	5015	7209	3274	2921	2925	2827	661	910	2005	2646
3.75-4.00													119	1355	2047	6606	5609	4649	2134	1115	972	2134	605	1154	720	470
4.00-4.25															436	1746	1911	3003	1793	1312	723	2024	1075	715	1034	958
4.25-4.50															80	426	2226	2482	2030	1232	625	1266	536	444	231	231
4.50-4.75																		816	1940	1183	222	579	121	249		
4.75-5.00																				370	533	1335	267	268		
5.00-5.25																					1549					

	Te (s)																							
H_S (m)	11.25-11.50	11.50-11.75	11.75-12.00	12.00-12.25	12.25-12.50	12.50-12.75	12.75-13.00	13.00-13.25	13.25-13.50	13.50-13.75	13.75-14.00	14.00-14.25	14.25-14.50	14.50-14.75	14.75-15.00	15.00-15.25	15.25-15.50	15.50-15.75	15.75-16.00	16.00-16.25	16.25-16.50	16.50-16.75	16.75-17.00	>17.00
0.25-0.50																								
0.50-0.75	24	24	10	14	26																			
0.75-1.00	702	681	329	281	259	139	121	75	94	70	49	45	23											
1.00-1.25	3627	2205	1690	1297	1206	982	945	634	599	367	299	242	204	121	50									
1.25-1.50	7764	6519	4239	3424	3178	2664	2446	1803	1050	1047	849	412	655	307	166	176	15	36	39					
1.50-1.75	12070	9731	9496	5963	4786	4305	3323	2066	2264	1631	1337	1120	641	866	580	319	485	140	158	21	23	27		
1.75-2.00	12276	9947	8642	7687	6370	4684	4982	2981	3274	2695	1783	1981	1480	1071	1159	946	770	338	358	239	33	38		70
2.00-2.25	9843	10572	7947	8768	7573	5293	5002	4140	3302	2788	2626	2332	1965	904	1706	1110	715	687	444	284	82	133	89	90
2.25-2.50	6499	7337	7529	5451	6004	5011	4263	3889	4263	2027	2314	1699	1474	1228	1420	1684	526	500	154	280	272	215	107	106
2.50-2.75	7854	7209	6863	7890	5517	4493	3585	3647	3669	2838	2344	3172	2250	880	537	477	298	537	489	374	122	59		139
2.75-3.00	8002	6776	6294	5546	6358	5683	2084	2105	1736	1515	1484	1672	1807	1361	692	845	880			309				83
3.00-3.25	3551	3534	2842	2807	5126	4124	2279	1576	1054	850	1393	1384	1220	1279	1212	834	1012	523	451	258			100	187
3.25-3.50	2557	2477	1739	775	2038	2564	1943	1956	1304	1318	1492	454	287	380	102	95		196	197	101	206	102		
3.50-3.75	2259	1542	1853	2629	1104	1470	971	1367	1201	608	608	850	762	330	457	226				117				
3.75-4.00	158	1053	1312	1022	1244	437		106	785	683	824	837	1087	1141	368	765	139			272				
4.00-4.25	2228	337	451	1030	2006	1094	1346	1429	527		255	1808	836	1705	1596	747	460	292	151	299				
4.25-4.50		237	249	923	1726	1670	1087	1382	1163							313	314							
4.50-4.75					1128	149	1223	164																
4.75-5.00								512	548															
5.00-5.25									386	1239														
5.25-2.50										430														

Table 6 Average Hindcast Wave Power (kW /m) by T_e and H_s at WETS during 1979-2013

	Te (s)																									
H_S (m)	4.75-5.00	5.00-5.25	5.25-5.50	5.50-5.75	5.75-6.00	6.00-6.25	6.25-6.50	6.50-6.75	6.75-7.00	7.00-7.25	7.25-7.50	7.50-7.75	7.75-8.00	8.00-8.25	8.25-8.50	8.50-8.75	8.75-9.00	9.00-9.25	9.25-9.50	9.50-9.75	9.75-10.0	10.0-10.25	10.25-10.50	10.50-10.75	10.75-11.00	11.00-11.25
0.25-0.50														1.0	1.0	1.0										
0.50-0.75			1.2	1.2	1.4	1.4	1.5	1.5	1.6	1.5	1.7	1.8	2.0	2.0	2.0	2.1	2.2	2.3	2.4	2.5	2.7	2.4	2.9	2.9	2.9	2.8
0.75-1.00	2.3	2.0	2.3	2.3	2.4	2.5	2.7	2.8	2.7	2.9	3.0	3.0	3.2	3.3	3.5	3.6	3.8	3.8	3.9	4.1	4.3	4.4	4.6	4.7	4.8	5.0
1.00-1.25	2.6	3.2	3.4	3.6	3.9	4.0	4.2	4.3	4.5	4.6	4.8	4.9	5.1	5.2	5.4	5.6	5.8	6.0	6.2	6.4	6.6	6.8	7.0	7.2	7.5	7.7
1.25-1.50		4.5	4.8	5.2	5.5	5.8	6.0	6.3	6.5	6.7	7.0	7.3	7.6	7.8	8.0	8.3	8.6	8.8	9.0	9.4	9.7	10.0	10.3	10.6	11.0	11.3
1.50-1.75			6.2	6.8	7.4	7.8	8.2	8.6	9.0	9.3	9.7	10.1	10.4	10.7	11.2	11.5	11.8	12.3	12.7	13.1	13.4	14.0	14.3	14.8	15.1	15.5
1.75-2.00				9.3	9.5	10.2	10.8	11.3	11.9	12.4	12.9	13.4	13.8	14.3	14.7	15.4	15.8	16.4	17.0	17.4	17.8	18.5	19.0	19.6	20.0	20.4
2.00-2.25					12.8	13.1	13.7	14.5	15.2	15.8	16.4	17.1	17.8	18.4	18.9	19.6	20.2	20.9	21.6	22.3	23.1	23.6	24.3	25.0	25.8	26.6
2.25-2.50						16.4	16.7	17.7	18.7	19.8	20.6	21.3	22.2	22.9	23.8	24.6	25.5	26.1	27.1	27.7	29.0	29.5	30.5	31.5	32.1	33.0
2.50-2.75							20.6	21.8	22.7	23.9	25.1	26.1	26.9	28.2	29.2	30.3	31.0	31.9	33.1	34.2	35.3	36.7	37.4	38.3	39.3	40.6
2.75-3.00									27.1	28.1	29.7	31.1	32.3	33.4	34.9	35.8	37.0	38.2	39.9	40.5	41.7	43.1	44.6	45.7	47.2	48.3
3.00-3.25										33.8	34.7	36.2	37.9	39.6	41.2	42.4	43.8	45.2	47.0	48.1	49.8	51.3	53.1	54.5	56.3	57.9
3.25-3.50											41.2	42.1	43.9	45.8	47.5	49.4	50.8	53.1	54.6	55.5	58.8	59.3	61.3	63.0	64.7	65.9
3.50-3.75												47.6	51.1	52.5	54.8	55.8	58.8	60.6	63.1	64.4	67.2	70.0	71.5	71.8	74.3	77.0
3.75-4.00													57.1	60.0	62.2	65.1	67.1	69.4	71.6	75.1	77.6	78.0	79.0	84.0	84.4	88.9
4.00-4.25														67.8	70.7	73.0	76.5	78.9	81.4	84.3	86.9	87.5	91.2	93.7	98.1	102.8
4.25-4.50															78.4	80.3	84.0	87.8	90.3	92.3	96.4	102.3	104.5	108.6	110.5	113.0
4.50-4.75																89.8	95.1	99.0	102.1	105.2	111.1	111.6	110.9	118.4	122.8	121.3
4.75-5.00																	102.0	107.0	111.7	117.1	117.7	124.2	123.6	130.8		
5.00-5.25																		119.0	121.3	125.7		142.3	137.4			
5.25-2.50																					149.3	149.3	148.5			
5.50-5.75																					160.0	165.0				

	Te (s)																							
H_S (m)	11.25-11.50	11.50-11.75	11.75-12.00	12.00-12.25	12.25-12.50	12.50-12.75	12.75-13.00	13.00-13.25	13.25-13.50	13.50-13.75	13.75-14.00	14.00-14.25	14.25-14.50	14.50-14.75	14.75-15.00	15.00-15.25	15.25-15.50	15.50-15.75	15.75-16.00	16.00-16.25	16.25-16.50	16.50-16.75	16.75-17.00	>17.00
0.25-0.50																								
0.50-0.75	2.7	3.0	3.4	3.6																				
0.75-1.00	5.1	5.0	5.4	5.2	5.9	5.9	6.7	6.9	6.7	6.8	6.8		7.6											
1.00-1.25	8.0	8.4	8.4	8.6	8.8	8.9	9.4	9.3	9.6	9.2	9.6	10.9	11.7	11.3	9.9									
1.25-1.50	11.7	12.0	12.3	12.5	12.8	13.0	13.7	13.9	14.3	15.1	15.0	15.1	15.4	16.1	15.8	17.3	19.1	20.0						
1.50-1.75	16.1	16.6	17.2	17.4	17.9	18.5	18.5	19.3	19.8	20.3	20.5	21.3	22.0	22.5	22.8	24.0	24.0	24.7	23.6		29.3			
1.75-2.00	21.1	21.7	22.4	22.8	23.8	24.4	25.2	25.5	25.7	27.1	28.0	29.0	29.1	30.5	30.8	30.4	31.6	31.8	35.2	35.4		34.8	40.4	
2.00-2.25	27.1	27.7	28.8	29.7	30.4	31.3	31.9	32.6	33.4	34.8	35.2	36.1	37.5	37.2	39.3	38.5	40.2	42.0	40.9	43.2	44.7	48.4		48.4
2.25-2.50	33.9	34.6	35.9	36.7	37.3	38.1	39.4	40.7	41.8	42.3	43.6	45.0	44.8	46.9	49.4	49.6	48.8	49.4	51.5	59.2	54.4	58.1	57.0	
2.50-2.75	41.9	42.9	44.1	45.5	46.3	47.5	48.4	49.4	50.5	51.4	53.1	54.8	56.2	58.4	60.8	56.2	60.1	61.8	64.0	64.4	63.7	62.2	69.9	
2.75-3.00	50.1	50.9	52.8	54.1	55.4	57.2	57.7	59.1	60.7	62.6	64.3	64.8	65.5	66.5	70.7	71.9	75.0	68.4	72.0	81.4				85.5
3.00-3.25	59.2	60.2	62.1	63.9	65.3	66.9	69.0	70.0	71.3	73.2	73.3	76.6	78.8	80.7	83.0	86.3	86.2	90.6	92.9	96.4			101.1	
3.25-3.50	69.0	71.2	72.1	74.1	77.1	77.9	79.8	83.0	84.8	87.1	88.6	89.1	97.1	95.5		94.3	95.3	102.7	104.7	109.7	110.2	108.0		
3.50-3.75	79.4	80.4	84.1	87.9	87.1	88.4	91.6	94.2	97.2	98.8	100.7	106.3	105.7	111.2	112.5	114.8			125.7					
3.75-4.00	89.8	93.6	96.5	96.6	98.3	101.4	102.1	105.5	109.8	115.7	114.7	119.1	123.6	131.5	126.1	127.7			140.5	151.5				
4.00-4.25	106.1	104.4	107.2	112.7	114.8	119.7	122.1	126.9	123.9	125.1	130.7	136.7	138.8	139.6	147.1	147.6	152.3	157.2	159.8					
4.25-4.50	112.8	115.4	126.0	124.3	127.8	131.7	131.8	139.5	144.0															
4.50-4.75		130.6	138.5	140.3	142.9	147.0	151.3																	
4.75-5.00							164.8	175.9																
5.00-5.25								186.6	195.6	204.5														
5.25-5.50									206.1	209.4														
5.50-5.75																								

Table 7 Average Hindcast Wave Power (kW /m) by T_e and H_s at the Kaneohe II site during 1979-2013

	Te (s)																									
H_S (m)	4.75-5.00	5.00-5.25	5.25-5.50	5.50-5.75	5.75-6.00	6.00-6.25	6.25-6.50	6.50-6.75	6.75-7.00	7.00-7.25	7.25-7.50	7.50-7.75	7.75-8.00	8.00-8.25	8.25-8.50	8.50-8.75	8.75-9.00	9.00-9.25	9.25-9.50	9.50-9.75	9.75-10.0	10.0-10.25	10.25-10.50	10.50-10.75	10.75-11.00	11.00-11.25
0.25-0.50								0.8	0.8		0.9		0.9	0.9	0.9	1.0	1.1									
0.50-0.75		1.3	1.1	1.3	1.4	1.4	1.4	1.6	1.7	1.6	1.7	1.8	2.0	2.0	2.1	2.2	2.3	2.4	2.5	2.6	2.7	2.7	3.0	2.9	3.0	3.1
0.75-1.00	2.0	2.1	2.2	2.3	2.4	2.6	2.7	2.8	2.8	3.0	3.0	3.2	3.3	3.5	3.6	3.7	3.9	4.1	4.2	4.3	4.5	4.6	4.8	5.0	4.9	5.2
1.00-1.25	3.0	3.1	3.4	3.6	3.9	4.1	4.2	4.4	4.5	4.8	4.9	5.1	5.3	5.4	5.6	5.9	6.0	6.3	6.5	6.7	6.9	7.1	7.3	7.5	7.8	8.0
1.25-1.50		4.3	4.7	5.1	5.5	5.8	6.1	6.4	6.7	6.9	7.2	7.5	7.8	8.1	8.4	8.7	9.0	9.2	9.5	9.9	10.1	10.6	10.8	11.1	11.5	11.8
1.50-1.75				6.9	7.3	7.8	8.3	8.7	9.2	9.6	10.1	10.5	10.8	11.2	11.6	12.0	12.5	12.9	13.3	13.7	14.1	14.6	15.0	15.5	15.8	16.3
1.75-2.00					9.5	10.2	10.9	11.5	12.1	12.7	13.2	13.7	14.4	15.0	15.4	16.0	16.5	17.0	17.6	18.2	18.8	19.4	19.9	20.6	21.1	21.4
2.00-2.25					12.8	13.2	13.7	14.6	15.4	16.3	16.9	17.6	18.5	19.1	19.8	20.5	21.3	21.9	22.6	23.6	24.2	24.9	25.6	26.3	27.0	27.6
2.25-2.50						17.4	16.7	18.1	19.0	20.1	21.1	22.0	23.0	24.0	24.9	25.7	26.5	27.4	28.4	29.3	30.3	31.0	32.1	32.9	33.9	35.0
2.50-2.75							19.9	22.3	22.9	24.3	25.6	26.9	28.0	29.2	30.1	30.5	32.4	33.9	34.8	36.0	37.1	37.8	39.2	40.2	41.1	42.8
2.75-3.00									26.5	29.3	30.4	31.9	33.5	34.9	36.3	37.6	38.8	39.7	41.4	43.0	44.1	45.5	46.9	48.1	49.2	50.5
3.00-3.25										34.0	36.2	37.8	39.1	40.9	42.8	44.6	45.9	48.0	48.9	51.1	51.8	53.9	55.7	57.4	58.0	59.7
3.25-3.50											40.6	43.4	46.0	47.5	49.8	51.5	54.0	55.7	57.1	59.6	60.8	63.4	63.4	65.2	68.4	71.5
3.50-3.75													51.5	56.0	56.8	59.9	61.9	63.8	65.5	67.9	69.6	72.5	73.4	75.8	80.2	80.2
3.75-4.00													59.5	61.6	66.0	68.1	71.0	72.6	76.2	79.6	81.0	82.1	86.4	88.8	89.9	94.1
4.00-4.25															72.6	75.9	79.6	83.4	85.4	87.5	90.4	96.4	97.7	102.2	103.4	106.5
4.25-4.50															79.7	85.1	89.0	91.9	96.7	102.7	104.1	105.5	107.2	110.9	115.5	115.7
4.50-4.75																		102.0	107.8	107.5	111.0	115.8	121.0	124.3		
4.75-5.00																				123.2	133.3	133.5	133.3	133.8		
5.00-5.25																					140.8					
5.25-5.50																										

	Te (s)																							
H_S (m)	11.25-11.50	11.50-11.75	11.75-12.00	12.00-12.25	12.25-12.50	12.50-12.75	12.75-13.00	13.00-13.25	13.25-13.50	13.50-13.75	13.75-14.00	14.00-14.25	14.25-14.50	14.50-14.75	14.75-15.00	15.00-15.25	15.25-15.50	15.50-15.75	15.75-16.00	16.00-16.25	16.25-16.50	16.50-16.75	16.75-17.00	>17.00
0.25-0.50																								
0.50-0.75	3.1	3.4	3.2	3.5	3.7																			
0.75-1.00	5.2	5.3	5.2	5.5	5.7	6.0	6.4	6.8	6.7	7.0	7.0	7.5	7.6											
1.00-1.25	8.3	8.3	8.5	8.9	9.3	9.5	9.5	9.8	9.8	9.7	10.3	9.7	11.3	11.0	12.6									
1.25-1.50	12.1	12.3	12.7	12.8	12.9	13.3	13.7	13.9	14.2	14.8	15.2	14.7	14.9	16.2	16.6	16.0	14.9	17.9	19.5					
1.50-1.75	16.8	17.0	17.5	18.1	18.4	18.8	19.2	19.7	20.4	20.6	20.3	21.1	21.4	21.7	22.3	22.8	24.2	23.3	22.6	21.0	22.8	27.2		
1.75-2.00	22.2	22.9	23.2	23.7	24.1	25.0	25.7	25.7	26.0	27.2	27.9	28.3	29.0	29.7	30.5	30.5	29.6	30.7	32.5	34.2	32.6	37.6		35.1
2.00-2.25	28.6	29.2	29.8	30.9	31.7	32.3	32.7	33.1	33.7	34.9	35.0	37.0	37.1	37.7	37.9	38.3	39.7	40.4	40.3	40.5	41.1	44.3	44.7	45.2
2.25-2.50	36.1	36.5	37.5	37.9	38.7	39.5	41.0	41.4	43.1	44.1	44.5	44.7	44.7	45.5	47.3	49.5	47.8	50.0	51.3	55.9	54.3	53.8	53.5	53.1
2.50-2.75	43.6	44.8	45.8	47.0	48.8	48.3	50.5	50.7	51.7	51.6	53.3	54.7	56.2	58.6	59.7	59.7	59.6	59.7	61.2	62.3	60.8	59.1		69.7
2.75-3.00	52.3	53.4	55.2	56.0	57.3	58.6	59.6	60.1	62.0	63.1	64.5	64.3	66.9	68.0	69.2	70.4	73.3			77.1				83.4
3.00-3.25	62.3	62.0	63.2	65.3	66.6	68.7	69.0	71.6	75.3	77.3	77.4	76.9	76.2	79.9	80.8	83.4	84.4	87.2	90.2	86.0			100.3	93.6
3.25-3.50	71.0	72.8	75.6	77.5	78.4	80.1	80.9	85.0	87.0	87.9	87.8	90.8	95.8	95.1	102.1	95.0		97.9	98.3	101.3	102.8	102.4		
3.50-3.75	83.7	85.7	88.3	90.7	92.0	91.9	97.1	97.6	100.1	101.4	101.3	106.2	108.8	109.9	114.2	112.8				116.8				
3.75-4.00	93.1	95.8	101.0	102.2	103.7	109.2		106.2	112.2	113.9	117.7	119.5	120.8	126.7	122.7	127.5	138.8			136.1				
4.00-4.25	106.1	112.4	112.8	114.4	118.0	121.6	122.4	129.9	131.7		127.7	139.1	139.3	142.1	145.1	149.5	153.2	146.2	151.0	149.6				
4.25-4.50		118.6	124.3	131.8	132.8	139.2	135.9	138.2	145.4							156.6	157.1							
4.50-4.75					141.1	148.9	152.8	163.6																
4.75-5.00								170.6	182.7															
5.00-5.25									193.2	206.5														
5.25-5.50										214.8														

Table 8 Occurrence (hours) of Hindcast T_e Versus H_s at the Kilauea site during 1979-2013

	Te (s)																										
H_S (m)	4.50-4.75	4.75-5.00	5.00-5.25	5.25-5.50	5.50-5.75	5.75-6.00	6.00-6.25	6.25-6.50	6.50-6.75	6.75-7.00	7.00-7.25	7.25-7.50	7.50-7.75	7.75-8.00	8.00-8.25	8.25-8.50	8.50-8.75	8.75-9.00	9.00-9.25	9.25-9.50	9.50-9.75	9.75-100	10.0-10.25	10.25-10.50	10.50-10.75	10.75-11.00	11.00-11.25
0.50-0.75	1	26	29	34	61	90	128	234	190	190	193	121	80	72	19	12	13	8									
0.75-1.00		45	402	728	1098	1467	1546	1530	1408	1298	1139	1158	930	782	608	442	361	292	156	146	110	52	30	14	8	7	3
1.00-1.25		8	105	1113	2691	5323	5932	5310	4467	3437	3265	2770	2448	2204	2061	1774	1561	1240	1033	860	721	452	360	216	177	121	68
1.25-1.50			5	73	761	2434	5237	6366	6189	4865	4151	3438	3150	2677	2353	2472	2261	2201	2028	1845	1642	1443	1198	1072	740	608	470
1.50-1.75					26	198	1072	2528	3268	3089	2855	2523	2473	2093	1990	1858	1673	1611	1792	1820	1776	1627	1602	1538	1458	1361	1151
1.75-2.00						6	33	227	647	952	1301	1443	1590	1548	1577	1527	1543	1411	1438	1478	1527	1534	1587	1496	1463	1469	1446
2.00-2.25							4	3	68	190	373	568	805	926	900	922	1020	1073	1171	1134	908	931	1006	1082	1147	1112	1139
2.25-2.50									5	30	95	192	429	448	544	737	796	943	739	849	760	730	651	688	700	801	722
2.50-2.75										5	29	88	156	239	364	329	420	470	575	535	490	585	522	572	577	668	636
2.75-3.00									1		3	19	41	93	176	225	204	303	363	303	290	297	369	438	340	324	350
3.00-3.25													11	35	82	109	139	200	171	186	196	195	177	206	245	229	200
3.25-3.50											1		2	10	21	37	53	108	121	122	161	128	123	146	197	147	160
3.50-3.75														2	2	11	22	83	63	48	65	86	58	55	74	85	98
3.75-4.00													1	2		4	5	23	20	31	22	32	36	41	43	29	36
4.00-4.25													1			1	1	4	2	14	18	19	14	22	20	33	26
4.25-4.50																	1		2	7	12	17	18	12	26	8	19
4.50-4.75																		2		2	4	3	10	4	17	7	2
4.75-5.00																						3	2	3	9	2	4
5.00-5.25																							1				
5.25-2.50																											
5.50-5.75																											2
5.75-6.00																									1		1
6.00-6.25																										1	

	Te (s)																								
H_S (m)	11.25-11.50	11.50-11.75	11.75-12.00	12.00-12.25	12.25-12.50	12.50-12.75	12.75-13.00	13.00-13.25	13.25-13.50	13.50-13.75	13.75-14.00	14.00-14.25	14.25-14.50	14.50-14.75	14.75-15.00	15.00-15.25	15.25-15.50	15.50-15.75	15.75-16.00	16.00-16.25	16.25-16.50	16.50-16.75	16.75-17.00	>17.00	
0.50-0.75																									1501
0.75-1.00	2	2																							15764
1.00-1.25	67	40	30	24	16	8	5	6	2	1	1														49917
1.25-1.50	384	277	173	139	108	65	49	27	32	20	10	4	1	2	0	1	1				1				60973
1.50-1.75	870	751	716	428	337	247	134	123	137	70	37	28	27	8	7	7	6	1	3	2	0	0	2	1	45324
1.75-2.00	1377	1140	1035	930	620	521	419	345	211	183	108	97	86	61	35	20	20	11	6	4	5	6	1	6	34490
2.00-2.25	1196	1130	894	952	912	857	657	624	470	382	268	195	145	100	79	59	46	35	34	20	20	16	9	26	25608
2.25-2.50	717	758	892	813	719	725	706	657	524	478	368	291	185	171	138	90	91	80	40	59	43	30	20	39	19493
2.50-2.75	611	594	652	623	622	525	563	482	432	444	398	364	299	257	205	144	106	121	82	83	57	39	23	87	15073
2.75-3.00	401	416	387	423	424	388	372	377	386	381	360	334	269	208	168	136	154	91	56	57	65	56	49	124	10221
3.00-3.25	217	279	252	251	283	339	320	286	253	234	226	240	228	221	212	162	138	106	91	97	96	55	37	129	7133
3.25-3.50	147	181	190	177	168	219	262	199	179	163	137	160	175	173	119	123	133	115	100	75	83	52	38	124	5029
3.50-3.75	118	109	127	127	118	148	137	155	153	121	122	134	107	83	107	104	96	103	112	62	57	36	31	147	3366
3.75-4.00	79	82	85	80	92	124	136	108	148	117	85	101	85	67	59	50	64	54	59	74	55	46	28	108	2311
4.00-4.25	38	73	57	66	79	60	80	95	89	88	90	62	51	47	50	58	37	55	60	38	26	20	16	92	1602
4.25-4.50	11	23	42	42	30	41	54	48	58	41	59	69	51	58	47	50	43	33	41	56	30	22	26	56	1153
4.50-4.75	5	9	5	21	11	20	30	31	19	34	41	44	44	36	37	37	31	22	13	39	31	30	24	33	698
4.75-5.00	5	5	7	7	15	11	8	15	21	30	44	32	45	15	17	26	21	20	14	16	19	24	10	27	477
5.00-5.25			1	2	7	7	11	20	13	14	9	29	21	14	7	6	11	18	11	13	14	14	9	29	281
5.25-5.50	1	1				4	6	10	7	6	10	16	7	12	11	8	6	6	20	25	6	3	9	29	203
5.50-5.75								2	5		3	12	13	5	5	5	5	5	8	9	16	8	8	18	129
5.75-6.00										2	1	1	6	7	5	5	5	3	2	3	4	4	1	11	62
6.00-6.25											1	1	1	3	2	4	3	2	5	4	3	3	6	7	46
6.25-6.50												2	1			2	3	3	1	1		1	2	10	26
6.50-6.75													1	3			2	3	3	1			1	9	23
6.75-7.00																		2	4	2				5	13
7.00-7.25																			1	3	1	1		6	12
7.25-7.50																					1	1		1	3
7.50-7.75																							1	3	4
																									300935

Table 9 Total Hindcast Wave Energy Flux (kWh/m) by T_e and H_s at the Kilauea site during 1979-2013

H_S (m)	Te (s) 4.50-4.75	4.75-5.00	5.00-5.25	5.25-5.50	5.50-5.75	5.75-6.00	6.00-6.25	6.25-6.50	6.50-6.75	6.75-7.00	7.00-7.25	7.25-7.50	7.50-7.75	7.75-8.00	8.00-8.25	8.25-8.50	8.50-8.75	8.75-9.00	9.00-9.25	9.25-9.50	9.50-9.75	9.75-100	10.0-10.25	10.25-10.50	10.50-10.75	10.75-11.00	11.00-11.25
0.50-0.75	1	29	34	43	84	135	187	363	290	304	298	199	137	145	41	25	29	18									
0.75-1.00		83	811	1586	2611	3567	3992	4062	3892	3713	3409	3621	3012	2647	2165	1627	1395	1191	674	636	507	253	148	74	42	38	17
1.00-1.25		20	312	3645	9574	20226	23783	22407	19722	15745	15597	13705	12612	11960	11422	10339	9427	7694	6749	5716	5037	3270	2703	1702	1394	987	566
1.25-1.50			21	334	3764	12834	29329	38087	39112	32210	28593	24771	23548	20904	18984	20878	19652	19899	18947	17873	16434	14965	12845	11860	8490	7270	5637
1.50-1.75					176	1432	8219	20415	27974	27727	27194	25102	25751	22724	22453	21828	20506	20354	23154	24361	24623	23377	23747	23400	22687	21983	19319
1.75-2.00						61	327	2442	7295	11386	16343	18910	21876	22313	23460	23748	24820	23398	24883	26035	27895	28998	31059	30157	30033	31268	31395
2.00-2.25							50	40	996	2924	5997	9521	14097	17025	17247	18342	21162	22914	25943	25956	21429	22575	24896	27706	30438	30328	31867
2.25-2.50									90	566	1896	4045	9358	10295	12947	18234	20406	25065	20380	24105	22348	22033	20333	22109	22981	27058	25122
2.50-2.75										114	691	2271	4152	6625	10492	9961	13171	15255	19342	18564	17534	21650	20039	22428	23072	27648	27024
2.75-3.00									27		90	585	1299	3101	6161	8126	7685	11813	14603	12648	12435	13105	16701	20433	16474	16029	17707
3.00-3.25													411	1384	3377	4615	6200	9293	8124	9150	9941	10214	9528	11376	13830	13441	12061
3.25-3.50											39		89	459	986	1833	2702	5823	6671	6909	9405	7797	7695	9409	13087	10044	11153
3.50-3.75														109	112	611	1303	5081	4034	3149	4410	6025	4181	4127	5602	6703	7994
3.75-4.00													58	121		268	330	1600	1429	2327	1752	2578	2958	3512	3784	2607	3347
4.00-4.25													65			71	75	307	161	1180	1581	1723	1347	2135	2002	3319	2700
4.25-4.50																	87		181	685	1195	1720	1910	1315	2920	924	2253
4.50-4.75																		195		215	443	349	1185	502	2139	897	261
4.75-5.00																						374	258	394	1214	288	590
5.00-5.25																							145				
5.25-2.50																											
5.50-5.75																											397
5.75-6.00																									204		210
6.00-6.25																										227	

H_S (m)	Te (s) 11.25-11.50	11.50-11.75	11.75-12.00	12.00-12.25	12.25-12.50	12.50-12.75	12.75-13.00	13.00-13.25	13.25-13.50	13.50-13.75	13.75-14.00	14.00-14.25	14.25-14.50	14.50-14.75	14.75-15.00	15.00-15.25	15.25-15.50	15.50-15.75	15.75-16.00	16.00-16.25	16.25-16.50	16.50-16.75	16.75-17.00	>17.00
0.50-0.75																								
0.75-1.00	12	12																						
1.00-1.25	583	349	277	221	154	79	48	60	22	12	10													
1.25-1.50	4759	3608	2327	1827	1476	899	703	389	489	308	157	60	15	33		15	13				18			
1.50-1.75	14984	13239	12869	7827	6299	4752	2637	2433	2771	1447	766	603	591	178	155	161	133	22	74	44			48	27
1.75-2.00	30801	26241	24354	22629	15352	13130	10809	9173	5693	5018	3021	2755	2470	1752	1036	584	617	346	187	122	143	198	34	201
2.00-2.25	34221	33347	26996	29337	28715	27815	21847	20860	16098	13462	9599	7081	5292	3681	2970	2315	1787	1359	1353	824	826	650	359	1124
2.25-2.50	25551	27600	33370	31351	28182	29208	28896	27353	22480	20826	16272	13192	8445	7936	6560	4328	4351	3871	1961	2967	2228	1555	1041	2092
2.50-2.75	26698	26698	29919	29076	29973	25811	28132	24584	22454	23436	21418	20108	16724	14675	11845	8513	6298	7285	5009	5055	3538	2496	1485	5772
2.75-3.00	20889	22291	21294	23703	24376	22913	22335	23017	24144	24354	23260	21995	18112	14207	11418	9596	11092	6573	4041	4195	4841	4327	3755	9863
3.00-3.25	13372	17717	16440	16675	19173	23680	22841	20784	18654	17484	17166	18648	18027	17850	17301	13502	11667	9017	7855	8517	8579	4957	3387	12125
3.25-3.50	10665	13415	14326	13744	13214	17708	21524	16797	15366	14268	12175	14485	16024	16304	11354	11854	13032	11523	10142	7719	8639	5438	4046	13702
3.50-3.75	9789	9304	11129	11335	10731	13748	13109	15027	15095	12251	12519	14146	11437	8925	11768	11758	11115	11861	13229	7348	6900	4382	3808	18932
3.75-4.00	7444	8050	8536	8203	9617	13185	14864	12033	16680	13475	10013	12063	10333	8330	7447	6388	8226	7116	7809	10019	7424	6362	3982	15732
4.00-4.25	4072	8022	6404	7496	9332	7278	9889	11980	11368	11438	12025	8419	7035	6591	7098	8398	5450	8191	9048	5814	4045	3197	2556	15184
4.25-4.50	1341	2823	5299	5454	4006	5571	7470	6721	8374	6067	8727	10590	7923	9123	7558	8140	7079	5532	7008	9688	5280	3883	4658	10368
4.50-4.75	677	1255	712	3044	1648	2984	4602	4913	3089	5600	6911	7463	7559	6295	6582	6732	5652	4114	2458	7452	6069	5920	4751	6807
4.75-5.00	754	769	1125	1142	2492	1900	1399	2628	3780	5521	8230	6040	8560	2937	3352	5249	4280	4197	2933	3390	4056	5258	2213	6187
5.00-5.25			178	353	1274	1294	2086	3874	2541	2793	1874	6013	4401	3069	1552	1320	2473	4136	2580	3063	3311	3364	2224	7399
5.25-5.50	186	179				809	1244	2155	1543	1340	2267	3688	1633	2830	2607	1950	1497	1502	5042	6506	1594	810	2427	8095
5.50-5.75								464	1186		729	2947	3335	1307	1305	1365	1345	1362	2224	2540	4593	2343	2327	5449
5.75-6.00										527	267	280	1612	1976	1430	1478	1487	916	601	928	1230	1266	316	3766
6.00-6.25											285	306	290	891	628	1249	977	637	1676	1349	1043	1031	2105	2551
6.25-6.50												642	337			671	1051	1079	368	365		372	752	3841
6.50-6.75													349	1074			752	1126	1169	400			396	3744
6.75-7.00																		815	1709	848				2319
7.00-7.25																			437	1342	445	450		2979
7.25-7.50																					481	510		514
7.50-7.75																							536	1666

Table 10 Average Hindcast Wave Power (kW/m) by T_e and H_s at the Kilauea site during 1979-2013

	Te (s)																										
H_S (m)	4.50-4.75	4.75-5.00	5.00-5.25	5.25-5.50	5.50-5.75	5.75-6.00	6.00-6.25	6.25-6.50	6.50-6.75	6.75-7.00	7.00-7.25	7.25-7.50	7.50-7.75	7.75-8.00	8.00-8.25	8.25-8.50	8.50-8.75	8.75-9.00	9.00-9.25	9.25-9.50	9.50-9.75	9.75-100	10.0-10.25	10.25-10.50	10.50-10.75	10.75-11.00	11.00-11.25
0.50-0.75	0.9	1.1	1.2	1.3	1.4	1.5	1.5	1.6	1.5	1.6	1.5	1.6	1.7	2.0	2.1	2.1	2.2	2.2									
0.75-1.00		1.9	2.0	2.2	2.4	2.4	2.6	2.7	2.8	2.9	3.0	3.1	3.2	3.4	3.6	3.7	3.9	4.1	4.3	4.4	4.6	4.9	4.9	5.3	5.3	5.4	5.6
1.00-1.25		2.5	3.0	3.3	3.6	3.8	4.0	4.2	4.4	4.6	4.8	4.9	5.2	5.4	5.5	5.8	6.0	6.2	6.5	6.6	7.0	7.2	7.5	7.9	7.9	8.2	8.3
1.25-1.50			4.2	4.6	4.9	5.3	5.6	6.0	6.3	6.6	6.9	7.2	7.5	7.8	8.1	8.4	8.7	9.0	9.3	9.7	10.0	10.4	10.7	11.1	11.5	12.0	12.0
1.50-1.75					6.8	7.2	7.7	8.1	8.6	9.0	9.5	9.9	10.4	10.9	11.3	11.7	12.3	12.6	12.9	13.4	13.9	14.4	14.8	15.2	15.6	16.2	16.8
1.75-2.00						10.2	9.9	10.8	11.3	12.0	12.6	13.1	13.8	14.4	14.9	15.6	16.1	16.6	17.3	17.6	18.3	18.9	19.6	20.2	20.5	21.3	21.7
2.00-2.25							12.4	13.4	14.6	15.4	16.1	16.8	17.5	18.4	19.2	19.9	20.7	21.4	22.2	22.9	23.6	24.2	24.7	25.6	26.5	27.3	28.0
2.25-2.50									17.9	18.9	20.0	21.1	21.8	23.0	23.8	24.7	25.6	26.6	27.6	28.4	29.4	30.2	31.2	32.1	32.8	33.8	34.8
2.50-2.75										22.8	23.8	25.8	26.6	27.7	28.8	30.3	31.4	32.5	33.6	34.7	35.8	37.0	38.4	39.2	40.0	41.4	42.5
2.75-3.00									27.2		29.9	30.8	31.7	33.3	35.0	36.1	37.7	39.0	40.2	41.7	42.9	44.1	45.3	46.6	48.5	49.5	50.6
3.00-3.25													37.4	39.5	41.2	42.3	44.6	46.5	47.5	49.2	50.7	52.4	53.8	55.2	56.5	58.7	60.3
3.25-3.50											39.4		44.7	45.9	46.9	49.5	51.0	53.9	55.1	56.6	58.4	60.9	62.6	64.4	66.4	68.3	69.7
3.50-3.75														54.3	56.0	55.5	59.2	61.2	64.0	65.6	67.8	70.1	72.1	75.0	75.7	78.9	81.6
3.75-4.00													58.4	60.7		66.9	66.0	69.6	71.5	75.0	79.6	80.5	82.2	85.7	88.0	89.9	93.0
4.00-4.25													64.6			70.8	75.5	76.6	80.3	84.3	87.9	90.7	96.2	97.0	100.1	100.6	103.8
4.25-4.50																	86.5		90.4	97.8	99.6	101.2	106.1	109.6	112.3	115.5	118.6
4.50-4.75																		97.4		107.5	110.7	116.5	118.5	125.4	125.8	128.2	130.3
4.75-5.00																						124.6	128.9	131.4	134.9	143.8	147.6
5.00-5.25																							145.4				
5.25-2.50																											
5.50-5.75																											198.4
5.75-6.00																									204.2		210.5
6.00-6.25																										227.4	

	Te (s)																							
H_S (m)	11.25-11.50	11.50-11.75	11.75-12.00	12.00-12.25	12.25-12.50	12.50-12.75	12.75-13.00	13.00-13.25	13.25-13.50	13.50-13.75	13.75-14.00	14.00-14.25	14.25-14.50	14.50-14.75	14.75-15.00	15.00-15.25	15.25-15.50	15.50-15.75	15.75-16.00	16.00-16.25	16.25-16.50	16.50-16.75	16.75-17.00	>17.00
0.50-0.75																								
0.75-1.00	6.0	5.8																						
1.00-1.25	8.7	8.7	9.2	9.2	9.6	9.9	9.5	10.0	11.0	11.7	10.0													
1.25-1.50	12.4	13.0	13.4	13.1	13.7	13.8	14.3	14.4	15.3	15.4	15.7	14.9	15.2	16.3		15.4	13.5				17.7			
1.50-1.75	17.2	17.6	18.0	18.3	18.7	19.2	19.7	19.8	20.2	20.7	20.7	21.6	21.9	22.2	22.2	22.9	22.1	22.2	24.8	22.2			23.9	27.1
1.75-2.00	22.4	23.0	23.5	24.3	24.8	25.2	25.8	26.6	27.0	27.4	28.0	28.4	28.7	28.7	29.6	29.2	30.8	31.5	31.1	30.5	28.6	33.0	33.9	33.4
2.00-2.25	28.6	29.5	30.2	30.8	31.5	32.5	33.3	33.4	34.3	35.2	35.8	36.3	36.5	36.8	37.6	39.2	38.8	38.8	39.8	41.2	41.3	40.6	39.9	43.2
2.25-2.50	35.6	36.4	37.4	38.6	39.2	40.3	40.9	41.6	42.9	43.6	44.2	45.3	45.6	46.4	47.5	48.1	47.8	48.4	49.0	50.3	51.8	51.8	52.0	53.6
2.50-2.75	43.7	44.9	45.9	46.7	48.2	49.2	50.0	51.0	52.0	52.8	53.8	55.2	55.9	57.1	57.8	59.1	59.4	60.2	61.1	60.9	62.1	64.0	64.6	66.3
2.75-3.00	52.1	53.6	55.0	56.0	57.5	59.1	60.0	61.1	62.5	63.9	64.6	65.9	67.3	68.3	68.0	70.6	72.0	72.2	72.2	73.6	74.5	77.3	76.6	79.5
3.00-3.25	61.6	63.5	65.2	66.4	67.8	69.9	71.4	72.7	73.7	74.7	76.0	77.7	79.1	80.8	81.6	83.3	84.5	85.1	86.3	87.8	89.4	90.1	91.5	94.0
3.25-3.50	72.5	74.1	75.4	77.7	78.7	80.9	82.2	84.4	85.8	87.5	88.9	90.5	91.6	94.2	95.4	96.4	98.0	100.2	101.4	102.9	104.1	104.6	106.5	110.5
3.50-3.75	83.0	85.4	87.6	89.3	90.9	92.9	95.7	96.9	98.7	101.2	102.6	105.6	106.9	107.5	110.0	113.1	115.8	115.2	118.1	118.5	121.1	121.7	122.8	128.8
3.75-4.00	94.2	98.2	100.4	102.5	104.5	106.3	109.3	111.4	112.7	115.2	117.8	119.4	121.6	124.3	126.2	127.8	128.5	131.8	132.4	135.4	135.0	138.3	142.2	145.7
4.00-4.25	107.2	109.9	112.3	113.6	118.1	121.3	123.6	126.1	127.7	130.0	133.6	135.8	137.9	140.2	142.0	144.8	147.3	148.9	150.8	153.0	155.6	159.8	159.8	165.0
4.25-4.50	121.9	122.7	126.2	129.8	133.5	135.9	138.3	140.0	144.4	148.0	147.9	153.5	155.4	157.3	160.8	162.8	164.6	167.6	170.9	173.0	176.0	176.5	179.1	185.1
4.50-4.75	135.3	139.4	142.4	144.9	149.8	149.2	153.4	158.5	162.6	164.7	168.6	169.6	171.8	174.9	177.9	181.9	182.3	187.0	189.1	191.1	195.8	197.3	198.0	206.3
4.75-5.00	150.9	153.8	160.7	163.1	166.1	172.7	174.8	175.2	180.0	184.0	187.0	188.7	190.2	195.8	197.2	201.9	203.8	209.9	209.5	211.9	213.5	219.1	221.3	229.1
5.00-5.25			177.6	176.7	182.0	184.9	189.6	193.7	195.5	199.5	208.2	207.3	209.6	219.2	221.7	220.0	224.8	229.8	234.6	235.6	236.5	240.3	247.1	255.1
5.25-5.50	185.9	178.5				202.3	207.4	215.5	220.4	223.4	226.7	230.5	233.3	235.9	237.0	243.7	249.6	250.4	252.1	260.2	265.6	269.9	269.7	279.1
5.50-5.75								232.2	237.2		243.0	245.6	256.6	261.5	261.1	273.0	269.0	272.5	278.0	282.2	287.0	292.9	290.9	302.7
5.75-6.00										263.4	267.0	280.4	268.7	282.3	286.0	295.6	297.5	305.3	300.7	309.2	307.4	316.5	316.1	342.4
6.00-6.25											285.4	305.6	290.0	297.1	314.1	312.1	325.8	318.5	335.1	337.2	347.7	343.6	350.9	364.4
6.25-6.50												321.1	337.0			335.4	350.2	359.6	368.4	364.5		372.3	376.0	384.1
6.50-6.75													348.8	358.0			375.9	375.2	389.6	400.3			395.9	416.0
6.75-7.00																		407.4	427.3	423.9				463.8
7.00-7.25																			436.7	447.3	444.9	450.0		496.4
7.25-7.50																					480.5	510.0		514.0
7.50-7.75																							535.7	555.5

Table 11 Occurrence (hours) of Hindcast T_e Versus H_s at the Paualela site during 1979-2013

H_S (m)	Te (s) 4.25-4.50	4.50-4.75	4.75-5.00	5.00-5.25	5.25-5.50	5.50-5.75	5.75-6.00	6.00-6.25	6.25-6.50	6.50-6.75	6.75-7.00	7.00-7.25	7.25-7.50	7.50-7.75	7.75-8.00	8.00-8.25	8.25-8.50	8.50-8.75	8.75-9.00	9.00-9.25	9.25-9.50	9.50-9.75	9.75-100	10.0-10.25	10.25-10.50	10.50-10.75	10.75-11.00	11.00-11.25
0.50-0.75					1	4	1	9	9	4	25	29	21	2														
0.75-1.00	5	5	47	82	124	169	211	143	251	208	330	271	207	250	135	113	78	86	26	18	21	4	1					
1.00-1.25	45	127	329	521	872	1089	1297	1132	1295	1224	1222	1100	1031	1047	950	945	757	640	428	380	244	208	108	69	45	20	12	6
1.25-1.50	47	202	650	1262	2260	2931	3533	3489	3210	2821	2361	2249	2148	1858	1763	1764	1481	1312	1041	1050	916	659	490	487	457	359	196	139
1.50-1.75	8	76	296	1021	2305	3475	4327	4404	4407	3671	3225	3094	2638	2288	2026	1827	1739	1558	1538	1296	1364	1268	1091	1003	826	727	735	504
1.75-2.00		8	36	308	908	1984	2646	3388	3281	3271	3006	2497	2166	2085	1878	1781	1512	1457	1340	1393	1421	1397	1437	1282	1231	1169	976	961
2.00-2.25			2	32	172	507	1008	1446	1863	2060	2027	1946	1761	1893	1671	1415	1360	1293	1289	1265	1332	1375	1337	1273	1202	1213	1249	1213
2.25-2.50				1	16	83	203	565	873	1086	1165	1240	1286	1362	1235	1193	1068	1006	1096	1177	1035	1016	993	972	925	972	896	965
2.50-2.75				1	4	4	45	118	325	395	570	704	817	885	767	839	741	692	649	729	687	705	762	738	746	748	729	701
2.75-3.00							6	29	68	185	346	520	580	600	559	502	523	469	531	560	502	426	470	446	503	525	511	543
3.00-3.25								7	16	83	166	343	256	420	362	397	364	297	289	255	314	327	274	278	304	340	367	344
3.25-3.50								1	5	27	84	125	157	193	220	280	318	228	181	226	172	174	139	134	155	172	165	165
3.50-3.75										2	21	36	93	127	124	214	211	140	109	103	95	75	84	67	72	127	99	111
3.75-4.00											12	4	25	70	95	140	104	94	107	78	70	69	35	45	50	50	56	44
4.00-4.25												1	9	31	42	58	68	88	51	74	42	33	14	23	36	45	26	34
4.25-4.50													2	11	25	48	50	61	47	19	15	20	27	14	19	14	5	11
4.50-4.75														5	23	20	26	19	31	12	6	0	3	12	8	6	2	13
4.75-5.00														4		16	25	19	28	4	6	5	2	6	1	2	3	2
5.00-5.25																4	4	8	10	0	2	2	2	2		2	3	2
5.25-2.50																	4	7	11	12	4	2	2	5				
5.50-5.75																	2	3	3	2	11							
5.75-6.00																		1			3							

H_S (m)	Te (s) 11.25-11.50	11.50-11.75	11.75-12.00	12.00-12.25	12.25-12.50	12.50-12.75	12.75-13.00	13.00-13.25	13.25-13.50	13.50-13.75	13.75-14.00	14.00-14.25	14.25-14.50	14.50-14.75	14.75-15.00	15.00-15.25	15.25-15.50	15.50-15.75	15.75-16.00	16.00-16.25	16.25-16.50	16.50-16.75	16.75-17.00	>17.00	
0.50-0.75																									105
0.75-1.00																									2785
1.00-1.25	4	4	1	3				2																	17157
1.25-1.50	89	73	42	23	11	4	6	0	3	3	2		2				1								41394
1.50-1.75	426	336	294	160	114	56	51	28	21	13	5	7	3	1	1	1		1		1					54256
1.75-2.00	783	640	530	427	305	259	205	139	104	77	48	24	11	11	13	11	9	3	4	2	3				48427
2.00-2.25	1042	880	811	679	571	396	356	311	206	174	146	87	62	37	34	23	22	9	10	10	14	9	4		39097
2.25-2.50	959	823	945	803	733	610	410	335	281	201	193	148	84	78	64	57	54	17	26	13	9	7	2	7	29288
2.50-2.75	770	779	769	736	674	696	556	498	404	312	260	207	210	135	88	84	59	40	27	23	18	8	6	16	21476
2.75-3.00	498	490	575	561	511	551	543	502	389	285	291	248	239	178	142	110	69	57	62	36	39	29	10	37	15856
3.00-3.25	379	393	328	373	398	345	405	378	365	341	254	194	176	168	154	116	106	94	50	59	29	29	20	56	11013
3.25-3.50	209	261	230	200	225	282	259	259	249	227	208	197	205	160	148	119	120	96	50	57	34	29	26	52	7223
3.50-3.75	103	121	157	159	113	147	122	155	189	167	180	158	127	140	105	103	81	73	56	41	23	25	20	36	4511
3.75-4.00	59	70	94	87	93	96	105	92	77	82	106	110	102	85	77	87	72	68	66	64	45	26	14	58	2983
4.00-4.25	32	40	39	64	93	68	80	71	73	82	60	66	84	94	50	60	51	69	57	48	34	29	16	44	2079
4.25-4.50	10	13	25	25	42	46	50	67	47	54	24	39	60	71	49	40	48	33	36	39	26	25	19	40	1316
4.50-4.75	5	7	7	9	14	16	18	16	45	29	37	21	28	18	26	34	21	28	31	24	18	11	17	18	684
4.75-5.00	5	5	4	9	13	5	14	18	35	29	28	41	36	19	12	18	24	18	14	10	19	29	10	16	554
5.00-5.25		5	5	2	9		2	10	12	15	15	19	22	15	21	8	6	16	21	15	11	8	10	23	311
5.25-5.50				2	4		3	2	1	6	5	4	5	7	15	1	4	3	7	16	12	8	9	25	186
5.50-5.75					1	1		1		1	5	6	6	9	8	3	2	2	4	2	3	8	10	20	113
5.75-6.00													1	2	4	4	2	2	3	1	2	4	4	12	45
6.00-6.25																3	4	3	1	2			3	7	23
6.25-6.50																	1	3	4	1	4	4	1	4	22
6.50-6.75																			2	4	4			4	14
6.75-7.00																					3		1	8	12
7.00-7.25																								4	4
7.25-7.50																								1	1
																									300935

Table 12 Total Hindcast Wave Energy Flux (kWh/m) by T_e and H_s at the Pauwela site during 1979-2013

H_S (m)	Te (s)																											
	4.25-4.50	4.50-4.75	4.75-5.00	5.00-5.25	5.25-5.50	5.50-5.75	5.75-6.00	6.00-6.25	6.25-6.50	6.50-6.75	6.75-7.00	7.00-7.25	7.25-7.50	7.50-7.75	7.75-8.00	8.00-8.25	8.25-8.50	8.50-8.75	8.75-9.00	9.00-9.25	9.25-9.50	9.50-9.75	9.75-100	10.0-10.25	10.25-10.50	10.50-10.75	10.75-11.00	11.00-11.25
0.50-0.75					1	6	1	14	15	7	45	52	41	4														
0.75-1.00	11	10	97	179	288	404	504	359	652	583	950	785	636	797	465	406	286	338	110	78	95	19	5					
1.00-1.25	129	386	1047	1735	3105	4080	5126	4681	5513	5432	5486	5202	5042	5326	5029	5153	4271	3751	2610	2451	1612	1382	768	518	352	161	101	48
1.25-1.50	194	863	2967	6113	11621	15755	19771	20454	19815	18090	15599	15637	15259	13781	13517	13896	12149	11008	9060	9481	8683	6495	4962	5102	4955	4032	2242	1658
1.50-1.75	41	452	1832	6687	16002	25427	33284	35285	37049	32168	29547	29440	26029	23403	21429	20057	19736	18348	18720	16419	17725	16964	15259	14489	12142	11016	11513	8159
1.75-2.00		59	297	2647	8267	18951	26626	35727	36087	37719	36303	31331	28364	28397	26632	26105	22966	22805	21678	23439	24569	25000	26532	24328	24123	23586	20171	20566
2.00-2.25			21	343	1985	6183	12876	19502	26301	30392	31310	31196	29619	33283	30291	26749	26538	26109	26944	27219	29621	31407	31630	30904	29949	31158	32933	32960
2.25-2.50				13	229	1256	3280	9487	15425	20067	22523	24897	26883	29786	27998	28163	26081	25512	28843	31814	28695	29102	29311	29520	28899	31251	29710	32809
2.50-2.75				17	71	76	868	2415	6954	8851	13469	17304	20958	23569	21278	24077	21971	21259	20686	23929	23392	24613	27479	27501	28432	29460	29600	29080
2.75-3.00							145	723	1776	5056	9861	15323	17862	19175	18526	17293	18683	17353	20351	22157	20626	17966	20361	19957	23087	24753	24877	27090
3.00-3.25								206	489	2653	5480	11863	9162	15808	14126	16141	15339	12971	13001	11871	15050	16200	14023	14572	16469	18885	21051	20252
3.25-3.50								33	177	1011	3273	5045	6604	8460	10115	13268	15693	11559	9505	12259	9648	10095	8288	8278	9741	11097	10885	11289
3.50-3.75										87	942	1665	4484	6385	6450	11637	11854	8181	6591	6359	6138	5015	5809	4745	5224	9478	7617	8780
3.75-4.00											602	214	1370	4008	5682	8717	6703	6333	7368	5584	5190	5301	2775	3631	4140	4250	4901	3971
4.00-4.25												57	554	2012	2841	4097	4953	6623	3989	6007	3522	2832	1244	2122	3395	4413	2611	3509
4.25-4.50													140	825	1907	3797	4050	5166	4130	1696	1398	1936	2733	1433	1962	1522	560	1278
4.50-4.75														396	1949	1727	2408	1784	3039	1239	625		333	1379	935	733	256	1700
4.75-5.00														356		1561	2534	1980	3045	441	694	614	259	773	137	272	414	284
5.00-5.25																442	455	933	1220		256	256	268	282		292	452	305
5.25-2.50																	489	879	1452	1648	570	298	312	789				
5.50-5.75																	273	422	426	285	1707							
5.75-6.00																		144			487							

H_S (m)	Te (s)																							
	11.25-11.50	11.50-11.75	11.75-12.00	12.00-12.25	12.25-12.50	12.50-12.75	12.75-13.00	13.00-13.25	13.25-13.50	13.50-13.75	13.75-14.00	14.00-14.25	14.25-14.50	14.50-14.75	14.75-15.00	15.00-15.25	15.25-15.50	15.50-15.75	15.75-16.00	16.00-16.25	16.25-16.50	16.50-16.75	16.75-17.00	>17.00
0.50-0.75																								
0.75-1.00																								
1.00-1.25	36	37	9	27				21																
1.25-1.50	1092	928	559	321	155	55	85		46	44	32		32				19							
1.50-1.75	7093	5769	5192	2899	2148	1078	1002	565	447	278	106	149	68	24	24	22		27		26				
1.75-2.00	17172	14428	12226	10186	7416	6448	5308	3641	2842	2102	1332	694	308	323	380	325	272	91	126	68	106			
2.00-2.25	29162	25275	24015	20515	17746	12630	11486	10362	7060	5998	5213	3176	2314	1415	1344	904	859	346	430	425	588	379	168	
2.25-2.50	33455	29465	34972	30491	28272	24192	16802	14020	11965	8716	8538	6677	3794	3641	3033	2768	2651	842	1326	675	466	383	108	385
2.50-2.75	32748	34127	34341	33743	31683	33607	27647	25225	20797	16487	14089	11387	11830	7764	5077	4992	3551	2465	1635	1476	1153	514	393	1101
2.75-3.00	25683	25597	30782	30905	28765	31731	32022	30392	24241	18203	18847	16356	16093	12185	9896	7887	4984	4192	4680	2767	2956	2230	769	3027
3.00-3.25	22892	24375	20912	24255	26532	23584	28356	26896	26618	25231	19266	15126	13982	13551	12717	9771	9085	8158	4394	5291	2678	2718	1846	5526
3.25-3.50	14599	18804	17026	15231	17479	22504	21095	21483	21123	19833	18503	17889	19025	15116	14178	11631	11898	9795	5162	5886	3531	3097	2819	5871
3.50-3.75	8359	10182	13349	13988	10162	13417	11418	14819	18617	16772	18407	16481	13469	15171	11636	11612	9269	8658	6619	4949	2887	3110	2515	4694
3.75-4.00	5450	6587	9193	8681	9508	10137	11282	10074	8637	9362	12451	13040	12486	10540	9705	11184	9494	9143	8925	8779	6248	3662	1982	8741
4.00-4.25	3385	4368	4257	7251	10857	8117	9749	8790	9401	10616	7945	8913	11664	13091	7203	8788	7571	10347	8793	7570	5439	4685	2614	7426
4.25-4.50	1182	1561	3076	3189	5506	6090	6821	9409	6693	7880	3565	5987	9322	11207	7988	6609	8020	5539	6224	6856	4649	4471	3482	7614
4.50-4.75	669	935	953	1295	2059	2366	2751	2485	7229	4772	6122	3579	4869	3177	4647	6222	3903	5311	5952	4725	3596	2221	3531	3838
4.75-5.00	738	757	605	1418	2105	823	2417	3096	6193	5223	5161	7676	6953	3785	2373	3607	5027	3799	3014	2178	4201	6485	2253	3877
5.00-5.25		820	864	348	1637		366	1880	2324	2974	3035	3928	4659	3246	4652	1786	1354	3651	4989	3631	2744	2006	2535	5987
5.25-5.50				378	769		635	410	206	1335	1141	903	1184	1673	3654	247	1019	775	1814	4204	3189	2164	2465	7239
5.50-5.75					213	223		232		240	1211	1485	1557	2370	2112	802	547	570	1151	588	875	2337	3010	6304
5.75-6.00													268	554	1156	1163	595	606	946	326	640	1299	1328	4069
6.00-6.25																940	1334	986	346	693			1086	2631
6.25-6.50																	353	1095	1460	359	1514	1567	385	1598
6.50-6.75																			778	1613	1648			1789
6.75-7.00																					1293		448	3907
7.00-7.25																								1988
7.25-7.50																								518

Table 13 Average Hindcast Wave Power (kW/m) by T_e and H_s at the Kilauea site during 1979-2013

H_S (m)	Te (s) 4.25-4.50	4.50-4.75	4.75-5.00	5.00-5.25	5.25-5.50	5.50-5.75	5.75-6.00	6.00-6.25	6.25-6.50	6.50-6.75	6.75-7.00	7.00-7.25	7.25-7.50	7.50-7.75	7.75-8.00	8.00-8.25	8.25-8.50	8.50-8.75	8.75-9.00	9.00-9.25	9.25-9.50	9.50-9.75	9.75-100	10.0-10.25	10.25-10.50	10.50-10.75	10.75-11.00	11.00-11.25
0.50-0.75					1.5	1.5	1.4	1.5	1.7	1.8	1.8	1.8	2.0	2.1														
0.75-1.00	2.1	2.0	2.1	2.2	2.3	2.4	2.4	2.5	2.6	2.8	2.9	2.9	3.1	3.2	3.4	3.6	3.7	3.9	4.2	4.3	4.5	4.9	5.2					
1.00-1.25	2.9	3.0	3.2	3.3	3.6	3.7	4.0	4.1	4.3	4.4	4.5	4.7	4.9	5.1	5.3	5.5	5.6	5.9	6.1	6.5	6.6	6.6	7.1	7.5	7.8	8.0	8.4	8.0
1.25-1.50	4.1	4.3	4.6	4.8	5.1	5.4	5.6	5.9	6.2	6.4	6.6	7.0	7.1	7.4	7.7	7.9	8.2	8.4	8.7	9.0	9.5	9.9	10.1	10.5	10.8	11.2	11.4	11.9
1.50-1.75	5.1	6.0	6.2	6.5	6.9	7.3	7.7	8.0	8.4	8.8	9.2	9.5	9.9	10.2	10.6	11.0	11.3	11.8	12.2	12.7	13.0	13.4	14.0	14.4	14.7	15.2	15.7	16.2
1.75-2.00		7.4	8.3	8.6	9.1	9.6	10.1	10.5	11.0	11.5	12.1	12.5	13.1	13.6	14.2	14.7	15.2	15.7	16.2	16.8	17.3	17.9	18.5	19.0	19.6	20.2	20.7	21.4
2.00-2.25			10.4	10.7	11.5	12.2	12.8	13.5	14.1	14.8	15.4	16.0	16.8	17.6	18.1	18.9	19.5	20.2	20.9	21.5	22.2	22.8	23.7	24.3	24.9	25.7	26.4	27.2
2.25-2.50				13.4	14.3	15.1	16.2	16.8	17.7	18.5	19.3	20.1	20.9	21.9	22.7	23.6	24.4	25.4	26.3	27.0	27.7	28.6	29.5	30.4	31.2	32.2	33.2	34.0
2.50-2.75				16.9	17.7	19.0	19.3	20.5	21.4	22.4	23.6	24.6	25.7	26.6	27.7	28.7	29.7	30.7	31.9	32.8	34.0	34.9	36.1	37.3	38.1	39.4	40.6	41.5
2.75-3.00							24.1	24.9	26.1	27.3	28.5	29.5	30.8	32.0	33.1	34.4	35.7	37.0	38.3	39.6	41.1	42.2	43.3	44.7	45.9	47.1	48.7	49.9
3.00-3.25								29.4	30.6	32.0	33.0	34.6	35.8	37.6	39.0	40.7	42.1	43.7	45.0	46.6	47.9	49.5	51.2	52.4	54.2	55.5	57.4	58.9
3.25-3.50								33.0	35.4	37.4	39.0	40.4	42.1	43.8	46.0	47.4	49.4	50.7	52.5	54.2	56.1	58.0	59.6	61.8	62.8	64.5	66.0	68.4
3.50-3.75										43.7	44.9	46.3	48.2	50.3	52.0	54.4	56.2	58.4	60.5	61.7	64.6	66.9	69.1	70.8	72.5	74.6	76.9	79.1
3.75-4.00											50.2	53.5	54.8	57.3	59.8	62.3	64.4	67.4	68.9	71.6	74.1	76.8	79.3	80.7	82.8	85.0	87.5	90.3
4.00-4.25												57.0	61.6	64.9	67.6	70.6	72.8	75.3	78.2	81.2	83.8	85.8	88.9	92.3	94.3	98.1	100.4	103.2
4.25-4.50													69.8	75.0	76.3	79.1	81.0	84.7	87.9	89.3	93.2	96.8	101.2	102.4	103.3	108.7	111.9	116.2
4.50-4.75														79.3	84.7	86.4	92.6	93.9	98.0	103.2	104.2		111.1	115.0	116.9	122.1	128.2	130.7
4.75-5.00														89.1		97.5	101.3	104.2	108.8	110.3	115.6	122.7	129.6	128.8	136.6	136.0	137.8	141.8
5.00-5.25																110.5	113.8	116.6	122.0		127.9	127.8	134.0	141.0		145.9	150.8	152.5
5.25-2.50																	122.2	125.6	132.0	137.3	142.6	148.8	156.0	157.9				
5.50-5.75																	136.6	140.6	142.0	142.6	155.1							
5.75-6.00																		144.3			162.3							

H_S (m)	Te (s) 11.25-11.50	11.50-11.75	11.75-12.00	12.00-12.25	12.25-12.50	12.50-12.75	12.75-13.00	13.00-13.25	13.25-13.50	13.50-13.75	13.75-14.00	14.00-14.25	14.25-14.50	14.50-14.75	14.75-15.00	15.00-15.25	15.25-15.50	15.50-15.75	15.75-16.00	16.00-16.25	16.25-16.50	16.50-16.75	16.75-17.00	>17.00
0.50-0.75																								
0.75-1.00																								
1.00-1.25	8.9	9.3	9.3	9.0				10.6																
1.25-1.50	12.3	12.7	13.3	13.9	14.1	13.8	14.2		15.2	14.6	15.9		16.0				19.3							
1.50-1.75	16.6	17.2	17.7	18.1	18.8	19.2	19.6	20.2	21.3	21.4	21.2	21.2	22.7	24.3	24.1	21.8		26.6		26.0				
1.75-2.00	21.9	22.5	23.1	23.9	24.3	24.9	25.9	26.2	27.3	27.3	27.8	28.9	28.0	29.4	29.2	29.5	30.2	30.3	31.5	33.9	35.3			
2.00-2.25	28.0	28.7	29.6	30.2	31.1	31.9	32.3	33.3	34.3	34.5	35.7	36.5	37.3	38.3	39.5	39.3	39.0	38.5	43.0	42.5	42.0	42.1	42.0	
2.25-2.50	34.9	35.8	37.0	38.0	38.6	39.7	41.0	41.9	42.6	43.4	44.2	45.1	45.2	46.7	47.4	48.6	49.1	49.5	51.0	51.9	51.8	54.7	53.9	55.1
2.50-2.75	42.5	43.8	44.7	45.8	47.0	48.3	49.7	50.7	51.5	52.8	54.2	55.0	56.3	57.5	57.7	59.4	60.2	61.6	60.5	64.2	64.0	64.2	65.5	68.8
2.75-3.00	51.6	52.2	53.5	55.1	56.3	57.6	59.0	60.5	62.3	63.9	64.8	66.0	67.3	68.5	69.7	71.7	72.2	73.5	75.5	76.9	75.8	76.9	76.9	81.8
3.00-3.25	60.4	62.0	63.8	65.0	66.7	68.4	70.0	71.2	72.9	74.0	75.9	78.0	79.4	80.7	82.6	84.2	85.7	86.8	87.9	89.7	92.3	93.7	92.3	98.7
3.25-3.50	69.9	72.0	74.0	76.2	77.7	79.8	81.4	82.9	84.8	87.4	89.0	90.8	92.8	94.5	95.8	97.7	99.2	102.0	103.2	103.3	103.8	106.8	108.4	112.9
3.50-3.75	81.2	84.1	85.0	88.0	89.9	91.3	93.6	95.6	98.5	100.4	102.3	104.3	106.1	108.4	110.8	112.7	114.4	118.6	118.2	120.7	125.5	124.4	125.7	130.4
3.75-4.00	92.4	94.1	97.8	99.8	102.2	105.6	107.4	109.5	112.2	114.2	117.5	118.5	122.4	124.0	126.0	128.6	131.9	134.5	135.2	137.2	138.8	140.8	141.6	150.7
4.00-4.25	105.8	109.2	109.2	113.3	116.7	119.4	121.9	123.8	128.8	129.5	132.4	135.0	138.9	139.3	144.1	146.5	148.5	150.0	154.3	157.7	160.0	161.6	163.4	168.8
4.25-4.50	118.2	120.1	123.0	127.6	131.1	132.4	136.4	140.4	142.4	145.9	148.5	153.5	155.4	157.8	163.0	165.2	167.1	167.9	172.9	175.8	178.8	178.8	183.3	190.4
4.50-4.75	133.8	133.6	136.2	143.8	147.1	147.9	152.9	155.3	160.6	164.5	165.4	170.4	173.9	176.5	178.7	183.0	185.8	189.7	192.0	196.9	199.8	201.9	207.7	213.2
4.75-5.00	147.7	151.4	151.3	157.6	161.9	164.7	172.6	172.0	176.9	180.1	184.3	187.2	193.1	199.2	197.8	200.4	209.5	211.1	215.3	217.8	221.1	223.6	225.3	242.3
5.00-5.25		164.1	172.9	174.2	181.9		183.0	188.0	193.6	198.3	202.3	206.7	211.8	216.4	221.5	223.3	225.6	228.2	237.6	242.1	249.5	250.8	253.5	260.3
5.25-5.50				188.8	192.1		211.5	204.9	206.1	222.5	228.2	225.8	236.9	238.9	243.6	246.7	254.7	258.4	259.1	262.7	265.7	270.6	273.9	289.6
5.50-5.75					213.4	223.0		231.8		239.8	242.3	247.5	259.5	263.4	264.0	267.2	273.6	285.2	287.8	293.8	291.8	292.2	301.0	315.2
5.75-6.00													267.8	277.1	289.0	290.8	297.3	303.2	315.3	326.3	319.8	324.6	332.0	339.1
6.00-6.25																313.5	333.5	328.8	346.1	346.6			361.8	375.8
6.25-6.50																	352.5	364.9	364.9	359.4	378.6	391.8	384.9	399.4
6.50-6.75																			389.1	403.2	412.1			447.2
6.75-7.00																					431.1		448.5	488.3
7.00-7.25																								497.1
7.25-7.50																								517.8

Table 14 Occurrence (hours) of Hindcast T_e Versus H_s at the Upolu site during 1979-2013

	Te (s)																												
Hs (m)	3.50-3.75	3.75-4.00	4.00-4.25	4.25-4.50	4.50-4.75	4.75-5.00	5.00-5.25	5.25-5.50	5.50-5.75	5.75-6.00	6.00-6.25	6.25-6.50	6.50-6.75	6.75-7.00	7.00-7.25	7.25-7.50	7.50-7.75	7.75-8.00	8.00-8.25	8.25-8.50	8.50-8.75	8.75-9.00	9.00-9.25	9.25-9.50	9.50-9.75	9.75-10.0	10.0-10.25	10.25-10.50	10.50-10.75
0.50-0.75						1	16	22	19	11	34	102	112	135	152	179	162	207	173	180	97	54	35	53	28	27	30	23	8
0.75-1.00	3	7	2	1	12	66	122	314	446	581	804	1038	1145	1298	1301	1407	1410	1180	1133	1135	1030	781	609	520	448	422	295	292	212
1.00-1.25			1	2	20	151	503	1306	2271	3287	4108	3930	3587	3483	3303	3120	2853	2608	2163	2061	1849	1510	1339	1173	1121	943	710	519	396
1.25-1.50					2	20	457	1830	3417	5802	7124	7625	6814	5653	4704	4037	3576	3031	2624	2405	1886	1662	1398	1130	974	868	754	611	600
1.50-1.75						1	47	433	1634	4203	6569	8053	8078	6777	4873	4014	3335	2746	2044	1774	1533	1195	1010	918	730	596	527	471	376
1.75-2.00								62	340	1295	3101	5023	5818	5356	4281	3193	2471	1925	1578	1371	1156	1011	855	635	566	509	446	464	291
2.00-2.25									19	190	814	1728	2634	3325	2808	2576	1754	1215	906	794	667	548	459	394	367	344	332	251	276
2.25-2.50										8	46	383	755	1338	1621	1590	1228	985	598	546	411	300	356	239	220	222	241	206	173
2.50-2.75												28	151	445	886	1026	828	706	581	453	243	165	175	163	135	161	140	125	110
2.75-3.00													7	83	350	336	482	491	360	301	175	136	83	100	84	68	57	48	50
3.00-3.25													1	2	34	105	251	309	232	232	186	73	68	64	49	70	52	46	33
3.25-3.50														1		27	69	153	164	160	114	69	66	40	47	36	21	18	27
3.50-3.75																3	22	57	108	87	59	82	78	52	39	21	18	14	7
3.75-4.00																	1	9	13	62	45	42	47	20	7	7	2	5	6
4.00-4.25																			2	25	18	25	33	30	5		9	6	4
4.25-4.50																					4	14	23	15		5		1	2
4.50-4.75																							6	5	13	7	5	1	4
4.75-5.00																						1	1		18	2	2		
5.00-5.25																							1		12				

	Te (s)																										
Hs (m)	10.75-11.00	11.00-11.25	11.25-11.50	11.50-11.75	11.75-12.00	12.00-12.25	12.25-12.50	12.50-12.75	12.75-13.00	13.00-13.25	13.25-13.50	13.50-13.75	13.75-14.00	14.00-14.25	14.25-14.50	14.50-14.75	14.75-15.00	15.00-15.25	15.25-15.50	15.50-15.75	15.75-16.00	16.00-16.25	16.25-16.50	16.50-16.75	16.75-17.00	>17.00	
0.50-0.75	3	3	5		1			1			1		1														1875
0.75-1.00	171	128	77	46	53	49	26	34	18	12	12	8	3			2	2	4	2								18661
1.00-1.25	349	269	235	187	182	129	82	90	85	54	61	30	28	15	13	7	7	4									50144
1.25-1.50	414	351	308	187	144	106	95	92	84	91	49	53	57	48	30	20	13	10	11	6	4	2					71179
1.50-1.75	380	339	280	252	198	122	127	82	67	60	43	53	37	37	30	18	7	10	7	1	2		1	1			64091
1.75-2.00	282	239	210	189	117	118	82	57	48	59	39	26	37	36	38	21	28	14	13	10	3	1		2	2		43418
2.00-2.25	265	205	137	123	83	77	73	53	44	40	17	15	13	23	7	8	8	4	8	8	1				1		23614
2.25-2.50	155	146	117	96	70	61	58	54	48	38	61	28	14	10	7	5	5	4	7	3	3					1	12457
2.50-2.75	64	73	63	62	63	33	24	19	38	19	11	17	16	18	18	9	1	6	3	1		1	3	2	4	1	7090
2.75-3.00	51	62	43	42	41	19	16	28	22	13	20	11	14	15	7	14	9	7	5	7	1	1				1	3660
3.00-3.25	24	10	15	20	17	14	19	15	16	11	11	5	5	3	6	6	3		3				1	1	1	6	2019
3.25-3.50	17	10	7	7	4	8	8	13	13	26	23	13	6	3	2	6	5	2	2								1187
3.50-3.75	12	18	8	5	4	3	5	14	5	10	2		6	5	5	3	2										754
3.75-4.00	12	6	8	8	6	2	0	2	4	6	5	6	11	2		2	13	5	3								367
4.00-4.25				2	4	5	3	1	4	3							4	3	19	8	5						218
4.25-4.50	1	1		1	1	1	0	2	4	7	3	1									4						90
4.50-4.75						1	6	4	1		3	1	1														58
4.75-5.00												3	1	1	1												30
5.00-5.25													2	1		3											19
5.25-2.50														2	2												4
																											300935

Table 15 Total Hindcast Wave Energy Flux (kWh/m) by T_e and H_s at the Upolu site during 1979-2013

H_S (m)	Te (s) 3.50-3.75	3.75-4.00	4.00-4.25	4.25-4.50	4.50-4.75	4.75-5.00	5.00-5.25	5.25-5.50	5.50-5.75	5.75-6.00	6.00-6.25	6.25-6.50	6.50-6.75	6.75-7.00	7.00-7.25	7.25-7.50	7.50-7.75	7.75-8.00	8.00-8.25	8.25-8.50	8.50-8.75	8.75-9.00	9.00-9.25	9.25-9.50	9.50-9.75	9.75-10.0	10.0-10.25	10.25-10.50	10.50-10.75
0.50-0.75						1	22	28	28	17	53	168	188	221	265	322	300	398	335	370	206	124	81	121	65	68	83	65	23
0.75-1.00	3	9	3	2	22	131	261	736	1097	1486	2144	2835	3245	3835	3964	4442	4563	3971	4003	4182	3885	3053	2482	2160	1916	1884	1350	1381	1025
1.00-1.25			2	5	61	461	1680	4652	8478	12951	16965	16885	16036	16027	15792	15390	14609	13821	11925	11756	10980	9214	8394	7464	7517	6478	5056	3747	2962
1.25-1.50					8	87	2142	9130	18272	32635	42306	47333	44233	38069	33022	29486	27308	23917	21397	20202	16351	14944	13070	10792	9624	8800	7968	6574	6709
1.50-1.75						6	303	2949	11780	32433	53230	68334	72176	63176	47392	40506	35066	29931	22972	20704	18627	14901	12900	12210	9989	8474	7643	6964	5741
1.75-2.00								546	3202	12972	32884	56164	68258	65974	54803	42712	34447	27751	23675	21489	18661	17020	14811	11391	10482	9693	8802	9439	6022
2.00-2.25									229	2405	10925	24584	39463	52398	46307	44487	31187	22633	17483	15858	13760	11655	10192	8956	8570	8365	8323	6494	7312
2.25-2.50										124	774	6740	14029	26143	33241	34115	27444	22940	14320	13682	10760	8059	9730	6840	6500	6749	7589	6709	5679
2.50-2.75												590	3401	10586	22235	26694	22669	20153	17279	13690	7679	5406	5888	5696	4805	5941	5326	4880	4407
2.75-3.00													195	2327	10521	10477	15632	16677	12674	11057	6701	5351	3358	4177	3618	3021	2635	2239	2407
3.00-3.25													31	64	1184	3867	9652	12410	9674	10118	8319	3401	3277	3190	2505	3744	2829	2574	1865
3.25-3.50														39		1173	3060	7063	7992	8051	5963	3734	3758	2333	2813	2224	1326	1187	1802
3.50-3.75																142	1100	3091	6001	5075	3572	5146	5156	3480	2727	1486	1325	1063	559
3.75-4.00																	59	553	827	4158	3106	2973	3485	1513	573	567	176	432	547
4.00-4.25																			144	1866	1420	2039	2756	2631	428		877	574	396
4.25-4.50																					346	1291	2190	1445		520		108	221
4.50-4.75																							638	534	1475	827	611	122	492
4.75-5.00																						119	113		2253	254	252		
5.00-5.25																							126		1642				

H_S (m)	Te (s) 10.75-11.00	11.00-11.25	11.25-11.50	11.50-11.75	11.75-12.00	12.00-12.25	12.25-12.50	12.50-12.75	12.75-13.00	13.00-13.25	13.25-13.50	13.50-13.75	13.75-14.00	14.00-14.25	14.25-14.50	14.50-14.75	14.75-15.00	15.00-15.25	15.25-15.50	15.50-15.75	15.75-16.00	16.00-16.25	16.25-16.50	16.50-16.75	16.75-17.00	>17.00
0.50-0.75	9	9	16		3			3			3		4													
0.75-1.00	861	645	400	255	300	274	157	209	114	77	79	52	21			10	11	23	11							
1.00-1.25	2661	2120	1883	1556	1523	1096	712	780	758	508	578	308	279	147	134	70	78	46								
1.25-1.50	4749	4082	3686	2298	1808	1340	1206	1183	1104	1222	670	766	793	681	450	293	203	151	182	101	75	38				
1.50-1.75	6051	5520	4711	4332	3408	2147	2260	1496	1256	1180	855	1046	742	772	648	378	140	211	161	22	46		22	25		
1.75-2.00	5913	5105	4596	4263	2685	2842	2000	1400	1212	1561	1038	698	978	941	993	588	813	398	372	282	89	32		63	57	
2.00-2.25	7183	5810	3923	3612	2482	2356	2258	1710	1457	1313	557	511	448	787	256	298	300	145	296	307	33				43	
2.25-2.50	5216	5079	4211	3557	2619	2300	2249	2170	1952	1548	2560	1226	630	451	309	223	242	186	323	140	154					55
2.50-2.75	2654	3114	2765	2736	2863	1554	1150	919	1897	955	589	860	842	982	1014	537	58	354	176	61		57	176	130	255	67
2.75-3.00	2553	3139	2270	2271	2245	1083	902	1661	1338	772	1239	670	897	1011	449	896	588	453	329	463	73	77				78
3.00-3.25	1405	585	895	1237	1098	918	1315	1022	1134	800	818	375	375	222	475	478	259		247				81	85	90	570
3.25-3.50	1170	713	493	522	295	633	622	1025	1050	2161	1945	1129	555	268	189	559	462	181	181							
3.50-3.75	958	1457	660	422	341	268	446	1293	462	982	193		588	527	533	330	226									
3.75-4.00	1085	546	750	778	607	218		206	441	638	553	698	1316	220		239	1668	653	401							
4.00-4.25				215	438	559	356	119	493	396							540	412	2739	1197	784					
4.25-4.50	108	112		117	122	129		254	545	960	438	151									638					
4.50-4.75						135	868	581	143		478	170	166													
4.75-5.00												544	194	181	196											
5.00-5.25													407	213		650										
5.25-2.50														444	454											

Table 16 Average Hindcast Wave Power (kW/m) by T_e and H_s at the Upolu site during 1979-2013

		Te (s)																												
		3.50-3.75	3.75-4.00	4.00-4.25	4.25-4.50	4.50-4.75	4.75-5.00	5.00-5.25	5.25-5.50	5.50-5.75	5.75-6.00	6.00-6.25	6.25-6.50	6.50-6.75	6.75-7.00	7.00-7.25	7.25-7.50	7.50-7.75	7.75-8.00	8.00-8.25	8.25-8.50	8.50-8.75	8.75-9.00	9.00-9.25	9.25-9.50	9.50-9.75	9.75-10.0	10.0-10.25	10.25-10.50	10.50-10.75
Hs (m)	0.50-0.75						1.4	1.4	1.3	1.5	1.5	1.6	1.6	1.7	1.6	1.7	1.8	1.9	1.9	1.9	2.1	2.1	2.3	2.3	2.3	2.3	2.5	2.8	2.8	2.9
	0.75-1.00	1.2	1.3	1.7	1.6	1.8	2.0	2.1	2.3	2.5	2.6	2.7	2.7	2.8	3.0	3.0	3.2	3.2	3.4	3.5	3.7	3.8	3.9	4.1	4.2	4.3	4.5	4.6	4.7	4.8
	1.00-1.25			2.3	2.7	3.1	3.1	3.3	3.6	3.7	3.9	4.1	4.3	4.5	4.6	4.8	4.9	5.1	5.3	5.5	5.7	5.9	6.1	6.3	6.4	6.7	6.9	7.1	7.2	7.5
	1.25-1.50					3.8	4.3	4.7	5.0	5.3	5.6	5.9	6.2	6.5	6.7	7.0	7.3	7.6	7.9	8.2	8.4	8.7	9.0	9.3	9.6	9.9	10.1	10.6	10.8	11.2
	1.50-1.75						5.6	6.5	6.8	7.2	7.7	8.1	8.5	8.9	9.3	9.7	10.1	10.5	10.9	11.2	11.7	12.2	12.5	12.8	13.3	13.7	14.2	14.5	14.8	15.3
	1.75-2.00								8.8	9.4	10.0	10.6	11.2	11.7	12.3	12.8	13.4	13.9	14.4	15.0	15.7	16.1	16.8	17.3	17.9	18.5	19.0	19.7	20.3	20.7
	2.00-2.25									12.0	12.7	13.4	14.2	15.0	15.8	16.5	17.3	17.8	18.6	19.3	20.0	20.6	21.3	22.2	22.7	23.4	24.3	25.1	25.9	26.5
	2.25-2.50										15.5	16.8	17.6	18.6	19.5	20.5	21.5	22.3	23.3	23.9	25.1	26.2	26.9	27.3	28.6	29.5	30.4	31.5	32.6	32.8
	2.50-2.75												21.1	22.5	23.8	25.1	26.0	27.4	28.5	29.7	30.2	31.6	32.8	33.6	34.9	35.6	36.9	38.0	39.0	40.1
	2.75-3.00													27.9	28.0	30.1	31.2	32.4	34.0	35.2	36.7	38.3	39.3	40.5	41.8	43.1	44.4	46.2	46.6	48.1
	3.00-3.25													31.0	31.9	34.8	36.8	38.5	40.2	41.7	43.6	44.7	46.6	48.2	49.8	51.1	53.5	54.4	56.0	56.5
	3.25-3.50														39.4		43.4	44.4	46.2	48.7	50.3	52.3	54.1	56.9	58.3	59.9	61.8	63.2	66.0	66.7
	3.50-3.75																47.3	50.0	54.2	55.6	58.3	60.5	62.8	66.1	66.9	69.9	70.8	73.6	75.9	79.9
	3.75-4.00																	58.9	61.4	63.6	67.1	69.0	70.8	74.2	75.6	81.8	81.0	87.9	86.4	91.1
	4.00-4.25																			72.1	74.6	78.9	81.6	83.5	87.7	85.6		97.5	95.6	99.1
	4.25-4.50																					86.4	92.2	95.2	96.3		104.1		108.4	110.3
	4.50-4.75																							106.4	106.9	113.5	118.2	122.1	121.6	123.1
	4.75-5.00																						118.9	113.2		125.2	126.9	126.0		
	5.00-5.25																							125.5		136.8				

		Te (s)																									
		10.75-11.00	11.00-11.25	11.25-11.50	11.50-11.75	11.75-12.00	12.00-12.25	12.25-12.50	12.50-12.75	12.75-13.00	13.00-13.25	13.25-13.50	13.50-13.75	13.75-14.00	14.00-14.25	14.25-14.50	14.50-14.75	14.75-15.00	15.00-15.25	15.25-15.50	15.50-15.75	15.75-16.00	16.00-16.25	16.25-16.50	16.50-16.75	16.75-17.00	>17.00
Hs (m)	0.50-0.75	3.0	2.8	3.3		2.7			3.0			3.5		3.9													
	0.75-1.00	5.0	5.0	5.2	5.5	5.7	5.6	6.0	6.2	6.3	6.4	6.6	6.5	6.9			5.2	5.4	5.8	5.7							
	1.00-1.25	7.6	7.9	8.0	8.3	8.4	8.5	8.7	8.7	8.9	9.4	9.5	10.3	10.0	9.8	10.3	10.1	11.1	11.5								
	1.25-1.50	11.5	11.6	12.0	12.3	12.6	12.6	12.7	12.9	13.1	13.4	13.7	14.5	13.9	14.2	15.0	14.6	15.6	15.1	16.6	16.8	18.7	19.1				
	1.50-1.75	15.9	16.3	16.8	17.2	17.2	17.6	17.8	18.2	18.7	19.7	19.9	19.7	20.1	20.9	21.6	21.0	20.0	21.1	23.1	22.3	22.8		22.3	25.0		
	1.75-2.00	21.0	21.4	21.9	22.6	23.0	24.1	24.4	24.6	25.3	26.5	26.6	26.9	26.4	26.1	26.1	28.0	29.0	28.5	28.6	28.2	29.7	32.2		31.3	28.3	
	2.00-2.25	27.1	28.3	28.6	29.4	29.9	30.6	30.9	32.3	33.1	32.8	32.8	34.1	34.5	34.2	36.5	37.2	37.5	36.3	37.0	38.4	33.2				43.4	
	2.25-2.50	33.7	34.8	36.0	37.0	37.4	37.7	38.8	40.2	40.7	40.7	42.0	43.8	45.0	45.1	44.1	44.5	48.3	46.5	46.2	46.6	51.2					54.8
	2.50-2.75	41.5	42.7	43.9	44.1	45.4	47.1	47.9	48.4	49.9	50.3	53.5	50.6	52.6	54.6	56.3	59.7	58.1	59.0	58.5	60.7		56.7	58.8	64.8	63.6	67.0
	2.75-3.00	50.1	50.6	52.8	54.1	54.8	57.0	56.4	59.3	60.8	59.4	62.0	60.9	64.1	67.4	64.1	64.0	65.3	64.7	65.8	66.2	73.2	76.5				78.2
	3.00-3.25	58.6	58.5	59.7	61.8	64.6	65.5	69.2	68.1	70.9	72.7	74.4	75.1	75.0	74.1	79.2	79.6	86.4		82.3				80.7	85.1	89.8	95.0
	3.25-3.50	68.8	71.3	70.5	74.5	73.8	79.2	77.8	78.9	80.8	83.1	84.6	86.8	92.5	89.5	94.7	93.1	92.4	90.3	90.7							
	3.50-3.75	79.8	81.0	82.5	84.4	85.2	89.5	89.2	92.4	92.4	98.2	96.5		98.0	105.3	106.5	110.2	113.1									
	3.75-4.00	90.4	90.9	93.7	97.3	101.1	108.9		102.8	110.3	106.4	110.6	116.3	119.7	110.1		119.3	128.3	130.7	133.7							
	4.00-4.25				107.7	109.6	111.8	118.6	119.2	123.3	132.1							134.9	137.4	144.2	149.7	156.9					
	4.25-4.50	108.3	112.2		116.6	122.4	128.7		127.0	136.3	137.2	146.0	151.1									159.5					
	4.50-4.75						134.6	144.7	145.3	142.9		159.3	169.6	166.1													
	4.75-5.00												181.4	193.7	181.4	196.0											
	5.00-5.25													203.5	213.4		216.6										
	5.25-2.50														221.8	226.8											

Table 17 Occurrence (hours) of Hindcast T_e Versus H_s at the South Point site during 1979-2013

H_S (m)	Te (s) 4.00-4.25	4.25-4.50	4.50-4.75	4.75-5.00	5.00-5.25	5.25-5.50	5.50-5.75	5.75-6.00	6.00-6.25	6.25-6.50	6.50-6.75	6.75-7.00	7.00-7.25	7.25-7.50	7.50-7.75	7.75-8.00	8.00-8.25	8.25-8.50	8.50-8.75	8.75-9.00	9.00-9.25	9.25-9.50	9.50-9.75	9.75-10.0	10.0-10.25	10.25-10.50	10.50-10.75
0.75-1.00	2	6		1	1										19	12	12	10	12	36	103	126	89	69	105	78	84
1.00-1.25			3	2		11	7	1	1	1	7	24	121	191	347	490	886	899	929	880	972	973	856	788	652	555	358
1.25-1.50				3	3	14	9	1	21	102	243	449	830	1345	2113	2959	3553	3932	3899	3759	3366	2952	2336	2093	1837	1515	1008
1.50-1.75					2	3	3	10	129	394	942	1691	2628	3437	4599	5455	6288	6267	5663	5110	4574	3902	3171	2732	2201	1655	1351
1.75-2.00								16	207	742	1488	2615	3884	4572	5403	5782	6006	5541	5302	4698	3979	3215	2686	2411	2079	1716	1299
2.00-2.25								2	216	647	1313	2623	3143	3800	4534	4167	3956	3859	3740	3286	2925	2467	2085	1682	1323	1130	934
2.25-2.50									63	506	1141	1688	1925	2427	2588	2490	2410	2432	2247	2174	1948	1705	1388	1175	994	833	675
2.50-2.75									16	159	344	684	983	1101	1407	1559	1297	1290	1323	1297	1131	1107	945	768	596	445	356
2.75-3.00										1	33	109	279	431	542	508	500	379	381	404	457	461	463	492	405	319	285
3.00-3.25												7	5	46	37	45	118	119	89	68	91	93	92	115	125	113	104
3.25-3.50																		3	17	24	22	29	15	15	21	31	42
3.50-3.75																						4	17	6	9	5	6
3.75-4.00																									2	2	1

H_S (m)	Te (s) 10.75-11.00	11.00-11.25	11.25-11.50	11.50-11.75	11.75-12.00	12.00-12.25	12.25-12.50	12.50-12.75	12.75-13.00	13.00-13.25	13.25-13.50	13.50-13.75	13.75-14.00	14.00-14.25	14.25-14.50	14.50-14.75	14.75-15.00	15.00-15.25	15.25-15.50	15.50-15.75	15.75-16.00	16.00-16.25	16.25-16.50	
0.75-1.00	71	39	20	9	10	7	1	1		2	7													932
1.00-1.25	281	202	116	82	41	31	29	32	20	17	8	4	3	1										10821
1.25-1.50	783	583	396	262	213	167	147	73	46	30	30	41	32	9	1	1	1		1	1	1			41160
1.50-1.75	1075	874	648	505	409	323	206	142	109	73	56	54	38	14	8	17	5	9	4	4	6	2	2	66790
1.75-2.00	1054	848	684	465	405	323	239	219	133	123	72	58	49	45	21	21	15	13	5	8	5	6		68452
2.00-2.25	718	561	473	389	393	284	204	159	108	95	92	56	39	22	25	20	8	13	7	5	7	3	1	51514
2.25-2.50	493	390	301	287	208	149	137	97	91	59	25	21	16	15	10	8	6	6	3	3	2			33136
2.50-2.75	292	229	205	150	115	104	124	95	57	31	18	14	5	10	4	4								18265
2.75-3.00	250	191	137	115	91	67	52	42	24	12	5	4	2	1	4	1	3	2	2	2	1			7457
3.00-3.25	101	100	90	86	55	36	33	17	12	10	4	3	2	3	2	1		3						1825
3.25-3.50	46	35	33	27	29	21	7	7	6	5						3	3							441
3.50-3.75	1	2	6	3	6	8	9	4	8	6	1	1	2	2	3	1								110
3.75-4.00				2	2	4	7	2	2	1	1	2	2	2										32
																								300935

Table 18 Total Hindcast Wave Energy Flux (kWh/m) by T_e and H_s at the South Point site during 1979-2013

	Te (s)																										
H_S (m)	4.00-4.25	4.25-4.50	4.50-4.75	4.75-5.00	5.00-5.25	5.25-5.50	5.50-5.75	5.75-6.00	6.00-6.25	6.25-6.50	6.50-6.75	6.75-7.00	7.00-7.25	7.25-7.50	7.50-7.75	7.75-8.00	8.00-8.25	8.25-8.50	8.50-8.75	8.75-9.00	9.00-9.25	9.25-9.50	9.50-9.75	9.75-10.0	10.0-10.25	10.25-10.50	10.50-10.75
0.75-1.00	3	9		1	2										74	48	51	42	52	162	460	563	375	313	462	341	411
1.00-1.25			8	7		39	23	4	4	5	37	126	647	1017	1939	2884	5290	5555	5791	5655	6588	6754	6068	5756	4933	4338	2783
1.25-1.50				13	15	66	50	6	135	679	1683	3202	6153	10312	16853	24283	30071	34249	35189	34904	32275	29074	23403	21405	19368	16343	11261
1.50-1.75					12	19	21	85	1103	3539	8833	16405	26531	36026	49884	61043	72774	74712	69592	64677	59182	52281	43550	38421	31534	24238	20285
1.75-2.00								173	2293	8651	18111	33313	51433	62909	76933	84944	91256	87563	86347	78779	68363	56880	48678	44804	39386	33497	25838
2.00-2.25								27	3044	9562	20397	42331	52682	66516	82611	78378	76657	77785	77580	70385	64341	55936	48542	40003	32144	28198	23907
2.25-2.50									1103	9324	22040	33885	40478	53001	58677	58732	58878	61046	58268	57975	53390	47840	40084	34669	30060	25805	21163
2.50-2.75									338	3563	7979	16697	24952	29335	39122	44935	38615	39605	41826	42384	37966	38275	33633	28054	22082	16745	13743
2.75-3.00										26	902	3158	8503	13680	17955	17506	17774	13933	14339	15738	18215	18949	19596	21281	17961	14551	13393
3.00-3.25												228	179	1708	1404	1756	4946	5221	4018	3062	4233	4517	4590	5843	6551	6064	5672
3.25-3.50																		149	881	1291	1260	1760	946	906	1304	1987	2724
3.50-3.75																						258	1132	437	694	364	440
3.75-4.00																									158	161	82

	Te (s)																						
H_S (m)	10.75-11.00	11.00-11.25	11.25-11.50	11.50-11.75	11.75-12.00	12.00-12.25	12.25-12.50	12.50-12.75	12.75-13.00	13.00-13.25	13.25-13.50	13.50-13.75	13.75-14.00	14.00-14.25	14.25-14.50	14.50-14.75	14.75-15.00	15.00-15.25	15.25-15.50	15.50-15.75	15.75-16.00	16.00-16.25	16.25-16.50
0.75-1.00	347	188	102	49	60	42	6	5		12	42												
1.00-1.25	2222	1622	973	701	360	281	260	293	178	140	78	41	32	11									
1.25-1.50	8939	6691	4683	3186	2629	2091	1837	940	612	393	416	591	474	132	16	16	13		14	16	17		
1.50-1.75	16575	13784	10416	8275	6908	5551	3616	2511	1994	1333	1045	1001	726	272	160	350	104	192	89	88	120	46	46
1.75-2.00	21328	17496	14520	10095	9084	7370	5412	5065	3140	2999	1771	1486	1254	1191	553	541	376	353	133	217	144	175	
2.00-2.25	18628	14819	12845	10745	10955	8102	5904	4763	3254	2972	2846	1739	1253	701	822	671	285	467	244	182	271	108	35
2.25-2.50	15890	12818	10137	9847	7296	5333	4920	3511	3385	2225	966	834	653	628	418	342	247	242	122	123	83		
2.50-2.75	11598	9318	8425	6240	4916	4588	5451	4219	2563	1425	853	668	254	492	203	212							
2.75-3.00	11998	9452	6893	5895	4668	3513	2752	2250	1314	685	279	226	119	54	235	62	181	125	131	132	68		
3.00-3.25	5692	5693	5194	4999	3304	2207	2063	1100	792	654	273	203	129	200	129	76		221					
3.25-3.50	3053	2368	2241	1892	2072	1502	496	510	454	371						257	256						
3.50-3.75	72	152	483	241	468	661	762	347	702	539	94	93	188	186	294	97							
3.75-4.00				176	185	384	698	190	198	103	103	211	212	209									

Table 19 Average Hindcast Wave Power (kW/m) by T_e and H_s at the South Point site during 1979-2013

H_S (m)	Te (s) 4.00-4.25	4.25-4.50	4.50-4.75	4.75-5.00	5.00-5.25	5.25-5.50	5.50-5.75	5.75-6.00	6.00-6.25	6.25-6.50	6.50-6.75	6.75-7.00	7.00-7.25	7.25-7.50	7.50-7.75	7.75-8.00	8.00-8.25	8.25-8.50	8.50-8.75	8.75-9.00	9.00-9.25	9.25-9.50	9.50-9.75	9.75-10.0	10.0-10.25	10.25-10.50	10.50-10.75
0.75-1.00	1.5	1.5		1.5	2.5										3.9	4.0	4.2	4.2	4.3	4.5	4.5	4.5	4.2	4.5	4.4	4.4	4.9
1.00-1.25			2.7	3.5		3.6	3.2	3.8	4.3	5.0	5.3	5.2	5.4	5.3	5.6	5.9	6.0	6.2	6.2	6.4	6.8	6.9	7.1	7.3	7.6	7.8	7.8
1.25-1.50				4.2	4.8	4.7	5.6	5.6	6.4	6.7	6.9	7.1	7.4	7.7	8.0	8.2	8.5	8.7	9.0	9.3	9.6	9.8	10.0	10.2	10.5	10.8	11.2
1.50-1.75					6.0	6.5	7.1	8.5	8.5	9.0	9.4	9.7	10.1	10.5	10.8	11.2	11.6	11.9	12.3	12.7	12.9	13.4	13.7	14.1	14.3	14.6	15.0
1.75-2.00								10.8	11.1	11.7	12.2	12.7	13.2	13.8	14.2	14.7	15.2	15.8	16.3	16.8	17.2	17.7	18.1	18.6	18.9	19.5	19.9
2.00-2.25								13.7	14.1	14.8	15.5	16.1	16.8	17.5	18.2	18.8	19.4	20.2	20.7	21.4	22.0	22.7	23.3	23.8	24.3	25.0	25.6
2.25-2.50									17.5	18.4	19.3	20.1	21.0	21.8	22.7	23.6	24.4	25.1	25.9	26.7	27.4	28.1	28.9	29.5	30.2	31.0	31.4
2.50-2.75									21.1	22.4	23.2	24.4	25.4	26.6	27.8	28.8	29.8	30.7	31.6	32.7	33.6	34.6	35.6	36.5	37.0	37.6	38.6
2.75-3.00										25.6	27.3	29.0	30.5	31.7	33.1	34.5	35.5	36.8	37.6	39.0	39.9	41.1	42.3	43.3	44.3	45.6	47.0
3.00-3.25												32.6	35.9	37.1	37.9	39.0	41.9	43.9	45.2	45.0	46.5	48.6	49.9	50.8	52.4	53.7	54.5
3.25-3.50																		49.5	51.8	53.8	57.3	60.7	63.1	60.4	62.1	64.1	64.9
3.50-3.75																						64.5	66.6	72.9	77.1	72.8	73.3
3.75-4.00																									79.1	80.5	82.3

H_S (m)	Te (s) 10.75-11.00	11.00-11.25	11.25-11.50	11.50-11.75	11.75-12.00	12.00-12.25	12.25-12.50	12.50-12.75	12.75-13.00	13.00-13.25	13.25-13.50	13.50-13.75	13.75-14.00	14.00-14.25	14.25-14.50	14.50-14.75	14.75-15.00	15.00-15.25	15.25-15.50	15.50-15.75	15.75-16.00	16.00-16.25	16.25-16.50
0.75-1.00	4.9	4.8	5.1	5.4	6.0	6.1	6.4	5.3		6.0	6.0												
1.00-1.25	7.9	8.0	8.4	8.5	8.8	9.1	9.0	9.2	8.9	8.3	9.8	10.4	10.7	10.8									
1.25-1.50	11.4	11.5	11.8	12.2	12.3	12.5	12.5	12.9	13.3	13.1	13.9	14.4	14.8	14.7	16.5	15.8	12.5		14.3	16.0	17.2		
1.50-1.75	15.4	15.8	16.1	16.4	16.9	17.2	17.6	17.7	18.3	18.3	18.7	18.5	19.1	19.5	20.0	20.6	20.8	21.4	22.2	22.0	19.9	23.1	23.1
1.75-2.00	20.2	20.6	21.2	21.7	22.4	22.8	22.6	23.1	23.6	24.4	24.6	25.6	25.6	26.5	26.3	25.8	25.1	27.2	26.6	27.1	28.7	29.2	
2.00-2.25	25.9	26.4	27.2	27.6	27.9	28.5	28.9	30.0	30.1	31.3	30.9	31.1	32.1	31.8	32.9	33.5	35.6	35.9	34.9	36.5	38.8	36.0	35.2
2.25-2.50	32.2	32.9	33.7	34.3	35.1	35.8	35.9	36.2	37.2	37.7	38.6	39.7	40.8	41.9	41.8	42.8	41.1	40.3	40.5	41.1	41.3		
2.50-2.75	39.7	40.7	41.1	41.6	42.7	44.1	44.0	44.4	45.0	46.0	47.4	47.7	50.8	49.2	50.7	53.1							
2.75-3.00	48.0	49.5	50.3	51.3	51.3	52.4	52.9	53.6	54.7	57.0	55.9	56.5	59.7	54.5	58.7	62.0	60.4	62.6	65.7	65.9	68.1		
3.00-3.25	56.4	56.9	57.7	58.1	60.1	61.3	62.5	64.7	66.0	65.4	68.3	67.8	64.5	66.7	64.3	75.8		73.7					
3.25-3.50	66.4	67.7	67.9	70.1	71.4	71.5	70.8	72.9	75.7	74.2						85.7	85.3						
3.50-3.75	72.4	76.2	80.5	80.2	78.1	82.6	84.7	86.8	87.7	89.9	94.0	92.8	94.0	93.2	97.8	96.5							
3.75-4.00				88.2	92.6	96.1	99.7	94.9	99.2	103.1	103.3	105.7	106.0	104.5									

5. Conclusions

A system of third-generation spectral wave models has produced 34 years of global and Hawai‘i wave hindcast through a hierarchy of nested computational grids. The high-resolution data around the Hawaiian Islands facilitates computation of wave energy parameters at the US Navy Wave Energy Test Site (WETS) in Kaneohe, Oahu. Two sites within WETS are documented in this report. One at 81 m depth corresponds to the location of a Waverider™ buoy and is referred to as WETS, the other at 58 m depth is referred to as Kaneohe II. Four other potential sites along the Hawaiian Island chain were selected to illustrate varied conditions.

Hindcast estimates show agreement with the data recorded by 6 offshore and 8 nearshore buoys along the island chain. The hindcast system reproduces the wave climate, dominant wave components, long-term statistical distributions, and individual swell and wind wave events in the recorded data. Discrepancies primarily occur on the southwest shores of Oahu and Lanai in the shadows of the north swells and east wind waves due to the lack of diffraction in the spectral wave models. This model limitation also has some influences on the northwest swells arriving at WETS, but the hindcast estimates are valid under the north swell and prevailing wind wave conditions.

The wave climate comprises year-round trade wind waves from the northeast to east and swells from the south that are augmented by energetic winter swells from the northwest to north as well occasional local storm waves. At WETS, wind waves with significant wave height less than 2 m account for 75% of the time and contribute to less than 40% of the total energy. Due to the winter swells, the mean wave power increases from 7.7 kW/m in August to 21.7 kW/m in December. Wave power flux over 15 kW/m occurs less than 30% of time, but accounts for more than 60% of total energy. The other potential sites show a similar pattern in that a small percentage of the larger events contribute to a major proportion of the total wave energy. The diverse and moderate wave conditions at WETS indicate it as suitable place for testing and development of wave energy convertors. The other potential sites complement WETS by providing the full range of wave components commonly observed in the Hawaiian Islands.

References

Arinaga, R.A. and Cheung, K.F. (2012). Atlas of global wave energy from 10 years of reanalysis and hindcast data. *Renewable Energy* 39, 49-64.

Booij, N., Ris, R.C., and Holthuijsen, L.H. (1999). A third generation wave model for coastal regions. Part I. Model description and validation. *J. Geophys. Res.* 104 (C4), 7649–7666.

Caruso, S. and Businger, S. (2006). Subtropical Cyclogenesis over the Central North Pacific. *Weather and Forecasting* 21(2), 193-205.

Cheung, K.F., Bai, Y., and Yamazaki, Y. (2013). Surges around the Hawaiian Islands from the 2011 Tohoku tsunami. *Journal of Geophysical Research*: *Oceans* 118(10), 5703-5719.

Filipot, J.-F. and Cheung, K.F. (2012). Spectral wave modeling for fringing reef environment. *Coastal Eng.* 67, 67–79.

Foster, J., Li, N., and Cheung, K.F. (2014). Sea state determination from ship-based geodetic GPS. *J. Atmos. Oceanic Technol.* http://dx.doi.org/10.1175/JTECH-D-13-00211.1.

Lenee-Bluhm, P., Paasch, R., and Özkan-Haller, T.H. (2011). Characterizing the wave energy resource of the US Pacific Northwest. *Renewable Energy* 36, 2106-2119.

Li, N. and Cheung, K.F. (2014). Wave Energy Test Site (WETS) Progress Report: Comparison of Wave Hindcast Model Results with Waverider Measurements: November 2012 – October 2013 (http://hinmrec.hnei.hawaii.edu/)

Saha, S., Moorthi, S., Pan, H.L., Wu, X., Wang, J., Nadiga, S., Tripp, P., Kistler, R.,Woolen, J., Behringer, D., Liu, H., Stokes, D., Grumbine, R., Gayno, G., Wang, J.,Hou, Y.T., Chuang, H., Juang, H.M.J., Sela, J., Irdell, M., Treadon, R., Klesits, D.,Felst, P.V., Keyser, D., Derber, J., Ek, M., Meng, J., Wei, H., Yang, R., Lord, S., vanden Dool, H., Kumar, A., Wang, W., Long, C., Chelliah, M., Xue, Y., Huang, B.,Schemm, J., Ebisuzaki, W., Lin, R., Xie, P.P., Chen, M., Zhou, S., Higgins, W., Zou,C.Z., Liu, Q., Chen, Y., Han, Y., Cucurull, L., Reynolds, R.W., Rutledge, G., and Goldberg, M. (2010). The NCEP climate forecast system reanalysis. *Bull. Am. Meteorol. Soc.* 91 (7), 1015–1057.

Skamarock, W. C., and Klemp, J. B. (2008). A time-split nonhydrostatic atmospheric model for weather and forecasting applications. *J. Comp. Phys.* 227, 3465-3485.

Stopa, J.E., Cheung, K.F., and Chen, Y.-L. (2011). Assessment of wave energy resources in Hawaii. *Renewable Energy* 36 (2), 554–567.

Stopa, J.E. and Cheung, K.F. (2014). Intercomparison of wind and wave data from the ECMWF reanalysis interim and the NCEP climate forecast system reanalysis. *Ocean Modell*. 75, 65–83.

Stopa, J.E., Cheung, K.F., Tolman, H.L., and Chawla, A. (2013a). Patterns and cycles in the climate forecast system reanalysis wind and wave data. *Ocean Modell*. 70, 207–220.

Stopa, J.E., Filipot, J.-F., Li, N., Cheung, K.F., Chen, Y.-L., and Vega, L. (2013b). Wave energy resources along the Hawaiian Islands chain. *Renewable Energy 55*, 305-321.

SWAN Team (2011). SWAN User Manual: SWAN Cycle III version 40.85, Delft University of Technology, 121 pgs.

Tolman, H.L. (2008). A mosaic approach to wind wave modeling. *Ocean Modell*. 25(1–2), 35–47.

Tolman, H. L., and Chalikov, D. (1996). Source terms in a third-generation wind-wave model. *J. Phys. Oceanog.* 26, 2497-2518.

Wessel, P., and Smith, W. H. F. (1991). Free software helps map and display data. *Eos Trans. AGU* 72(41), 445–446.

Appendix A

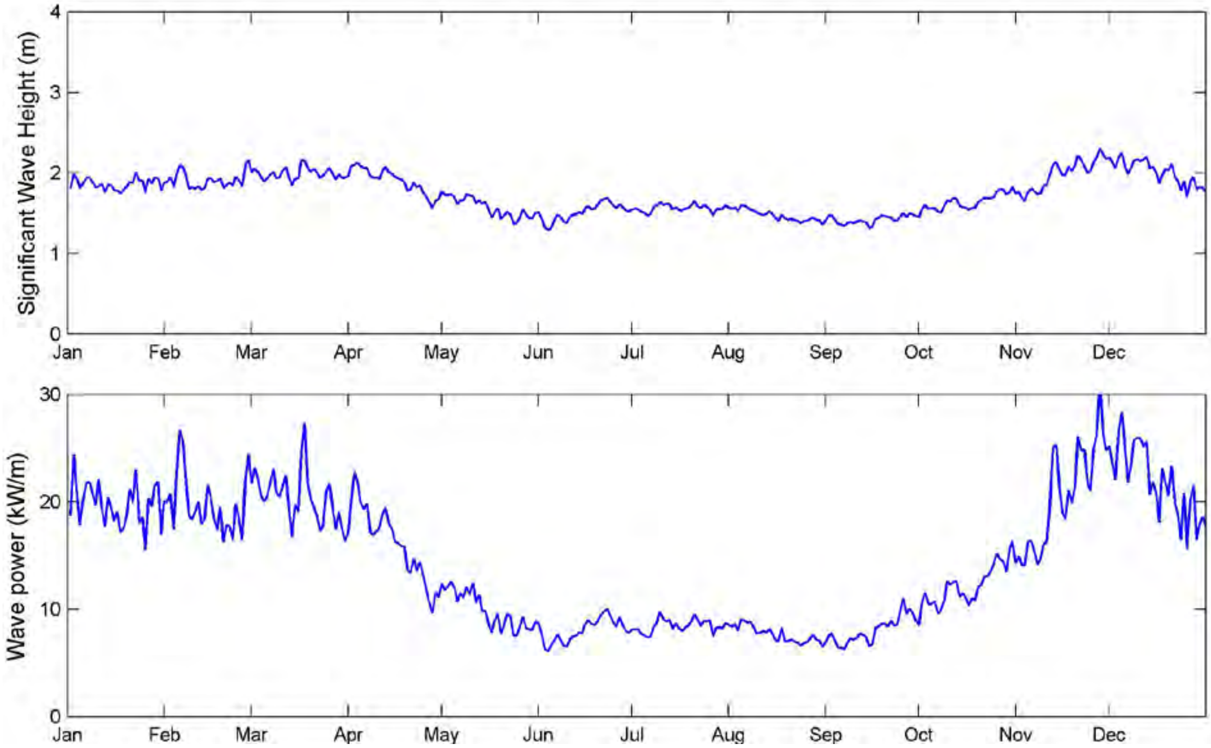

Figure A1– Average daily significant wave height and wave power at WETS.

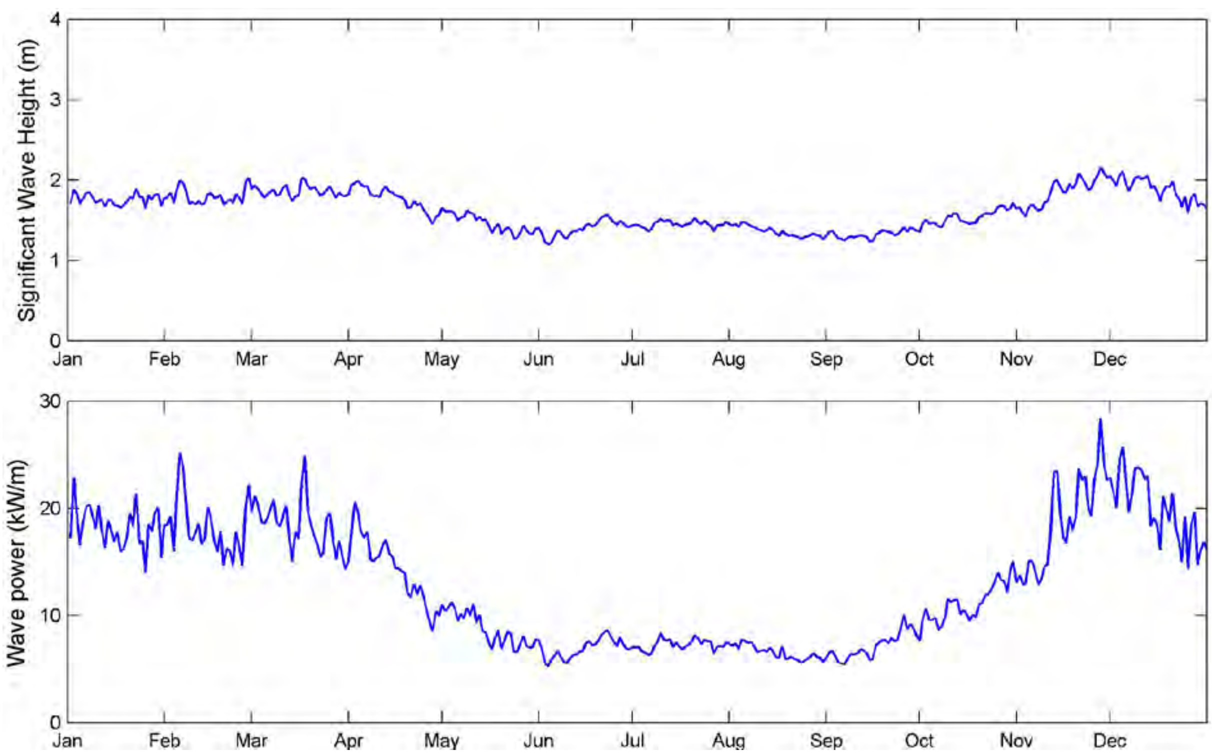

Figure A2– Average daily significant wave height and wave power at the Kaneohe II site.

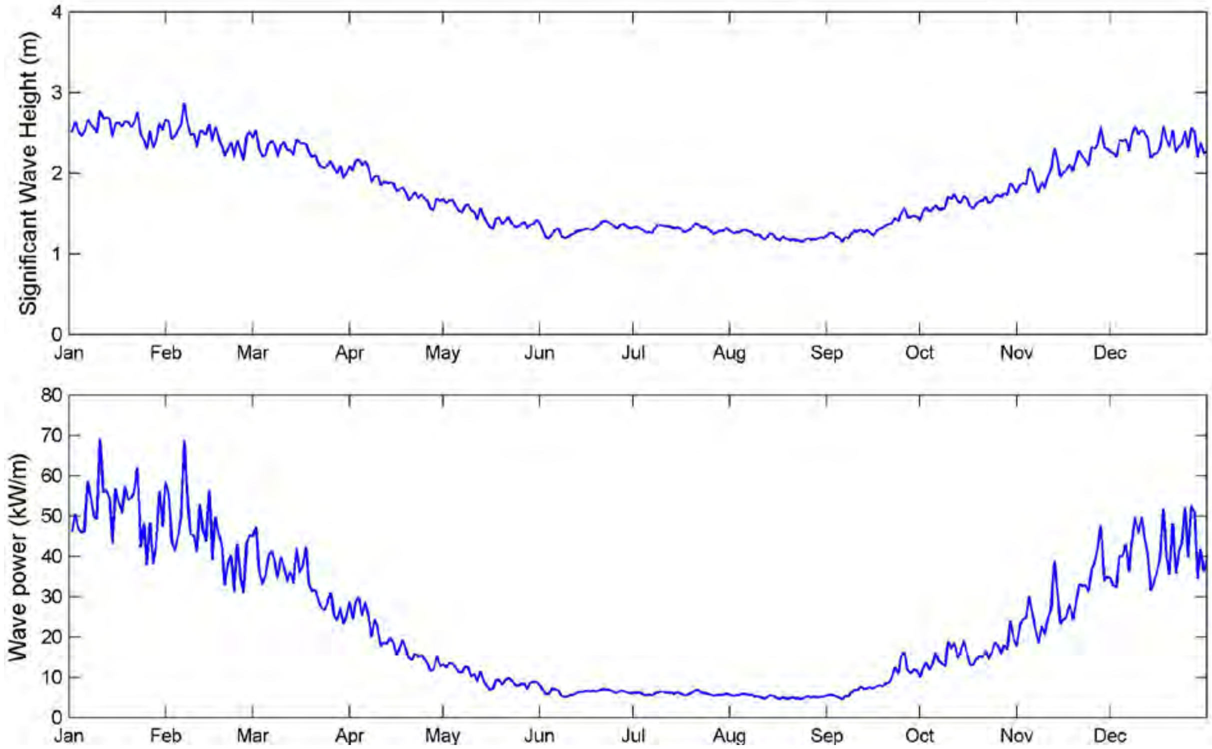

Figure A3– Average daily significant wave height and wave power at the Kilauea site.

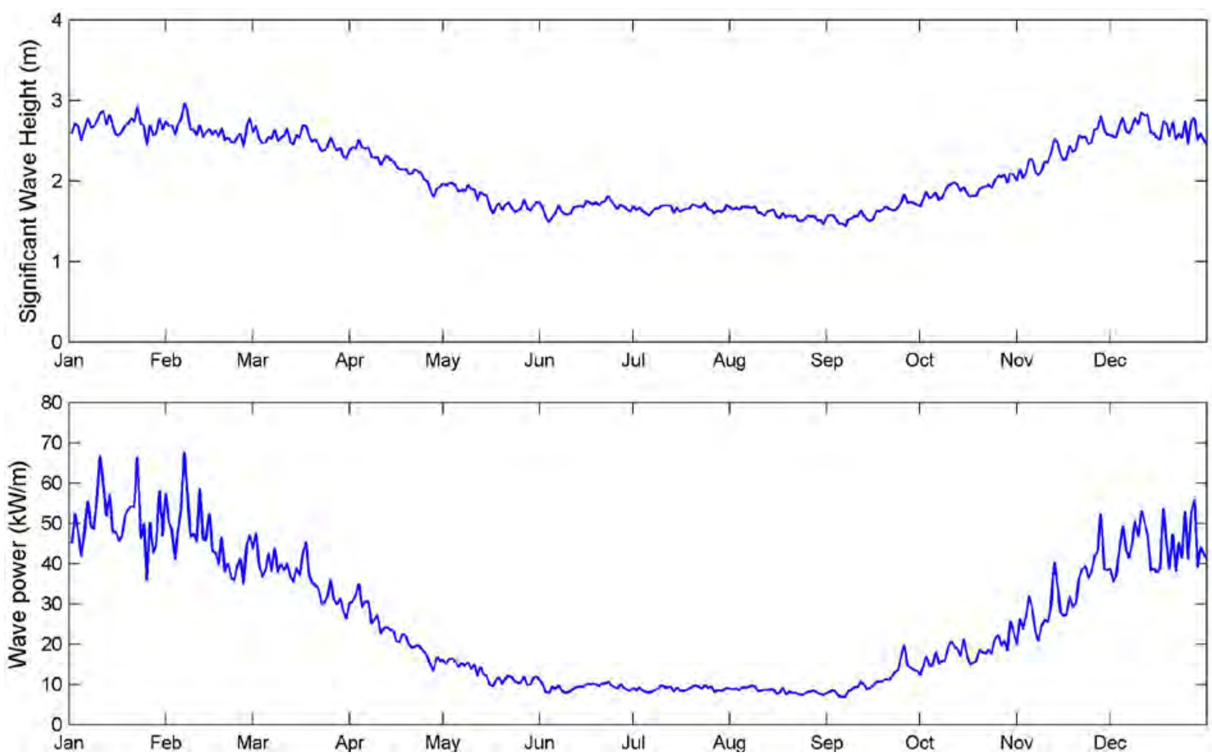

Figure A4– Average daily significant wave height and wave power at the Pauwela site.

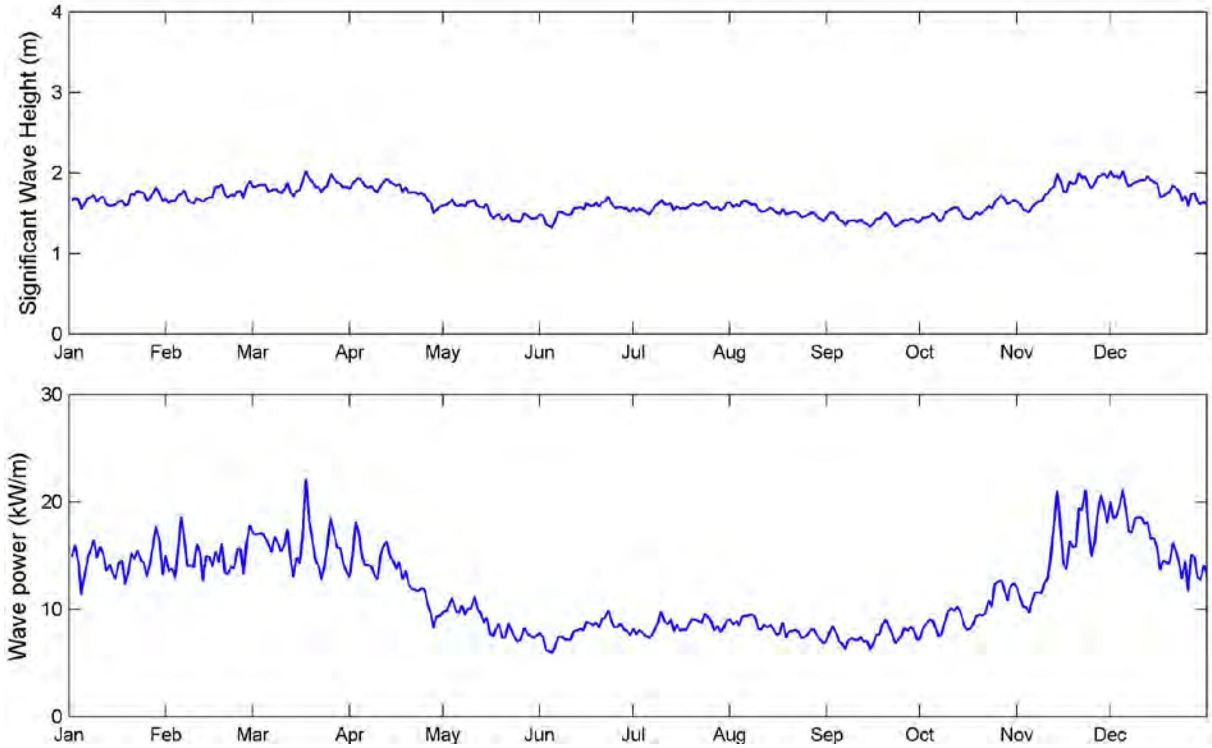

Figure A5– Average daily significant wave height and wave power at the Upolu site.

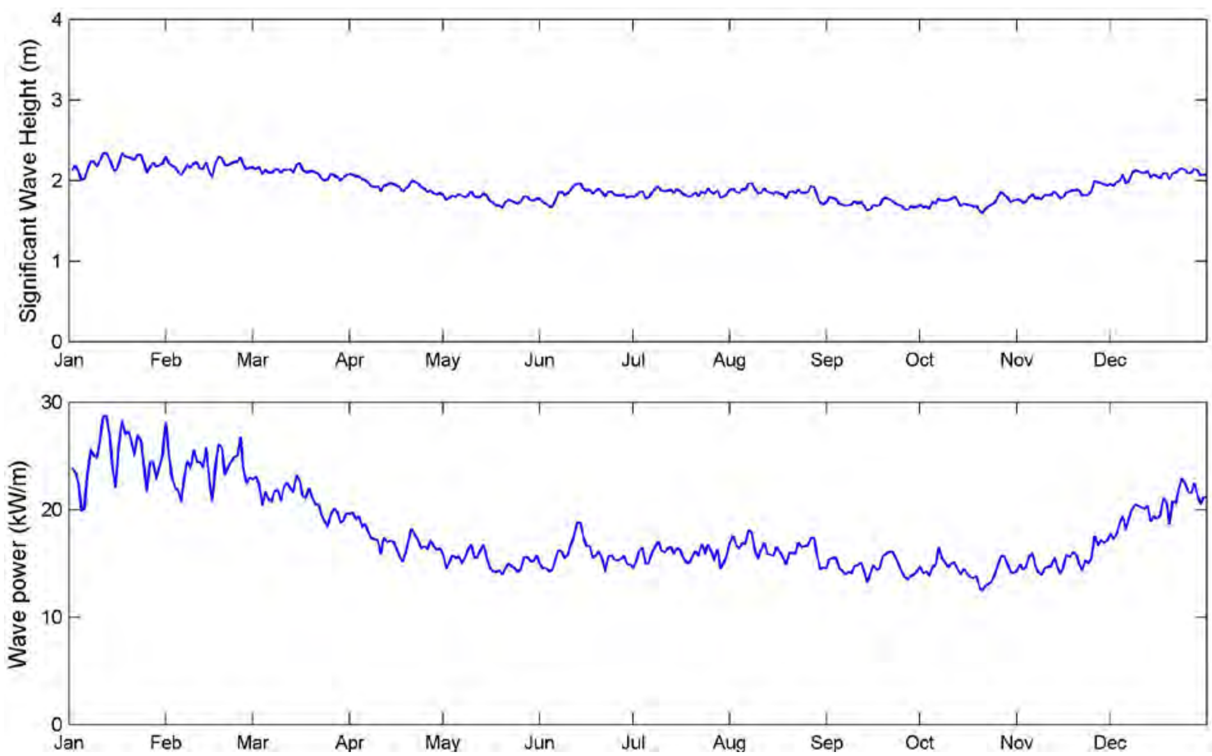

Figure A6– Average daily significant wave height and wave power at the South Point site.

Appendix B

Table B1 Monthly Average Wave Energy Parameters at WETS

	Jan	Feb	Mar	Apr	May	Jun	Jul	Aug	Sep	Oct	Nov	Dec
Significant wave height (m)	1.86	1.91	1.98	1.89	1.57	1.52	1.57	1.47	1.43	1.65	2.00	2.00
Wave power (kW/m)	19.7	19.8	20.1	15.9	9.8	8.1	8.6	7.7	8.2	12.4	20.8	21.7
Energy period (s)	9.7	9.3	8.7	7.9	7.3	6.7	6.6	6.7	7.4	8.2	8.9	9.4
Spectral width	0.37	0.37	0.38	0.36	0.36	0.36	0.35	0.35	0.37	0.37	0.37	0.37
Max directionally resolved wave power (degree)	14.5	19.2	28.4	39.8	45.5	55.9	58.2	59.9	41.5	29.6	27.5	21.6
Directionality coefficient	0.83	0.82	0.81	0.80	0.81	0.84	0.87	0.86	0.82	0.80	0.81	0.81

Table B2 Monthly Average Wave Energy Parameters at the Kaneohe II site

	Jan	Feb	Mar	Apr	May	Jun	Jul	Aug	Sep	Oct	Nov	Dec
Significant wave height (m)	1.76	1.80	1.85	1.76	1.45	1.41	1.46	1.36	1.33	1.55	1.87	1.87
Wave power (kW/m)	18.1	18.2	18.1	14.1	8.6	6.9	7.4	6.6	7.3	11.3	19.0	19.7
Energy period (s)	9.7	9.3	8.7	7.9	7.3	6.6	6.6	6.6	7.4	8.2	8.9	9.5
Spectral width	0.38	0.38	0.38	0.37	0.37	0.37	0.35	0.36	0.38	0.38	0.38	0.38
Max directionally resolved wave power (degree)	10.4	15.0	23.4	34.4	40.2	50.9	53.3	54.3	36.7	25.2	22.6	16.6
Directionality coefficient	0.84	0.83	0.82	0.81	0.82	0.84	0.87	0.86	0.82	0.81	0.82	0.82

Table B3 Monthly Average Wave Energy Parameters at the Kilauea site

	Jan	Feb	Mar	Apr	May	Jun	Jul	Aug	Sep	Oct	Nov	Dec
Significant wave height (m)	2.56	2.45	2.21	1.82	1.44	1.29	1.30	1.20	1.32	1.66	2.10	2.38
Wave power (kW/m)	51.4	44.5	32.5	18.2	9.6	6.3	5.9	5.1	8.6	16.0	29.5	41.9
Energy period (s)	11.8	11.4	10.5	9.0	7.8	6.9	6.6	6.6	8.0	9.2	10.2	11.2
Spectral width	0.32	0.34	0.36	0.38	0.38	0.38	0.37	0.38	0.38	0.37	0.36	0.34
Max directionally resolved wave power (degree)	-16.3	-13.2	-7.1	4.6	12.1	27.2	37.8	36.4	14.6	1.9	-3.1	-10.7
Directionality coefficient	0.90	0.88	0.86	0.82	0.80	0.79	0.82	0.81	0.82	0.85	0.86	0.88

Table B4 Monthly Average Wave Energy Parameters at the Pauwela site

	Jan	Feb	Mar	Apr	May	Jun	Jul	Aug	Sep	Oct	Nov	Dec
Significant wave height (m)	2.67	2.61	2.46	2.14	1.73	1.62	1.62	1.55	1.58	1.89	2.36	2.63
Wave power (kW/m)	50.8	45.4	35.5	22.0	12.2	9.0	8.7	8.1	10.9	18.2	32.5	44.8
Energy period (s)	11.3	10.9	9.8	8.4	7.4	6.5	6.4	6.4	7.6	8.7	9.6	10.7
Spectral width	0.34	0.36	0.39	0.41	0.41	0.42	0.41	0.42	0.41	0.41	0.39	0.37
Max directionally resolved wave power (degree)	-14.2	-9.5	1.4	21.5	34.9	53.6	60.3	62.0	33.1	13.0	7.1	-4.5
Directionality coefficient	0.83	0.81	0.78	0.74	0.75	0.78	0.84	0.83	0.77	0.76	0.77	0.80

Table B5 Monthly Average Wave Energy Parameters at the Upolu site

	Jan	Feb	Mar	Apr	May	Jun	Jul	Aug	Sep	Oct	Nov	Dec
Significant wave height (m)	1.65	1.70	1.79	1.73	1.48	1.48	1.53	1.48	1.37	1.50	1.77	1.77
Wave power (kW/m)	14.2	14.6	15.3	12.6	8.4	7.6	8.2	7.9	7.3	9.7	15.3	15.6
Energy period (s)	8.8	8.4	8.0	7.4	6.9	6.4	6.5	6.6	7.0	7.6	8.1	8.4
Spectral width	0.41	0.42	0.41	0.39	0.41	0.41	0.40	0.41	0.43	0.43	0.40	0.41
Max directionally resolved wave power (degree)	23.2	28.4	39.1	49.6	53.4	59.0	57.4	58.4	49.9	42.3	40.7	36.0
Directionality coefficient	0.77	0.78	0.80	0.82	0.82	0.84	0.85	0.82	0.79	0.79	0.81	0.79

Table B6 Monthly Average Wave Energy Parameters at the South Point site

	Jan	Feb	Mar	Apr	May	Jun	Jul	Aug	Sep	Oct	Nov	Dec
Significant wave height (m)	2.20	2.16	2.07	1.90	1.75	1.80	1.82	1.83	1.69	1.71	1.82	2.05
Wave power (kW/m)	24.8	23.6	20.5	16.7	15.0	15.6	15.7	16.0	14.5	14.1	15.2	20.2
Energy period (s)	9.0	8.9	8.6	8.6	9.0	8.8	8.6	8.7	9.1	8.8	8.3	8.5
Spectral width	0.49	0.50	0.50	0.52	0.52	0.53	0.53	0.52	0.51	0.51	0.49	0.49
Max directionally resolved wave power (degree)	220.6	217.0	191.3	164.4	167.3	163.9	160.4	164.3	177.4	176.4	167.1	189.1
Directionality coefficient	0.70	0.68	0.66	0.64	0.65	0.64	0.66	0.66	0.64	0.64	0.65	0.67